NOVEL MECHANISMS FOR BUFFERING THE HAEMODYNAMIC EFFECTS OF DIETARY SALT AND THE RELEVANCE OF SKIN SODIUM IN HUMANS

VIKNESH SELVARAJAH

Selwyn College

and

Division of Experimental Medicine and Immunotherapeutics

Department of Medicine

University of Cambridge

This dissertation is submitted for the degree of Doctor of Philosophy

May 2018

SUMMARY

Novel mechanisms for buffering the haemodynamic effects of dietary salt and the relevance of skin sodium in humans

Dr Viknesh Selvarajah

Background: Hypertension is one of the most common diseases in the United Kingdom and it remains an important risk factor for cardiovascular morbidity and mortality. Dietary sodium is an important trigger for hypertension and humans show a heterogeneous blood pressure (BP) response to salt intake. The mechanisms for this have not been fully explained, with renal sodium handling thought to play a central role. Animal studies have shown that dietary salt loading results in Na^+ accumulation and lymphangiogenesis in skin mediated by vascular endothelial growth factor-C (VEGF-C), both attenuating the rise in BP. This represents an additional system for maintaining BP and volume homeostasis in response to salt load. The focus of this thesis is to determine whether these dermal mechanisms exist in humans.

Methods: The technique of measuring skin Na^+ and K^+ using inductively coupled plasma optical emission spectrometry was developed in a pilot study of healthy adults. In a further study in healthy adults, the effects of dietary salt modulation on skin Na^+, the effect of sex and the relationship between skin Na^+ and haemodynamic parameters and plasma VEGF-C were studied. Skin Na^+ concentrations were expressed as the ratio Na^+:K^+ to correct for variability in sample hydration. The effect of dietary salt intake on skin gene expression of factors that potentially influence BP such as VEGF-C and the hypoxia inducible factor (HIF) transcription system was assessed, exploring possible mechanisms linking skin Na^+ to haemodynamic variables.

Results: Skin Na^+:K^+ increased with dietary salt loading and this effect appeared to be greater in men while only women showed a rise in ambulatory mean BP. Skin Na^+:K^+ correlated with blood pressure, stroke volume and peripheral vascular resistance in men, but not in women. No change was noted in plasma vascular endothelial growth factor-C.

Conclusions: These findings suggest that the skin may buffer dietary Na^+, reducing the hemodynamic consequences of increased salt and this may be influenced by sex. Skin Na^+ may influence blood pressure, stroke volume and PVR.

PREFACE

This dissertation is the result of my own work and includes nothing which is the outcome of work done in collaboration except as declared and specified in the text. It is not substantially the same as any that I have submitted, or, is being concurrently submitted for a degree or diploma or other qualification at the University of Cambridge or any other University or similar institution. I further state that no substantial part of my dissertation has already been submitted, or, is being concurrently submitted for any such degree, diploma or other qualification at the University of Cambridge or any other University or similar institution. It does not exceed the prescribed word limit of 60,000 words.

ACKNOWLEDGEMENTS

I am grateful to all the people who helped the work presented in this thesis possible in the face of adversity. In particular, my supervisors Professor Ian Wilkinson and Dr Carmel McEniery, who have gone above and beyond in providing me with the support, patience, guidance and generosity throughout my PhD. I am profoundly grateful to my college tutor Dr Gavin Jarvis and my consultant colleague Dr Kevin O'Shaughnessey for supporting and encouraging me in this endeavour.

I would like to thank the British Heart Foundation and the National Institute for Health Research for supporting my PhD.

I am indebted to my colleagues at the Division of Experimental Medicine and Immunotherapeutics who have supported and encouraged me along the way. I am deeply grateful to Dr Kaisa Mäki-Petäjä and Dr Stephen Smith for their invaluable help and Dr Joseph Cheriyan for his guidance and support. A big thank you to Sarah, Nikki. Jane, Annette, Jean and Karen for their support over the course of this work. I have had the great pleasure of working with Kat, Marie and Lucy and I thank them for their help and encouragement.

I am extremely grateful for the contribution of my collaborators without whom the analytical work in this thesis would not have been possible. Dr Sylvaine Bruggraber and Liliana Pedro from the Elsie Widdowson Lab, Dr Yury Alaverdyan from the Cambridge Graphene Centre, Keith Burling from the Addenbrookes Core Assay Biochemistry lab were extremely supportive and helpful throughout and I cherish what they have taught me. I would also like to thank the Cambridge University Hospitals NHS Foundation Trust Human Research Tissue Bank for their support.

I would like to thank my parents for their support and encouragement. Finally, I would have been unable to complete this without the love and support of my step-son Scott and my wife Anthea, whose extraordinary resilience, resourcefulness and wisdom has kept me going and made this possible.

TABLE OF CONTENTS

LIST OF FIGURES

CHAPTER 1

CHAPTER 2

CHAPTER 3

CHAPTER 4

CHAPTER 5

CHAPTER 6

CHAPTER 7

LIST OF TABLES

CHAPTER 1

CHAPTER 2

CHAPTER 3

CHAPTER 4

CHAPTER 5

CHAPTER 6

ABBREVIATIONS

ANS	Autonomic nervous system activity
BSA	Body surface area
cDNA	Complementary DNA
CKD	Chronic kidney disease
CT	Cycle threshold
CVD	Cardiovascular disease
DBP	Diastolic blood pressure
DdCT	Double delta cycle threshold
DNA	Deoxyribonucleic acid
EMIT	Experimental Medicine and Immunotherapeutics
ECG	Electrocardiogram
ECF	Extracellular fluid
eNOS	Endothelial nitric oxide synthase
eV	Electron volt
EXTL2	Exeostosin Like Glycosyltransferase 2 (EXTL2)
FC	Fold change
GAG	Glycosaminoglycans
HR	Hours
HRV	Heart rate variability (HRV)
HIF	Hypoxia inducible factor
HRV	Heart rate variability
ICP-OES	Inductively Coupled Plasma/Optical Emission Spectrometry
ICF	Intracellular fluid
i.d	Internal diameter
iNOS	Inducible nitric oxide synthase
LVM	Left ventricular mass
MAP	Mean arterial pressure
MCD	Mean capillary density
mmHg	Millimetres of mercury
MRC	Medical Research Council

mRNA	Messenger RNA
MPS	Mononuclear phagocyte system
NaCl	Sodium chloride
NO	Nitric oxide
PBS.	Phosphate-buffered saline
PHD2	Prolyl hydroxylase domain 2
PPM	Parts per million
qPCR	Quantitative polymerase chain reaction
RAAS	The renin-angiotensin-aldosterone system
SBP	Systolic blood pressure
sFLT-4	Soluble receptor for VEGF-C
SHR	Spontaneously hypertensive rats
SS	Salt sensitive
SV	Stroke volume
SSBP	Salt sensitivity of blood pressure
SR	Salt resistant
UNaV	Urinary 24-hour sodium excretion

Chapter 1 BACKGROUND

1.1 HYPERTENSION

Blood pressure is a quantitative phenotype with a continuous distribution in human populations. Hypertension is defined as systolic blood pressure ≥140 mmHg or diastolic blood pressure ≥ 90 mmHg, measured at the brachial artery. It is a common disorder, affecting a third of the human population, and its prevalence is increasing worldwide. [1,2] Hypertension represents an important global health challenge, being considered one of the foremost modifiable risk factors for stroke, heart failure, ischaemic heart disease and chronic kidney disease. [1,3,4] Globally, the control of hypertension continues to be inadequate despite improved therapies and unhealthy lifestyle factors are thought to be a critical factor. [5] Furthermore, cardiovascular risk does not start at the conventional cut-off point 140/90 mmHg but starts at a systolic blood pressure of 115 mmHg and a diastolic pressure of 75 mmHg. [6] Therefore, understanding and addressing the factors that increase blood pressure has important health implications that extends beyond the scope of hypertension.

1.1.1 Pathophysiology of hypertension

Despite its prevalence, the precise origins of hypertension remain unclear. Hypertension is believed to be multifactorial with various pathophysiologic mechanisms. The maintenance of a normal blood pressure is dependent on the balance between the cardiac output and peripheral vascular resistance.[7] Hypertension in believed to start with a raised cardiac output resulting from extracellular volume expansion, which transforms in time to a raised peripheral vascular resistance (PVR), this being determined by the number and contractile state of resistance vessels that are less than 150µm in diameter. [8,9]Previous work suggests that there is structural remodelling of these vessels in hypertension, which results in a fixed, irreversible, increase in PVR. [9] There is also a reduction in the density of arterioles and capillaries in the skin and skeletal muscle, termed microvascular rarefaction, which contributes to the raised BP by increasing PVR. [10,11]

Two main forms of hypertension exist. Secondary hypertension is defined as raised blood

pressure resulting from a recognisable and potentially correctable cause while in primary or essential hypertension, no such cause is identified. In unselected populations, between 1 – 5% of hypertensives have secondary hypertension, the principal forms of which are listed in Table 1. Notably, most of these conditions involve aberrations in body sodium regulation. The pathogenesis of essential hypertension remains elusive despite decades of extensive research efforts. It is believed to be a complex disorder reflecting interplay between genetic susceptibility and environmental triggers, and it is unclear which specific mechanisms are involved.

Table 1.1: Causes of secondary hypertension. [12] Disorders in italics involve dysregulation of body sodium homeostasis.

Renal	Endocrine	Drugs
Renal artery stenosis	*Hyperaldosteronism*	Cocaine
Renal parenchymal	*Conn's syndrome*	Alcohol
disease	*Bilateral adrenal hyperplasia*	*Corticosteroids*
Adult Polycystic Kidney	*Phaeochromocytoma*	*Oral contraceptive in pill*
disease	*Cushing's syndrome*	*Nonsteroidal anti-inflammatory drugs*
Renal tumours	Hyperthyroidism	*Vascular endothelial growth factor*
Liddle's syndrome	*Hypothyroidism*	*inhibitors*
Gordon 's syndrome	Hyperparathyroidism	Monoamine oxidase inhibitors
	Acromegaly	Heavy metals

1.1.2 Central blood pressure and arterial stiffness

Blood pressure measured at the brachial artery (peripheral blood pressure) has played a central role in our evaluation and management of cardiovascular disease, but in recent years greater emphasis has been placed on the importance of central or aortic blood pressure and arterial stiffening. **Central blood pressure** (CBP) refers to the pressure experienced by the large vessels and the heart and has been shown to be a better predictor of cardiovascular events than peripheral blood pressure. [13-15] This may be because the heart, kidneys and

brain are exposed to aortic rather than brachial pressure. [16]

Stiffness refers to the ability to resist deformation. **Arterial stiffness** is associated with advancing age and is increasingly recognised as a surrogate endpoint for cardiovascular disease. [17] Stiffening in the large central arteries is positively associated with systolic hypertension, coronary artery disease, stroke, heart failure and atrial fibrillation. [18-21] Aortic stiffening generally results from a complex interplay between factors such as haemodynamic forces, calcification, salt intake, glycaemic state and the degeneration of elastin fibres with deposition of stiffer collagen. [22,23] The large arteries, such as the aorta, provide a conduit for circulating blood and buffer arterial pressure changes that occur during the cardiac cycle, enabling a constant blood flow to the peripheral vascular beds. During myocardial contraction a wave that travels through the aortic trunk and arterial tree is generated. The rate which this aortic pressure waves travel is the **pulse wave velocity** (PWV). Aortic pulse wave velocity (aPWV) as measured by carotid-femoral pulse wave velocity, is the gold standard measure of arterial stiffness. [17]. Carotid-femoral pulse wave velocity is known to be independent predictor of cardiovascular events and mortality in the general population. [24] An increase of aortic pulse wave velocity of 1 m/s confers an increased cardiovascular risk by more than 10%.[25] The forward going aortic pulse wave gets reflected from the periphery and normally returns in diastole, augmenting or increasing systolic pressure in the central arteries and maintaining coronary blood flow. The **augmentation index** (AIx) is a measure of pulse wave reflection and quantifies the extent of augmented pressure relative to the central pressure. AIx has been shown to predict cardiovascular events in patients with hypertension and ischaemic heart disease, as well as all-cause mortality in patients with renal impairment. [17] CBP, aPWV and AIx can now be determined reliably using non-invasive techniques and should be considered for the evaluation of cardiovascular risk. [17]

1.2 ROLE OF SODIUM IN HYPERTENSION AND CARDIOVASCULAR DISEASE

Sodium is an alkali metal which serves as an essential nutrient in all animals. It is the dominant ion of the extracellular fluid where it functions as an osmotic skeleton, maintaining extracellular volume and adequate tissue perfusion. Sodium maintains the normal transmembrane electrochemical gradient, transmission of nerve impulses and normal cell metabolism. [26,27] The terms sodium and salt are often used synonymously, with salt comprising of 40% sodium 60% chloride by weight. Over 90% of dietary sodium is consumed as salt.

For the purpose of this thesis:
Salt refers to sodium chloride

Na^+ refers to both ionised or non-osmotically bound sodium

Dietary sodium is consumed as salt

1 mmol sodium = 23 mg sodium
1 gram of sodium chloride (salt) = 390mg (17 mmol) of sodium
6 grams of sodium chloride (salt) = 2.3g (100mmol) of sodium

Excessive dietary sodium, principally as the chloride salt, has long been considered a pivotal factor in development of hypertension. [28] The average daily sodium intake worldwide in 2010 estimated at 3.95 g per day, exceeding the maximum UK recommended intake of 2.3 g per day. [29,30] Essential hypertension is virtually absent in populations with a sodium intake of less than 1.2 g per day and tends to occur in populations consuming more than 2.3 g of sodium a day, suggesting that the development of hypertension requires a threshold level of sodium intake. [31] The first scientific report describing a direct relationship between sodium intake and hypertension is credited to Dr Lewis Dahl, who showed that mean salt intake correlates with the prevalence of hypertension. [32,33] Subsequently, numerous epidemiological and interventional studies have demonstrated a positive relationship between salt intake and blood pressure. The International Study of Salt and BP (INTERSALT) study showed that an increase in daily sodium intake of 50 mmol resulted in an increase in systolic BP of 5 mmHg over a 30-year period, after adjusting for potentially confounding

variables such as BMI and alcohol intake. [34] The DASH (Dietary Approaches to Stop Hypertension – Sodium) trial showed that a reduction in salt intake resulted in a stepwise decrease in BP and this was more pronounced in individuals of African origin, older participants and those with hypertension. [35] The PURE study, which included 102,216 adults from 18 countries, showed increments of 2.11 mmHg in SBP and 0.78 mmHg in DBP for each 1 g increment in estimated sodium intake. [36]

Dietary sodium reduction should theoretically reduce cardiovascular disease by lowering blood pressure and this has formed the basis for population wide sodium reduction as a means to reduce cardiovascular disease. [37] Interventional trials proving this are lacking, but observational data from the Trials of Hypertension Prevention (TOHP), which consisted of 2974 healthy, normotensive individuals, showed a direct linear association between sodium intake and cardiovascular events as well as all-cause mortality over a 20 year period. [38,39] Thus, the evidence for reducing population salt intake is strong. Approximately 80% of salt consumed is processed and obtained from outside the home and keeping salt intake below the recommended targets is challenging. [28] The World Health Organisation has proposed salt reduction as the key dietary target for 2025 to reduce mortality from cardiovascular disease, the main non-communicable diseases. [40] The UK salt reduction strategy started in 2003 and since then national adult daily sodium intake has fallen from 3.7g in 2001 to 2.9 g in 2014, and there are ongoing efforts to improve public awareness and reduce the salt content of manufactured foods. [41]

1.2.1 Salt sensitivity of blood pressure

Salt sensitivity of blood pressure (SSBP) is a physiological trait in mammals, including humans, by which blood pressure exhibits changes parallel to changes in salt intake. [42] Although most populations, including the UK, have sodium intakes exceeding 2.3 g a day most people remain normotensive, suggesting that some individuals are more sensitive to salt than others. Acute and chronic salt loading and depletion experiments support this view. [43,44] This apparent heterogeneity in blood pressure response to salt has caused controversy regarding recommendations to reduce salt intake in the general population. [42,45]

SSBP has significant prognostic and therapeutic implications. Weinberger et al showed that normotensive individuals who are salt sensitive had a significantly greater increase in systolic and diastolic pressure over time than those who were salt resistant, and are more likely to develop hypertension in the future. [46] This suggests a possible pathophysiological connection between SSBP and the development of essential hypertension. SSBP is associated with endothelial dysfunction and has been shown to be an independent risk factor for left ventricular hypertrophy, renal impairment and cardiovascular events. [47-49] SSBP is also independently associated with mortality in both normotensive and hypertensive individuals. [50] Furthermore, women with a history of pre-eclampsia have a tendency for salt-sensitivity before menopause, which may contribute to their excess cardiovascular risk.[51] Thus, it can be seen that the salt sensitivity trait has clinical relevance and implications that extends beyond BP.

1.2.1.1 Determination of salt sensitivity - its challenges and clinical application

The assessment of salt sensitivity of blood pressure is difficult because of the lack of universal consensus on definition. [42] A large number other studies have been done using a variety of dietary approaches, thresholds and measures of BP for defining salt sensitivity. [42,52] In these methods of assessment, individual displaying a significant BP response to dietary sodium modulation were termed salt sensitive (SS), all those that do not classified as salt resistant. (SR).

SSBP has been was arbitrarily defined as a ≥ 10% increase in MAP between low and high

intakes. [53] Weinberger et al defined SSBP as a ≥ 10 mmHg increase in mean arterial pressure (MAP) after an infusion of 2 L of normal saline over 4 hours, relative to MAP after 1 day of a low sodium (10 mmol) diet and administration of frusemide. [50] Using this technique in 378 healthy volunteers, Weinberger et al showed that 26% of normotensive individuals are salt sensitive. [43] In a study of 198 hypertensives, they showed 73% of blacks were salt sensitive compared with 56% of whites [43]. Factors associated with SSBP include hypertension, diabetes mellitus, black race, intrinsic kidney disease and older age. [54] Thus the SSBP phenotype may be present in a significant proportion of the human population and racial variations exist. Recently, ambulatory BP has been used where an increase in 24-hr MAP of ≥ 4 mmHg with increased salt intake has been introduced as an alternative definition.[55,56] SSBP determined by BP responses to dietary modulation has been found to be a reproducible trait. [57]

There are several limitations for the above definitions and techniques for salt sensitivity. Determining salt sensitivity by salt loading and depletion is impractical in routine clinical practice, compromising its clinical utility. Although individuals are commonly dichotomised as SS or SR, BP responses to sodium manipulation follow a Gaussian distribution and SSBP is a continuous, normally distributed quantitative trait. [43,58] Defining an individual as SS or SR depends on the arbitrarily chosen thresholds for the magnitude of BP changes. Furthermore, short term salt loading and depletion studies (days to weeks) may not reflect the long-term effects of a particular level of dietary salt intake. The sequence of sodium intake has also been a source of controversy. Subjecting individuals to a low sodium intake is believed to result in variable degrees of renin-angiotensin-aldosterone system activation. Therefore, starting with a low-salt intake may influence the effect of subsequent high-salt intake on sodium. [42,43]

Salt sensitivity of blood pressure describes a clinical phenotype with a significant prognosis for cardiovascular health. Theoretically, reducing salt intake would be more important in salt sensitive than for salt resistant water individuals, not only for its benefits for BP control, but also for the additional effects on cardiovascular risk. [42] An understanding of the underlying mechanisms for differential BP response to a salt load and reliable biomarkers for the SSBP phenotype are currently lacking. Trials evaluating the relative efficacy of antihypertensives in

salt sensitive hypertensives are also inadequate. Thus, SSBP may be relevant, but its clinical applications are still uncertain.

1.2.2 How sodium modulates blood pressure

1.2.2.1 Traditional paradigms - the two-compartment model for body water and sodium

Total body water (TBW) has traditionally been divided into two compartments, intracellular fluid (ICF) and extracellular fluid (ECF), with the latter consisting of the intravascular and interstitial spaces. Total body sodium (TBNa) has been divided similarly. The interstitium is the space located between the capillary walls and cells, being further subdivided according to body site and tissue type(see Figure 1.1). [59,60] The intravascular and interstitial spaces are considered to be in a state of equilibrium, in which fluids with nearly constant osmolyte concentrations surround the body cells. This conventional model, the 'equilibrium theory', derives from Claude Bernard's 19th century paradigm of a "milieu interieur", which introduced the physiological concept of homeostasis. [61,62] In the two-compartment model, sodium ions act as the principal extracellular osmoles, holding water in the extracellular space. [63] Conversely potassium ions retain water within cells with this balance being maintained by the Na^+-K^+- ATPase pump in the cell membrane. In this model, sodium accumulation is primarily extracellular and inevitably leads to commensurate water retention, such that accumulation of 140 mmol of sodium must inevitably lead 1 litre of water in the extracellular fluid, thus maintaining iso-osmolality. [63,64] Extracellular sodium content is maintained within narrow limits to prevent perturbations in fluid balance, and multiple physiological systems operate to maintain extracellular sodium levels. [63]

The mechanisms by which sodium influences blood pressure are not fully understood. In the classical Guytonian model, increased salt intake leads to a corresponding expansion in extracellular volume. This leads to an increase in plasma volume, venous return and cardiac output, which is turn causes a rise in systemic blood pressure. [65] This increase in extracellular volume can be counterbalanced by pressure natriuresis carried out by the kidneys. [66] The kidney is therefore believed to be the main organ regulating the haemodynamic response to salt intake.

Figure 1.1: Body fluid compartments. In the average male, intracellular fluid and extracellular fluid domains consist of about 57% and 43% of total body water respectively. The ECF compartment is further subdivided into interstitial fluid, lymph, plasma, bone and connective tissue, adipose tissue, and transcellular water. Percentages are percent of TBW. Taken from Bave et al. [60]

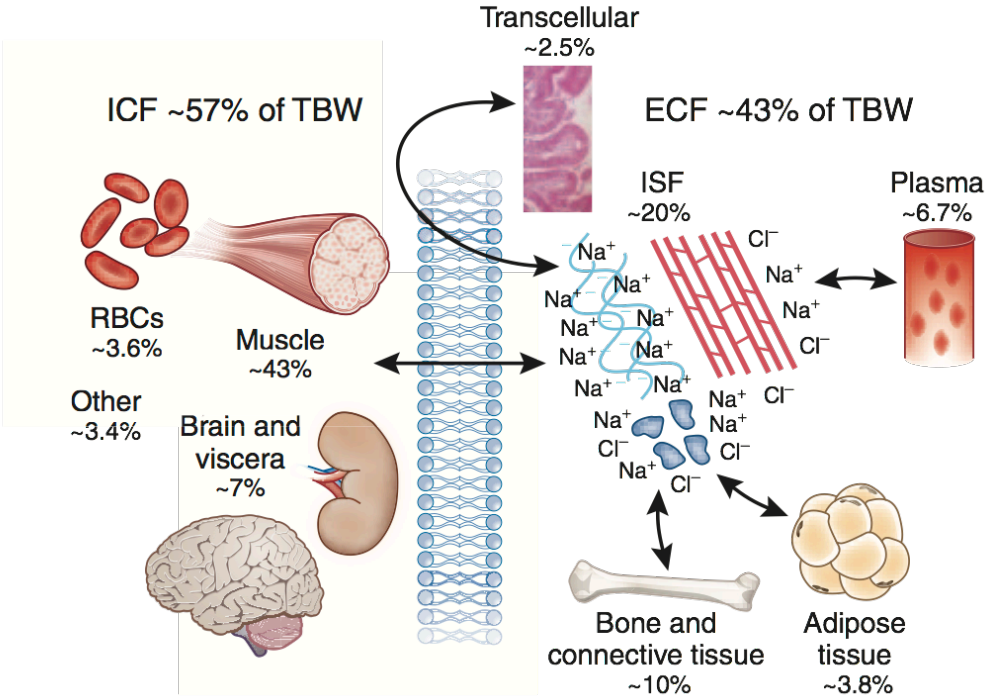

1.2.2.2 The role of the kidney in salt sensitivity

The kidney has traditionally been considered to be at the centre of BP control, with blunted renal sodium excretion thought to result in a rise in BP via an increase in extracellular volume (Figure 1.2). This is supported by physiological and genetic observations. [67,68] Systemic blood pressure determines renal perfusion, which can directly regulate sodium reabsorption in the proximal tubule. In the Guytonian model, this acute pressure natriuresis response is a uniquely powerful means of BP around a set point (Figure 1.2).This implies that a mismatch between renal perfusion pressure and sodium excretion could cause BP to rise in the face of dietary salt intake. [69] Renal sodium absorption per se is increased in hypertensive individuals and differs across ethnic groups. It is likely that genetic polymorphisms contribute to this phenomenon via effects on sodium transporters in the kidney, NKCC2 and ENaC, and regulatory molecules of the renin-angiotensin aldosterone system. [70-72] Further compelling evidence for the central role of the kidney in hypertension comes from cross transplantation studies between normotensive and hypertensive rat strains showing how normotensive recipients develop hypertension after receiving kidneys from hypertensive donors. [73] Thus, a wealth of evidence supports the traditional nephrocentric view of hypertension and salt sensitivity in humans. Despite this, specific renal mechanisms in the majority of salt-sensitive individuals are lacking.

Figure 1.2: The nephrocentric model of salt sensitivity. Renal responses to salt loading in salt resistant (dotted red line) and salt sensitive (green line) individuals. The traditionally held view is that renal sodium excretion rises rapidly and to match an increase in sodium intake, so that BP changes only minimally. In salt sensitive individuals is believed that renal sodium excretion is impaired, resulting in an increase in extracellular fluid volume and blood pressure. (Taken from Kurtz et al and Brands MW) [74,75]

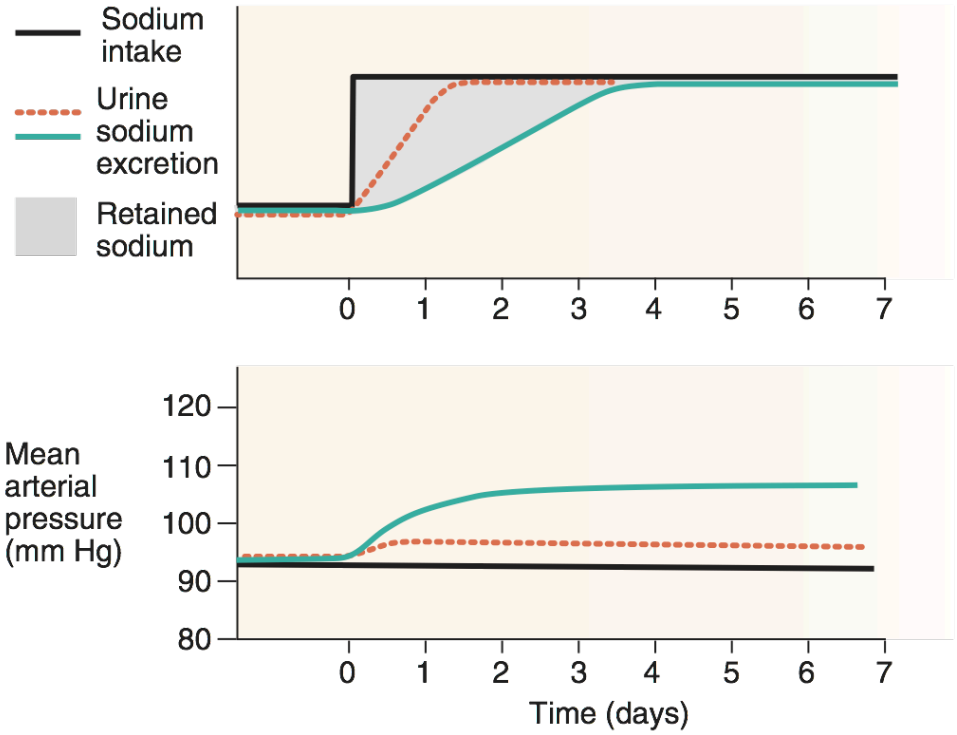

1.2.2.3 Other mediators of salt sensitivity

Several natriuretic and anti-natriuretic neuro-hormonal systems have been implicated in salt sensitivity.

The renin-angiotensin-aldosterone system (RAAS): The RAAS is the principal volume-regulatory effector in mammals and a major regulator of blood pressure within the human body. [76]It is sensitive to changes in salt intake. [77] Short-term salt loading and depletion studies by Macgregor and Weinberger showed that individuals who are salt sensitive display a blunted renin, aldosterone and angiotensin-2 response to salt depletion. [78,79] This is

believed to be due to the excessive BP response to salt loading, as preventing the expected decrease in aldosterone and angiotensin-2 that accompanies salt loading prevents the expected natriuresis. [80] Thus, the blunted RAAS system is a phenotypic characteristic of SSBP.

The sympathetic nervous system: Studies in rats and humans have shown that the pressor response to salt is associated with increased plasma and urine catecholamine levels. [81] In hypertensive humans plasma catecholamines decrease more in those who are salt resistant compared to those who are salt sensitive, and this is likely to contribute to the difference in haemodynamic response. [82-84] Salt sensitive hypertensive humans are also known to have a greater pressor response to exogenous norepinephrine than salt resistant hypertensives, regardless of salt intake. [83,85]

Atrial natriuretic peptides (ANPs): These are peptide hormones that are synthesised, stored and released by atrial myocytes in response to atrial distension, angiotensin 2, endothelin and sympathetic stimulation. The salt sensitive sub-strain of spontaneously hypertensive rats (SHR) fail to respond to volume expansion during salt loading with an increase in ANP, compared with salt resistant SHR controls. [86] Low levels of circulating N-terminal ANP have been shown to predict SSBP in the Framingham Offspring cohort. [87] However, the opposite has also been observed. [88] The available evidence suggests that ANP may play a pathogenic role in some cases of SSBP.

The endothelin system: Endothelins are vasoactive peptides that are known to modulate vascular function, fluid-electrolyte homeostasis, cardiac function, and neuronal function. [89] Urinary endothelin displays a circadian rhythm and correlates negatively with BP and positively with Na^+ excretion during salt loading. Humans with SSBP have low levels of urinary endothelin and this is believed to contribute to impaired natriuresis with salt loading. [90]

Nitric oxide (NO): Dietary salt loading increases the excretion of NO metabolites in salt resistant individuals while the opposite is seen in humans who are salt sensitive. It is believed that an endogenous inhibitor of NO may play a role in SSBP. [91] Differences in NO

production may exist in salt sensitive and salt resistant individuals. Black SS appear to have a greater BP reduction with intravenous L-arginine compared to SR controls. This apparent deficit in NO production by those with the SSBP triggered may explain their endothelial dysfunction and inability to vasodilate with salt loading. [83]

1.2.2.4 Genetics of salt sensitivity in humans

Several lines of evidence support a genetic basis for SSBP. BP changes with dietary salt modulation has been found to have a higher correlation between monozygotic twins compared with sibling pairs.[92] Investigators in the GenSalt study, a dietary salt modulation population study in 1906 rural Chinese, observed that 22-33% of the BP changes occurring in response to a change in response salt intake could be attributed to genetic effects. [93] The higher prevalence of SSBP in people of blacks compared with Caucasians suggests a genetic influence on this trait. It has been postulated that people of African origin evolved in an environment low in sodium and genetic mechanisms aimed at retaining sodium evolved. [94] However, the exact genetic factors contributing to salt sensitivity in blacks is still unclear.

Studies searching for candidate genes for SSBP have focussed on traditional pathways believed to mediate SSBP, as described in 1.2.2.1 - 1.2.2.3. These include genes for angiotensin converting enzyme (ACE), angiotensinogen (AGT), angiotensin II type 1 receptor, epithelial sodium channel (ENaC) , 11-beta hydroxy steroid dehydrogenase (11-BHSD), alpha and beta adrenoceptors, endothelial nitric oxide synthase and adducin. [95] These studies have shown association between these candidate genes and the SSBP trait, but have been plagued by several methodological challenges such as study size and lack of replication across multiple studies. [42]

Mendelian syndromes of hypertension have been considered important for the understanding the genetic basis for SSBP and essential hypertension. [96] In keeping with the nephrocentric model SSBP, mendelian hypertension results from mutations leading to sodium retention while mendelian hypotension results from mutations causing renal sodium loss. [42] Mutations in the aldosterone synthase/11β-hydroxysteroid dehydrogenase, mineralocorticoid receptor, and β and γ subunits of the epithelial sodium channel (ENaC)

cause monogenic hypertension[97]. However, these syndromes are rare, accounting for less than 1% of the prevalence of essential hypertension, and their relationship to salt sensitivity in the general population is still unclear. Furthermore, individuals with these mutations were not formally assessed for the SSBP trait. [75]

More recently genome wide association studies (GWAS) have been used to identify single-nucleotide polymorphisms associated with SSBP. These have identified genes that influence BP variability but, to date, statistically significant associations have yet to be found and confirmed that meet genome-wide significance thresholds. [42,98] In summary, SSBP appears to be an inherited trait but our knowledge of genetic mechanisms for the general population remains incomplete.

1.2.2.5 Relevance of other ions

In addition to sodium, dietary chloride also appears to play an important role in the pathogenesis of primary hypertension. [99] The concentrations of sodium (135 – 145 mmol/l) and chloride (95 – 106 mmol/l) are predominant in the serum and are the main constituents of serum osmolarity. The chloride component of salt may determine the volume expansion leading to the rise in BP; neither of these findings is seen if sodium is given with another anion, such as citrate, or chloride with another cation such as ammonium. [100,101] The reasons for these observations are not clear, though most of our dietary salt intake comes in the form of sodium chloride. A growing body of evidence supports the relative importance of transmembrane Cl^- fluxes via chloride channels in the maintenance of cell volume, apoptosis, insulin secretion, neuronal excitability and propagation of atherosclerosis. [102,103]

Potassium intake is also known to be a factor in hypertension associated with salt intake, with previous evidence suggesting that dietary potassium modulates salt sensitivity. [104]. Possible mechanisms include potassium-induced effects on vascular tone and renal sodium retention. [31] Population studies have shown an inverse relationship between dietary potassium and blood pressure. [31] In addition to the adverse effects of low dietary potassium intake, the ratio of dietary sodium–to-potassium intake based on urine sodium-to-potassium ratio can also independently influence blood pressure. [105] A higher sodium-to-potassium intake ratio is also associated with an increase in overall cardiovascular mortality. [106] The

mechanisms for these observations are unclear and could be related to the influence of dietary potassium on renal sodium reabsorption. [105]

1.2.3 Novel paradigms

1.2.3.1 Rethinking the mechanisms for salt sensitivity

In the classical model a defect in renal sodium excretion is the basis for salt sensitivity, and humans who are salt-resistant are protected from salt-induced BP rises because they can rapidly excrete a salt load without retaining sodium. [107] Several studies in animals and humans oppose this view. Short term salt loading studies have shown that the amount of body sodium retained by healthy salt-resistant rats and humans is comparable, or in fact higher, than those who are salt-sensitive normotensives of hypertensives (Figure 1.3). [108-115] In salt loading experiments in lasting 4 weeks, Titze et al showed that salt resistant rats accumulated greater levels of total body sodium than salt sensitive rats, without showing the same rise in BP [116] In a short-term salt loading experiment in healthy normotensive humans in a metabolic ward, Heer et al observed the retention of very large amounts of body sodium (1704 ± 309.8 mmol) without a significant increase in BP. [117] Thus, salt resistant individuals undergo sodium retention without a BP rise during acute salt loading. These observations oppose the view that salt-sensitivity is simply due to a deficit in renal excretion of excess sodium.

Figure 1.3: Results of salt loading studies in normotensive African-Americans. Schmidlin et al measured cumulative sodium retention and mean arterial pressure before and after increasing dietary sodium intake from 30 mmol to 250 mmol per day. Salt-resistant and salt-sensitive subjects have comparable degrees of sodium accumulation despite having different haemodynamic responses. (Taken from Schmidlin et al. [111])

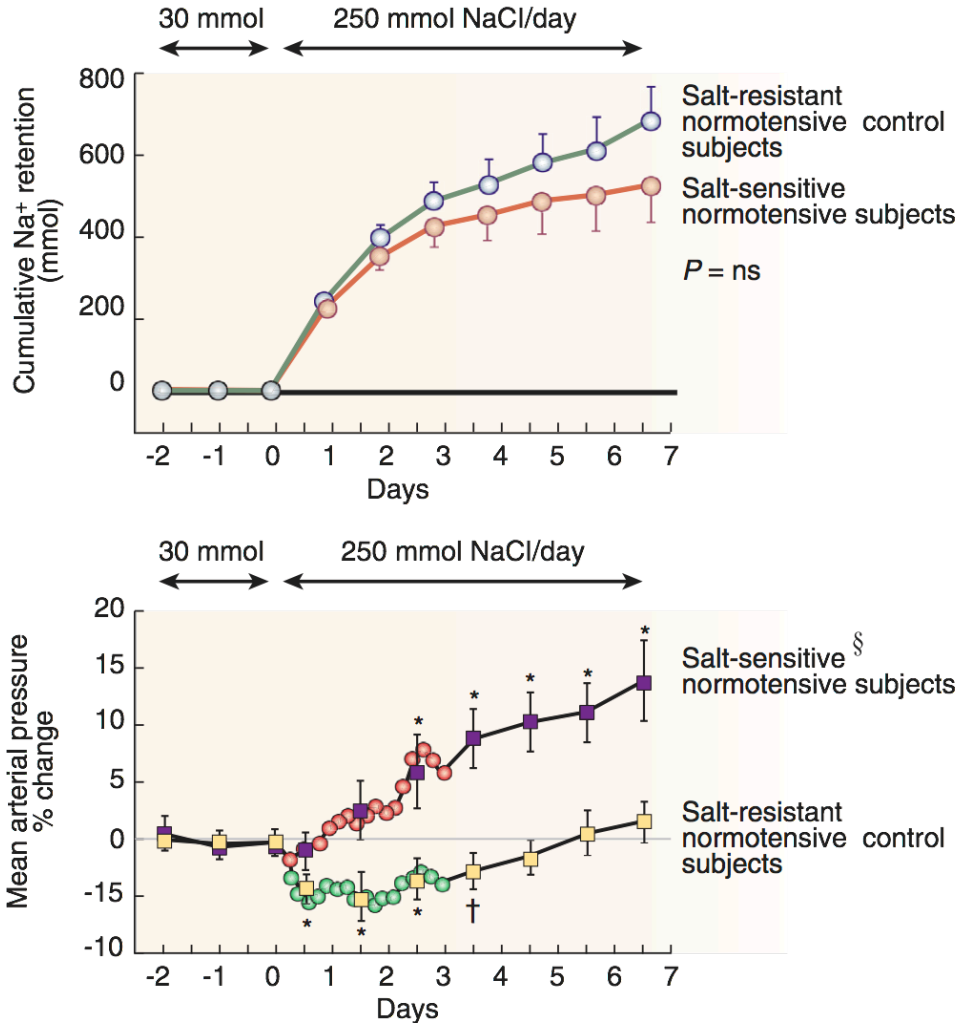

Contrary to the traditionally held view, salt-resistant subjects experienced substantial increases in blood volume with short-term salt loading (days to weeks). [110,111,117,118] In healthy normotensive subjects acute salt loading results in increases in blood volume, stroke volume and cardiac output that is comparable to salt-sensitive subjects, even though salt resistant subjects do not have an increase in blood pressure. [110,111,119-121] Studies in heathy and hypertensive humans revealed that salt-resistant subjects compensate for the increase in cardiac output during salt loading via concomitant vasodilation and decrease in peripheral

vascular resistance (PVR) [111,118,121,122] The mechanisms for this are unclear.

These findings contradict the view that increasing salt intake in salt-resistant individuals does not increase BP because they are able to rapidly excrete excess sodium and avoid expansion of blood volume. Instead, salt-resistance may be explained by the ability to respond to a salt load with compensatory vasodilation.[75] This raises questions regarding pathophysiology of salt sensitivity the possibility of alternative mechanisms that underlie the normal response to salt intake.

1.2.3.2 A `three-compartment model' of body sodium

As described in 1.2.2.1, in the classical paradigm an increase in salt intake leads to increased sodium accumulation in the extracellular space with a corresponding increase in extracellular volume. However, more long term studies looking at sodium balance in humans have shown that large amounts of sodium can accumulate without being paralleled by commensurate water retention, termed non-osmotic water retention. [117,123-125] Under close monitoring, the excretion of sodium via urine, stool and sweat did not match the amount of sodium ingested. [117,123] Recently the Mars 500 study, a long-term study that simulated a space flight to Mars in healthy males, investigated sodium metabolism at constant salt intake under controlled conditions for 105 and 250 days. [125] This study showed that sodium is rhythmically stored and released completely independent from salt intake. At a constant salt intake, a circaseptan variability in sodium excretion was observed. There was considerable variability in day-to-day 24-hr sodium excretion with fluctuations in aldosterone, cortisol, and cortisone with a periodicity of 1 week. It was observed that BP, body weight and extracellular water were not coupled to urine sodium excretion as expected, and the rhythmical accumulation and release of total body sodium was independent of salt intake (Fig 1.4). [125] The underlying mechanisms are still unclear.

Figure 1.4: Observations from the Mars 105 and 250 long-term studies in sodium metabolism. (A) Changes in systolic blood pressure (SBP) and urinary aldosterone, cortisol, cortisone, and cortisol/cortisone excretion at varying levels of sodium intake. (B)In the longer study, subjects were re-exposed to a high salt intake of 12 g per day salt for consecutive weeks after being on 6 g per day. SBP increased. Body weight increased initially before during the transition but then returned to baseline. Extracellular water (measured using impedance) increased and then decreased. Aldosterone excretion had an expected sustained decrease while total body sodium seemed had no relation to the other parameters. Taken from Rakova et al. [125]

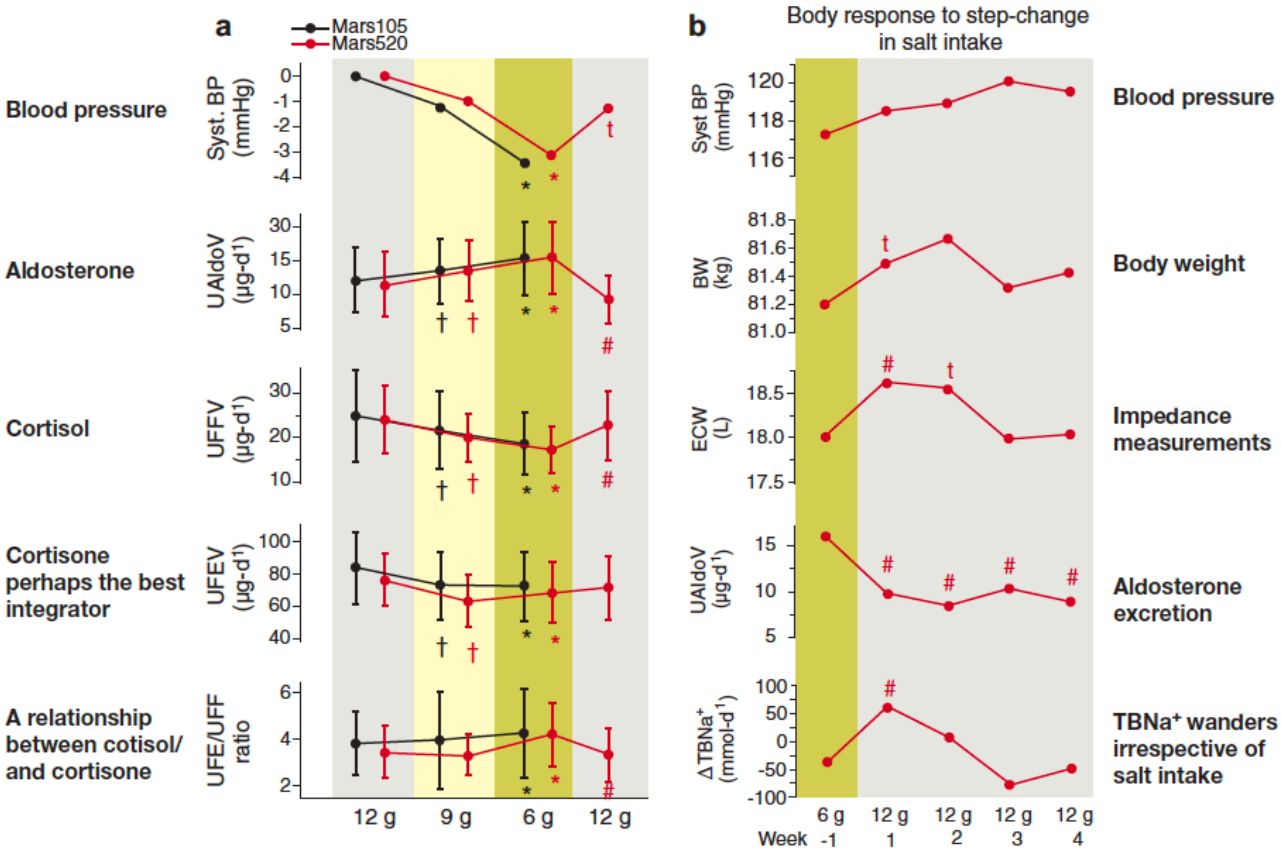

These observations supporting the existence non-osmotic storage of excess sodium (sodium accumulation without commensurate water retention) in an additional third compartment. Several lines of evidence suggest this additional compartment is the interstitium. In cartilage, chondrocytes are known to be subjected to relatively higher sodium concentrations of 250 - 350 mmol/l, which is much higher than the mean serum sodium

concentration of 140 mmol/l, suggesting that extracellular sodium concentration is not uniform and may reach high levels in the interstitium. [126,127] Edelman et al observed the penetration of $^{22}Na^{+}$ and $^{24}Na^{+}$ radioisotopes and deuterium into human tissues, showed that tissues such as bone, cartilage and connective tissue account for 50% of the total body sodium content. [128] This would suggest that the interstitium can accumulate excess sodium in the face of positive sodium balance without equilibrating with extracellular fluid or plasma.

In 1909, Wahlgren measured the chloride content of skin, intestine, liver, muscle, lungs, skeletal bone, brain and blood in salt-loaded dogs. He observed that one-third of total body chloride was stored in the skin but could not measure sodium. [129] This led Cannon to suggest, in 1929, that the skin and connective tissues could serve as a reservoir for sodium chloride during times of dietary excess. [61] Subsequent salt loading experiments in rats have supported this view, showing skin sodium concentrations can rise to 180 - 190 mmol/l without the expected rise in skin water content, indicating water-free sodium retention and hypertonicity. [130] These studies revealed that glycosaminoglycan polymerisation enables osmotically inactive sodium storage in the skin, serving as an important mechanism for buffering volume and blood pressure changes with salt intake. [130-134] Titze et al found that osmotically inactive sodium storage in salt resistant rats was three-fold higher than in salt sensitive rats, as determined by the relationship between body sodium and body water. [116]They concluded that salt sensitivity is associated with a reduced capacity for osmotically-inactive sodium storage and that such sodium storage serves as an important mechanism for buffering volume and blood pressure changes with salt intake.

In summary, this novel evidence opposes the traditional views that salt intake leads to a corresponding expansion in extracellular volume, extracellular sodium is tightly regulated and that intravascular and interstitial sodium are a state of equilibrium. It can be seen that the interstitium, particularly the skin, functions as a reservoir for sodium and constitutes a local hypertonic environment which is not readily equilibrated with plasma. Sodium accumulation in the interstitial space may have implications for salt sensitivity.

1.2.3.3 The role of glycosaminoglycans in sodium homeostasis

The interstitium consists of a framework of fibres of which collagen is predominant, a gel phase of glycosaminoglycans and a solution of electrolytes and proteins. The relative composition of these constituents varies considerably between tissues. [135] Glycosaminoglycans (GAGs) are unbranched polyanionic polysaccharide chains of variable length consisting of repeating disaccharide units. [136,137] There are five types identified: hyaluronan, chondroitin sulphate, dermatan sulphate, heparan sulphate and keratan sulphate. With the exception of hyaluronan, all GAGs are covalently bound to core protein backbones, forming proteoglycans (Fig 1.5). [138] GAGs are highly negatively charged at physiological pH because of their carboxyl and sulphate groups. [139] The cation binding capacity of GAGs is mainly dependent on the degree of sulfatation and the resulting osmotic pressure contributes to the hydration of the interstitium. [135,140] GAGs may also play an important role in enabling osmotically inactive skin Na^+ in the interstitium and sodium homeostasis.

Farber was the first to propose sodium binds to GAGs , describing how chondroitin sulphate binds to sodium in bovine nasal cartilage and functions as a sodium exchange resin. [141] Ivanova et al first described this process occurring in the skin, observing an increase in skin Na^+ and sulphated GAGs in salt loaded albino Wister rats. [131] More recently, Titze et al found that skin Na^+ concentration in rat skin increased from 152mmol/l to 180 mmol/l with 8 weeks of salt loading, with parallel increase in GAG content. [130] Conversely, they found that a low salt diet resulted in lower skin Na^+ and sulphated GAG content and subsequent release of skin Na^+. [142] Dietary salt intake is therefore directly linked to polymerization and sulfatation of glycosaminoglycans in the interstitium, providing an additional storage capacity for sodium. Recently, Fischereder et al showed that skin GAGs content correlated with Na^+ concentration in renal transplant donors and recipients, suggesting that skin Na^+ storage is regulated by GAGs in humans. [143]

There are several limitations of the above studies. They quantified GAGs using gene expression of enzymes involved in GAG chain elongation such as chondroitin synthase and xylosyltransferase, due to the technical challenges of analysing GAGs. [130,142,143] It is believed

that sodium is bound to GAGs without being osmotically active through their high negative charge density, but this remains to be proven. [130] The exact nature of GAG-Na^+ interactions are unclear - this is believed to be electrostatic such that and GAGs and Na^+ are in a state of incomplete ionisation. [141,144] Nevertheless, GAGs appear to mediate an important mechanism for sodium storage and release in accordance with physiological needs.

Figure 1.5: An illustration of proteoglycans and glycosaminoglycans. Proteoglycans are the major structural components of the interstitium and they consist of multiple glycosaminoglycans (GAGs) attached to a linking protein. GAGs have fixed negative charges in the form of carboxyl (COO−) and sulfate (SO3−) groups. The polyanionic nature of the GAG network forms the basis for electrostatic interactions with sodium ions. Taken from Nijst et al. [145]

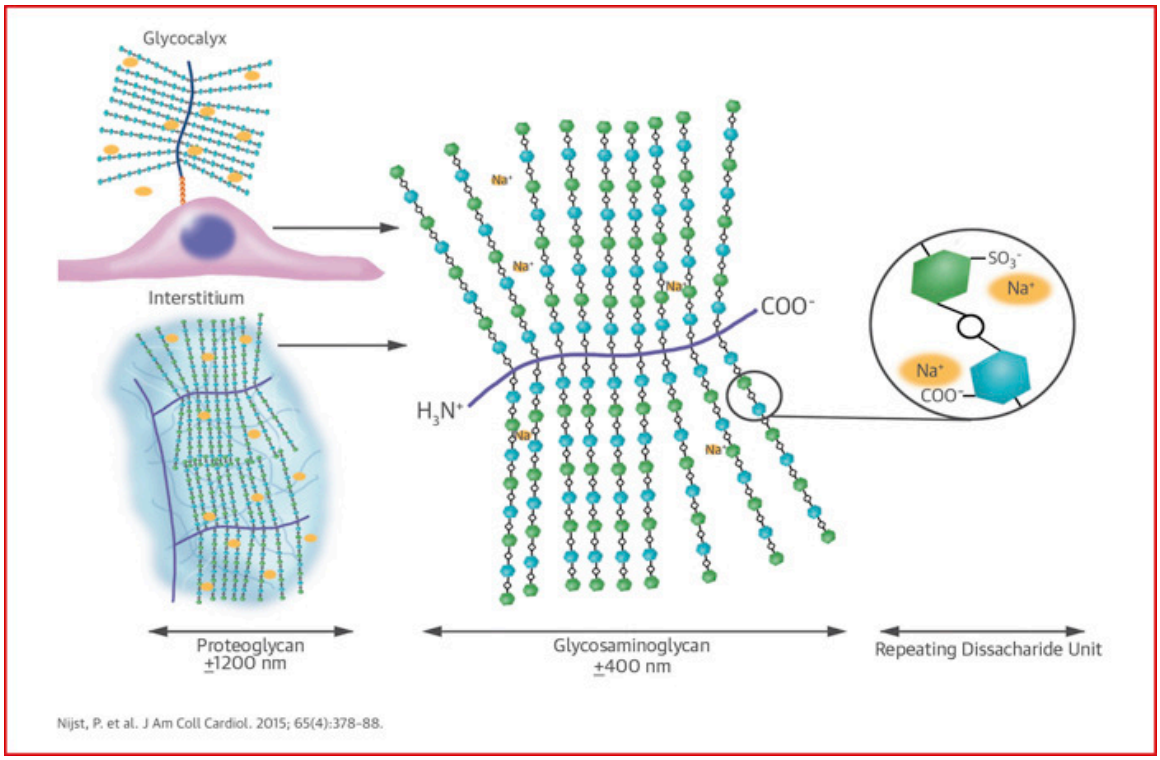

1.2.3.4 Tissue macrophages influence sodium balance, interstitial volume and blood pressure

In recent years it has become apparent that cells of the innate and adaptive immune system play a role in hypertension and cardiovascular disease. [146] Macrophages, together with dendritic cells, monocytes and bone marrow precursor cells form the mononuclear phagocytotic system and are present in every peripheral tissue of the body. [147] Macrophages serve diverse and essential functions in development, homeostasis, tissue repair and immunity. [148] Macrophages appear to recognize NaCl-induced hypertonicity as a chemotactic stimulus and migrate in the direction of high salt concentration. [149] Macrophage transcriptional and translational expression profiles are influenced transcriptional by ambient NaCl concentrations. [150,151]

Recently, further work in rat skin by Jen Titze's group showed that macrophages mediate an additional adaptive mechanism that functions during periods of high salt intake (Figure 1.6). [133,134] In their rat model high salt intake increased skin Na^+ concentration and the resultant hypertonicity caused recruitment of macrophages, which activated tonicity-responsive enhancer binding protein (TonEBP). TonEBP binds to the vascular endothelial growth factor C (VEGF-C) gene and increases its expression. By mediating VEGF-C, the macrophage response restructured the interstitial lymphatic network which enabled drainage of water and electrolytes into the systemic circulation. VEGF-C also and induced expression of endothelial nitric oxide synthase (eNOS) which causes vasodilation via nitric oxide (NO) production. These processes appeared to buffer the haemodynamic response to salt loading. [133] VEGF-C inhibition using soluble VEGFR3 and macrophage-inhibition using clodronate liposomes resulted increased in skin electrolyte and water content, decreased eNOS expression and elevated MAP in response to a high salt diet. [133] More recent work in mice has also confirmed that antagonism of VEGF-C and TonEBP via genetic deletion results a greater rise in MAP with salt loading, correlating with the rise in Cl^- but not Na^+ [152]. This may suggest a central role for Cl^- in salt-sensitive hypertension that has yet to be elucidated.

Figure 1.6: A novel extra-renal mechanism for buffering dietary salt. Under normal conditions Na^+ binds to negatively charged GAGs in the dermal interstitium, without commensurate water, allowing high concentrations of Na^+ to accumulate in the skin. During salt loading, the Na^+ binding capacity of GAGs is exceeded and interstitial hypertonicity develops, leading to an influx of macrophages, which release an osmosensitive transcription factor (TonEBP). This induces the secretion of VEGF-C in an autocrine manner, leading to lymphangiogenesis. The enhanced lymphatic network increases Na^+ transport back into the circulation, for eventual removal by the kidneys, preventing a blood pressure rise with salt loading (Image Adapted from Marvar et al courtesy of Gökçen Ackali)[153].

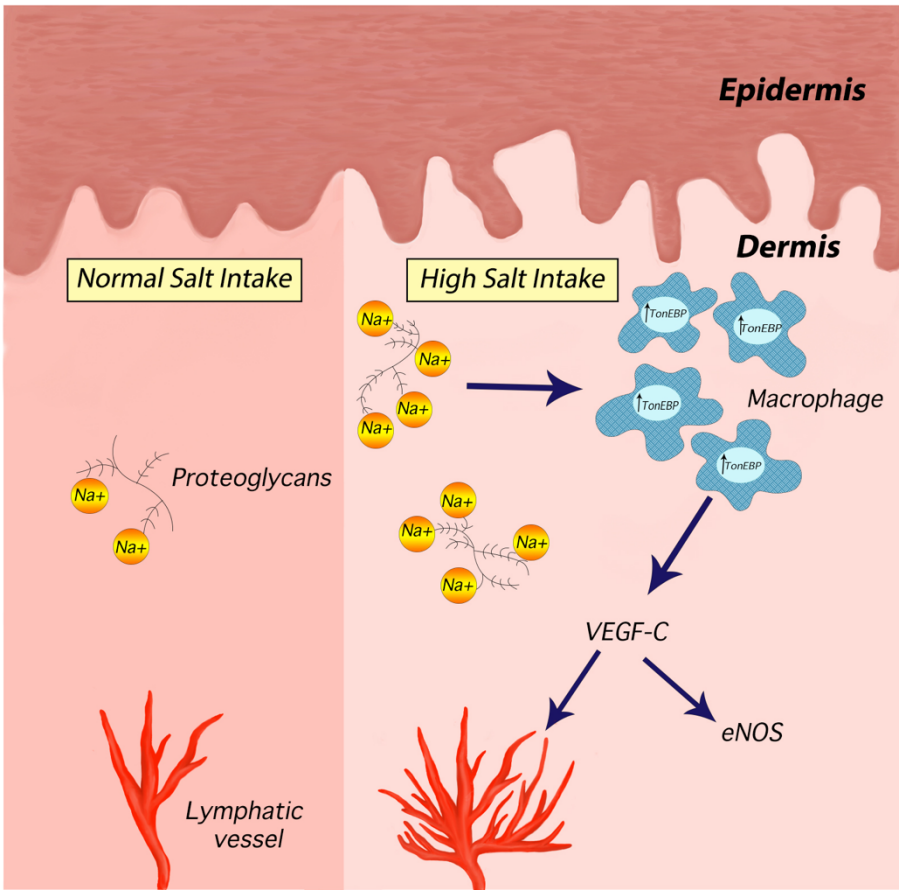

In summary, macrophages exert a homeostatic function in the skin via TonEBP and VEGF-C, regulating clearance of osmotically inactive stored salt via cutaneous lymphatic vessels. The interstitium, including the lymphatics, acts as a third separate and locally regulated compartment. This appears to constitute an extra-renal mechanism controlling blood pressure during high salt intake, mediating a vasodilatory response. Incorporating this model into the traditional paradigm of sodium homeostasis, the skin may act as a buffer as well as a reservoir for sodium, while the kidney controls sodium excretion and reabsorption,

controlling serum osmolality and total body water. It is conceivable that people predisposed to salt-sensitive hypertension have defects in the pathway described above and these individuals are less effective at buffering the increase in volume resulting from salt intake, resulting in a rise in BP. Future challenges include ascertaining how different antihypertensive agents affect the distribution of sodium and water between the subcutaneous lymphatic system and the intravascular space and how this system interacts with other organs that modulate BP like the kidney and brain.

1.2.3.4.1 VEGF-C and its role in BP control

Vascular endothelial growth factor (VEGF) was initially discovered as a tumour-derived soluble factor that induces endothelial cell permeability and angiogenesis. [154] Seven members of the VEGF family have been identified so far (Figure 1.7). The effects of VEGF are mediated by tyrosine kinase receptors: VEGFR-1, VEGFR-2, and VEGFR-3. VEGFR-2 is expressed on endothelial cells and activation by VEGF stimulates to release NO release by endothelial cells. VEGFR-3 is expressed on lymphatic vessels and mediates lymphangiogenesis in response to VEGF-C and VEGF-D[154,155] The activation of VEGFR-1 and VEGFR-2 receptors by VEGF C this may be relevant to sodium homeostasis and BP regulation, as discussed previously.

Figure 1.7: The different types of VEGF and VEGF-receptors in humans.

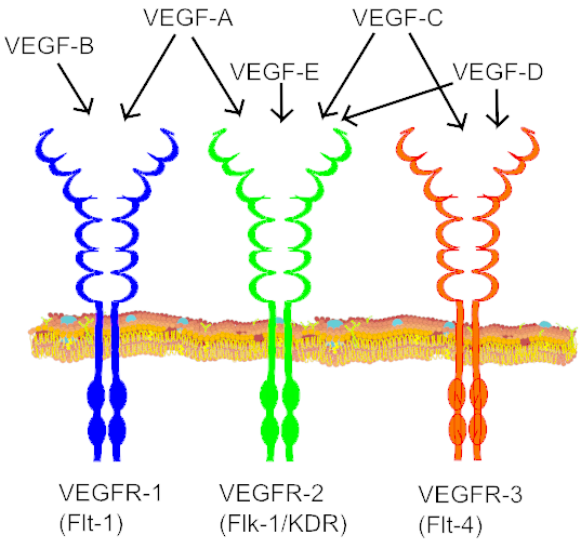

Evidence for a role for VEGF in BP control in humans comes from the use of VEGF inhibitors in the treatment of various malignancies. [156] Bevacizumab is a recombinant humanized monoclonal antibody that binds to circulating VEGF-A and prevents its association with endothelial receptors. [155] It was the first FDA-approved VEGF pathway inhibitor intended for systemic use in various cancer types, including breast, colorectal, renal, and lung cancer. Hypertension and proteinuria were described as side-effects in up to 36% of patients and this was attributed to endothelial dysfunction and podocyte dysregulation, via its interactions with VEGFR-2 receptors. [157] A recent study in rats using sunitinib, a multi-targeted tyrosine kinase receptor inhibitor which would affect VEGF-A and VEGF-C, showed that sunitinib caused a rise in BP that was exacerbated by a high salt diet. In this study macrophage infiltration and lymphangiogenesis was increased by high salt intake but the lymphangiogenesis was not significantly impaired by sunitinib, suggesting that salt sensitivity with this class of drug may involve other mechanisms. [158] Direct evidence for VEGF-C involvement in BP control is lacking. In a cross-over study in patients with chronic kidney disease (CKD) plasma VEGF-C was significantly higher following a high-salt diet (200 mmol Na^+ a day) for compared to a low salt (50 mmol a day), suggesting VEGF-C was induced by high salt intake. [159]This was not observed in healthy volunteers. [159] Further studies are required to substantiate the clinical and therapeutic relevance of VEGF-C in regulating sodium homeostasis and BP in humans.

1.2.4 Dietary sodium and arterial stiffness

Several lines of evidence suggest a relationship between arterial stiffness and salt intake. A previous observational study in two Chinese populations, showed the age-related rise in aortic PWV was blunted in the population with a lower salt intake. [160] Humans with salt-sensitivity have increased arterial stiffness compared with salt-resistant subjects with the same BP levels. [161] A recent meta-analysis of 11 randomized controlled trials of salt restriction and arterial stiffness showed that average reduction in sodium intake of 89.3 mmol/day was associated with a 2.84% (95% CI: 0.51–5.08) reduction in PWV. [162] These studies were done in hypertensives and normotensives using applanation tonometry, doppler transducer and pressure transducer techniques to measure PWV. [163-173] The length of dietary intervention ranged from 1 to 6 weeks. The improvement in PWV with dietary salt

reduction was independent of baseline BP and BP change between interventions. [162] The maximum benefit from salt intake restriction was seen expected for hypertensive patients on antihypertensive drug treatment. [163-173] in one study, the reduction in PWV was observed the greater in black compared with white and Asian hypertensive patients, with the three ethnic groups showing similar changes in BP. [168]

The pathomechanics of dietary sodium's influence on arterial stiffness is unclear. In addition to its effects on BP, sodium may directly affect arterial wall components. In hypertensive rats, high sodium intake leads to cardiac hypertrophy, fibrosis, hypertrophy of large arteries and enhanced extracellular matrix. [174] Et-taoil et al showed that high sodium intake and indapamide therapy decreased and increased aortic hyaluronan content respectively in a rat model. [175] They showed that the reduction in systemic arterial compliance with indapamide was associated with increased media thickness and reduced aortic hyaluronan content and these changes occurred under stable BP conditions. The hypothesised that the RAAS system controls hyaluronan synthesis and high salt intake suppresses renin. [176]

Pressure may also affect arterial wall sodium and GAG content. Hollander et al examined the effects of surgical coarctation in dogs on arterial wall Na^+, Cl^- and sulfated GAGs at constant sodium intake [177]. They found that in the aortic hypertensive segments created by coarctation, sodium and chloride concentrations were 18.2% and 25% higher than in control respectively. They noted that sulfated GAGs increased by 27 - 35% in the coarcted dogs. The authors concluded that the increase in pressure on the coarcted aortas induced an increase in sulfated GAG synthesis, and the rise in sodium content was a consequence. It is possible that a similar Na^+-GAGs relationship exists in the vascular interstitium and the skin.

Evidence from human studies show that moderate dietary sodium intake reduces arterial stiffness independent of BP. Considering arterial stiffness as a predictor of cardiovascular and all-cause mortality, this adds to the value of dietary salt reduction in the reducing cardiovascular disease. Animal experiment suggest possible relationship between dietary sodium, shear stress and arterial wall constitution, but the link between sodium intake and arterial stiffness remains unexplained.

1.3 SKIN ELECTROLYTES IN HUMANS

1.3.1 Skin structure and physiology

In humans, the skin is the largest organ in the body, constituting 6% of body weight and incorporating blood flow of up to 60% of cardiac output. [178] The skin incorporates all major support systems such as blood vessels, lymphatics muscle and nerves. The skin consists of 2 tissue layers: the epidermis, the external layer consisting of non-stratified epithelial cells and the dermis, which consists mainly of connective tissue (See Figure 1.7). [178] The epidermis is approximately 50–200 µm thick and acts as a physical barrier against micro-organisms and water loss. [179] The dermis is a tough, flexible and very elastic layer between 1.5 and 3 mm thick, arranged into two sub-layers: the papillary dermis and the reticular dermis. Despite its greater volume, the dermis is relatively acellular compared with the epidermis and consists of fibroblasts, blood vessels, lymphatics and nerves interspersed in an extracellular matrix. Most of the functionality in the dermis is dependent on its extracellular matrix, which is composed of macromolecules such as collagen, elastin and proteoglycans, the most abundant being dermatan sulphate. [178,180]

Figure 1.7: Skin structure with relative thickness of epidermis and dermis. Proteoglycans are most abundant in the dermis, suggesting this is where non-osmotic sodium storage is likely to occur. [179]

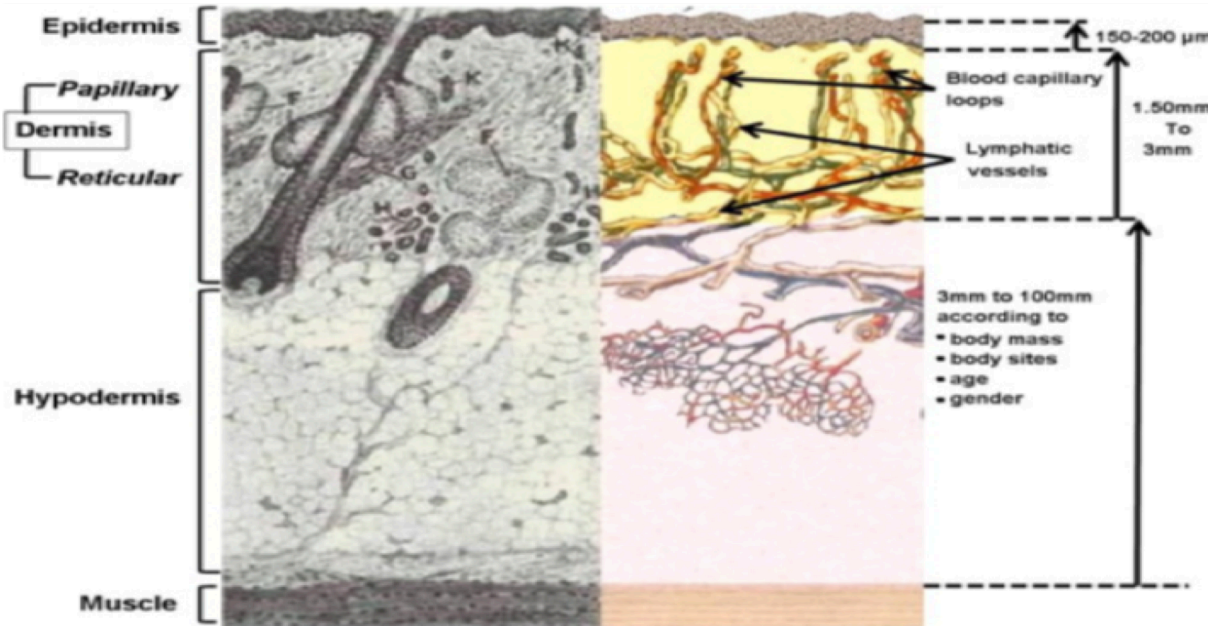

1.3.2 The skin as a depot for NaCl in humans

Studies in rodents suggests the skin functions as a reservoir for sodium and a buffer for dietary salt. [116,130,131] A review of the literature shows a paucity of information on skin sodium concentrations in humans, with most studies done between 50 - 90 years ago. [181-188]Most of these studies included skin K^+ analysis. Skin Cl^- measurement may have started earlier and relied on different quantification techniques. [129,189] Table 1.2 summarises 10 studies that measured skin Na^+ and K^+ and their methods. In table 1.2 elemental concentrations measured in fresh tissue is expressed wet weight Na^+ and K^+ and concentrations measured in dried tissue is termed dry weight Na^+ and K^+. The exact relevance of skin electrolytes was not understood but the skin was considered as depot for sodium, chloride and water. [186,190,191]

As shown in table 1.2, these showed a wide range of values for skin Na^+ and K^+. Several factors could account for this. Essential elements are often distributed heterogeneously in solid biological tissue structures and their quantification would depend on the sensitivity of the technique used and potential contamination. [192] Skin $Na^+$and K^+ were measured using precipitation techniques, which would have had variable sensitivity, until flame photometry was available in the 1940s. [193] A number of studies used skin samples taken post-mortem, which could have had elemental shifts secondary to tissue autolysis[181,182,186,194,195] 6 studies analysed full-thickness skin biopsies. [143,181-184,186,195] It can be seen that analysis of epidermis tissue alone yielded higher potassium values, suggesting an anatomical variation in skin potassium distribution. [185,187,188]In 1928 Urbach conducted salt loading experiments in a small number of humans, which involved the administration of oral NaCl 10g daily over a period of 1 week. [183,190] He observed the sodium chloride content of human skin increased by 15 – 20%. This finding and earlier work by Wahlgren in dogs lead him to conclude that the skin was a repository for sodium chloride in 1928. [129,190]No similar studies on humans have been published since.

More recently 2 studies analysed human skin Na^+ using modern techniques. Kopp et al used human cadaveric lower limb specimens with atomic spectrometry after ashing the specimens. They obtained sodium concentrations of significant variability. [195] However, they did not perform skin biopsies on live patients. Very recently, Fischereder et al measured skin Na^+ in renal transplant donors and recipients under general anaesthetic, using inductively coupled plasma optical emission spectrometry. [143] They obtained skin Na^+ and K^+ with significant variability and did not publish their sample preparation methods.

The skin has long been considered a depot for sodium, chloride and water, although the influence of this on BP was not previously studied. [190,191]The literature on human skin Na^+ measured with direct chemical analysis has yielded a wide range of values with several limitations. None of the above studies looked at the relationship between skin Na^+ and blood pressure, sex or age. Based on current evidence a universally accepted normal range for skin electrolytes in lacking.

Table 1.2 - Previous studies assessing skin Na^+ and K^+ content. [143,181-184,186,195]

Study	Study Size	Source	Local anaesthetic	Analysis method	Na^+ (wet) mg/g	Na^+ (dry) mg/g	K^+ (wet) mg/g	K^+ (dry) mg/g	% Water
Brown 1926	10	Epidermis & dermis (Chest and waist) Cadavers	Nil	Precipitation with $BaCl_2$	-	3.60 ± 0.37	-	2.39 ± 0.51	
Brown 1927	27	Epidermis & dermis (Chest and waist) Cadavers	Nil	Precipitation with $BaCl_2$	1.58 ± 0.20	-	0.91 ± 0.24	-	63.5 ± 3.7
Urbach 1928	26	Epidermis & dermis (Various regions) Healthy volunteers	Nil	Precipitation with $BaCl_2$	0.95 – 1.39	-	-	-	
Cornbleet 1942	10	Epidermis & dermis (Various regions) Healthy volunteers	Nil	Calorimetric method (Yoshimatsu)	-	3.50 ± 0.02	-	2.47 ± 0.04	
Suntzeff 1945	18	Epidermis (Mastectomies & limb amputations)	Nil	Flame photometry	1.22 ± 0.02	-	3.22 ± 0.03	-	
Eisele 1945	18	Epidermis and dermis (Mastectomies & limb amputations	Nil	Butler-Tuthill method	2.14 ± 0.18	7.56 ± 1.03	0.64 ± 0.13	2.28 ± 0.50	70.8 ± 20.1
Zheutlin 1950	12	Epidermis (Mastectomies)	Nil	Flame photometry	1.06 ± 0.19	3.07 ± 0.58	3.15 ± 0.30	9.07 ± 1.13	65.1± 3.1
Hodgeson 1960	45	Epidermis (Various regions) Healthy volunteers	Procaine 0.5%	Flame photometry	2.00 ± 0.44	5.63 ± 1.34	1.37 ± 0.28	3.84 ± 0.84	
Hodgeson 1960	20	Epidermis (Various regions) Patients under GA	Nil	Flame photometry	1.83 ± 0.49	5.23 ± 1.33	2.07 ± 0.57	6.03 ± 2.07	
Kopp 2011	21	Epidermis & dermis (Limb amputations)	Nil	Atomic spectrometry	1.77 ± 0.37	-	-	-	
Fischereder 2017	21	Epidermis & dermis (Abdomen) Healthy kidney donors	Nil	ICP-OES	-	6.57 ± 4.03	-	1.76 ± 1.09	
Fischereder 2017	27	Epidermis & dermis (Abdomen) Dialysis patients	Nil	ICP-OES	-	7.05 ± 3.34	-	1.92 ± 0.98	

Values are mean ± SD

1.3.3 Sodium MRI of the skin

Traditional methods for estimating tissue sodium in humans are invasive and rely on tissue biopsies or administration of a radioactive or stable isotope. For over 30 years the use of ^{23}Na-MRI spectroscopy has enabled the non-invasive assessment of sodium concentrations in human tissue in vivo. [196] Recently ^{23}Na-MRI spectroscopy has been used in human skin. [195,197-204] Sodium (^{23}Na) possesses a quadrupolar nucleus with 3/2 spin, yielding the second strongest nuclear magnetic resonance signal after protons (^{1}H) in biological tissue [205]. ^{23}Na-MRI spectroscopy is able to simultaneously measure proton and sodium signal intensity, giving a measure of the ratio of sodium to water in vivo. This technique was first developed in the skin by Kopp et al, who used a 3 tesla magnetic resonance (MR) system to assess the sodium : water ratio in calf skin and muscle, which was quantified in mmol/l. [195].

Using ^{23}Na-MRI, several this group revealed several trends in skin and muscle sodium storage. In a study of 56 normotensives and 57 hypertensives, Kopp et al showed that skin and muscle sodium storage increased with age and was higher in men than women (Figure 1.8). [197] Skin Na^+ and water accumulation paralleled increased systolic blood pressure while the age-dependent increases in muscle Na^+ content in men was not associated with increase in water content, indicating water-free Na^+ storage(Figure 1.8). [197] When skin and muscle content was controlled for age, patients with refractory hypertension had increased tissue Na^+ content compared with controls, suggesting a link between tissue Na^+ and essential hypertension. [195] A subsequent study in 38 subjects again showed higher skin Na+ in men than women, which remained statistically significant after correcting for age and BMI. [203]

Figure 1.8: Trends in skin and muscle Na^+ and water and determined with ^{23}Na MRI. Na^+ and water content in relation to age. A: Muscle Na^+ detected by ^{23}Na-MRI in women (n=44) and men (n=69) with or without the diagnosis of hypertension. An additional analysis of muscle water content was performed in 25 women and 35 men in this study group. B:^{23}Na-MRI analysis of skin Na^+ and ^{1}H-MRI measurements of skin water in the same women and men.

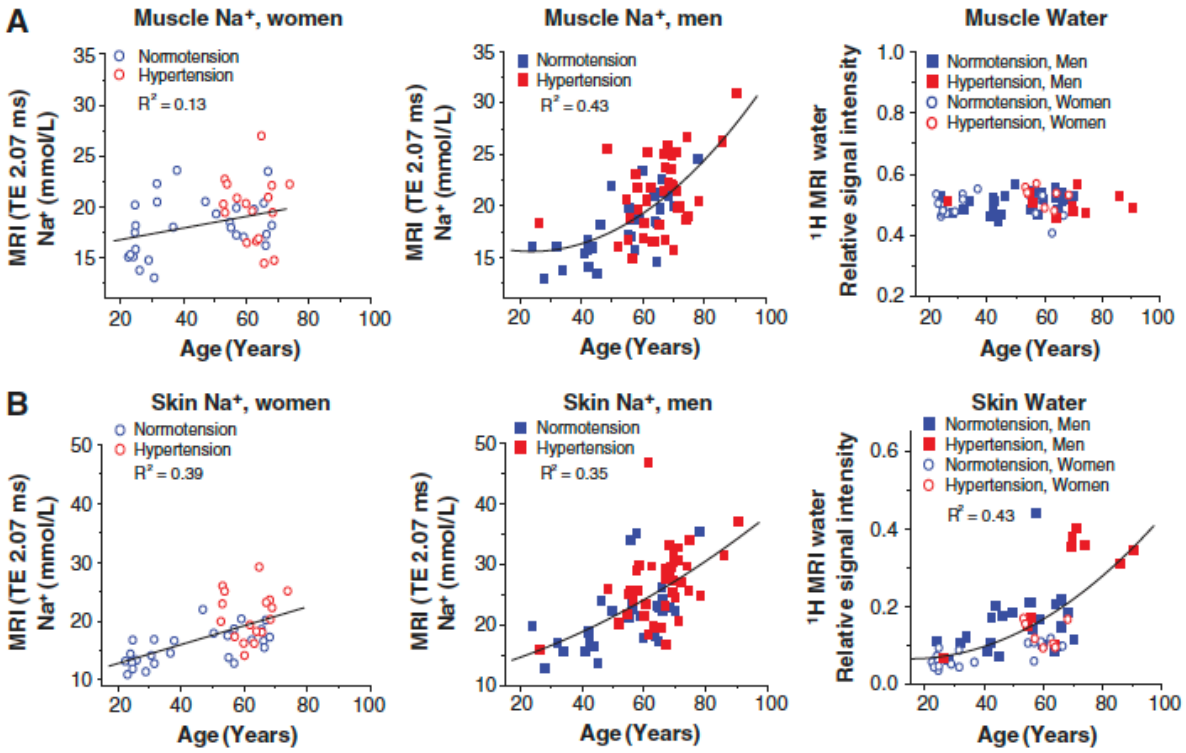

^{23}Na-MRI in haemodialysis patients showed that a dialysis session reduced skin Na^+ by 19% and patients with higher serum VEGF-C levels showed better dialytic Na^+ removal. [198] In their 27 healthy controls there was an age-related rise in skin Na^+ which corresponded with a decline in serum VEGF-C. The authors concluded that skin Na^+ stores can be mobilised by haemodialysis and VEGF-C facilitates Na^+ flow between the interstitium and systemic circulation in humans, supporting earlier work in rodents. [133,198] In a small study of 9 heart failure patients, diuretic treatment with frusemide was observed to reduce skin Na by 34%, suggesting that diuretic treatment can mobilize skin Na^+ stores. Recently, Schneider et al showed that skin sodium content positively correlated with systolic BP and was an strong, independent predictor of left ventricular mass (LVM) in patients with mild chronic kidney

disease (Figure 1.9). [204] The relationship between left ventricular mass skin Na^+ was unaffected by BP, leading the authors to conclude that sodium had BP-independent effects on the myocardium and skin Na^+ could reflect Na^+ accumulation in the myocardium, which could have detrimental effects. [204]

Figure 1.9: Relationship between skin Na and left ventricular mass. LVM was measured with 1.5 tesla MRI in 89 participants with mild renal impairment (mean eGFR 51 ml/min per 1.73 m^2. This was independent of sex, height, SBP and body hydration as measured by bioimpedence. [204]

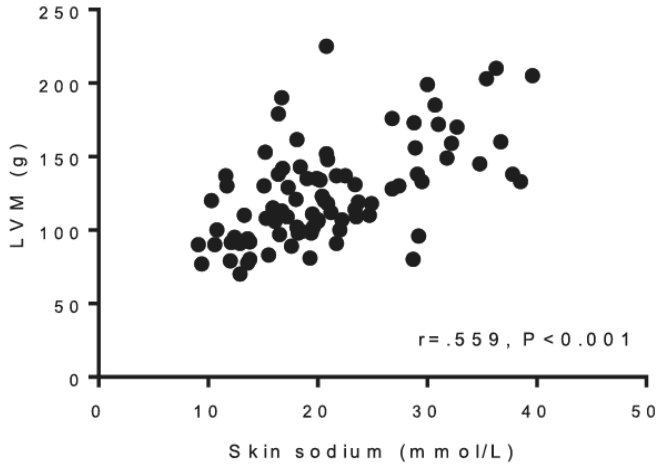

^{23}Na-MRI has revealed relationships between skin Na^+ and age, sex, BP and LVM, making it a potential biomarker for cardiovascular disease. [204] There are several limitations this technique for quantifying skin Na^+ using this method. MRI sensitivity for sodium is 9.2% of the sensitivity to protons and therefore the signal to noise ratio is much higher for sodium. [205] Variability in Na^+ signal intensity may be seen between in different tissues and discordance may occur between MRI Na^+ measurements and direct chemical measurements. [205-207] Thus, ^{23}Na MRI is unlikely to provide an exact quantification of tissue sodium and values need to be interpreted with caution. It is unclear whether Na^+ bound to GAGs and ionised Na^+, as well as intracellular and extracellular sodium are detected differently by ^{23}Na MRI. This could lead to a discordance between direct chemical measurements and ^{23}Na MRI measurements. In summary despite its limitations ^{23}Na MRI has provided important insights into the relevance of skin Na^+ in humans.

1.3.4 Dermal sodium distribution

There is a paucity of data describing electrolyte distributions in the skin. Microstructural analysis of sodium distribution in rodents has shown that sodium is concentrated under the keratinocyte layer. [208] Electron probe analysis and more recently, 7-tesla ^{23}Na-MRI have revealed a similar accumulation of sodium, below the epidermis, in the papillary dermis. [199,209] Mechanisms proposed for this 'band' of high sodium concentration in the skin include active sodium transport, combined with cutaneous blood capillary loops, creating a functional kidney-like countercurrent system for concentration of sodium chloride under the skin. [208] Two functions of this apparent dermal sodium barrier have been proposed. It is possible that it acts as physiological fluid barrier with high osmolality inside or directly under the epidermis. [208,209] Jantsch et al showed that skin Na^+ accumulation occurs during cutaneous bacterial infections and endogenously boosts antimicrobial capacity in humans and in mice. [210] This suggests that the dermal sodium functions as an antimicrobial barrier. Further work is needed to explain the exact mechanisms that generate and maintain this apparent pattern of sodium distribution skin, as well as the distribution of other elements such as chloride.

1.4 DERMAL CONTROL OF BP IN HUMANS

The focus of hypertension research has traditionally been the kidney, brain, heart and blood vessels. Emerging evidence In humans suggests that the skin modulates BP via regulation of cutaneous blood flow and salt metabolism. [211] Blood flow in the skin is dynamic and mediates thermoregulation, ranging from as low as 1% rising from to as high as 60-70% in erythroderma and heat stress. [211,212] Mechanisms such as sympathetic neural control of skin blood flow are believed control cutaneous vasodilation that occurs with heat stress. [212] The skin is a rich source of nitric oxide, containing ten times the levels in the circulation. [213] On this background several new mechanisms linking the skin to BP have been recently identified.

Ultraviolet A irradiation of the skin has been observed to induce NO release, reducing systemic BP. [214,215] Human skin contains photo-labile NO derivatives like nitrite and *S*-nitroso thiols, which after UVA irradiation, decompose and lead to the formation of vasoactive NO. [214] This process of photo-relaxation, as described by Furchgott, may account for the latitudinal and seasonal variations of BP and CVD. [211]

The hypoxia inducible factor (HIF) transcription system, acting via the heterodimeric transcription factors HIF-1α and HIF-2α, plays a central role in the cellular response to hypoxia. [216] Recent evidence suggests that the HIF-1α: HIF-2α ratio in the skin affects MAP in via regulation of nitric oxide synthase 2(NOS 2), a key regulator of vascular tone. [217] HIF-1α and HIF-2a act antagonistically - HIF-1a promotes nitric oxide production by keratinocytes via NOS 2 while HIF-2α promotes keratinocyte arginase expression and urea production. [218] HIF-1α also up-regulates VEGF A, which influences NO via VEGFR2 receptors, influencing vascular tone. [219,220] Cowburn et al recently showed that mice with keratinocyte HIF-1α deletion had increased vascular tone and elevated systemic BP. Conversely, deletion of HIF-2α activity in keratinocytes resulted in increased skin NO levels and reduced systemic BP. [217] In accordance with this, they showed decreased epidermal expression of HIF-1α and increased epidermal HIF-2α expression in hypertensive humans correlated significantly with increased mean blood pressure. These findings provide a novel mechanism for systemic BP regulation by the skin. Recent evidence suggest that HIF metabolism may also be influenced

by dietary salt. In the renal medulla dietary salt suppresses HIF prolyl-hydroxylase 2 (PHD2), which degrades HIF-1α and HIF-2α,increasing natriuresis[221,222] It would be plausible that if a similar mechanism exists in the skin, high salt intake could alter levels of HIF isomers, potentially influencing PVR. [217] This would need to be explored in further work.

As described in in 1.2.3.1 - 1.3.3, the skin appears to buffer dietary salt and rodent models, dermal Na^+ accumulation in response to acute salt loading protects against a BP rise. The role of GAGs and macrophages in this process are described in 1.2.3.3 and 1.2.3.4 respectively. Cross sectional data in humans show that long-term, higher skin sodium storage is associated with higher BP. The mechanisms for this association are yet unknown and may explain BP differences between the sexes and the increase in BP with age.

Capillary rarefaction is the reduction in the density of capillaries and has been observed in the skin of hypertensives using video microscopy. [11,223-227] Capillary rarefaction is believed to be structural in origin, associated with either impaired angiogenesis or capillary attrition, or functional, associated with impaired recruitment of non-perfused capillaries. [224] The mechanisms by which capillary rarefaction is thought to lead to hypertension is subject to debate. Capillaries do not have vascular smooth muscle and cannot increase resistance to blood flow by vasoconstriction. It has been suggested that capillaries can contribute to peripheral vascular resistance by virtue of their narrow calibre or reduction in the number, leading to an increase in resistance in the remaining capillaries. [223,224,228] Prasad et al showed a negative correlation between capillary density in the forearm and SBP in patients with essential hypertension. [223] He et al showed that in hypertensive humans a modest reduction in salt intake improves dermal capillary density as assessed by capillaroscopy. [11] This trend was seen across different racial groups and suggests that salt intake is linked to microvascular rarefaction. Mechanisms whereby salt affects the microcirculation remain unclear. A reduction in capillary reserve may have deleterious effects on organs affected by hypertension such as the brain and heart, though there is a paucity of data linking microvascular rarefaction to clinical outcomes. Recently, in the Maastricht study skin capillary density independently associated with albuminuria, suggesting a role for capillary rarefaction in albuminuria and microvascular damage.

Thus, the evidence for BP regulation in the skin is growing with the promise of novel pathways and cutaneous therapeutic targets.

1.5 SEX DIFFERENCES IN RESPONSE TO DIETARY SALT

Studies in animals and humans have consistently shown sex differences in hypertension, with females having lower blood pressure than males across a variety of species and animal models. [229-231] Studies on the impact of biological sex on the haemodynamic effects of dietary salt are sparse and controversial. [45] Kojima et al reported in a dietary salt modulation study of 174 Japanese essential hypertensives that women were sensitive while men were not. [232] Overlack et al reported greater SSBP in women in dietary salt modulation study of 163 white, non-obese normotensive subjects. [44] In the GenSalt study in 1906 Chinese, women exhibited larger changes in blood pressure than men in response to changes from low-to-high or high-to-low salt intake. [58] It should be noted only the GenSalt study controlled dietary salt intake with respect to body weight, which is a potential confounder in sex-comparisons [58] In a study by Weinberger et al in 374 normotensive, where SSBP was determined differently (salt loading with an infusion of 2 L of normal saline over 4 hours and salt depletion with a low sodium (10 mmol) diet and frusemide), sex differences in SSBP were not observed. [50] In contrast, in rodent studies of salt sensitivity, male Dahl salt sensitive rats had a higher BP and more than female Dahl salt sensitive rats in response to a high sodium diet, suggesting that the males were more salt sensitive than females. [233] This was attributed to testosterone-dependent hypertension and upregulation of intrarenal angiotensinogen in males.

Several putative factors have been proposed to contribute SSBP in females. SSBP tends to me more marked in post-menopausal women, but it is not known if this observation may be attributable to ageing or differences in sex hormones. Shulman et al showed an increase in SSBP in the absence of a BP rise in 40 normotensive women following surgical hysterectomy, supporting the latter. [234]A relationship between ovarian hormones and SSBP via differential effects on renal sodium absorption has been suggested. In a study by Pechere-Bertschi et al

in 35 healthy normotensive women not on the oral contraceptive pill, dietary salt moderation had similar effects on blood pressure during the luteal and follicular phases of the menstrual cycle. [235] This occurred despite renal blood flow being significantly greater during the luteal phase. In a further study by this group, the effects of modern low dose oestrogen and progesterone-only contraceptive treatment was studied in 27 normotensive women. The use of oral contraceptives but not associated with an increase in SSBP in response to dietary salt modulation. [236]

In summary sex differences in SSBP have been suggested but further studies are needed to confirm this and explain the underlying pathomechanics. Differences in skin sodium storage as determined by ^{23}Na-MRI spectroscopy may allude to extra-renal mechanisms that could explain sex differences in salt sensitivity.

1.6 SUMMARY

The relationship between dietary sodium and BP and the underlying mechanisms explaining the heterogeneity in response to salt intake are poorly understood. In the last 15 years we have witnessed a renaissance in our understanding of sodium physiology and how humans handle dietary sodium, with a paradigm shift away from the traditional nephrocentric view that pressure natriuresis exclusively determines salt sensitivity. Emerging novel data on the storage of sodium in the interstitium and the study of possible differences in such storage between SS and SR individuals has highlighted the relevance of interstitial electrolytes and the roles played by GAGs, the lymphatics and cells of the mononuclear phagocytotic system. Sodium distribution the skin may facilitate water conservation and cutaneous antimicrobial defence. The use of magnetic resonance imaging techniques to measure such interstitial sodium storage has led to an appreciation of trends and differences in interstitial sodium storage in humans and may also lead to the development of a radiological marker for the SSBP phenotype. The skin is now emerging as a potentially important site of extra-renal sodium homeostasis and BP regulation.

There are several areas of uncertainty. The function of skin as a buffer for dietary salt has not been proven by ^{23}Na MRI, which has not been used to measure changes in skin Na^+ with dietary salt modulation. ^{23}Na magnetic resonance imaging (MRI) studies in humans have shown a direct relationship between skin Na^+ and BP, but the mechanisms underlying this are unknown. [197,204] It is unknown if age and sex differences in the capacity to store skin Na^+ could explain the observed tendency for SSBP in women and older individuals. [197,204] Although MRI data were confirmed by direct ashing of human cadaveric samples, they have not yet been confirmed by direct chemical analysis of skin electrolytes in humans. [195] It is unclear if other factors other than GAGs, such as sodium transporters, influence the storage and distribution of sodium in the skin.

1.7 HYPOTHESES

The principle hypothesis is that the skin functions as a buffer for dietary sodium and modulates its haemodynamic effects.

This hypothesis was interrogated in 2 clinical studies and related experiments, discussed in Chapters 2 - 6 respectively. Their main hypotheses are summarised below:

1. In humans the skin acts as a reservoir to buffer increases in body sodium and the degree of change in skin sodium with dietary salt loading relates to the BP change.

2. Increased sodium intake leads to a rise in plasma VEGF-C and the degree of change determines the haemodynamic response to dietary salt loading.

3. Levels of sodium in the skin are positively associated with plasma VEGF-C levels.

4. Dietary salt loading leads to changes in skin capillary density in healthy humans.

5. Increased salt intake in humans lead to changes in dermal expression of glycosaminoglycans, Ton-EBP and VEGF-C in humans.

6. The hypoxia inducible factor (HIF) transcription system in the skin is altered by dietary salt loading and relates to associated BP changes.

7. The ENaC sodium is transporter is involved in skin sodium distribution and flux.

1.8 AIMS

The above hypotheses were tested in 6 studies, described in detail in Chapters 2 - 6 respectively. Firstly, the feasibility of measuring skin $Na^+$and K^+ concentrations using ICP-OES was assessed using skin samples obtained from the tissue bank and skin biopsies in healthy volunteers. Next, the techniques developed in skin elemental analysis were used to study changes in skin electrolytes alongside haemodynamic and biochemical measurements in another group of healthy volunteers within a double-blind, randomized, crossover study comparing high and low dietary salt intakes. Within this group capillaroscopy was used to measure changes in skin capillary concentration and skin changes gene expression with salt loading were investigated. Finally, the feasibility of determining skin elemental distribution patterns and underlying molecular mechanisms was assessed.

Study 1 (Chapter 2): To measure skin electrolyte concentrations in skin samples obtained under general anaesthesia to assess the effects of local anaesthetic on skin Na^+, K^+ and water content.

Study 2 (Chapter 3): To assess the feasibility of measuring skin elemental concentrations in skin biopsy samples taken from healthy volunteers and to observe the naturally occurring inter-individual variation.

Study 3 (Chapter 4): To measure skin Na^+ and K^+ in 48 healthy volunteers and observe the effects of varying salt intake on skin electrolytes and plasma VEGF-C. Furthermore, to study the correlation between skin sodium, blood pressure, other hemodynamic variables and plasma VEGF-C.

Study 4 (Chapter 4): To measure changes in skin capillary concentrations with varying salt intake in a sub-set of participants in Study 3.

Study 5 (Chapter 5): To measure changes in dermal gene expression for glycosaminoglycans, Ton-EBP, VEGF-C and hypoxia inducible factor isomers with dietary salt loading in a sub-set

of participants in Study 3.

Study 6 (Chapter 6): To assess the feasibility of studying skin sodium distribution profiles using scanning electron microscopy with energy dispersive X-ray spectroscopy (SEM-EDX), alongside immunohistochemical localisation of ENaC in the skin.

Chapter 2 METHODS DEVELOPMENT

2.1 INTRODUCTION

The quantification of the essential elements Na^+ and K^+ in human skin forms a central tenet of this thesis. An equally important consideration was the avoidance of elemental contamination, defined as the inadvertent addition of target analytes to samples during sample collection, transportation or analysis. [237] Skin elemental analysis was done in the following stages:

- Skin biopsies were taken from volunteers under local anaesthetic in the EMIT unit
- Storage of skin samples in cryovials at −80°C
- Division of skin samples under microscopy
- Skin elemental analysis by Inductively Coupled Plasma/Optical Emission Spectrometry (ICP-OES) at the MRC Elsie Widdowson Laboratory

Elemental contamination could have occurred at all stages, including the use of local anaesthetic (lidocaine hydrochloride), which contains Na^+. The methods for skin Na^+ and K^+ analysis and assessment of elemental contamination were developed concurrently during the following studies:

1. **Gelatine analysis** - gelatine samples were used to simulate skin samples to determine if Na^+ and K^+ contamination occurred during division and handling prior to elemental analysis.

2. **Tissue Bank skin analysis** - this study assessed the feasibility of measuring Na^+ and K^+ in human skin using ICP-OES. Skin elemental concentrations were measured in 17 skin samples obtained under general anaesthesia to assess the effects of local anaesthetic on skin Na^+, K^+ and water content. Due to the large size of samples, skin samples were divided prior to analysis by ICP-OES.

3. **VARSITY methods study** - a pilot study in 48 healthy humans assessing the feasibility of measuring skin elemental concentrations in healthy subjects and the naturally occurring inter-individual variation.

4. **VARSITY study** - a study in 48 healthy humans looking at the effects of varying salt intake on skin Na^+ and K^+. During this study, Na^+-free lignocaine was developed and trialled. Skin samples were divided prior to analysis by ICP-OES, with one portion used for elemental analysis and the other retained for other experiments later.

In this chapter methods used for skin elemental analysis and the measures taken to avoid contamination are described. Description of routine measurements are given in relevant experimental chapters. Detailed descriptions of the VARSITY methods and VARSITY studies are given in Chapter 3 and 4 respectively.

2.2 SKIN BIOPSY TECHNIQUE

Skin biopsies were carried out using sterile technique in a closed, temperature-controlled room (23 ± 2°C). An area of skin was selected on the lower back and cleaned using 2% chlorhexidine gluconate solution (ChloraPrep™), which was confirmed by ICP-OES analysis not to contain Na^+ or K^+. The skin was injected with lignocaine hydrochloride local anaesthetic (Xylocaine 1% with 2% adrenaline, AstraZeneca). This has a significant Na^+ content (116mmol/l) and no K^+ content as measured with ion-sensitive electrodes (Siemens Dimension RXL auto analyser) at the Cambridge Core Biochemical Assay Laboratory. In view of this, injections were carried out at a depth of approximately 11mm into the subcutaneous layer to avoid introducing lignocaine Na^+ and water into the dermis (Figure 2.1). A single full-thickness skin punch biopsy was taken with disposable punch skin biopsy needles (Miltex™) of 4-5mm width. Any attached subcutaneous tissue was immediately removed by macroscopic dissection using a blade Bard-Parker™ surgical blade. Skin tissue handled with sterile forceps and immediately placed in a 2ml cryovial (Thermoscientific). All surgical instruments were sterilised and autoclaved prior to use. In the VARSITY methods study the cryovial was then placed on ice before being stored at −80°C until analysis. For the main VARSITY study, samples were snap frozen in liquid nitrogen before storage at −80°C.

Figure 2.1: Illustration of skin biopsy procedure showing injection of local anaesthetic deep into the subcutaneous fat.

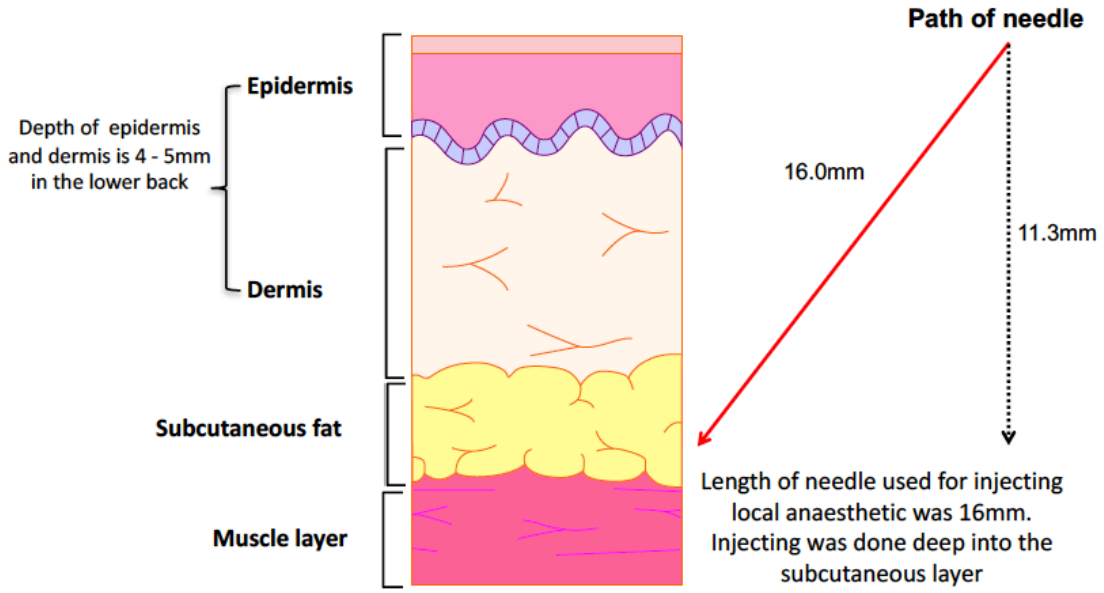

2.3 SKIN ELEMENTAL ANALYSIS

2.3.1 Inductively Coupled Plasma/Optical Emission Spectrometry (ICP-OES)

ICP-OES is a sensitive, powerful analytical tool for the determination of trace elements in a variety of sample matrices, including biological tissue. [238,239] Its high sensitivity allows elemental analysis in small tissue samples. ICP-OES has been used in Forensic Science for over 30 years for trace element analysis of evidential human tissue. [240] Very recently ICP-OES has been used successfully to measure skin Na^+ and K^+ in human skin. [143] This technique was available at the MRC Elsie Widdowson Laboratory, where it was previously used for trace element analysis in human and animal tissue. [241,242] Skin samples require acid digestion and homogenisation to allow elemental analysis, and ICP-OES has the capacity to handle samples of extreme pH. For these reasons ICP-OES was chosen for skin elemental analysis undertaken in this thesis.

The major components and layout of an ICP-OES system are illustrated below in Figure 2.2. With this technique, the analyte is transported into the instrument as a stream of liquid. Within the instrument the liquid is converted into an aerosol through nebulisation. The aerosol is then injected into argon plasma at a temperature of 10 000K in aerosol form, allowing analyte elements to be liberated as free atoms and ions in the gaseous state. [239,243]Collisional excitation within the plasma confers additional energy to the atoms, promoting them to excited states. The excited state species can then relax to the ground state by the emitting photons. These photons have characteristic wavelengths which can be used to identify the elements from which they originated. The total number of photons is directly proportional to the concentration of the originating element in the sample, and this way elemental concentration is measured. [239] The main advantage of this technique over other alternatives originates from its efficient and reproducible vaporisation, atomisation, excitation and ionisation for a wide range of elements and sample matrices. This is mainly due to the high temperature of the argon plasma, which is much higher than the maximum temperature of furnaces (3300K). [243]

Figure 2.2 Major components and layout of a typical ICP-OES system. Taken from Boss et al[238]

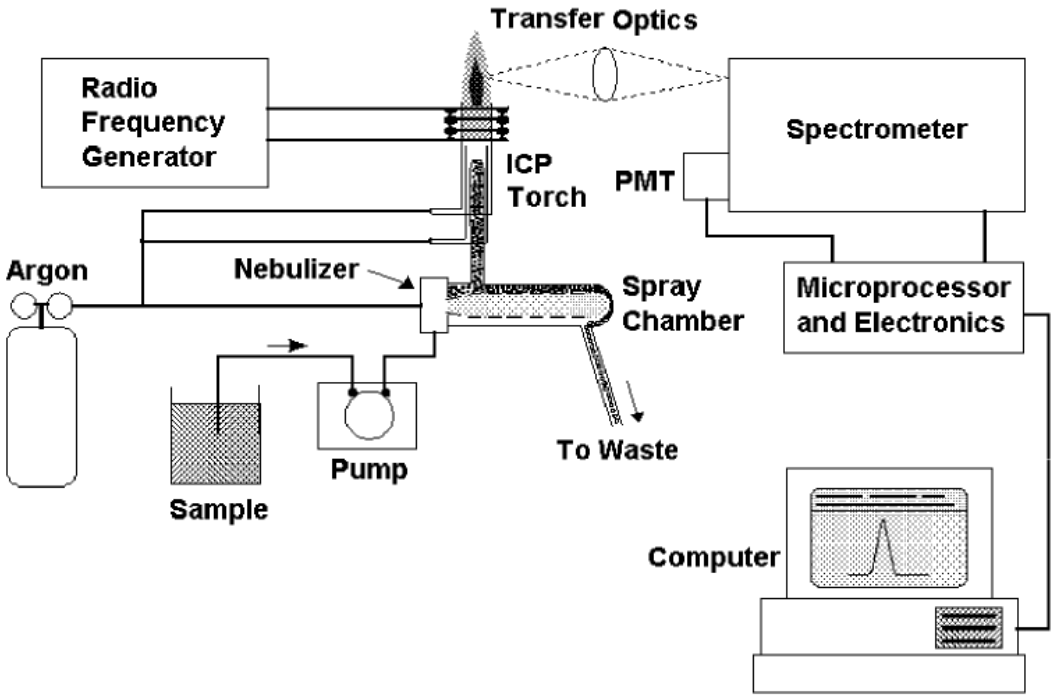

2.3.2 Sample preparation

Skin samples were analysed by ICP-OES in liquid form, as explained above. To achieve this, samples were freeze dried and underwent cold acid digestion at the MRC Elsie Widdowson Laboratory. The steps and techniques used for skin preparation for analysis by ICP-OES are summarised below in Figure 2.3. Environmental elemental contamination during sample preparation is a potential problem in all laboratories, with the main contributor being dust and atmospheric particulates. [237] The MRC Elsie Widdowson Laboratory specialises in trace element analysis and had precautionary measures already in place to reduce environmental elemental contamination. This included the use of clean room environment for sample preparation and ICP-OES analysis, and the use of personal protective equipment.

2.3.2.1 Freeze-drying

Elemental concentrations measured in solid biological tissue are calculated from the detected elemental output divided by the weight of sample, as opposed to volume, in the case of biological fluids. This presents a challenge as the weight of a sample varies with degree of hydration. The weight of tissue when it obtained is termed tissue wet weight. The weight of tissue after water is removed by a drying technique is termed dry weight. Elemental measurements per wet weight of tissue may have potential inaccuracies introduced by changes in sample hydration during sample processing, which is why previous studies in humans and rats have expressed skin Na^+ and K^+ concentrations per unit dry weight. [134,182,184,186-188,244,245] Tissue drying has been carried out using different methods, including dry ashing, oven drying and freeze-drying. Freeze drying was used for as it available and in use at the MRC Elsie Widdowson Laboratory.

Freeze-drying is a process by which water is removed from frozen tissue by sublimation at a low temperature and under vacuum. A vacuum is needed as sublimation can only occur when the partial pressure of the water vapour exceeds that of the atmosphere. Freeze drying facilitated acid digestion and the measurement of sample water content. The skin samples were weighed in a pre-weight polypropylene vial using an electrobalance to determine their wet weights and then freeze-dried overnight in a Mini Lyotrap system (LTE scientific, Greenfield, Oldham, UK) until they reached a constant weight (dry weight). This took up to 48 hours. The vials were re-weighed after drying to determine water content, as the difference between wet weight and dry weight.

2.3.2.2 Sample acid digestion

Freeze-dried skin samples were digested directly in the vial by adding a digestion solution containing 1:1 (volume for volume) mixture of 69% HNO_3 and 40% H_2O_2. The volume of the digestion solution was adjusted to the sample dry weight to ensure complete digestion - a skin sample of 7mg dry weight required 150 µL of digestion solution. Samples were vortexed thoroughly to provide a homogeneous matrix for digestion. Following this, the samples were incubated overnight at room temperature followed by a second incubation overnight in a water bath at 40^{o}C. More digestion solution was added if the solution was not clear and

the incubation at 40°C repeated. All samples were digested to completeness before being diluted 1:40 with ultra-high purity (UHP) water containing strontium (Sr, 1ppm final concentration). Digestion blank controls were prepared alongside the skin samples as empty vials and analysed collectively with the digested skin samples.

Figure 2.3: Techniques used for skin preparation for analysis by ICP-OES.

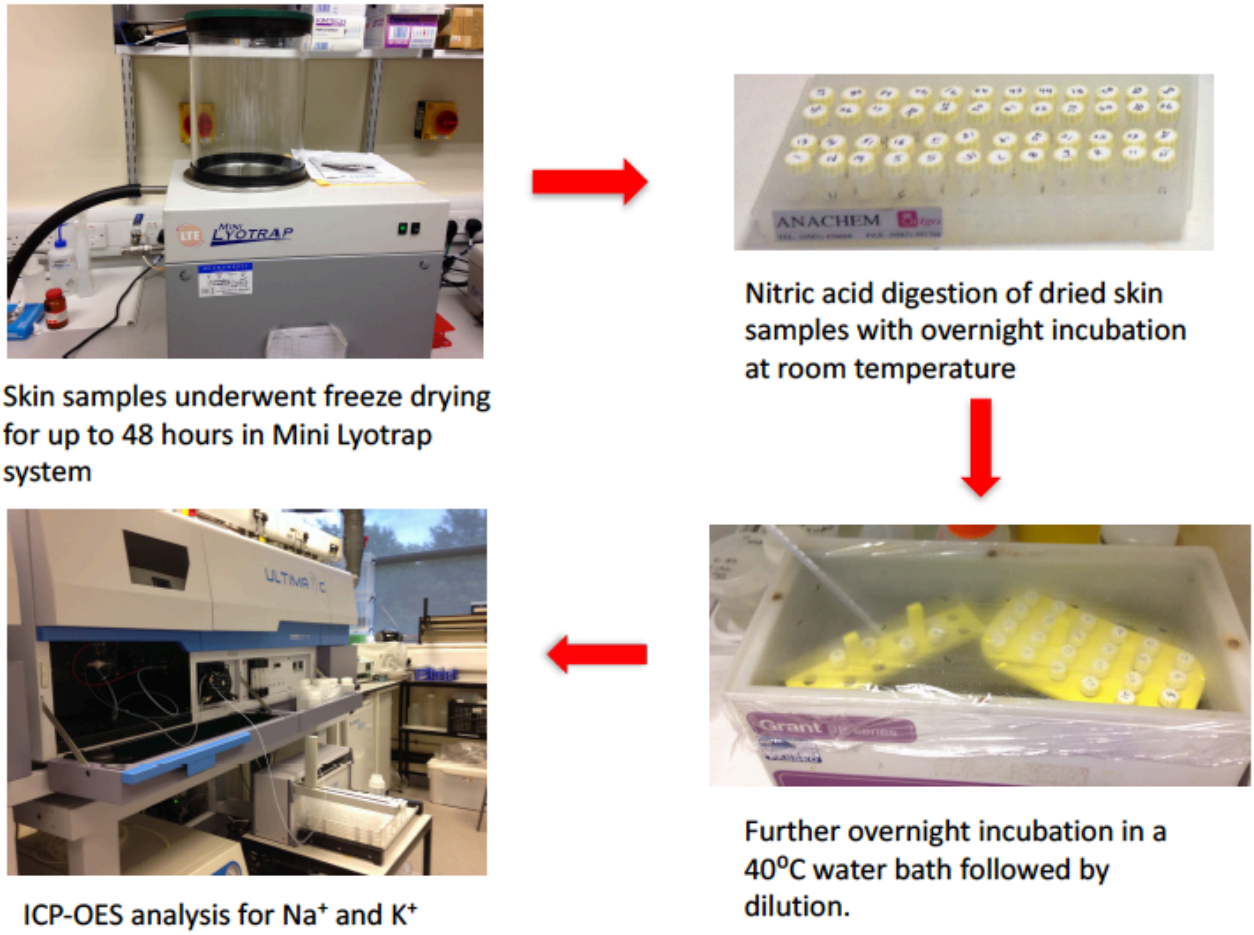

2.3.3 ICP-OES settings

The skin elemental concentrations of Na^+ and K^+ were determined using a Jobin Yvon Horiba – ULTIMA 2C ICP-OES system equipped with a concentric PFA micro-flow nebuliser with sample flow rate 0-2ml/min, a 50ml glass cyclonic spray chamber and a radial torch with an 3mm internal diameter (i.d.) alumina injector. Sample solutions were introduced from an auto-sampler (Jobin Yvon Horiba AS500) using a sample probe with 0.25mm i.d. sample tubing and 0.38mm i.d. pump tubing (orange/green). Instrument operating conditions are listed in Table 2.1. Strontium, added during sample preparation, was measured alongside Na^+ and K^+ to control for possible error in sample dilutions and uptake. Peak profiles were used to measure individual elements as described in table 2.2. A series of external calibration standards were prepared from 1000 ppm commercial stock solutions in 2% HNO_3 (Na, Fluka Tracepure; K, Perkin-Elmer Pureplus), with final concentrations per element ranging from 0 to 15 ppm in a diluent matched to the digested solution (final concentration 0.86% HNO_3, 1ppm Sr). The Na^+ and K^+ concentrations were calculated against the linear regression obtained from the calibration standards. Drift check solutions and blank (diluent) solutions were measured after every block of approximately 6 samples to monitor contamination during the ICP-OES analysis process. Blank solutions contained ultra-pure water (Arium Pro Ultrapure Water Systems, Sartorius) in place of sample digests.

Table 2.1: Running conditions used for ICP-OES.

Analytical Conditions	Na:K
RF power (W)	1000
Plasma gas (L min^{-1})	12
Sheath gas (L min^{-1})	2
Auxiliary gas (L min^{-1})	0.0
Speed pump (rates min^{-1})	10
Nebulizer gas flow rate (L/min^{-1})	0.73
Nebulizer pressure (bar)	2.75
Number of replicates	3

Table 2.2: Peak profile measurement parameters

Element	Na	K	Sr
Wavelength (nm)	588.995	766.490	346.446
Number of points	21	11	9
Integration time (s)	0.5	0.5	0.5
Increments (nm)	0.001	0.002	0.002
Photomultiplicator tube voltage (V)	911	990	750
Photomultiplicator tube gain (%)	100	100	100
Points used	5	5	5
Number of replicates	3	3	3
Calculation mode	Gauss	Gauss	Gauss

2.3.4 Assessment of Matrix effect

In analytical chemistry, matrix refers to the components of a sample other than the analyte. [246] Matrix effect is defined as the combined effect of all components of the sample on the measurement of the analyte. [246]It represents the quantification of sample interference on the measurement of Na^+ and K^+ through our method. This effect will be different depending on the method, sample, analyte and technique of analysis. Matrix effects are primarily caused by the disturbance of the ion beam path through the ion optics and the mass spectrometer by the high concentration of the matrix element. To measure matrix effect, a pooled sample was created from the skin digest samples and aliquoted and spiked with Na^+ and K^+ with final concentrations per element ranging from 0 to 15 ppm and maintaining a sample dilution of 1:40. The slopes of the linear regressions obtained for each element are compared with the slopes of the external calibration linear regression in diluent described above and a correction factor calculated.

2.3.5 Expression of skin elemental concentrations and water content

Skin Na^+ and K^+ were quantified by ICP-OES in milligrams. Concentrations were calculated for each sample by dividing the measured Na^+ and K^+ by the weight of the sample. The sample wet weight was used to obtain skin Na^+_{wet} and K^+_{Wet} in mg/g. The sample dry weight was used to obtain skin Na^+_{Dry} and K^+_{Dry} in mg/g. Water content was taken as the weight loss with freeze drying - the difference between wet weight and dry weight (in milligrams). This was expressed as a percentage of wet weight to give percentage water content (% water). The ratio of Na^+ and K^+ to water were used as an estimate of osmotically inactive storage of these elements in the skin. This ratio was calculated as follows:

1. Na^+_{Dry} and K^+_{Dry} were converted from mg/g to mmol/g and the total amount of Na^+ and K^+ in each sample was calculated in mmol.

2. The sample water content (in grams) was converted to volume of water using the formula: 1ml = 1mg of water.

3. The total amount Na^+ and K^+ in each sample was divided by the volume of water and the ratio of Na^+ and K^+ to water expressed as mmol/l.

2.3.6 Assessment of drying consistency

The consistency of freeze drying over a range of skin sample weights is unknown. If water removal is less efficient in larger samples, their recorded dry weights would be higher than their true dry weights. Consequently, skin elemental concentrations expressed per milligrams of dry weight would be underestimated in in these samples. To assess if this was present sample wet weights were plotted against percentage weight loss with freeze drying (% water) to look for the existence of a significant negative correlation.

2.4 GELATINE ANALYSIS

2.4.1 Introduction

In the Tissue Bank skin analysis and the VARSITY study it was necessary to halve skin samples divided before elemental analysis by ICP-OES. In this experiment, the contamination of skin samples with Na^+ and K^+ during this procedure was assessed. Gelatine samples were used to simulate skin samples undergoing the same procedures to assess Na^+ and K^+ contamination. Gelatine is a mixture of peptides and proteins produced by partial hydrolysis of collagen extracted from the skin, bones and connective tissues of animals such as cattle, chicken, pigs and fish. [247] It is a viscoelastic substance, mainly composed of carbon, hydrogen, nitrogen and oxygen. It is also known to contain Na^+ and K^+ within its matrix. [248,249] Gelatine therefore shares similar properties to skin and was deemed a suitable substrate to assess elemental contamination in skin samples. During this experiment, elemental contamination from 2ml cryovials (Thermoscientific) used to store skin samples was also assessed, as the use of solutions containing Na^+ and K^+ during their manufacture was unknown.

2.4.2 Aims

1. Assess if the procedures involved in dividing skin samples prior to elemental analysis in the introduced Na^+ and K^+ contamination and variability.

2. Determine whether storage of samples in cryovials introduced contamination.

2.4.3 Methods

An initial analysis of 10 pieces of gelatine from several regions of a 4 x 2 cm gelatine block was carried out at the MRC Elsie Widdowson laboratory to determine Na^+ and K^+ content. Subsequently, all procedures planned for skin samples were carried out on the same gelatine block at the EMIT unit, as shown in Figure 2.4. Firstly 5 mm punch biopsies were

carried out using sterile technique. 10 x 5mm punch-biopsy samples were removed with sterile non-toothed forceps and a blade Bard-Parker™ surgical blade. Sterile gloves were used when handling the samples. Samples were placed in cryovials, snap-frozen in liquid nitrogen and kept in a- 80 °C freezer for 72 hours. The samples were individually removed and placed on a tray containing dry ice covered in aluminium foil. Dry ice was used to keep samples frozen and reduce moisture loss. Each sample was halved longitudinally with a scalpel under an 10x microscopic view. One half was placed in a new cryovial and the other half was placed in the original cryovial. Samples placed back in the original cryovial were labelled Group 1 (G1) and those placed in a new cryovial were labelled Group 2 (G2). All samples were placed on dry ice before being stored in a - 80 °C freezer for 48 hours. The gelatine samples were transported to MRC Elsie Widdowson laboratory analysis by ICP-OES analysis as previously described in 2.2. The procedures for sample preparation for ICP-OES as outlined in 2.3.2 and 2.3.3 were carried out. Differences in dry weight values for Na^+ and K^+ (Na^+_{Dry} and K^+_{Dry}) between Groups 1 & 2 were used to determine if there was any contamination and variability introduced by sample division. During sample preparation 4 empty 2ml cryovials had ultra-pure water (Arium® Pro Ultrapure Water Systems, Sartorius) added in place of sample digests to determine Na^+ and K^+ content in empty cryovials.

Figure 2.4: Gelatine sample handling and analysis

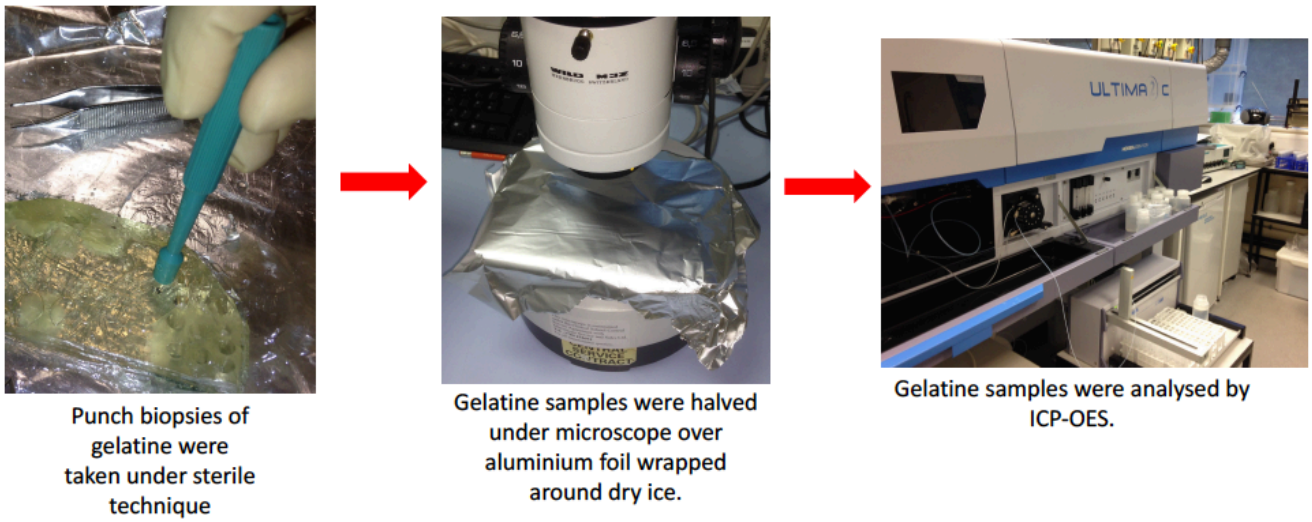

2.4.4 Results

Gelatine elemental concentrations and water content are shown in Table 2.3. Results are expressed as mean ± standard deviation. 2 samples were rejected (1 from each group) due these samples being dropped during handling and were likely to have incurred environmental contamination. The results for the remaining 9 samples per group are shown in table 2.3. No significant difference was noted between the 2 groups for Na^{+}_{Dry} (3.64 ± 0.68 vs.3.66 ± 0.58 mg/g; p = 0.95) and K^{+}_{Dry} (0.05 ± 0.00 vs. 0.05 ± 0.00 mg/g; p=0.81). Water content was similar in both groups (90.6 ± 1.1 % vs. 90.1 ± 1.5 %, p=0.42). Concentrations of Na^{+} and K^{+} in the blank cryovials was negligible (< 0.001 mg/ml).

Table 2.3: Elemental concentrations for gelatine samples for Group 1 (G1) and Group 2 (G2).

Samples	G1	G2	P for difference
$Na^{+}_{Wet,}$ mg/g	0.34 ± 0.04	0.35 ± 0.04	0.22
$Na^{+}_{Dry,}$ mg/g	3.64 ± 0.68	3.66 ± 0.58	0.95
$K^{+}_{Wet,}$ mg/g	0.01 ± 0.00	0.01 ± 0.00	0.69
$K^{+}_{Dry,}$ mg/g	0.05 ± 0.00	0.05 ± 0.00	0.81
% water	90.6 ± 1.1	90.1 ± 1.5	0.42

2.4.5 Discussion

The data suggests that Na^+ and K^+ contamination did not occur during the dividing of samples prior to elemental analysis. Moreover, the results show low standard deviations for Na^+ and K^+, suggesting that contamination during the procedures for sample handling and instrumentation was unlikely. There was also no detectable Na^+ and K^+ contamination from the cryovials used to store samples. There were several limitations of this experiment that would have affected the ability to generalise the findings for human skin samples. Firstly, local anaesthetic injections were not used as injecting lignocaine into gelatine samples was not possible. Secondly, the water content of gelatine was high (>90%) compared to human skin. [182,186,187] Furthermore, the homogeneity of Na^+ and K^+ distribution in gelatine was unknown and may have been different from human skin. In conclusion, the findings of this experiment suggest that the procedures involved in dividing skin samples prior to elemental analysis and the storage of samples in cryovials did not introduced Na^+ and K^+ contamination and variability. It was therefore deemed appropriate to use these procedures when handling skin samples.

2.5 ANALYSIS OF TISSUE BANK SKIN

2.5.1 Introduction

Skin biopsies in this thesis were taken with lignocaine local anaesthetic, as described in 2.2. Although Injections were carried out deep into the subcutaneous layer, there was still a risk of Na^+ and water contamination of biopsy tissue. The purpose of this study was to evaluate skin electrolyte and water content without the influence of local anaesthetic injection in to the skin and the feasibility of measuring skin Na^+ and K^+ with ICP-OES using the techniques described in 2.3.

2.5.2 Aims

The primary aim of this study was to evaluate the Na^+ and K^+ concentrations and water content in healthy human skin without the influence of local anaesthetic. A further aim was to assess the feasibility of skin elemental analysis with ICP-OES.

2.5.3 Methods

2.5.3.1 Samples

We obtained healthy skin specimens from the Cambridge University Hospitals NHS Foundation Trust Human Research Tissue Bank. The skin samples were all healthy breast reduction surgical resections obtained from 17 women under general anaesthesia. The skin specimens were previously collected during surgery and placed on a small piece of foil and the plunged into liquid nitrogen for a up to 10 seconds. Once frozen each sample was placed into a pre-cooled cryovial and then stored at - 80 °C. All tissue acquisition procedures and experimental protocols were approved by Cambridge University Hospitals Human Research Tissue Bank, under the generic ethics approval (11/EE/0011). Only data on age and sex was provided under this ethics approval.

2.5.3.2 Sample processing and analysis

The skin samples were large in comparison to punch biopsy samples obtained from the VARSITY Methods and VARSITY studies, and this would have led to longer cold acid digestion times. For this reason, samples were divided using the techniques described with gelatine samples in 2.4.3. Each sample was halved longitudinally with a scalpel under 10x microscopic view, as described in 2.4.3, to ensure even splitting of the epidermis and dermis. Samples were cut on aluminium foil over dry ice to keep them frozen and avoid loss of moisture. Samples were then sent on dry ice to the MRC Elsie Widdowson laboratory to determine Na^+ and K^+ content by ICP-OES analysis as previously described in 2.2. The procedures for sample preparation for ICP-OES were carried out as outlined in 2.3.2 and 2.3.3.

2.5.3.3 Expression of skin elemental concentrations

Skin Na^+ and K^+ concentrations and water content were calculated and expressed as described in 2.3.5.

2.5.3.4 Assessment of drying consistency

This was assessed as described in 2.3.6.

2.5.4 Results

Samples from 17 women were analysed for Na^+ and K^+ concentrations and water content. Results are expressed as mean ± standard deviation in Table 2.4. Mean age was 43.4 ± 15.9 with range 19 - 72. Mean Na^+ concentration was 2.25 ± 0.23 mg/g of wet skin and 6.35 ± 1.75 mg/g of dry skin. Mean K^+ concentration was 0.57 ± 0.17 mg/g of wet skin and 1.56 ± 0.50 mg/g of dry skin. The mean water content was 62.9 ± 6.5 %. Measured water content was not correlated with sample wet weights, suggesting that freeze drying removed water consistently in this sample set. (Figure 2.4).

Table 2.4: Results for skin elemental and water content in Tissue Bank samples.

Variable	Mean ± SD
Age, years	43.4 ± 15.9
Wet weight, g	60 ± 3
Dry weight, g	20 ± 10
Skin Na^{+}_{Wet}, mg/g	2.25 ± 0.23
Skin Na^{+}_{Dry}, mg/g	6.35 ± 1.75
Skin Na^{+}: water, mmol/l	156.2 ± 8.8
Skin K^{+}_{Wet}, mg/g	0.57 ± 0.17
Skin K^{+}_{Dry}, mg/g	1.56 ± 0.50
Skin K^{+}: water, mmol/l	23.4 ± 7.7
Water content, %	62.9 ± 6.5

Figure 2.4: Effects of sample wet weights on % water content.

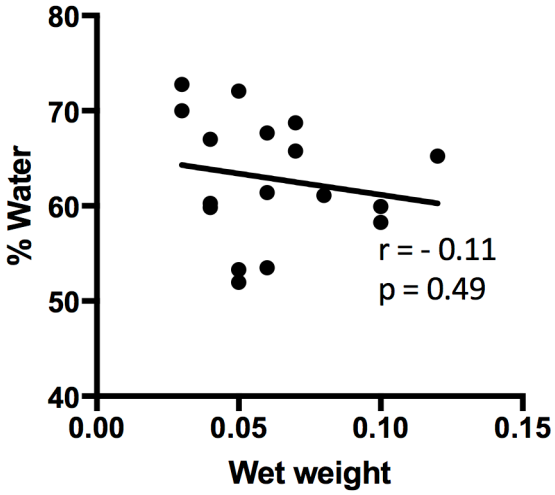

2.5.5 Discussion

The main aim of this study was to measure skin Na^+ and K^+ and water content without the influence of local anaesthetic. The values for skin Na^+ and K^+ per unit wet and dry weight fall within published ranges (Chapter 2.3). Tissue Bank samples had a water content of 62.9 ± 6.5 %, which is similar to previously published values in human skin. [182,187] Skin Na^+ to water ratio was 156.2 ± 8.8 mmol/l while K^+ to water ratio was 23.4 ± 7.7 mmol/l. In these absence of serum Na^+ and K^+ concentrations these values suggest storage of these elements in the skin without commensurate water accumulation. The freeze-drying technique did not appear to be affected by sample wet weights.

There are several weaknesses of this analysis. The skin samples were not collected prospectively, and it was not possible to ensure that Na^+ containing substances were used during the surgical procedure or collection. The samples were only from women and this could have affected their generalisability for men. The measurements of Na^+ and K^+ to water ratios did not differentiate between extracellular and intracellular Na^+ and K^+ and could not be compared with the serum concentrations. Despite these limitations, the results skin Na^+ and K^+ and water content measured with modern techniques are similar to previously published values and will inform later work.

2.5.6 Conclusions

It is feasible to perform skin elemental analysis with ICP-OES using the techniques described.

2.6 DEVELOPMENT OF SODIUM FREE LIDOCAINE SOLUTION

2.6.1 Introduction

Xylocaine 1% with 2% adrenaline (AstraZeneca) is the conventional form of local anaesthetic used in Addenbrookes Hospital. It contains the excipients sodium metabisulphate, sodium hydroxide and sodium chloride, as confirmed by AstraZeneca. These excipients are added to increase the osmolality and pH of Xylocaine, which minimises the risk of tissue reaction and improves tolerability during tissues injection. [250,251] Sodium metabisulphate is also used to prevent oxidation and improve the shelf life of the solution. The sodium content of Xylocaine is a potential source of contamination during skin elemental analysis in human volunteers. It was therefore necessary to create an alternative Na^+ free anaesthetic. Dextrose, which has previously been used as an excipient for lidocaine solutions, was chosen as substitute for the above Na^+-based excipients. [252] Commercially available lidocaine local anaesthetic solutions have pH of around 3.5-7.0. [253] In designing a lidocaine/dextrose solution, the pH would also have to be similar for tolerability.

2.6.2 Aims

1. To develop a Na^+-free lidocaine/dextrose solution with suitable osmolality and pH for use in the VARSITY main study.

2. To confirm that this lidocaine/dextrose solution does not contain Na^+ or K^+.

2.6.3 Methods

Conventional lidocaine (Xylocaine 1% with 2% adrenaline, AstraZeneca) was analysed at the Addenbrookes Core Assay Biochemistry lab (CBAL) for Na^+ and K^+ using an ion selective electrode (Siemens Dimension RXL auto-analyser). The osmolality of Xylocaine 1% was measured using method of freezing point depression with an Advance Micro-Osmometer model 3300 (Advanced Instruments, Norwood, USA). Tayside Pharmaceuticals, a MHRA-approved Pharmaceutical company in Dundee, made up solutions of lidocaine 1% and dextrose as an alternative excipient at different concentrations (2.5%, 5% and 10%). Ultra-pure water was used to make up lidocaine solutions and precautions were taken to avoid introducing sodium during the manufacturing process. The osmolality of these different lidocaine/dextrose solutions were measured and plotted against dextrose concentrations to determine the concentration of dextrose that would have a similar osmolality to conventional lidocaine. Lidocaine 1% was subsequently produced with this concentration of dextrose and tested for osmolality at the CBAL and pH at Tayside Pharmaceuticals. Due to technical challenges adrenaline was not included in the solution. Na^+ and K^+ concentrations were determined by ICP-OES in the final vials of lidocaine/dextrose to be used in VARSITY study.

2.6.4 Results

The osmolality of Xylocaine 1% with 2% adrenaline (AstraZeneca) was measured as 277 mOsm/kg. Osmolalities for lidocaine 1% and dextrose solutions at different dextrose concentrations are shown in Table 2.5. Osmolality had a linear relationship with dextrose concentration (Figure 4.5). Using dextrose 3.5% gave a similar osmolality to Xylocaine. Lidocaine 1% with dextrose 3.5% was produced by Tayside Pharmaceuticals. This was found to have an osmolality of 269 mOsm/kg and pH of was 5.0. 12 vials of lidocaine 1% with dextrose 3.5% were analysed by ICP-OES and were found to have Na^+ and K^+ concentrations of less than 0.1 mmol/l.

Table 2.5: Results for osmolalities at different concentrations of dextrose.

Dextrose concentration, %	Osmolality mOsm/kg
2.5	213
5	369
10	686

Figure 2.5: Linear plot of osmolality values for lidocaine and dextrose solutions at different dextrose concentrations.

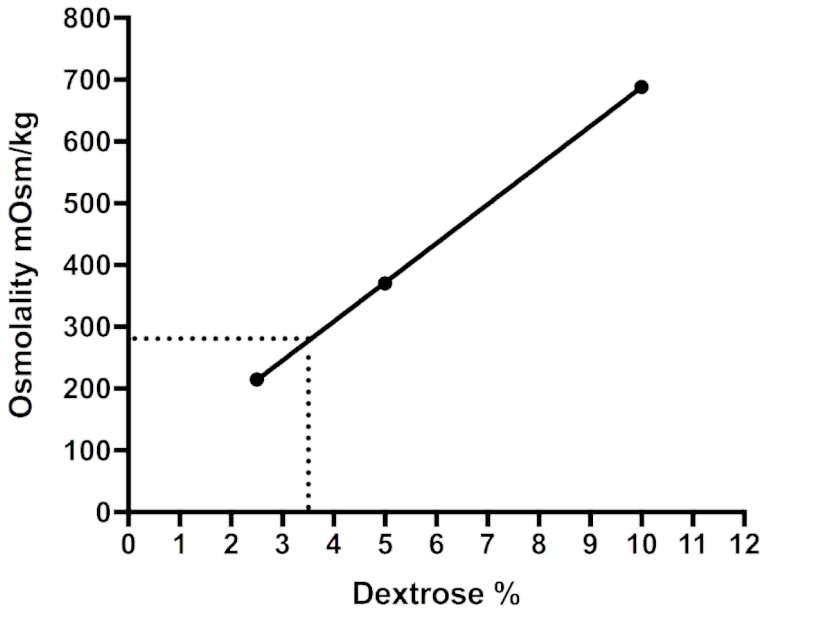

2.6.5 Discussion

Lidocaine 1% and dextrose 3.5% has been shown to have a similar osmolality and pH as conventional lidocaine. This Na^+ free lidocaine was manufactured in time for the last 16 volunteers for VARSITY study. A concentration of < 0.1 mmol/l for Na^+ and K^+ was regarded as negligible for the purpose of avoiding elemental contamination. The use of lidocaine 1% and dextrose 3.5% would avoid Na^+ contamination of skin, but not water contamination, which would still have to be considered.

.

Chapter 3 VARSITY METHODS PILOT STUDY

3.1. INTRODUCTION

The recent discovery of novel mechanisms in the skin for buffering dietary salt in rodent models has highlighted the relevance of skin electrolytes. [133,134,152] At the commencement of this work the available data on skin electrolyte content in humans was sparse with significant heterogeneity and limitations, as shown in Table 1.2 in 3.2. [181-188] In the last 7 years, ^{23}Na-MRI measurements have revealed relationships between skin Na^+ and age, sex, BP and LVM, making it a potential biomarker for cardiovascular disease. [197,204] Direct chemical measurements of human skin have not evaluated the relationship between skin electrolytes and these variables. [181-188,197,204] To interrogate the hypotheses of this thesis outlined in 1.7, a reliable technique for skin elemental quantification and an evaluation of the normal variation in healthy humans was essential. On this background, VARSITY Methods was conducted as a pilot observational cross-sectional study to assess the feasibility of measuring skin Na^+ and K^+ concentrations in healthy subjects and the naturally occurring inter-individual variation. This study was meant to inform the analysis of Na^+ and K^+ content of skin samples in the main VARSITY study, which assessed the effects of dietary salt on skin Na^+. As described in 2.6, the use local anaesthetic for skin biopsies was associated with the risk of sodium contamination. To assess whether contamination occurred, skin Na^+ values obtained from VARSITY methods were compared with the analysis of Tissue Bank skin samples, described in 2.5.

3.2 AIMS

1. The primary aim of this study was to assess the feasibility of measuring skin Na^+ and K^+ concentrations in healthy subjects define the usual concentrations of sodium and potassium in the skin of healthy adult humans.

2. The secondary aim was to examine the naturally occurring variations in skin Na^+ and its relationship with putative factors such as age, sex, BMI, BSA and BP.

3. A further aim was to assess the presence of sodium contamination from local anaesthetic use.

3.3 METHODS

3.3.1 Study design & protocol

VARSITY Methods was a single-centre observational, cross-sectional study. Participants attended a single study visit, having refrained from caffeine, alcohol, strenuous exercise and the application of moisturiser or fake tan to their lower back for the previous 6 hours. Height and weight were assessed and, after a minimum of 5 minutes rest, seated brachial blood pressure was recorded. Body surface area (BSA) was calculated using the Du Bois formula [254]: $BSA = 0.007184 \times Weight(kg)^{0.425} \times Height(cm)^{0.725}$.Twenty millilitres of blood were drawn into three EDTA tubes and a clotted tube. For each participant a single EDTA sample was centrifuged at 4°C (3200 rpm for 15 minutes) and the serum separated and stored at - 80°C prior to analysis for VEGF-C.

3.3.2 Subjects

Participants were healthy individuals aged between 18 to 70 years at the time of screening. Exclusion criteria included hypertension (sustained blood pressure >140/90mmHg), current use of antihypertensive drugs, diuretics or salt supplements**,** renal impairment**,** heart failure or pregnancy. Participants were recruited from Cambridge using adverts placed through the university and hospital common areas as well as sending letters to their general practitioners. We set a recruitment target of 48 participants, stratified by screening age as set below in table 3.1.

Table 3.1: Age categories for recruitment in VARSITY Methods.

Age Range (years)	Sample Size
18 to 30	16
31 to 50	16
51 to 70	16

3.3.3 Haemodynamic assessments

In all participants, brachial blood pressure was measured using a validated semi-automated oscillometric device (HEM-705CP, Omron Corporation) after 5 minutes of rest in seated position. BP was measured in the non-dominant arm in triplicate, with approximately a 1-minute interval between readings. The average of three readings was recorded in use for analysis. Further readings were taken if there was a difference of > 5 mmHg was observed between the 2nd and 3rd readings.

3.3.4 Biochemical measurements

Serum and 24-hr urine electrolytes (Na^+, K^+ and creatinine), plasma renin and aldosterone were measured in an accredited laboratory (Cambridge University Hospitals Department of Clinical Biochemistry). Estimated glomerular filtration rate was measured using the Modification of Diet in Renal Disease (MDRD) formula. [255] Plasma VEGF-C measurement was carried out at the Addenbrookes Core Biochemical Assay Laboratory (CBAL) using a validated sandwich ELISA (MesoScale$_{TM,}$ Rockville, USA), in which a VEGF-C-specific antibody was used to bind the serum VEGF-C. Reproducibility of the assay was checked by the team at CBAL by running quality control samples at the beginning and end of each batch.

3.3.5 Skin biopsy procedure

As described in 2.2, full-thickness skin punch biopsies (4mm diameter) were carried out over the lower back region using 2 – 4 ml of local anaesthetic (Xylocaine 1% with 2% adrenaline, AstraZeneca) in all participants. The skin was cleaned using 2% chlorhexidine gluconate solution. Skin tissue was handled with forceps and immediately placed in a cryovial in ice before being stored at − 80°C until analysis.

3.3.6 Skin elemental analysis

Whole skin samples were then sent on dry ice to the MRC Elsie Widdowson laboratory to determine Na^+, K^+ and water content by ICP-OES analysis as previously described in 2.2. The procedures for sample preparation for ICP-OES were carried out as outlined in 2.3.2 and 2.3.3.

3.3.7 Expression of skin elemental concentrations

Skin Na^+ and K^+ concentrations and water content were calculated and expressed as described in 2.3.5.

3.3.8 Assessment of drying consistency

This was assessed as described in 2.3.6.

3.3.9 Statistical analysis

Statistical analysis was performed using SPSS 23.0 (SPSS Inc., Chicago, IL, USA). Graph-Pad Prism 7.0 (GraphPad Software Inc., La Jolla, CA, USA) was used to construct graphs and figures. Results are expressed as means ± SD unless otherwise stated. Differences in skin Na^+ were examined in different tertiles of age using ANOVA analysis. Post hoc test were performed using the Bonferonni algorithm. Correlation coefficients between skin $Na^+$and putative parameters such as age, sex, body mass index (BMI), body surface area (BSA) and

BP were calculated using Pearson's method for normally distributed variables and Spearman's method for non-normally distributed variables. Multiple regression analysis was then performed to examine the parameters that independently influence skin Na^+ and K^+. The unpaired 2-tailed Student's *t*-test was used to compare normally distributed skin biochemical parameters between sexes and between VARSITY methods and Tissue Bank. The Mann Whitney test was used to compare non-normal distributed data. Test for normality were carried out using the Shapiro-Wilk test.

3.4 RESULTS

3.4.1 Subjects and exclusions

48 healthy participants were recruited over a 2-year period from 2011 to 2013, with 16 recruited in each age category specified in table 3.1. Skin samples were analysed for all 48 participants in 5 batches. After reviewing results for skin analysis for both VARSITY main and VARSITY methods 11 participants were excluded. 8 were excluded because of an analytical problem with the ICP-OES instrument during analysis of the 2nd batch, resulting in a dramatic shift in sensitivity. This was determined by the trace element analysis teams at the MRC Elsie Widdowson Laboratory after reviewing skin electrolyte values from both studies. This was attributed to a drop in ICP-OES argon pressure during the analysis. 3 further participants were excluded because of low sample wet weights (< 0.01 g), leading to variability in the freeze-drying process and elemental analysis, as discussed further in 4.5.1.2.

3.4.2 Baseline characteristics

The baseline characteristics for the remaining 37 participants used in the analysis are summarised in Table 3.2, with values shown for the whole group and participants divided into tertiles of age. Mean age was 39 ± 16 years and 18 were men.36 out of 37 participants were Caucasian, in keeping with the demographics of the Cambridge region. The mean 24-hour sodium excretion of 117.1 ± 45.9 mmol, approximating to a salt intake of 7g a day. This is below the UK average daily sodium intake, recently estimated at 130 mmol. [256] No participants were current smokers. 3 women were on hormone replacement therapy and 6 were on contraceptive treatment. As seen in Table 3.2 the expected age-related rise in blood pressure and decline in renal function was observed. [257,258] VEGF-C displayed a high variability using our ELISA assay and mean plasma concentration was 106.4 ± 107.9 pg/ml, showing no variation with age.

Table 3.2: Baseline demographic data for Varsity Methods. Data is presented for the whole population and tertiles of age.

Variables	All subjects	Age tertile			
		1	2	3	*P* for difference*
n	37	12	12	13	
Age	39 ± 16	22	37	58	< 0.001
BMI, kg/m^2	23.5 ± 3.0	22.6 ± 3.4	24.2 ± 3.1	23.6 ± 2.5	0.41
BSA, m^2	1.81 ± 0.18	1.81 ± 0.16	1.88 ± 0.19	1.74 ± 0.16	0.15
Gender (M/F)	18/19	6/6	7/5	5/8	0.94
Seated SBP, mmHg	124 ± 12	121 ± 11	121 ± 9	132 ± 12	**0.02**
Seated DBP, mmHg	78 ± 9	75 ± 9	75 ± 6	83 ± 10	**0.04**
MAP, mmHg	90 ± 10	90 ± 9	90 ± 7	99 ± 10	**0.02**
Serum Na, mmol l^{-1}	139.4 ± 2.1	139.4 ± 2.0	138.8 ± 1.8	140.1 ± 2.3	0.29
GFR, ml/min/1.72m^2	95.6 ± 19.2	107.3 ± 18.9	94.6 ± 19.4	84.8 ± 12.6	**0.01**
Renin, mU/l	20.1 ± 11.0	20.8 ± 8.3	24.0 ± 14.9	15.9 ± 7.9	0.18
Aldosterone, pmol/l	268.2 ± 185.1	330.5 ± 222.1	253.2 ± 161.4	224.5 ± 165.9	0.35
VEGF-C pg/ml	106.4 ± 107.9	80.8 ± 71.7	131.6 ± 177.0	111.3 ± 58.3	0.58
24-Urinary Na$^+$, mmol	117.1 ± 45.9	102.0 ± 31.0	128.0 ± 61.4	97.4 ± 26.2	0.39

Data presented as mean ± SD. Difference between age groups was analysed using one-way Anova with post-hoc Bonferonni algorithm. P value < 0.05 taken to be significant.

3.4.3 Assessment of drying consistency

Measured water content did not correlate with sample wet weights (Figure 3.1), suggesting that overall, freeze drying removed water consistently in this sample set. This suggested that Na^{+}_{Dry} and K^{+}_{Dry} could be used in the analysis.

Figure 3.1: Effects of skin sample wet weights on % water content.

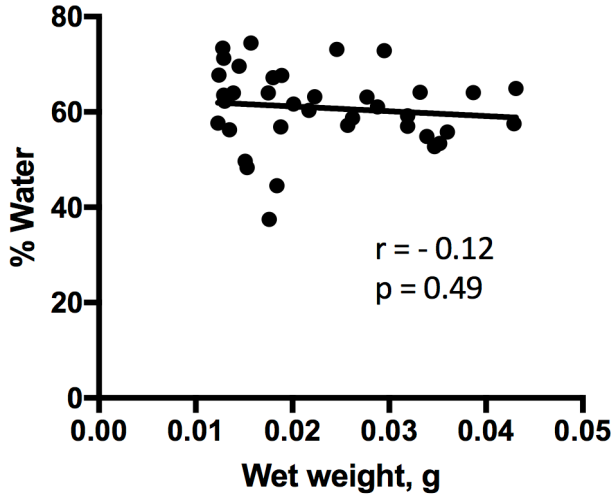

3.4.4 Skin biochemical variables

Results for skin biochemical analyses are shown in Table 3.3 with values shown for the whole group and participants divided into tertiles of age. Mean Na^{+} concentration was 2.15 ± 0.27 mg/g of wet skin and 5.69 ± 1.30 mg/g of dry skin. Mean K^{+} concentration was 0.69 ± 0.18 mg/g of wet skin and 1.82 ± 0.52 mg/g of dry skin. The mean skin water content was 60.9 ± 8.2 %. The ratio of Na^{+} to water in skin was higher in the skin than in serum (157.6 ± 41.6 vs. 139.4 ± 2.1 mmol/l , p = 0.01) and more variable (range 118.6 - 236.1 mmol/l). No difference was noted in skin electrolytes or water content between the different tertiles of age. Sex specific skin biochemical analyses are shown in Table 3.4.

Table 3.3: Skin biochemical parameters for Varsity Methods. Data is presented for the whole population and tertiles of age.

	All subjects	Age Tertile			P for difference*
		1	2	3	
n	37	12	12	13	
Age	43	22	37	58	< 0.001
Na_{Wet} mg g^{-1}	2.15 ± 0.27	2.09 ± 0.30	2.15 ± 0.26	2.19 ± 0.28	0.69
Na_{Dry} mg g^{-1}	5.69 ± 1.30	5.47 ± 1.37	6.06 ± 1.40	5.57 ± 1.17	0.50
Na/H_2O mmol l^{-1}	157.6 ± 41.6	158.9 ± 59.0	149.9 ± 24.3	163.6 ± 36.8	0.72
K_{Wet} mg g^{-1}	0.69 ± 0.18	0.73 ± 0.17	0.71 ± 0.19	0.64 ± 0.19	0.42
K_{Dry} mg g^{-1}	1.82 ± 0.52	1.88 ± 0.41	1.97 ± 0.57	1.62 ± 0.54	0.22
% water	60.9 ± 8.2	62.9 ± 6.4	61.0 ± 9.9	58.8 ± 8.0	0.47

Data presented as mean ± SD. Difference between age groups was analysed using one-way Anova with post-hoc Bonferonni algorithm. P value < 0.05 taken to be significant

Table 3.4: Skin biochemical parameters for Varsity methods according to sex.

	All subjects	Age Tertile			P for difference*
		1	2	3	
n	37	12	12	13	
Age	43	22	37	58	< 0.001
Na_{Wet} mg g^{-1}	2.15 ± 0.27	2.09 ± 0.30	2.15 ± 0.26	2.19 ± 0.28	0.69
Na_{Dry} mg g^{-1}	5.69 ± 1.30	5.47 ± 1.37	6.06 ± 1.40	5.57 ± 1.17	0.50
Na/H_2O mmol l^{-1}	157.6 ± 41.6	158.9 ± 59.0	149.9 ± 24.3	163.6 ± 36.8	0.72
K_{Wet} mg g^{-1}	0.69 ± 0.18	0.73 ± 0.17	0.71 ± 0.19	0.64 ± 0.19	0.42
K_{Dry} mg g^{-1}	1.82 ± 0.52	1.88 ± 0.41	1.97 ± 0.57	1.62 ± 0.54	0.22
% water	60.9 ± 8.2	62.9 ± 6.4	61.0 ± 9.9	58.8 ± 8.0	0.47

Data presented as mean ± SD. Difference between age groups was analysed using one-way Anova with post-hoc Bonferonni algorithm. P value < 0.05 taken to be significant

Women had lower skin K^+_{Wet} and skin K^+_{Dry} and a trend for lower skin Na^+_{Wet} and skin Na^+_{Dry} compared to men. No significant correlations were seen between Na^+_{Wet} or Na^+_{Dry} and putative parameters such age, BMI, BSA, SBP, DBP or MAP (Table 3.5 and 3.6). A significant correlation was seen between skin Na^+_{Wet} and K^+_{Wet} ($r = 0.47$, $p = 0.003$) as seen in Figure 3.2.

Table 3.5: Correlation between skin Na^{+}_{Wet} and putative variables in VARSITY methods.

Variable	Correlation Coefficient	Significance
Age, years	0.16	0.34
BMI, Kg/m^2	- 0.19	0.28
BSA, m^2	- 0.04	0.83
SBP, mmHg	- 0.22	0.19
DBP, mmHg	- 0.29	0.09
MAP, mmHg	- 0.27	0.11
Renin, mU/l	- 0.07	0.67
Aldosterone, pmol/l	- 0.04	0.83
VEGF-C pg/ml	- 0.04	0.84

Table 3.6: Correlation between skin Na^{+}_{Dry} and putative variables in VARSITY methods.

Variable	Correlation Coefficient	Significance
Age, years	0.01	0.97
BMI, Kg/m^2	0.10	0.55
BSA, m^2	0.23	0.17
SBP, mmHg	0.06	0.74
DBP, mmHg	0.12	0.47
MAP, mmHg	0.10	0.57
Renin, mU/l	0.03	0.87
Aldosterone, pmol/l	0.01	0.98
VEGF-C, pg/ml	0.10	0.57

Data presented as mean ± SD. Correlation and significance was determined using the Pearson's correlation test.

Figure 3.2: Relationship between skin Na^{+}_{Wet} and K^{+}_{Wet} in VARSITY methods (n = 37).

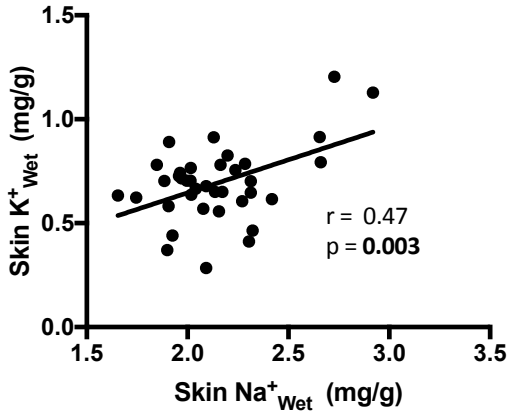

3.4.5 Comparison with Tissue Bank samples

Comparison between skin biochemical parameters for VARSITY methods and Tissue Bank samples is shown in Table 3.7. There was no significant difference in Skin Na^{+}_{Dry} or Skin Na^{+}_{Wet} between both sets of samples. Levels of skin K^{+} per unit wet weight (K^{+}_{Wet}) was lower in the Tissue Bank samples (0.57 ± 0.17 mg/g vs 0.69 ± 0.76 mg/g; p = 0.02). There was no significant difference skin K^{+} per unit wet dry weight. Tissue Bank samples were significantly larger than Varsity methods samples (0.062 ± 0.0026 mg vs. 0.023 ± 0.009 mg, p < 0.001). The measured water content was similar between both sample sets (62.3 ± 6.5 % vs. 60.9 ± 8.3 %, p = 0.29).

Table 3.7: Skin biochemical parameters Tissue Bank skin samples compared with Varsity Methods

	Varsity methods	Tissue Bank	P for difference
n	17	37	
Age	43 ± 16	39 ± 16	0.38
Gender (M/F)	0/17	18/19	-
Skin Na_{Wet} mg g^{-1}	2.25 ± 0.23	2.15 ± 0.27	0.18
Skin Na_{Dry} mg g^{-1}	6.35 ± 1.76	5.69 ± 1.30	0.17
Skin Na (mmol/l)	156.2 ± 8.8	157.6 ± 41.6	0.89
Skin K_{Wet} mg g^{-1}	0.57 ± 0.17	0.69 ± 0.76	**0.02**
Skin K_{Dry} mg g^{-1}	1.56 ± 0.50	1.82 ± 0.52	**0.10**
Wet weight g	0.062 ± 0.026	0.023 ± 0.009	**< 0.001**
% water	62.3 ± 6.5	60.9 ± 8.3	0.29

Data presented as mean ± SD. Difference between groups was analysed using the unpaired t test with normally distributed data and the Mann-Whitney U test for non-normal data. P value < 0.05 taken to be significant.

3.5 DISCUSSION

The Varsity methods study showed that human skin Na^+ and K^+ can be quantified in healthy humans using skin biopsies and ICP-OES. No significant associations were seen between skin Na^+ and age, BP or other putative parameters. The use of local anaesthetic did not appear to affect skin Na^+ and water content.

Table 3.8 shows all studies of that analysed Na^+ or K^+ in full thickness skin, with data from Varsity methods included for comparison. It can be seen that the values for skin Na^+, K^+ and water content are within the range of values for previous direct chemical measurements in full thickness human skin done more than 70 years ago. [181-184,186] These studies used precipitation techniques to quantify skin electrolyes, which would have had greater variability and less sensitivity than ICP-OES. Recently, during the course of this work, 2 further studies on skin Na^+ analysis using modern techniques were published. [143,195] Kopp et all used atomic spectroscopy to measure wet skin Na^+ in cadaveric calf skin. Their values for wet skin Na^+ appeared lower than in VARSITY methods, though cadaveric tissue could have had elemental shifts secondary to tissue autolysis. [194] Fischereder et al used ICP-OES to measure skin Na^+ and K^+ in abdominal skin obtained from 27 kidney transplant recipients on haemodialysis and 21 healthy donors under general anaesthetic. [143] This group used a similar technique for skin elemental analysis but used a pressure digestion system instead of freeze drying. Their values for skin Na^+_{Dry} were similar to Varsity methods, but with higher variability. Fischereder et al analysed skin Na^+_{Wet} in their 48 patients and their values showed a significant variability of 1.0 - 14.0 mg/g. [143]

Table 3.8: Previous studies assessing skin Na^+ and K^+ content in full thickness skin samples with data from VARSITY methods included for comparisons. [143,181-184,186,195]

Study	Study Size	Source	Local anaesthetic	Analysis method	Na^+ (wet) mg/g	Na^+ (dry) mg/g	K^+ (wet) mg/g	K^+ (dry) mg/g	% Water
Brown 1926	10	Epidermis & dermis Chest and waist Cadavers	Nil	Precipitation with $BaCl_2$	-	3.60 ± 0.37	-	2.39 ± 0.51	
Brown 1927	27	Epidermis & dermis Chest and waist Cadavers	Nil	Precipitation with $BaCl_2$	1.58 ± 0.20	-	0.91 ± 0.24	-	63.5 ± 3.7
Urbach 1928	26	Epidermis & dermis Various regions Healthy volunteers	Nil	Precipitation	0.95 – 1.39	-	-	-	
Cornbleet 1942	10	Epidermis & dermis Various regions Healthy volunteers	Nil	Calorimetric method (Yoshimatsu)	-	3.50 ± 0.02	-	2.47 ± 0.04	
Eisele 1945	18	Epidermis and dermis Mastectomies Limb amputations	Nil	Butler-Tuthill method	2.14 ± 0.18	7.56 ± 1.03	0.64 ± 0.13	2.28 ± 0.50	70.8 ± 20.1
Kopp 2011	21	Epidermis & dermis Calf Limb amputations	Nil	Atomic spectrometry	1.77 ± 0.37	-	-	-	
VARSITY methods	**37**	**Epidermis & dermis** **Lower back**	**Yes**	**ICP-OES**	**2.15 ± 0.27**	**6.11 ± 1.17**	**0.57 ± 0.17**	**2.06 ± 0.52**	**62.4 ± 9.0**
Fischereder 2017	21	Epidermis & dermis Abdomen Healthy kidney donors	Nil	ICP-OES	-	6.57 ± 4.03	-	1.76 ± 1.09	
Fischereder 2017	27	Epidermis & dermis Abdomen Dialysis patients	Nil	ICP-OES	-	7.05 ± 3.34	-	1.92 ± 0.98	

Elemental measurements per wet weight of tissue may have potential inaccuracies introduced by changes in sample hydration during sample processing, which is why previous animal studies expressed skin Na^+ and K^+ concentrations per unit dry weight after samples underwent dry ashing. [134,244,245] There is no definite consensus on how skin electrolyte concentrations should be expressed. For the purpose of making comparisons to previous studies and evaluating the normal variation in healthy subjects, skin Na^+ and K^+ in this study were expressed in terms wet and dry weight.

The use of lidocaine 1% local anaesthetic for skin biopsies was a potential source of sodium

and water contamination for VARSITY methods. Comparison with Tissue Bank samples showed no significant difference is skin Na^+ or water content (Table 3.7). This suggests no significant sodium and water contamination for VARSITY methods. Furthermore, previous studies which did not use local anaesthetic and had similar skin Na^+ values (Table 3.8).

^{23}Na-MRI studies assessing in human skin in-vivo showed a variation of skin Na^+ storage with age and sex and a positive correlation between skin Na^+ and SBP. [195,197,198,204] This has not been shown by this study or other previous studies that involved direct chemical measurements of skin Na^+**.**[143,181-184,186,195,197,204] Skin Na^+ quantification with ^{23}Na-MRI has yielded values ranging from 10-40 mmol/l of water. [195,197,198,204] In VARSITY methods mean Na^+:water ratio was higher at 157.6 mmol/l (range 118.6 - 236.1 mmol/l). This indicates a difference in sensitivity between both techniques for quantifying skin Na^+, whereby ^{23}Na MRI may quantify Na^+ in ionised form and bound to GAGs differently, as suggested by previous ^{23}Na MRI studies in cartilage. [259] It is also not known if skin sodium follows a topographical variation. This could be of relevance as it may explain some of the differences between ^{23}Na MRI analysis of calf skin and the analysis of back skin in VARSITY methods, as well as previous studies that looked at skin from various regions (Table 3.8).

Skin K^+appeared to be lower in women than in men (Table 3.4) and lower in the Tissue Bank breast skin samples compared to VARSITY methods (Table 3.7). The reasons for these observations is unclear and previous studies did not evaluate sex specific differences in skin K^+.[181,182,184,186-188]The epidermis has a significant K^+ content and this difference could be explained by the epidermis being thinner in women. [188,260] Structural differences between lower back and breast skin could potentially explain differences in skin K^+ content. There was a trend for lower skin Na^+ in women in VARSITY methods, in keeping with the findings in ^{23}Na MRI studies which showed lower Na^+ skin storage in women. The reasons for this are unclear. Men have a thicker epidermis and dermis at all ages and may have higher levels of dermal glycosaminoglycans, leading to sex-specific difference in skin Na^+ storage [261,262]

As shown above the values obtained for skin mean Na^+: water ratio show a higher ratio than plasma**,** which may be in keeping with the existence of non-osmotic sodium storage in the

skin as observed in previous rat studies. [132,133,244,245] In this study, the mean skin Na^+ concentration was 2.15 mg/g of wet weight. If skin sodium follows a uniform distribution, in a 70 kg human with skin constituting 6 % of body wet weight, this translates into a total Na^+ content of approximately 8.6 g on a basal salt intake of 7g a day. This approximates to around 10 - 14 % of total body sodium. [263]

Skin Na^+ positively correlated with skin K^+ per wet weight of skin (Figure 3.1) This finding was noted recently by Fischereder et al and could reflect the balance of intracellular and extracellular cations in the skin.[143] Further work is needed to understand the relevance the mechanisms underpinning this relationship.

There are several limitations to this pilot study. VARSITY methods had a small study size and data from 11 participants were retrospectively excluded because of analytical issues, and this would limit the generalisability of its findings and the ability to detect significant relationships between skin Na^+ and other parameters. Our skin biopsies were small and taken from the lower back, and we had no means of ascertaining if they were representative of the whole skin or if skin Na^+ varies with region and time.

3.6 CONCLUSIONS

This pilot study has shown the feasibility of skin elemental analysis with ICP-OES using the techniques described. The sex differences in skin electrolytes observed were further evaluated in our main study.

Chapter 4 VARSITY STUDY

4.1 INTRODUCTION

Large population studies suggest that excessive dietary sodium, principally as the chloride salt, is an important trigger for hypertension. [34,36] The mechanisms for this relationship are still debated. [42,45] Recent observations oppose the traditional view that body sodium balance functions as a two-compartment model, supporting the existence of non-osmotic sodium retention in a third compartment. In support of this, studies in rat models have shown that the skin is capable of osmotically inactive Na^+ storage, via glycosaminoglycans, serving as an important mechanism for buffering volume and blood pressure changes with salt intake. [131,133,134] High salt intake in rats also stimulates tonicity-responsive enhancer binding protein (TonEBP;NFAT5) secretion by mononuclear phagocyte system (MPS) cells, which mediates vascular endothelial growth factor C (VEGF-C) expression. This results in enhanced interstitial lymphatic drainage and increased expression of endothelial nitric oxide synthase (eNOS), which buffers the hemodynamic response to salt loading. [133,134] However, the relevance of these mechanisms in humans is unclear.

Previous studies have not examined the relationship between dietary salt, skin $Na^+$and blood pressure. A few studies have examined VEGF-C in humans, with plasma VEGF-C being shown to be higher in hypertensives compared to normotensives and a trend for decline in circulating VEGF-C with age. [133,198] Recent ^{23}Na magnetic resonance imaging (MRI) studies in humans have shown a direct relationship between skin Na^+ and BP, as well as age and sex differences in the capacity to store skin Na^+.[197,204] Although MRI data were confirmed by direct ashing of human cadaveric samples, they have not yet been confirmed by direct chemical analysis of skin electrolytes in humans. [195] Moreover,^{23}Na MRI has not been used to measure changes in skin Na^+ with dietary salt modulation.

The ability to taste salt, or salt taste sensitivity, is believed to be a primary determinant of salt intake. The threshold for detect the taste of salt has been observed to be greater in subjects with hypertension and diabetes, and positively correlated with age and BP. [264,265] Mechanisms for these observations are unclear. The transduction of the taste of salt is believed to occur via specific apical amiloride -sensitive (ENaC) sodium channels in the

lingual epithelium and factors such as aldosterone secretion and dietary salt depletion are known to modulate this process. [266-268] It is unknown if VEGF-C influences the ability to taste salt.

Capillary rarefaction is the reduction in the density of capillaries and has been observed in the skin of hypertensives using video microscopy, and is believed to influence systemic BP and target organ damage [11,224,225] Salt intake has been shown to influence skin capillary rarefaction in subjects with mild hypertension, with a negative correlation seen between skin capillary density and urine sodium excretion. [11] The relevance of skin capillary rarefaction and the effect of dietary salt modulation on skin capillary density in healthy subjects is uncertain.

On this background the VARSITY study was a double-blind, randomized, crossover study in healthy subjects comparing the effects of a high and low dietary salt intake on skin electrolytes, haemodynamic and biochemical variables, including plasma VEGF C. Therefore, the work in this chapter sought to determine if the mechanisms described in rodent skin models function in humans. Furthermore, the VARSITY study assessed changes in skin capillary density and ability of subjects to detect the taste of salt with dietary salt modulation.

4.2 HYPOTHESES

Primary hypothesis:

Skin Na^+ and plasma VEGF-C increase with dietary salt loading and the degree of BP change relates to the change in these parameters - individuals with a greater rise in skin Na^+ and VEGF-C will have the smallest rise in blood pressure.

Secondary hypotheses:

. Skin Na^+ is positively associated with plasma VEGF-C levels, blood pressure and other hemodynamic variables.

. The ability to taste sodium is positively associated with plasma VEGF-C levels.

. Skin capillary density decreases with dietary salt loading and correlates with skin Na^+

4.3 AIMS

Primary aim:

To study the change in skin Na^+ with an increased dietary salt intake by direct chemical measurements in young healthy adults.

Secondary aims:

To study the following:

1. The change in the following variables with dietary salt modulation:
   - Plasma VEGF-C and sFLT-4 (soluble receptor for VEGF-C)
   - Plasma renin and aldosterone
   - Blood pressure (clinic and ambulatory)
   - Cardiac output (CO) and peripheral vascular resistance (PVR)
   - Arterial stiffness (as measured with pulse wave velocity and augmentation index)
   - Heart rate variability (a measure of autonomic nervous system activity)
   - Ability to taste salt
   - Skin capillary density

2 The correlation between skin sodium, blood pressure, other hemodynamic variables and plasma VEGF-C.

3 The relationship between the ability to taste sodium and plasma VEGF-C levels.

4 The effect of dietary salt on skin capillary density.

4.4 METHODS

4.4.1 Study design and protocol

The VARSITY study was a 4-week single-centre, double-blind, randomized, crossover study as depicted in 4.1. Volunteers were screened and placed on a 4g low salt diet (equivalent to 70 mmol of sodium/day) at visit 1 to standardize the background sodium intake. Participants were outpatients and given a printed booklet provided by practicing dietitians on how to maintain a low salt diet, with email and telephone advice offered throughout the duration of the study. Baseline salt consumption was assessed by checking 24-hour urinary sodium excretion (UNaV) up to 3 days after visit 1.

Figure 4.1 Illustration of the VARSITY study's 4-week double blind crossover design. Participants had a 7-day run in on a 4g low salt diet before being asked to take either 200 mmol slow sodium or placebo tablets for 7 days. This was followed by a 7-day washout period before they received the second treatment for 7 days. A skin biopsy was taken after 7 days of 200 mmol slow sodium and placebo.

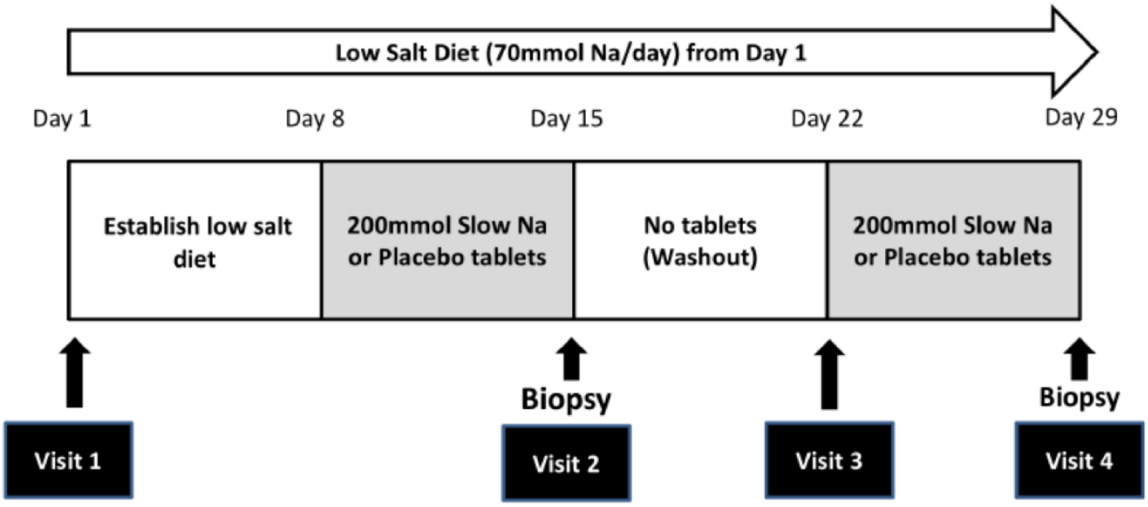

Participants with high baseline salt intakes were given further advice on dietary salt restriction. After a 1-week run-in period on a low-sodium diet, participants then received at 200 mmol/day of slow sodium tablets (HK Pharma, UK) for 7 days or an equal number of placebo tablets (99.25 % lactose, 0.75 % magnesium stearate; Rayonex, UK) during weeks 2 and 4. The order of treatment was randomised. Study compliance was assessed by checking 24-hour UNaV within 48 hours of visits 2, 3, and 4, with participants and investigators blinded to the results. Medication compliance was assessed by participants returning used tablet bottles. Each participant was seen at approximately the same time at each study visit in a temperature-controlled study room. Weight was measured at every visit using the same calibrated scales, with one layer of clothing and no shoes. Participants were required to refrain from caffeine, alcohol, strenuous exercise and the application of moisturizer or fake tan to their lower back for 6 hours prior to study visits. At each visit, seated brachial BP was recorded after a minimum of 5 minutes rest. After a further 10 minutes rest in supine position, brachial BP, CO, stroke volume (SV), pulse wave analysis, aortic pulse wave velocity and heart rate variability were taken.

Ambulatory blood pressure monitoring (ABPM) was carried out with the 24-hour UNaV collections within 48 hours of visits 2, 3, and 4. Venepuncture and venous blood samples were collected in a standard 4.7 ml serum gel tube for electrolytes, a 2.6 ml EDTA tube for plasma renin and aldosterone and a 4.7 ml EDTA tube for plasma VEGF-C and sFLT-4. At each visit, the participants' ability to taste salt was tested with salt solutions of different strengths. At visits 2 and 4, a skin capillaroscopy and a skin biopsy was carried out after hemodynamic measurements.

4.4.1.1 Study blinding and randomisation

The order in which the participants received placebo or slow sodium tablets was determined with automated randomisation computer program (Microsoft excel version 14.0). This was conducted by Dr Kaisa Mäki-Petäjä from the EMIT unit before the start of the study, who labelled the order of placebo and slow sodium tablets in pre-prepared bottles. I was blinded to the randomisation and tablet preparation. The randomisation code was kept by Dr Kaisa Mäki-Petäjä and used by her for unblinding following skin elemental analysis and analysis of haemodynamic and biochemical variables.

4.4.2 Subjects

Participants were healthy individuals aged between 18 and 50 years and recruited by advertisement. Exclusion criteria included hypertension (sustained blood pressure>140/90 mm Hg), current use of antihypertensive drugs, diuretics, salt supplements**,** renal impairment, or pregnancy. All participants gave informed consent prior to study participation. Ethical approval for the study was obtained from a National Research Ethics Committee (REC Reference: 11/H0304/003) and was performed according to Good Clinical Practice and according to the principles of the Declaration of Helsinki.

4.4.3 Haemodynamic assessments

4.4.3.1 Blood pressure

4.4.3.1.1 Clinic blood pressure

In all participants, brachial blood pressure was measured using a validated semi-automated oscillometric device (HEM-705CP, Omron Corporation) after 5 minutes of rest in seated position BP was measured in the non-dominant arm in triplicate, with approximately a 1-minute interval between readings. The average of three readings was recorded in use for analysis. Further readings were taken if there was a difference of > 5 mmHg was observed between the 2nd and 3rd readings. After 10 minutes rest in supine position, brachial blood pressure was taken in an identical manner.

4.4.3.1.2 Ambulatory blood pressure

Ambulatory blood pressure monitoring (ABPM) was carried out within 48 hours of each visit using Mobil-O-Graph® (IEM, USA). The ABPM device was placed on the non-dominant arm. Ambulatory BP recordings were analysed with the Mobil-O-Graph® system software package. A total of 40 readings were taken in a 24-hour period - 30 during the day (0800 - 2159 hrs) and 10 at night (2200 - 0759 hrs). ABPM Recordings were rejected if less than 30 readings were recorded.

4.4.3.2 Central haemodynamic measurements

4.4.3.2.1 Pulse wave analysis and arterial wave reflections

Radial artery waveforms were measured using a high-fidelity micromanometer (SPC- 301; Millar Instruments) from the wrist of the non-dominant arm with the participant lying supine after a further five minutes of rest, as previously described. [269] Pulse wave analysis was carried out using SphygmoCor software (AtCor Medical, Sydney) was used to calculate augmentation index (AIx), the difference in pressure between the first and second systolic peaks of the pulse wave, expressed as a percentage of the pulse pressure. AIx

measurements with an operator index of below 80% were rejected. Heart rate was recorded during measurement of the radial artery waveform and central mean arterial pressure (MAP) was obtained as the value given by the software derived from integration of the waveform, as previously described. [269] The equipment used for pulse wave analysis and a typical SphygmoCor software output are shown in Figures 4.2 and 4.3 respectively.

Figure 4.2: Equipment used for pulse wave analysis.

Figure 4.3: An example of SphygmoCor software output for pulse wave analysis.

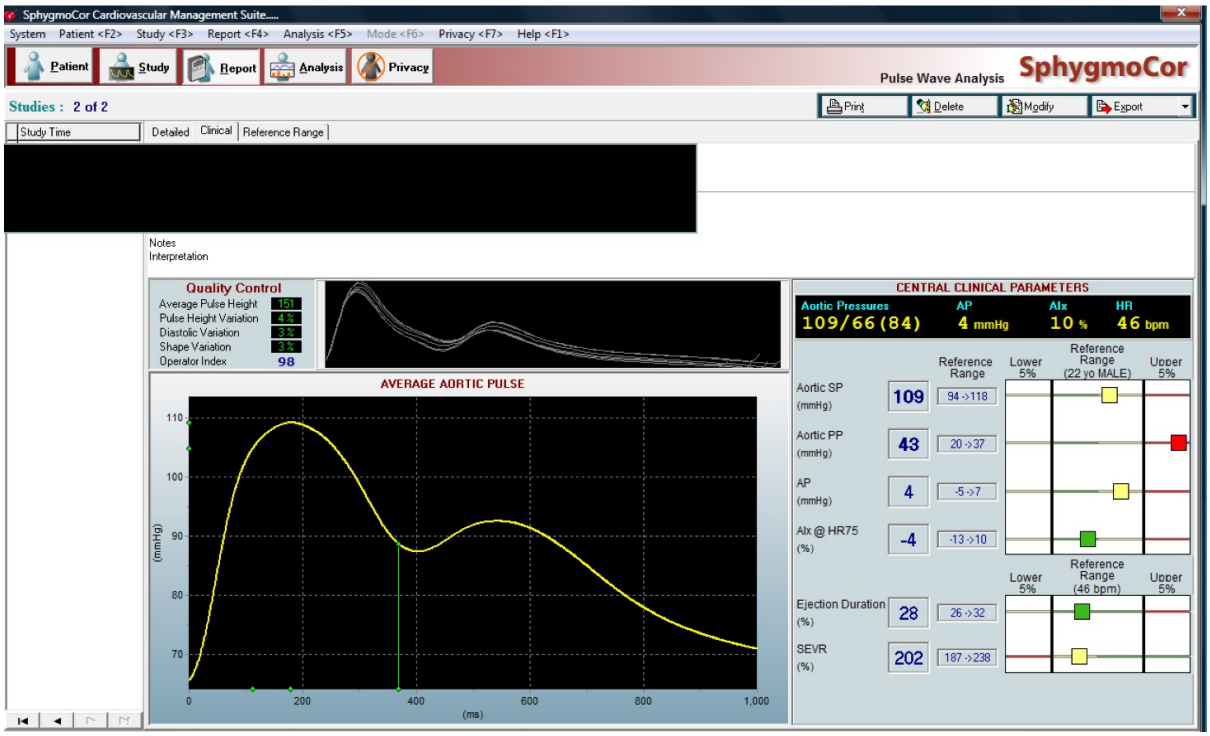

4.4.3.2.2 Aortic pulse wave velocity

Carotid-femoral aortic pulse wave velocity (aPWV) was measured using the SphygmoCor system (AtCor Medical, Sydney). Subjects had at least 15 minutes rest before supine blood pressure was measured in triplicate and the mean was entered into the SphygmoCor software. Electrocardiogram (ECG) electrodes were attached to each subject to enable gating of arterial waveforms when they were recorded. Sequentially recording of ECG-gated carotid and femoral artery waveforms was then performed using applanation tonometry, as described previously. [269] Waveforms were gated to the ECG R wave. Measurements were made in triplicate. The path-length for the determination of aPWV was measured as the surface distance between the suprasternal notch and femoral site minus the distance between the suprasternal notch and point of maximum carotid pulsation, which was marked in the skin. This measurement was made using a tape measure and entered into the software. aPWV was calculated by the SphygmoCor software, dividing the surface distance by the by the wave transit time. The mean of 2 aPWV readings was taken and accepted if the SD was less than ± 0.5 m/s. The method used to calculate aPWV is illustrated in Figure 4.4.

Pulse wave analysis and arterial wave reflections and aortic pulse wave velocity were performed by myself after I received training from Dr Kaisa Mäki-Petäjä and Jean Smith and Jean Woodcock Smith. I performed measurements independently after I was able to achieve AIx measurements with an operator index of below 80% and aPWV readings with SD of less than ± 0.5 m/s.

Figure 4.4: The method used to calculate aPWV

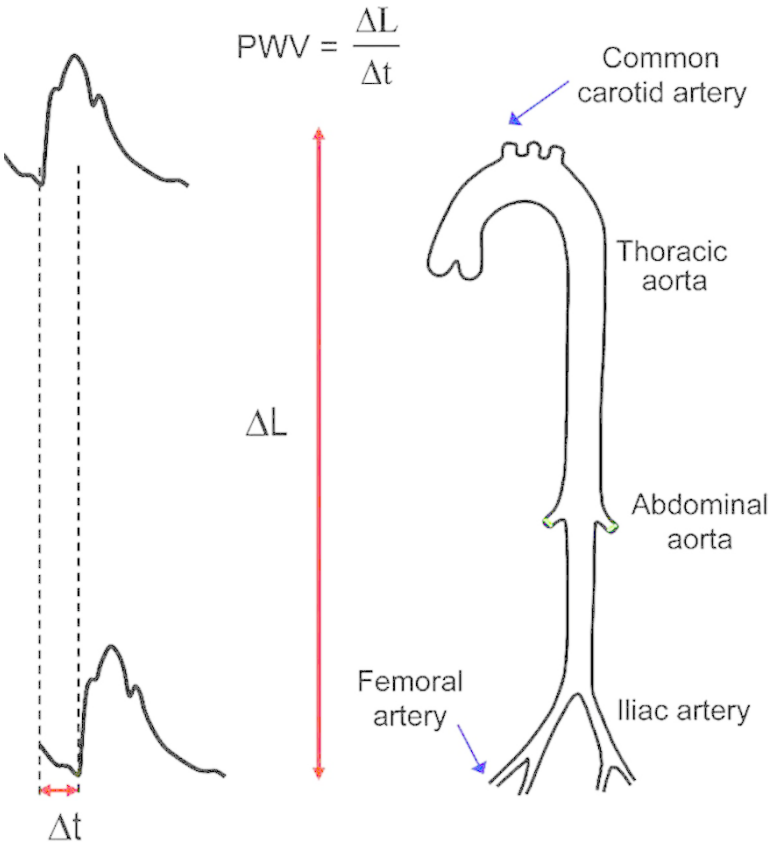

Figure 4.5: An example of a SphygmoCor aPWV output.

4.4.3.3 Cardiac output

Cardiac output (CO) and stroke volume (SV) were determined by a non-invasive, inert gas rebreathing technique with the InnoCor$_{TM}$ gas analyser system (Innovision, Odense, Denmark) as shown in Figures 4.6 and 4.7. In this technique, the concentration of an absorbed gas (nitrous oxide, N2O) and a non-absorbed gas (sulphur hexafluoride, SF6) using a photoacoustic multi-gas analyser. The difference in absorption of the two gases is proportional to pulmonary blood flow, and hence cardiac output. This technique has previously been validated against thermodilution and direct Fick methods for measurement of pulmonary blood flow and cardiac output. [270-274] CO and SV were analysed after central haemodynamic measurements were taken. While resting in supine position, subjects continuously rebreathed a gas mixture (1% Sulphur hexafluoride, 5% Nitrous oxide, and 94% oxygen) over 20 seconds with a respiratory rate of 20 breaths/min. Continuous samples of expired gases were analysed by an infrared photoacoustic gas analyser (InnoCor; Innovision A/S, Chicago, IL, USA) to determine CO and SV. All measurements were taken by myself after

I received training from Dr Kaisa Mäki-Petäjä.

Figure 4.6: Equipment used for the Innocor® inert gas rebreathing technique.

Figure 4.7: An example of InnoCor® software output.

4.4.3.4 Peripheral vascular resistance

Peripheral vascular resistance (PVR) was calculated using supine mean arterial pressure within 1 hour of Innocor measurements as follows:

$$\text{PVR (dynes s}^{-1}\text{cm}^{-5}) = \frac{\text{Mean arterial pressure (mmHg) x 80}}{\text{Cardiac output (l min}^{-1})}$$

4.4.3.5 Heart rate variability

Heart rate variability (HRV) was measured at every visit using the SphygmoCor$_{TM}$ HRV System, as previously described. [275] This system utilises a 3-lead ECG to non-invasively provide an assessment of sympathetic and para-sympathetic autonomic function in both the time and frequency domains, using software that calculates the statistical parameters of the normal R–R intervals by excluding ectopic beats of the electrocardiogram (ECG). Participants initially had a resting 12-lead electrocardiograph at screening to confirm the presence of normal sinus rhythm. HRV was measured at rest in the supine position over a period of 10 minutes with participants placed in a quiet, darkened room at approximately the same time of day at every visit. Participants are asked to maintain a regular breathing pattern during measurements. An example of HRV data output on the SphygmoCor$_{TM}$ system is shown in Figure 4.8. The variables measured were:

3. power in the low-frequency (LF) range, representing mostly sympathetic activity
4. power in the high-frequency (HF) range, representing parasympathetic function and is considered to be a marker of vagal activity
5. total power of all frequencies, representing all cyclic components of HRV

The high frequency and low frequency components of HRV were normalized by dividing their absolute powers by the sum of high-frequency power and low-frequency power (total power), multiplied by 100. I performed all HRV measurements after I received training from Dr Kaisa Mäki-Petäjä and Jean Smith and Jean Woodcock Smith.

Fig 4.8: HRV data output obtained using SphygmoCor$_{TM}$ HRV System. As seen above spectral analysis of a series of successive R-R intervals provides the frequency domain analysis. This divides the heart rate spectrum into different components that quantify sympathetic and vagal influences on the heart: Total Power, High Frequency Power and Low Frequency Power.

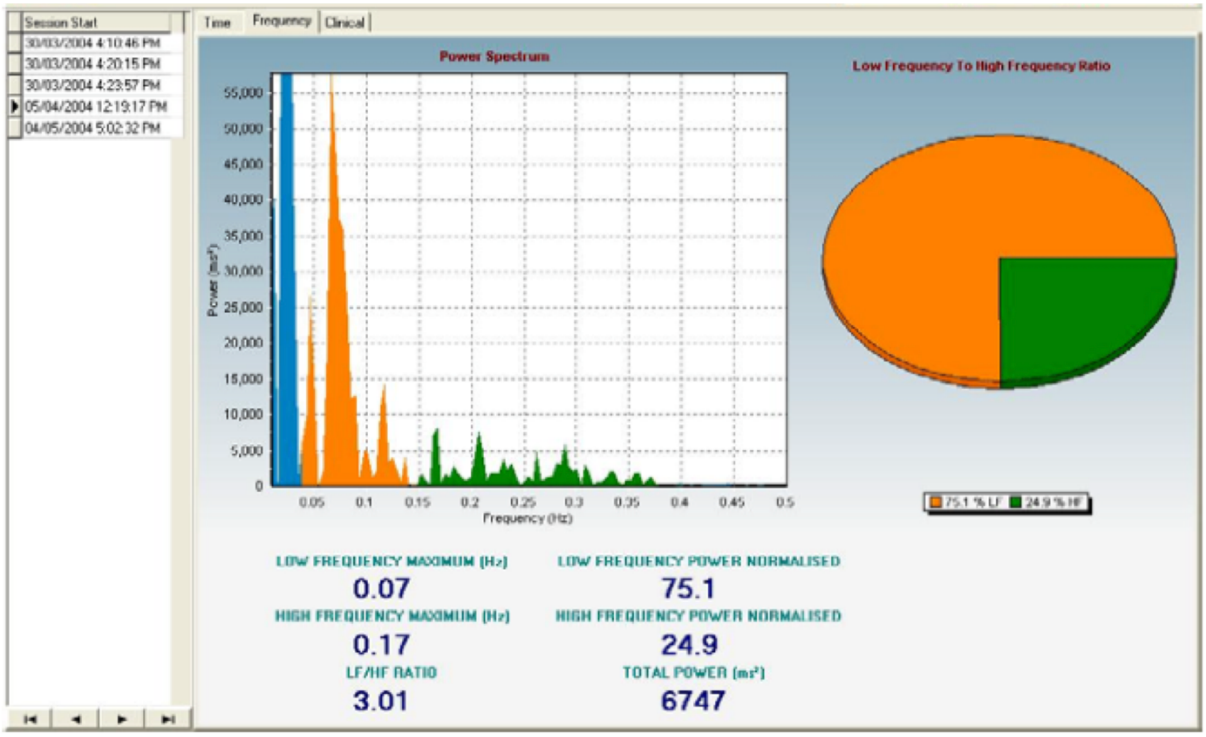

4.4.4 Biochemical measurements

4.4.4.1 Serum and plasma biochemistry

Serum electrolytes (Na^+, K^+, Cl^- and creatinine), plasma renin and plasma aldosterone were measured in an accredited laboratory (Cambridge University Hospitals Department of Clinical Biochemistry). Estimated glomerular filtration rate was measured using the Modification of Diet in Renal Disease (MDRD) formula. [255]

4.4.4.2 VEGF-C and sFLT-4

Plasma VEGF-C and sFLT-4 were measured at each visit. For each participant, a single EDTA sample was centrifuged at 4°C (3200 rpm for 15 minutes), and the plasma separated and stored at - 80°C prior to analysis for VEGF-C and sFLT-4 (soluble receptor for VEGF-C) by sandwich immunoassay. For VEGF-C, in view of the high standard deviation for our previous assay, we used an alternative Quantikine ELISA kits from R&D Systems (Abingdon, United Kingdom). This was recently used for a similar study on the effect of dietary salt modulation on plasma VEGF-C. [159] sFLT-4 was measured by an in-house electrochemical luminescence immunoassay on the MesoScale Discovery (Rockville, MA, USA) assay platform using antibodies and standards from an R&D Systems DuoSet at the Core Biochemical Assay Laboratory (CBAL) in Cambridge. Reproducibility of the VEGF-C and sFLT-4 assays were checked by the team at CBAL by running quality control samples at the beginning and end of each batch.

4.4.4.3 24-hour urine biochemistry

The 24-hour urine collections were made for Na^+, K^+, Cl^- , creatinine and albumin within 48 hours of each visit, starting at 08:00 and discarding the first morning void. Urine electrolytes were measured in an accredited laboratory (Cambridge University Hospitals Department of Clinical Biochemistry). Samples with a 24-hour urine creatinine value of less than 5.3 mmol, the lower limit of normal at the Cambridge University Hospitals Department of Clinical Biochemistry, were regarded as incomplete and rejected. Urinary creatinine clearance was calculated using the following formula as previously described[276]:

$$\text{Creatinine clearance (ml/min)} = \frac{\text{Urine Creatinine concentration (mmol) x urine volume (ml)}}{\text{Plasma creatinine (mmol) x 1440}} \text{ x 1440}$$

Creatinine clearance (ml/min) = [Urine Creatinine concentration (mmol) x urine volume (ml)]/plasma creatinine (mmol) x 1440

Fractional excretion of sodium (FeNa) is the percentage of the sodium filtered by the kidney which is excreted in the urine. This was measured in 24-hour urine collections using the following formula as previously described[277]:

$$\text{Fractional Excretion of Sodium (FENa)} = \frac{\text{Urine sodium (mmol) x Serum Creatinine (mmol)}}{\text{Serum Na (mmol) x Urine Creatinine (mmol)}} \text{ x 100}$$

4.4.5 Skin biopsy procedure

As described in 2.2, skin punch biopsies of 5mm diameter were taken from the lower back, using local anaesthetic (lidocaine) by myself. The first biopsy was done on the right at the 2nd visit. The second biopsy was done on the left at the 4th visit in an approximately symmetrical position. Any fat obtained with the biopsied tissue was removed. Skin samples were placed in cryovials and snap frozen in liquid nitrogen once they were obtained and then stored at −80°C until analysis. As described in 2.5, after 32 participants completed the study, we developed Na^+-free lidocaine using Dextrose as an excipient (Lidocaine 1% with Dextrose 3.5%, Tayside Pharmaceuticals, Dundee). This was used in the remaining 16 participants. Skin Na^+ values for obtained with each type of local anaesthetic were compared at the end of the study.

4.4.6 Skin elemental analysis

Skin samples were halved longitudinally with a scalpel under microscopic view, ensuring even splitting of the epidermis and dermis, as described in 2.5.3. One portion of each skin sample was sent on dry ice to the MRC Elsie Widdowson laboratory to determine Na^+, K^+ and water content by ICP-OES analysis as previously described in 2.2. The remaining portion was

stored at −80°C in the EMIT unit for further analysis. The procedures for sample preparation for ICP-OES were carried out as outlined in 2.3.2 and 2.3.3.

4.4.7 Expression of skin elemental concentrations

Skin Na^+ and K^+ concentrations and water content were calculated and expressed as described in 2.3.5. Elemental measurements per wet weight of tissue may have potential inaccuracies introduced by changes in sample hydration during sample processing, which is why previous animal studies or skin Na^+ with dietary modulation expressed skin Na^+ and K^+ concentrations per unit dry weight after samples underwent dry ashing. [134,244,245]Therefore, Na^+_{Dry} was used to compare changes in skin Na^+ with salt loading.

4.4.8 Assessment of drying consistency

This was assessed as described in 2.3.6.

4.4.9 Salt taste sensitivity

Salt taste sensitivity in participants was evaluated using a staircase method with paired difference testing, which was originally described by Cornsweet and used in previous studies of salt taste sensitivity. [264,265,278,279]. Salt (NaCl) solutions of different concentrations were made up by dissolving table salt (Waitrose, UK), weighed with a digital weighing scale (Mettler PM 400, Hampton) in double distilled deionised water obtained by reverse osmosis (ROS) using a Fresenius AquaUNO$_{TM}$ system at the Addenbrookes Hospital Haemodialysis unit. 6 solutions of NaCl at concentrations 0.05%, 0.10%, 0.2%, 0.4%, 0.8% and 1.6% were used in the test. These were constituted as follows:

1. 0.05% NaCl - 0.05 g NaCl in 100 ml ROS water
2. 0.1% NaCl - 0.1 g NaCl in 100 ml ROS water
3. 0.2% NaCl - 0.2 g NaCl in 100 ml ROS water
4. 0.4% NaCl - 0.4 g NaCl in 100 ml ROS water
5. 0.8% NaCl - 0.8 g NaCl in 100 ml ROS water
6. 1.6% NaCl - 1.6 g NaCl in 100 ml ROS water

Salt taste testing was carried out in a single-blind manner by myself. Each participant was presented with a pair of liquids (salt solution and ROS water) in a random order with increasing concentrations of NaCl (as shown in Table 4.1), and asked if either solution contains salt. A whole-mouth gustatory test procedure was used for the different solutions. Participants were asked to apply 1 ml of solution evenly on the tongue using a 5 ml syringe, hold the solution for a few seconds and then swallow it. Participants were each given a cup of ROS water to rinse their mouths before tasting each solution. The following 2 parameters for salt taste sensitivity were assessed:

Salt recognition threshold - This was the lowest concentration of NaCl at which the participant recognized the solution as being salty. [280] This is a measure of salt taste sensitivity.

Salt detection threshold - This was the lowest concentration at which a participant could distinguish between ROS water and salt solution. [281] This is a measure of salt taste acuity.

Table 4.1: Scheme and order of solutions used to test salt taste sensitivity. Participants we given solutions in the order A - F with solution 1 and 2 given in random order.

Solution	Salt – Y/N	**Solution**	Salt – Y/N
Solution A1 0% NaCl		Solution A2 0.05% NaCl	
Solution B1 0% NaCl		Solution B2 0.1% NaCl	
Solution C1 0% NaCl		Solution C2 0.2% NaCl	
Solution D1 0% NaCl		Solution D2 0.4% NaCl	
Solution E1 0% NaCl		Solution E2 0.8% NaCl	
Solution F1 0% NaCl		Solution F2 1.6% NaCl	

Published values for salt detection and recognition threshold have varied in the literature with different techniques used. Rabin et al recorded a mean salt detection threshold of the 0.165 % in 203 normotensive adults. [282] Choe et al recorded salt recognition threshold range of 0.045 - 0.285% in 218 healthy adults. [283] Prior to being used in the VARSITY study the above solutions were tested on 3 volunteers from the EMIT unit. 2 recorded salt recognition thresholds of 0.2 % NaCl and the 3rd recorded a threshold of 0.1 %.On the basis of these observations the range of salt concentrations in Table 4.1 were chosen for the VARSITY study. Salt recognition and detection thresholds were assessed in all participants in each visit after haemodynamic measurements at Visits 1 and 3, and after capillaroscopy at Visits 2 and 4.

4.4.10 Skin capillaroscopy

Skin capillary density was measured by intravital microscopy following a validated technique. [225,284] Participants were studied at approximately the same time between 0900 and 1100 on visit 2 and 4 and were asked to have an overnight fast from midnight prior to these visits. Measurements were carried out in a temperature-controlled room (21 – 24 degrees Celsius) after at least 20 minutes of acclimatisation. Measurements were performed in the morning with participants in the seated position and the left hand supported at the level of the heart. Movement of the hand was restricted by placing the hand palm down on a table. Video-microscopy was performed on the dorsal skin of the middle phalanx with a hand-held digital capillaroscope (Optilia$_{TM}$, Sweden), containing a 6500 K LED colour lamp (Figure 4.9).

Fig 4.9: Equipment and techniques for skin capillary density measurement. A: The Optilia$_{TM}$ hand-held digital capillaroscope, showing equipment set up. B: Technique of video-microscopy. C: The Accoson$_{TM}$ Duplex Aneroid cuff which was applied to the wrist for venous congestion.

A. **B.**

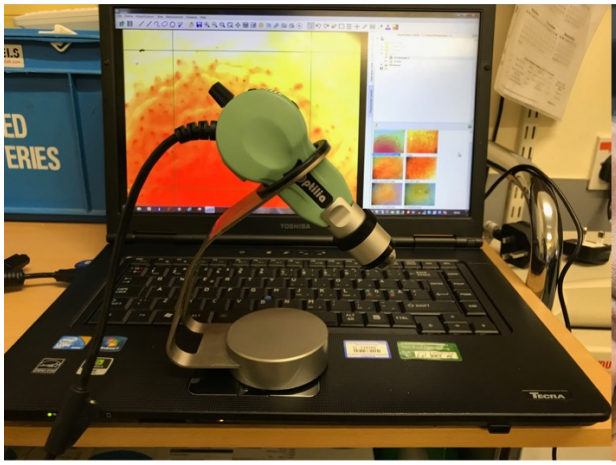

C.

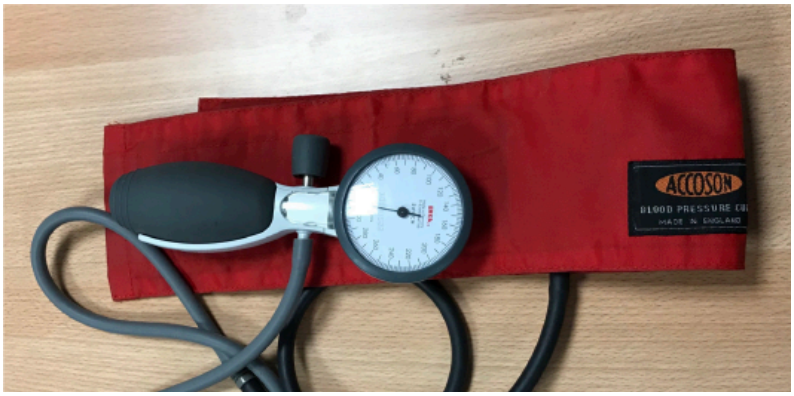

This device has been previously used to quantity skin capillaries in neonates. [285] A drop of liquid paraffin oil was applied to the skin to reduce light reflection. A system magnification of 200x was used. Images were processed with OptiPix capillaroscopy research software (Optilia$_{TM}$, Sweden) and stored as JPEG images, which were analysed offline to count the total number of visible (i.e. perfused) capillaries. For each participant, I selected a region of interest on the middle phalanx and captured 4 images taken 1 minute apart at baseline. A further 4 images were taken from the same point after venous congestion, which was achieved using the application of a cuff (Accoson$_{TM}$ Duplex Aneroid Hand Model) to the wrist, inflated to 60 mmHg for 2 minutes (Figure 4.9C). Venous occlusion was previously

shown to effectively maximise the number of visible capillaries. [284] The increase in capillary density during venous occlusion (capillary recruitment) has been noted to be attenuated in hypertensives. [228]

The number of visible capillaries per 1.0 mm^2 field was calculated from each capillaroscopy image taken at unoccluded and post venous congestion using a software program developed by Dr Stephen Smith from the EMIT unit (Figure 4.10). This novel program was written in the Python (version 2.7) programming language and used a Canny edge finding algorithm to detect and count visible capillaries per 1.0 mm^2. Counted capillaries were highlighted in blue (Figure 4.10).

4.10: Examples of skin capillary images. (A)Capillaroscopy image obtained at 200x using the Optilia$_{TM}$ system. (B)Capillaries within a 1.0 mm^2 field were identified using the software program.

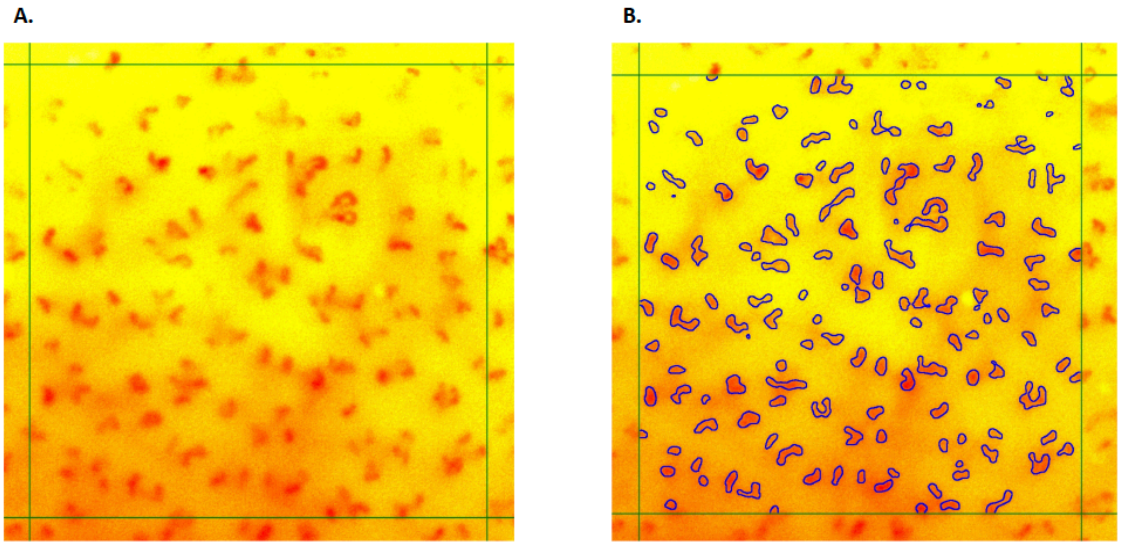

.

The accuracy of the software was tested by a visual inspection by Dr Smith and myself and corrections were made if necessary. The average capillary count for 4 images was used to obtain the mean capillary density (MCD) per mm^2. Capillaroscopy images were reviewed and software analysis run by Dr Stephen Smith, who was blinded to the order of treatment. Participants were excluded if the images were of inadequate quality and the software was unable to detect capillaries, as judged by both Dr Stephen Smith and myself, and if the SD for a set of 4 images pre or post cuff exceeded 19/mm^2. Capillaroscopy is only possible in the lighter pigmented subjects and therefore, only Caucasians were included in this present study.

4.4.11 Statistical analysis

4.4.11.1 Primary outcome and power calculations

The planned primary outcome measure for which the Varsity main study the change in skin Na^+ with salt loading, as measured per dry weight (Na^+_{Dry}). As published data available on changes in skin sodium concentration in response to salt loading in humans were lacking, the initial sample size of 48 was based on other salt loading studies of a similar design. A planned interim analysis was done after 26 participants completed the study and revealed freeze drying was not consistent across samples and Na^+_{Dry} values were not reliable. A pragmatic approach was taken, and a further analysis was planned after 48 participants completed the study. When the study was completed the limitations of freeze drying skin samples persisted. For this reason the primary outcome we changed from absolute dry Na^+ to Na^+:K^+ ratio.

4.4.11.2 Main study analysis

Normally distributed data are presented as mean ± SEM and non-normal data as median and interquartile range(IQR). Tests for normality were carried out using the Shapiro Wilk's test. Student's paired t-tests were applied to paired observations after placebo and slow sodium for normally distributed data and the Wilcoxon signed-rank test for non-normally distributed data. Independent samples t-tests were applied to unpaired observations for normally distributed data and the Man Whitney test for non-normally distributed data. Correlation coefficients between skin Na^+:K^+ and putative parameters such as age, sex, body mass index (BMI) and haemodynamic variables were calculated using Pearson's method for normally distributed variables and Spearman's method for non-normally distributed variables. I then performed multiple regression analysis to examine the parameters that independently influence skin Na^+:K^+. The presence of carry-over effect for changes in skin Na^+ was checked using univariate analysis of variance as previously described. [286] A probability of < 5% was used to reject the null hypothesis. Statistical analysis was performed with the SPSS software (version 23.0). Graph-Pad Prism 7.0 (GraphPad Software Inc., La Jolla, CA, USA) was used to construct graphs and figures.

4.4.11.2.1 Sex specific analysis

In analysing the data it became apparent that that skin Na^+:K^+ differed by gender and a post-hoc gender specific analysis was therefore undertaken. The effects of contraceptive treatment on skin biochemistry is unknown. A further analysis of women according to contraceptive treatment was undertaken to see if this influenced observed sex differences.

4.4.11.3 Salt taste sensitivity

The Wilcoxon signed-rank test was used to compare salt recognition and detection thresholds post placebo and slow sodium treatments. Spearman's correlation coefficient by rank was used to analyse the correlation between the salt recognition or detection thresholds and plasma VEGF-C, as well as putative parameters such as age, BMI, BP, plasma renin and aldosterone. Multiple regression analysis was then performed to examine the parameters that independently influence salt recognition and detection thresholds. P-values less than 0.05 were considered significant.

4.4.11.4 Skin capillaroscopy

Mean capillary density at baseline (unoccluded) and after venous occlusion was compared using the Student's paired *t* test. The relationship between mean capillary density and putative parameters such as age, body mass index (BMI) and haemodynamic variables were calculated using Pearson's method for normally distributed variables and Spearman's method for non-normally distributed variables. We then performed multiple regression analysis to examine the parameters that independently infuence skin capillary density.

4.5. Results

4.5.1 Analysis of whole study population

4.5.1.1 Baseline characteristics

A total of 24 men and 24 women completed the study with a mean age of 30 ± 2 years (range 18–49 years). Baseline characteristics are shown in Table 4.2. Our study population had a lower baseline sodium intake compared to the current average intake in England (approximately 130 mmol/day). [256]

Table 4.2: Baseline variables for the whole VARSITY study population

Baseline variables	(n=48)
Age, years	30 ± 1
Ethnicity (Caucasian)	45/48
Body weight, kg	69.2 ± 1.6
Height, cm	171 ± 1
BMI, kg ms^{-2}	23.0 (21.9 – 24.4)
Haemodynamic variables	
Seated SBP, mmHg	120 ± 1
Seated DBP, mmHg	74 ± 1
Seated MAP, mmHg	89 ± 1
Seated HR, BPM	72 ± 1
Supine SBP, mmHg	118 ± 1
Supine DBP, mmHg	70 ± 1
Supine MAP, mmHg	87 ± 2
Supine HR, BPM	65 ± 1
24-hr MAP	93 ± 1
24-hr SBP	118 ± 1
24-hr DBP	73 ± 1
Night-time SBP, mmHg	110 ± 1
Night-time DBP, mmHg	65 ± 1
Night-time MAP, mmHg	85 ± 1
Augmentation index, %	9.0 ± 2.0
PWV m/s	5.3 (4.8 – 5.8)
Cardiac output, litres/min	6.0 ± 0.2
Stroke volume, ml	90.8 ± 3.3
PVR, dynes s^{-1} cm^{-5}	1166 (997.5 – 1420)
High frequency $power_{Normalised}$, %	77.0 ± 3.9
Low frequency $power_{Normalised}$, %	52.2 ± 3.1
Biochemical variables	
eGFR, ml/min/1.72m^2	111.6 (95.0 – 122.6)
Renin, mU/l	13.5 (8.3 – 18.8)
Aldosterone, pmol/l	121 (80– 209)
Plasma VEGF C, pg/ml	585.7 (438.6 - 1038)
sFlt-4, pg/ml	9.6 ± 0.7
24-hr Urine Na^+	93.8 ± 8.1
24-hr Urine K^+	69.8 ± 5.1
24-hr Urine Cl^-	108.7 ± 9.0

Normally distributed data presented as mean ± SEM. Non-normally distributed data are presented as median and IQR.

4.5.1.2 Assessment of drying consistency

The mean sample weight was 0.015 ± 0.006g. Measured skin sample water content was negatively correlated with sample wet weights (Figure 4.11), suggesting that overall, freeze drying did not remove water consistently across all samples, with smaller samples recording greater proportional water contents because of greater water removal. Consequently, Na^{+}_{Dry} and K^{+}_{Dry} were negatively correlated with sample weights, with a tendency for smaller samples to have higher measured Na^{+}_{Dry} and K^{+}_{Dry} content (Figure 4.12). This suggested that Na^{+}_{Dry} and K^{+}_{Dry} could not be used in the analysis. For this reason Na^{+} values expressed as Na^{+}:K^{+} ratios to correct for this variation due to sample weight.

Figure 4.11: Effects of skin sample wet weights on % water content.

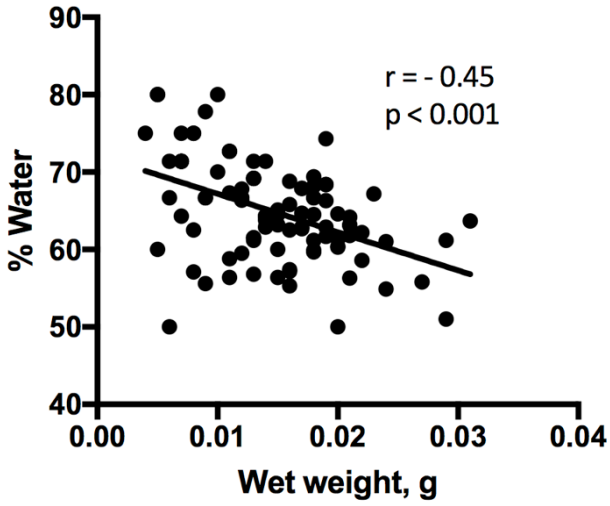

Figure 4.12: Variation of skin Na^+_{Dry} and K^+_{Dry} with sample wet weight

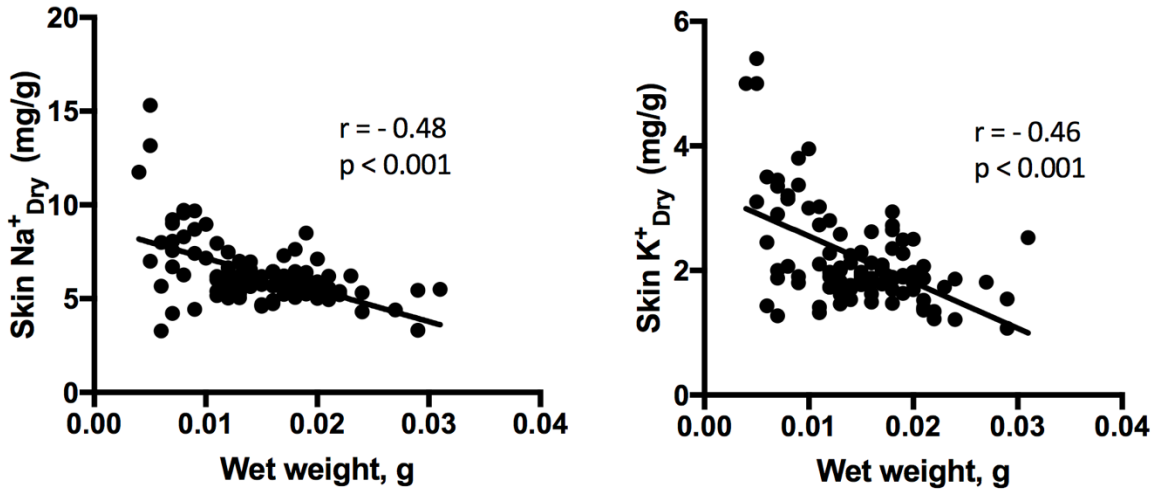

4.5.1.2 Primary outcome and skin biochemical variables

The primary endpoint was the change in skin Na^+:K^+ between the placebo and slow sodium phases. Skin biochemical responses to placebo vs. slow sodium are shown in Table 4.3. There was an increase in skin Na^+:K^+ between the placebo and slow sodium phases (from 2.91 ± 0.08 to 3.12 ± 0.09; p = 0.01; Figure. 4.13). There was a significant increase in skin Na^+_{Wet} with salt loading with no change in skin K^+_{Wet}, in keeping with previous salt loading studies in rats. In multiple regression analysis with age, BMI, clinic mean arterial pressure (MAP) and sex entered into the model, sex was found to be the only independent factor influencing skin Na^+:K^+ values (R^2 for the model=0.316, P<0.001). This was primarily because in women, skin K^+ was lower and the Na^+:K^+ ratio was consequently higher. Therefore, subsequent skin analyses were sex-specific. For this thesis, haemodynamic and biochemical data are presented for the whole VARSITY study population and by sex.

Table 4.3: Skin biochemical responses to placebo vs. slow sodium.

Variable	n = 48		
	Placebo	Slow sodium	P-value
Skin wet weight, mg	0.015 ± 0.001	0.015 ± 0.001	0.70
Skin Na^+, mg/g	2.09 ± 0.04	2.20 ± 0.05	**0.04**
Skin K^+, mg/g	0.74 ± 0.02	0.73 ± 0.03	0.62
Skin Na^+: K^+	2.91 ± 0.08	3.12 ± 0.09	**0.01**

Figure 4.13: Skin Na^+:K^+ response to placebo vs. slow sodium.

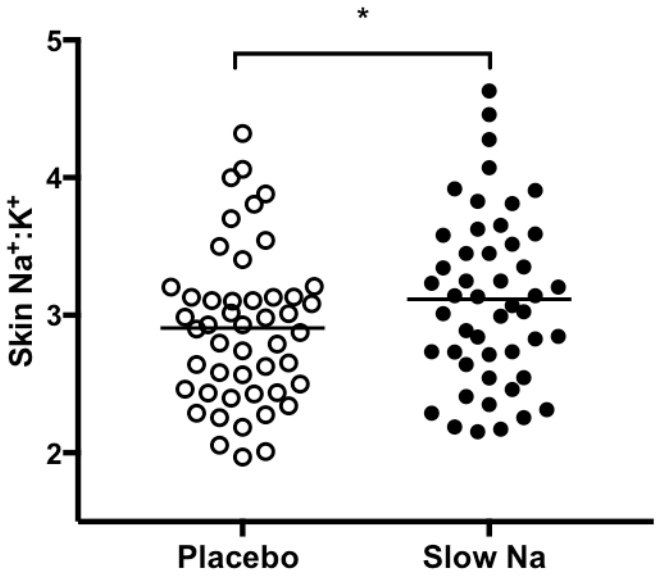

Data for the whole VARSITY study population.
Bars are mean for the group. * indicates p = 0.01.

4.5.1.3 Haemodynamic responses to placebo vs. slow sodium

Haemodynamic responses to placebo vs. slow sodium for the whole study population are shown in Table 4.4. There was no significant difference in weight or clinic BP measurements. There was a significant increase in ambulatory 24-hr SBP, MAP, day SBP, night SBP and night MAP with salt loading. Stroke volume increased with salt loading (97 ± 4 vs. 103 ± 4 ml, $p < 0.05$) with no significant change seen in cardiac output or PVR. Pulse wave velocity and augmentation index did not change with salt loading. No significant difference was noted in normalised high frequency and low frequency components of HRV.

Table 4.4 – Differences in haemodynamic responses to placebo vs. slow sodium

Variable	n = 48		
	Placebo	Slow sodium	P-value
Body weight, kg	68.8 ± 1.6	68.6 ± 1.6	0.07
Office measurements			
Seated SBP, mmHg	117 ± 1	117 ±	0.92
Seated DBP, mmHg	72 ± 1	72 ± 1	0.81
Seated MAP, mmHg	87 ± 1	87 ± 2	0.85
Seated HR, bpm	73 ± 2	70 ± 1	0.06
Supine SBP, mmHg	114 ± 1	115 ± 1	0.44
Supine DBP, mmHg	67 ± 1	67 ± 1	0.83
Supine MAP, mmHg	83 ± 1	83 ± 1	0.72
Supine HR, bpm	62 ± 1	60 ± 1	0.06
Ambulatory BP, mmHg			
24-hr SBP	117 ± 1	120 ± 1	**0.01**
24-hr DBP	72 ± 1	72 ± 1	0.36
24-hr MAP	93 ± 1	94 ± 1	**0.03**
Day SBP	121 ± 1	123 ± 1	**0.03**
Day DBP	76 ± 1	75 ± 1	0.83
Day MAP	96 ± 1	97 ± 1	0.12
Night SBP	109 ± 1	112 ± 1	**< 0.01**
Night DBP	64 ± 1	65 ± 1	0.06
Night MAP	85 ± 1	87 ± 1	**0.01**
Central haemodynamics			
CSBP, mmHg	97 ± 1	98 ± 1	0.26
CDBP, mmHg	68 ± 1	68 ± 1	0.92
CMAP, mmHg	82 ± 1	82 ± 1	0.12
Augmentation index, %	9.1 ± 2	9.5 ± 2	0.67
PWV ms^{-1}	5.1(4.7 – 5.5)	5.2(4.9 – 5.7)	0.28
Cardiac output, litres/min	6.1 ± 0.2	6.4 ± 0.2	0.11
Stroke volume, ml	96.9 ± 3.6	102.8 ± 4.2	**0.046**
PVR, dynes s^{-1} cm^{-5}	1050 ± 46	1128 ± 47	0.57
Heart rate variability			
High frequency $power_{Normalised,}$%	48.2 ± 2.8	52.1 ± 3.1	0.27
Low frequency $power_{Normalised,}$%	53.1 ± 2.9	47.9 ± 3.1	0.11

Normally distributed data presented as mean ± SEM. Non-normally distributed data are presented as median and IQR. Student's paired t-tests were applied to paired observations after placebo and slow sodium for normally distributed data and the Wilcoxon signed-rank test for non-normally distributed data.

4.5.1.4 Biochemical responses to placebo vs. slow sodium

Serum, plasma and urine biochemical responses to placebo vs. slow sodium for the whole study population are shown in Table 4.5. Slow sodium caused the expected increases in 24-hour urine Na^+ and Cl^-, serum Na^+ and Cl^-, and suppression of plasma renin and aldosterone. Serum eGFR and urine creatinine clearance increased with slow sodium, consistent with glomerular hyperfiltration as previously seen in salt-loaded healthy adults. [287,288] Fractional excretion of sodium (FeNa) was significantly higher after slow sodium, as previously described in healthy adults. [288] No significant change in plasma VEGF-C levels or sFLT-4 (soluble receptor for VEGF-C) between placebo and slow sodium was observed.

Table 4.5 – Differences in biochemical responses to placebo vs. slow sodium for the whole VARSITY study population.

Variable	n = 48		
	Placebo	**Slow sodium**	**P-value**
Serum measurements			
Na^+, mmol/l	139 ± 0.2	141 ± 0.3	**< 0.001**
Cl^-, mmol/l	103 ± 0.3	105 ± 0.4	**< 0.001**
K^+, mmol/l	4.3 ± 0.04	4.4 ± 0.05	0.51
eGFR, ml/min/1.72m^2	111.1 ± 3.2	117.2 ± 3.6	**0.001**
Plasma measurements			
Renin, mU/l	20 (14 – 27)	7 (3–11)	**< 0.001**
Aldosterone, pmol/l	221 (140 – 344)	70 (69 – 80)	**< 0.001**
VEGF-C, pg/ml	672 (396 – 1013)	686 (458 – 1085)	0.85
sFlt-4, pg/ml	9.7 ± 0.8	9.8 ± 0.7	0.60
Urinary measurements			
Volume, ml/24hr	1741 ± 122	2032 ± 145	0.01
Na^+, mmol/24hr	72.9 ± 6.3	221.9±16.5	**< 0.001**
Cl^-, mmol/24hr	93.4 ± 7.1	236.1 ± 12.7	**< 0.001**
K^+, mmol/24hr	60.8 (46.9 – 78.1)	57.3 (41.6 – 78.2)	0.08
Creatinine clearance, ml/min	112.4 ± 6.0	124.3 ± 5.9	**0.02**
Albumin, mg/24h	5.8 ± 1.1	6.8 ± 1.5	0.15
FE_{Na}, %	0.36 ± 0.03	0.94 ± 0.06	**< 0.001**

Normally distributed data presented as mean ± SEM. Non-normally distributed data are presented as median and IQR. Student's paired t-tests were applied to paired observations after placebo and slow sodium for normally distributed data and the Wilcoxon signed-rank test for non-normally distributed data.

4.5.2 Sex-specific analysis

4.5.2.1 Baseline characteristics

Sex-specific baseline characteristics are shown in Table 4.6. Men had higher weight, BP, stroke volume, eGFR and renin. Women had higher augmentation index.

Table 4.6 – Differences in demographics and baseline variables for by gender

Baseline variables	Males (n=24)	Females (n=24)	P-value
Age, years	28 ± 2	32 ± 2	0.14
Ethnicity (Caucasian)	22/24	23/24	-
Body weight, kg	74.3 ± 2.5	64.1 ± 1.5	**< 0.001**
Height, cm	178 ± 2	165 ± 2	**< 0.001**
BMI, kg ms^{-2}	22.7 (21.6 – 24.0)	23.9 (22.1 – 25.4)	0.29
Haemodynamic variables			
Seated SBP, mmHg	123 ± 2	116 ± 2	**0.004**
Seated DBP, mmHg	67 ± 2	72 ± 2	0.45
Seated MAP, mmHg	90 ± 2	90 ± 2	0.89
Seated HR, BPM	71 ± 2	73 ± 2	0.32
Supine SBP, mmHg	122 ± 2	115 ± 2	**0.03**
Supine DBP, mmHg	67 ± 2	72 ± 2	**0.04**
Supine MAP, mmHg	87 ± 2	87 ± 2	0.99
Supine HR, BPM	64 ± 2	67 ± 2	0.37
24-hr MAP	95 ± 2	91 ± 1	**0.02**
24-hr SBP	122 ± 2	114 ± 1	**< 0.001**
24-hr DBP	74 ± 2	72 ± 1	0.43
Night-time SBP, mmHg	113 ± 2	107 ± 1	**0.01**
Night-time DBP, mmHg	66 ± 2	64 ± 1	0.44
Night-time MAP, mmHg	88 ± 2	83 ± 1	0.05
Augmentation index, %	2.8 ± 2.0	15.0 ± 2.6	**0.003**
PWV m/s	5.3 (4.8 – 5.7)	5.2 (4.8 – 5.8)	0.61
Cardiac output, litres/min	6.3 ± 0.3	5.6 ± 0.3	0.06
Stroke volume, ml	101.9 ± 4.7	79.6 ± 3.6	**< 0.001**
PVR, dynes s^{-1} cm^{-5}	1156 (982.3 – 1324)	1183(1032 – 1690)	0.22

Biochemical variables			
eGFR, ml/min/1.72m^2	114.3 (107.7 – 124.4)	97.2 (88.4 - 117.2)	**0.01**
Renin, mU/l	18.0 (13.0 – 25.5)	9.0 (7 – 14)	**< 0.001**
Aldosterone, pmol/l	166.0 (110 – 194)	110.5 (69.0 – 279.5)	0.27
Plasma VEGF C, pg/ml	542.7 (412.5 - 842.5)	644 (469.7 - 1172.0)	0.22
sFlt-4, pg/ml	9.1 ± 0.9	10.1 ± 1.0	0.45
24-hr Urine Na^+, mmol/24hr	102.0 ± 12.4	84.9 ± 10.1	0.31
24-hr Urine K^+, mmol/24hr	75.0 ± 8.9	64.2 ± 4.4	0.29
24-hr Urine Cl^-, mmol/24hr	115.4 ± 12.7	101.5 ± 12.8	0.45

Normally distributed data presented as mean ± SEM. Non-normally distributed data are presented as median and IQR. The values for males and females was analyzed using the unpaired t test with normally distributed data and Man Whitney test for non-normal data. P value < 0.05 taken to be significant.

4.5.2.2 Skin biochemical variables

Sex-specific skin Na^+, K^+ and Na^+:K^+ values are presented in Table 4.7 and Figure 4.14. Men showed a significant increase in skin Na^+:K^+ of 11.2% (p=0.008) from placebo to slow sodium phases, whilst women showed a non-significant increase of 4.0% (p=0.31). On formal repeated measures ANOVA testing, there was no significant difference between genders (p=0.31). Neither sex showed a significant change in skin K^+ with a change in salt intake, in keeping with previous animal studies. [244,245] Women had a lower skin K^+ compared to men ($p < 0.01$ post placebo and slow sodium) and consequently had higher Na^+:K^+ ratio than men ($p < 0.001$ post placebo and salt). No evidence of carry-over effect was seen for skin Na^+:K^+ or skin Na^+ for either sex using univariate analysis of variance with order of treatment (placebo or slow sodium) as a fixed factor (p = 0.68).

Table 4.7: Differences in skin biochemical responses to placebo vs. slow sodium by sex.

Variable	Men (n=24)			Women (n=24)		
	Placebo	Slow sodium	P-value	Placebo	Slow sodium	P-value
Skin wet weight, g	0.014±0.001	0.015±0.001	0.68	0.015±0.001	0.015±0.001	0.35
Skin Na^+, mg/g	2.02±0.06	2.27±0.08	**0.02**	2.15±0.05	2.14±0.03	0.84
Skin K^+, mg/g	0.80±0.03	0.82±0.04	0.59	0.68±0.03	0.65±0.02	0.28
Skin Na^+:K^+	2.59±0.09	2.88±0.12	**0.008**	3.23±0.10	3.36±0.12	0.31

Student's paired t-tests were applied to paired observations after placebo and slow sodium for normally distributed data and the Wilcoxon signed-rank test for non-normally distributed data.

Figure 4.14: Differences in skin biochemical responses by sex. Responses to placebo vs. slow sodium in (A) men and (B) women.

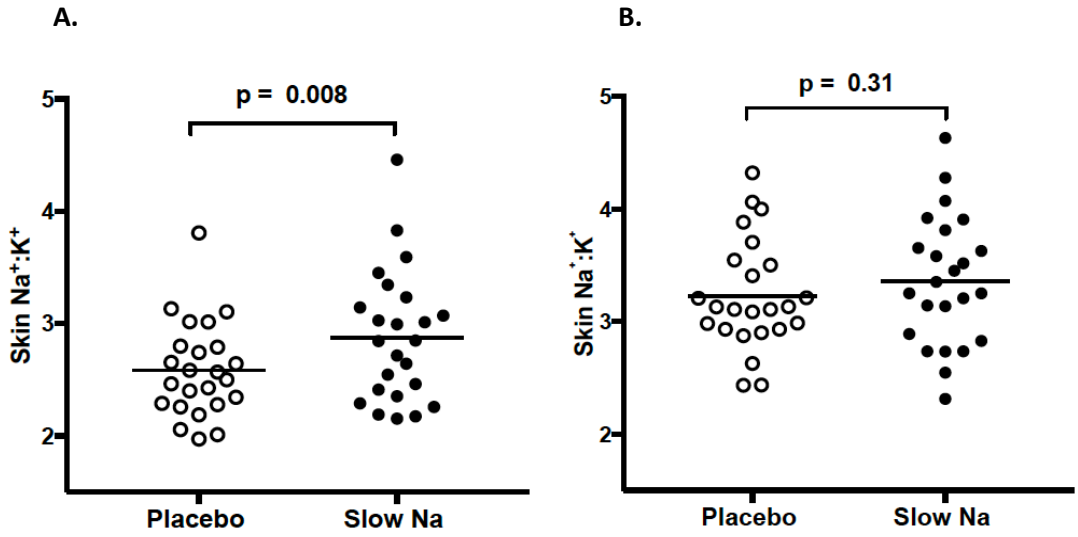

Sex specific data for the VARSITY study. Bars are mean for the group.

4.5.3.3 Haemodynamic responses to placebo vs. slow sodium

Hemodynamic responses to placebo vs. slow sodium are shown in Table 4.8. In men there were no differences in haemodynamics following salt loading, whilst women had higher 24-hour systolic BP (SBP), 24-hour MAP, daytime SBP, night-time SBP, diastolic BP (DBP) and MAP. Only women had an increase in body weight post slow sodium (63.5 ± 1.6 vs. 64.2 ± 1.6 kg; $p = 0.01$).

Table 4.8 – Differences in haemodynamic responses to placebo vs. slow sodium by sex.

Variable	Males (n=24)			Females (n=24)		
	Placebo	Slow sodium	P-value	Placebo	Slow sodium	P-value
Body weight, kg	73.6±2.5	73.6±2.5	0.93	63.5±1.6	64.2±1.6	**0.01**
Office measurements						
Seated SBP, mmHg	120±2	119±2	0.85	114±2	114±2	0.72
Seated DBP, mmHg	71±2	71±2	0.98	73±2	73±1	0.75
Seated MAP, mmHg	87±1	87±2	0.65	87±2	88±1	0.43
Seated HR, bpm	72±2	68±2	0.12	74±2	72±2	0.30
Supine SBP, mmHg	116±2	116±4	0.91	111±2	113±2	0.27
Supine DBP, mmHg	65±2	65±2	0.72	68±2	69±1	0.55
Supine MAP, mmHg	83±2	82±1	0.62	83±2	84±2	0.33
Supine HR, bpm	60±2	58±2	0.15	64±2	63±2	0.23
Ambulatory BP, mmHg						
24-hr SBP	121±1	122±2	0.57	114±1	118±1	**< 0.001**
24-hr DBP	73±2	73±2	0.46	71±1	73±1	0.05
24-hr MAP	96±2	96±2	0.89	91±1	93 ± 1	**< 0.001**
Day SBP	124±1	125±2	0.32	118±1	121±2	**0.02**
Day DBP	76±2	76±2	0.34	75±2	76±2	0.33
Day MAP	98±2	98±2	0.93	95±1	97±2	0.05

Night SBP	114±2	115±2	0.52	105±1	110 ± 1	**< 0.001**
Night DBP	65±2	66±2	0.65	63±1	65 ± 1	**0.01**
Night MAP	88±2	89±2	0.80	82±1	86 ± 1	**< 0.001**
Central haemodynamics						
CSBP, mmHg	99±1	99±2	0.99	95±2	98±2	0.11
CDBP, mmHg	67±2	66±2	0.21	69±2	70±1	0.22
CMAP, mmHg	82±2	80±2	0.12	83±2	85±2	0.22
Augmentation index, %	4.5±2	4.5±2	0.98	13.7±3	14.5±3	0.58
PWV ms^{-1}	5.2(4.7 – 5.6)	5.3(4.9 – 6.0)	0.10	5.0(4.7 – 5.5)	5.2(4.8 – 5.4)	0.93
Cardiac output, litres/min	6.6±0.3	7.0±0.4	0.08	5.6±0.3	5.8±0.3	0.10
Stroke volume, ml	107.9±5.2	116.8±6.5	0.09	86.0±4.0	88.9±3.6	0.29
PVR, dynes s^{-1} cm^{-5}	1048±51	1045±64	0.57	1251±72	1212±66	0.46

Normally distributed data presented as mean ± SEM. Non-normally distributed data are presented as median and IQR. Student's paired t-tests were applied to paired observations after placebo and slow sodium for normally distributed data and the Wilcoxon signed-rank test for non-normally distributed data.

4.5.3.4 Biochemical responses to placebo vs. slow sodium

Differences in biochemical responses to placebo vs. slow sodium are shown in Table 4.9. As expected, in both sexes, slow sodium increased 24-hour UNaV, serum Na^+ and Cl^-, and suppressed plasma renin and aldosterone. There were no significant changes in plasma VEGF-C levels or sFLT-4 (soluble receptor for VEGF-C) between placebo and slow sodium in either sex.

Table 4.9 – Differences in biochemical responses to placebo vs. slow sodium by sex.

Variable	Males (n=24)			Females (n=24)		
	Placebo	Slow sodium	P-value	Placebo	Slow sodium	P-value
Serum measurements						
Na^+,mmol/l	140±0.4	141±0.3	**0.001**	139±0.3	140±0.4	**< 0.001**
Cl^-,mmol/l	103±0.4	106±0.5	**< 0.001**	103±0.4	105±0.6	**< 0.001**
K^+,mmol/l	4.4±0.06	4.4±0.07	0.97	4.3±0.07	4.3±0.09	0.69
eGFR, ml/min/1.72m^2	114.7 (103.9 – 127.5)	117.1(107.3 – 136.7)	0.24	99.2 (84.1 – 119.2)	105.9 (94.2-127.8)	**< 0.001**
Plasma measurements						
Renin, mU/l	24(15–30)	11(4–13)	**< 0.001**	17 (9 – 21)	3 (2 – 7)	**< 0.001**
Aldosterone, pmol/l	221(143–318)	80(69–111)	**< 0.001**	240 (137 – 435)	69 (69 – 75)	**< 0.001**
VEGF-C, pg/ml	540 (352 – 881)	625 (460 – 1066)	0.20	830 (467 – 1404)	755 (412 – 1130)	0.39
sFlt-4, pg/ml	8.9±1.1	9.1±1.0	0.79	10.3±1.0	10.6±0.9	0.57

Urinary measurements						
Volume, ml/24hr	1540±174	1678±203	0.25	1935±166	2299±186	**0.004**
Na^+, mmol/24hr	86.3±10.3	221.9±16.5	**< 0.001**	60.0±6.8	227.1±19.9	**< 0.001**
Cl^-, mmol/24hr	103.7±11.6	228.1±14.4	**< 0.001**	83.8±8.2	241.3±21.5	**< 0.001**
K^+,mmol/24hr	63.3(51.2 – 93.5)	55.1(39.9 – 73.8)	0.15	56.9(40.5 – 76.7)	58.7(41.6 – 77.9)	0.49
Creatinine clearance, ml/min	111.1±9.1	125.3±9.6	0.14	108.1±8.0	122.4±7.6	0.06
Fractional $Excretion_{Na}$, %	0.44±0.06	0.93±0.08	**< 0.001**	0.28±0.03	0.94±0.09	**< 0.001**

4.5.3.5 Effects of contraceptive use in women

10 women were on contraceptive treatment, of which 6 were on the combined pill and 4 were on progesterone-only pill or progesterone implants. Contraceptive treatment did not seem to affect the skin Na^+ or skin Na^+:K^+ response to dietary salt loading (Table 4.10 and Figure 4.15). Women on contraceptive treatment had higher skin K^+ levels post slow sodium ($p = 0.03$) but not post placebo ($p = 0.11$) compared with females not on contraceptive treatment. Consequently, females on contraceptive treatment had a trend for lower skin Na^+:K^+ levels post placebo ($p = 0.05$) and post slow sodium ($p = 0.09$) compared with females not on contraceptive treatment. Baseline characteristics and haemodynamic responses to salt loading were similar in women with and without contraceptive use (Table 4.11 and 4.12).

Table 4.10: Differences in skin biochemical responses to placebo vs. slow sodium in women according to contraceptive (OCP) use.

Variables	No contraceptive use n = 14			Contraceptive use n = 10		
	Placebo	Slow sodium	P-value	Placebo	Slow sodium	P-value
Skin Na^+, mg/g	2.15 ± 0.07	2.15 ± 0.05	0.92	2.16 ± 0.07	2.12 ± 0.07	0.92
Skin K^+, mg/g	0.65 ± 0.03	0.62 ± 0.02	0.43	0.73 ± 0.05	0.70 ± 0.04	0.50
Skin Na^+:K^+	3.37 ± 0.12	3.53 ± 0.13	0.43	3.04 ± 0.17	3.12 ± 0.20	0.69

Normally distributed data presented as mean ± SEM. The change between placebo and slow sodium for both groups was analyzed using the student's paired t test. P value < 0.05 taken to be significant.

Figure 4.15: Comparison of skin Na^+:K^+ responses by use of contraception. Skin Na^+:K^+ changes with salt loading in women not on contraceptive treatment (A ; n=14) and women on contraceptive treatment (B ; n=10).

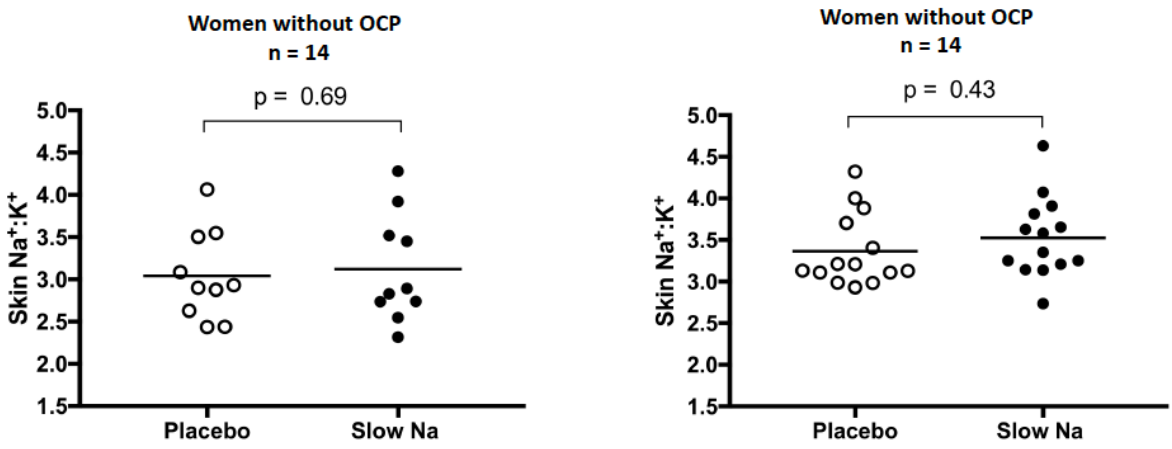

Bars are mean for the group. Comparisons within groups were made using the unpaired t test.

Table 4.11– Differences in demographics and baseline variables for women according to contraceptive use.

Baseline variables	No contraceptive (n=14)	On contraceptive (n=10)	P-value
Age, years	33 ± 3	30 ± 2	0.55
Ethnicity (Caucasian)	13/14	10/10	-
Body weight, kg	65.0 ± 2.2	62.9 ± 2.0	0.52
Height, cm	163 ± 2	166 ± 1	0.31
BMI, kg ms^{-2}	24.4 ± 0.7	22.8 ± 0.8	0.14
Haemodynamic variables			
Seated SBP, mmHg	117 ± 2	114 ± 4	0.51
Seated DBP, mmHg	75 ± 2	76 ± 2	0.80
Seated MAP, mmHg	89 ± 2	89 ± 3	0.91
Seated HR, BPM	75 ± 3	71 ± 2	0.36
Supine SBP, mmHg	115 ± 3	115 ± 4	0.94
Supine DBP, mmHg	72 ± 2	72 ± 3	0.99
Supine MAP, mmHg	87 ± 2	86 ± 3	0.96
Supine HR, BPM	67 ± 2	66 ± 2	0.67
24-hr MAP	91 ± 1	92 ± 2	0.62
24-hr SBP	114 ± 2	114 ± 2	0.99
24-hr DBP	72 ± 1	73 ± 1	0.59
Night-time SBP, mmHg	106 ± 2	108 ± 2	0.50
Night-time DBP, mmHg	62 ± 2	66 ± 2	0.59
Night-time MAP, mmHg	82 ± 1	85 ± 2	0.13
Augmentation index, %	17.8 ± 3.4	11.0 ± 3.8	0.21
PWV m/s	5.4 (4.9 – 5.9)	5.0 (4.5 – 5.8)	0.19
Cardiac output, litres/min	5.3 ± 0.3	6.0 ± 0.4	0.17
Stroke volume, ml	75.3 ± 4.1	85.7 ± 6.2	0.16
PVR, dynes s^{-1} cm^{-5}	1265 (1011 – 1880)	1183(1046 – 1348)	0.22

Biochemical variables			
eGFR, ml/min/1.72m^2	95.1 (88.7 – 115.2)	103.7 (87.1 – 151.1)	0.73
Renin, mU/l	14.1 ± 2.1	7.0 ± 0.8	**0.02**
Aldosterone, pmol/l	113 (69 – 247)	87 (70 – 385)	0.83
Plasma VEGF C, pg/ml	831.9 ± 116.1	840.3 ± 195.9	0.97
sFlt-4, pg/ml	9.0 ± 1.3	11.8 ± 1.6	0.19
24-hr Urine Na^+,mmol	101.1 ± 14.7	65.4 ± 11.6	0.08
24-hr Urine K^+,mmol	61.6 ± 5.8	67.3 ± 6.9	0.53
24-hr Urine Cl^-,mmol	122.7 ± 19.0	76.1 ± 13.5	0.07

Normally distributed data presented as mean ± SEM. Non-normally distributed data are presented as mean and IQR. The values for women with and without contraceptive use was analyzed using the unpaired t test with normally distributed data and Man Whitney test for non-normal data. P value < 0.05 taken to be significant.

Table 4.12 – Differences in haemodynamic responses to placebo vs. slow sodium according to contraceptive use

Variables	No contraceptive (n=14)			On contraceptive (n=10))		
	Placebo	**Slow sodium**	**P-value**	**Placebo**	**Slow sodium**	**P-value**
Body weight, kg	64.2 ± 2.3	64.8 ± 2.4	0.12	62.4 ± 2.0	63.2 ± 1.7	**0.03**
Office measurements						
Seated SBP, mmHg	115 ± 2	116 ± 2	0.48	111 ± 3	111 ± 3	0.85
Seated DBP, mmHg	74 ± 2	74 ± 2	0.96	71 ± 2	72 ±2	0.63
Seated MAP, mmHg	88 ± 2	88 ± 2	0.68	85 ± 3	86 ± 2	0.50
Seated HR, bpm	77 ± 2	75 ± 3	0.42	69 ± 3	68 ± 3	0.55
Supine SBP, mmHg	111 ± 3	115 ± 3	0.15	111 ± 3	110 ± 2	0.79
Supine DBP, mmHg	68 ± 2	70 ± 2	0.33	68 ± 2	68 ± 1	0.64
Supine MAP, mmHg	83 ± 2	85 ± 2	0.18	82 ± 2	82 ± 2	0.74
Supine HR, bpm	67 ± 2	64 ± 2	0.31	62 ± 3	61 ± 3	0.58
Ambulatory BP, mmHg						
24-hr SBP	114 ± 1	118 ± 2	**0.02**	113 ± 2	118 ± 2	**0.004**
24-hr DBP	71 ± 2	72 ± 2	0.54	71 ± 1	74 ± 1	**0.03**
24-hr MAP	91 ± 2	93 ± 2	0.07	90 ± 1	94 ± 2	**0.001**
Day SBP	119 ± 2	121 ± 3	0.19	117 ± 2	121 ± 3	0.05

Day DBP	75 ± 3	75 ± 2	0.95	75 ± 1	77 ± 2	0.17
Day MAP	95 ± 2	96 ± 2	0.47	94 ± 2	97 ± 2	**0.04**
Night SBP	104 ± 2	109 ± 2	**0.001**	106 ± 2	111 ± 1	**0.001**
Night DBP	61 ± 2	64 ± 2	0.10	64 ± 1	67 ± 1	0.07
Night MAP	81 ± 2	85 ± 2	**0.008**	83 ± 2	87 ± 1	**0.005**
Central haemodynamics						
CSBP, mmHg	95 ± 2	101 ± 3	**0.01**	95 ± 3	93 ± 3	0.44
CDBP, mmHg	69 ± 2	71 ± 2	0.62	69 ± 2	69 ± 2	0.96
CMAP, mmHg	82 ± 2	87 ± 2	**0.01**	83 ± 3	81 ± 2	0.44
Augmentation index, %	15.7 ± 3.6	19.1 ± 3.8	0.10	10.9 ± 4.9	8.1 ± 4.3	0.10
PWV ms^{-1}	5.6 ± 0.3	5.5 ± 0.2	0.91	5.0 ± 0.1	5.0 ± 0.1	0.95
Cardiac output, litres/min	5.5 ± 0.3	5.6 ± 0.3	0.46	5.8 ± 0.5	6.2 ± 0.5	0.43
Stroke volume, ml	82.8 ± 4.7	85.2 ± 4.6	0.42	90.4 ± 6.9	94.0 ± 5.7	0.51
PVR, dynes s^{-1} cm^{-5}	1268 ± 91	1278 ± 92	0.79	1229 ± 123	1119 ± 87	0.36

Normally distributed data presented as mean ± SEM. Student's paired t-tests were applied to paired observations after placebo and slow sodium

4.5.3.5 Correlations for skin Na^+:K^+

Univariate analyses revealed significant correlations between skin Na^+:K^+ and haemodynamic variables in men, as shown in Figure 4.16. Skin Na^+:K^+ correlated positively with supine MAP post placebo ($r=0.53$, $p<0.01$) and post slow sodium ($r=0.51$, $p=0.01$). Skin Na^+:K^+ was negatively correlated with SV and positively correlated with PVR post placebo and slow sodium. Plasma VEGF-C, after logarithmic transformation, showed a positive correlation with skin Na^+:K^+ post slow sodium ($r=0.51$, $p=0.01$) but not placebo ($r=0.06$, $p=0.79$) (fig. 3). These correlations were independent of age and BMI on multiple regression analysis. In women univariate analysis revealed a significant correlation only for skin Na^+: K^+ and PVR post salt ($r = 0.49$, $p=0.02$). On multiple regression analysis, this correlation was not independent of age.

Figure 4.16: Correlation between skin Na^+:K^+ and haemodynamic variables in men. (A) Supine brachial mean arterial pressure (MAP) post placebo. (B) Stroke volume post placebo. (C) Peripheral vascular resistance (PVR) post placebo. (D) Supine brachial MAP post slow sodium. (E) Stroke volume post slow sodium. (F) PVR post slow sodium.

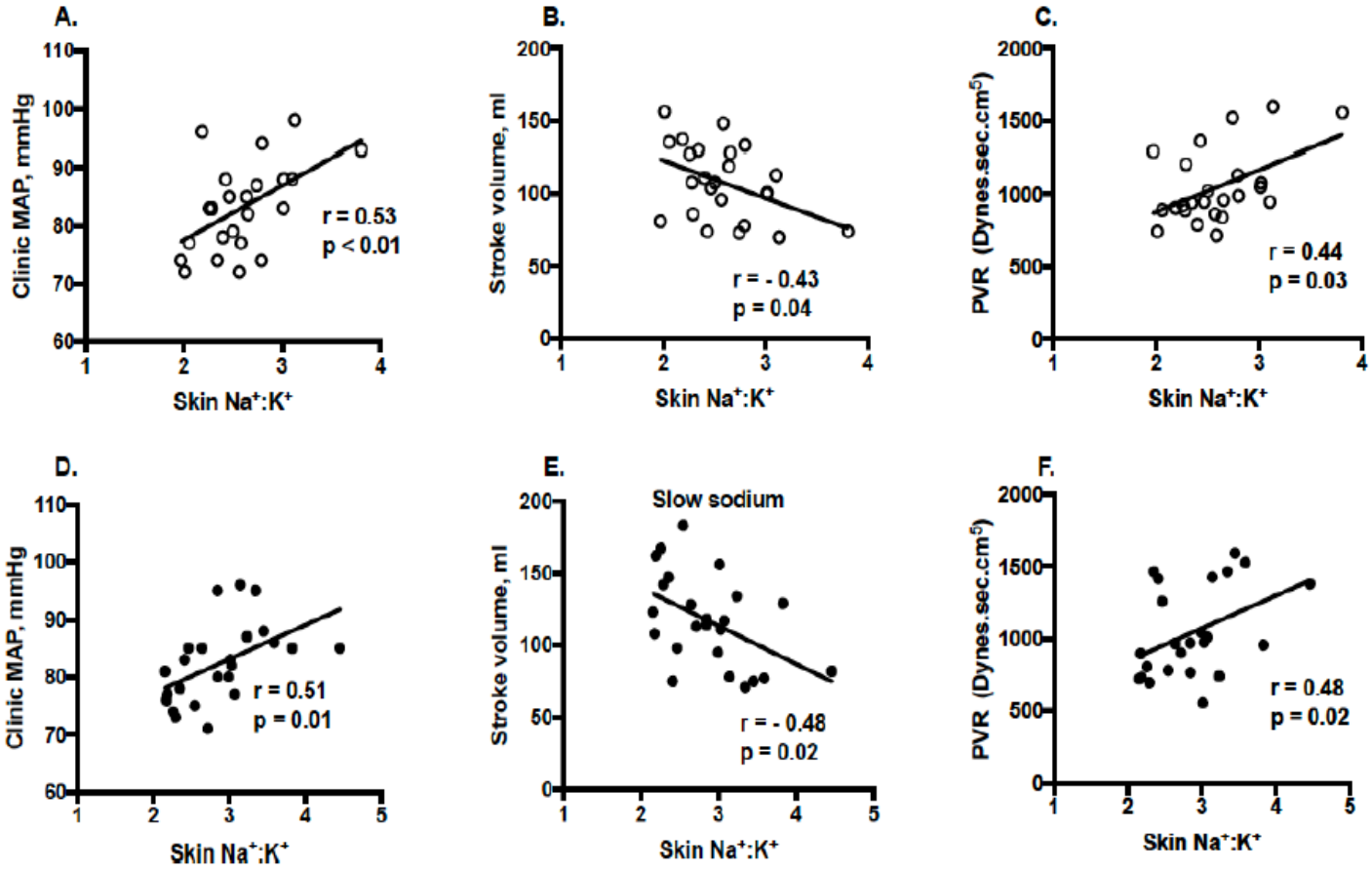

Figure 4.17: Correlation between skin Na^+:K^+ and plasma VEGF-C. A : Post-placebo. B: Post slow sodium

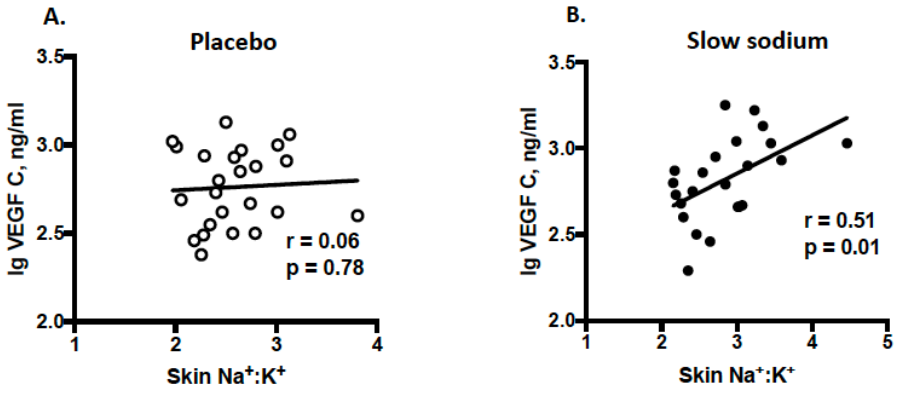

4.5.3.6 Effect of lidocaine type

14 male participants received conventional local anaesthetic (Xylocaine 1% with adrenaline, Astra Zeneca). 10 male participants received Na^+- free lidocaine using Dextrose as an excipient (Lidocaine 1% with Dextrose 3.5%, Tayside Pharmaceuticals, Dundee). In view of sex differences in skin Na^+:K^+ a comparison of results was done in males receiving both types of lidocaine . Skin Na^+:K^+ values post placebo and slow sodium were pooled for each group. As seen in Figure 4.18, no significant difference to suggest Na^+ contamination was evident.

Figure 4.18 : Comparison of skin Na^+:K^+ by type of local anaesthetic. Skin post-placebo and post-slow sodium samples from male participants who received conventional local anaesthetic (n = 14) and sodium-free anaesthetic (n = 10) in the VARSITY study are shown.

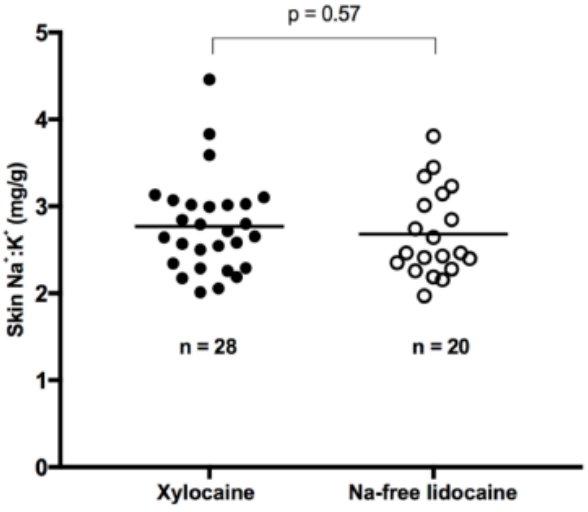

Bars are mean for the group. Comparisons between groups were made using the unpaired t test.

4.5.3 Salt taste sensitivity

Baseline salt recognition and detection thresholds are shown in Figure 4.19. Most participants had salt recognition and detection thresholds at 0.05 - 0.10 % NaCl. Univariate analyses did not reveal any significant correlations between salt recognition or detection thresholds and VEGF-C or other putative variables at baseline (Tables 4.13 and 4.14). These findings were similar in men and women (data not shown)

Figure 4.19: Baseline salt recognition thresholds (A) and detection thresholds (B) for the whole VARSITY study population (n = 48).

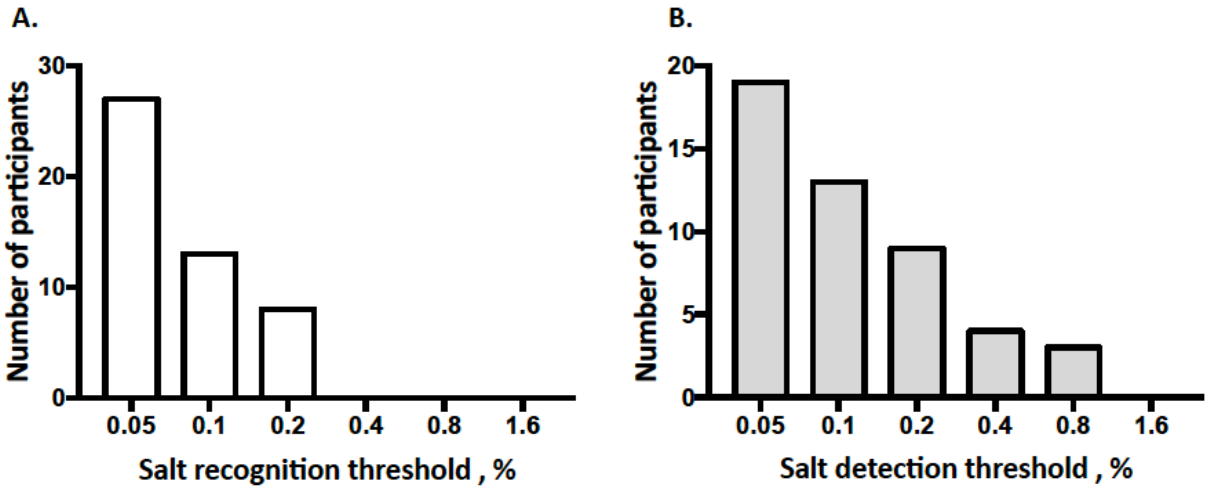

Table 4.13: Correlation between salt recognition threshold and putative variables in VARSITY methods.

Variable	Correlation Coefficient	Significance
Age, years	- 0.18	0.22
BMI, Kg/m^2	- 0.11	0.47
Supine MAP, mmHg	0.05	0.76
24-hr MAP	0.02	0.91
Renin, mU/l	- 0.01	0.94
Aldosterone, pmol/l	0.04	0.79
VEGF-C, pg/ml	- 0.11	0.49

Correlations were analyzed using Spearman's correlation coefficient by rank.

Table 4.14: Correlation between salt detection threshold and putative variables in VARSITY methods.

Variable	Correlation Coefficient	Significance
Age, years	- 0.18	0.22
BMI, Kg/m^2	- 0.07	0.62
Supine MAP, mmHg	- 0.01	0.97
24-hr MAP	- 0.11	0.47
Renin, mU/l	- 0.06	0.68
Aldosterone, pmol/l	- 0.19	0.20
VEGF-C, pg/ml	- 0.08	0.63

Correlations were analyzed using Spearman's correlation coefficient by rank.

The change in salt recognition and detection thresholds with placebo and slow sodium are shown in Figure 4.20. A significant change in salt detection threshold was observed,

indicating rise in the lowest concentration at which participants could distinguish between ROS water and salt solution. No change in salt recognition threshold was noted.

Figure 4.20: Response for salt recognition threshold (A) and detection thresholds (B) placebo vs. slow sodium for the whole VARSITY study population.

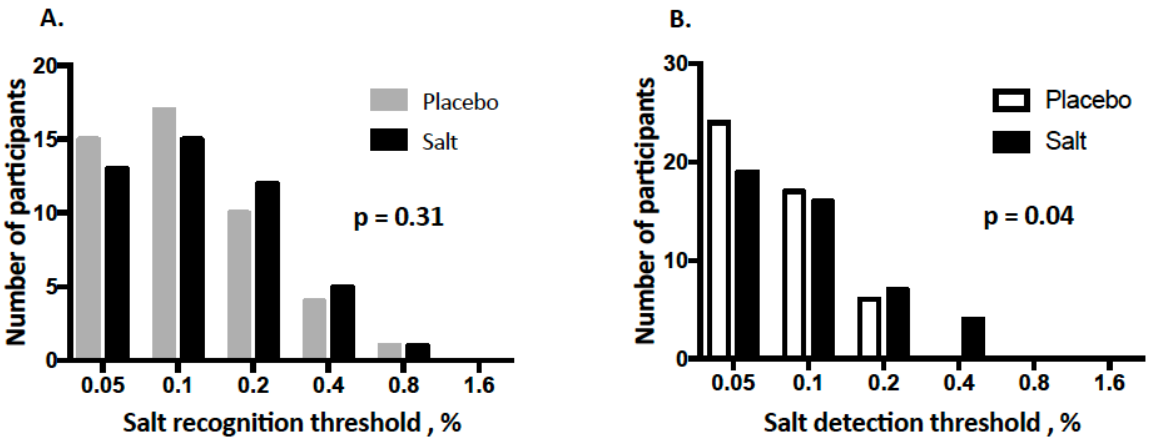

The Wilcoxon signed-rank test was used to compare salt recognition and detection thresholds post placebo and slow sodium treatments.

Univariate analyses did not reveal any significant correlations between the change in salt recognition or detection thresholds between placebo and slow sodium and the change in plasma VEGF-C, renin or aldosterone (Table 4.15).

Table 4.15: Correlation between observed difference (δ) in salt detection threshold and putative variables in VARSITY methods.

Variable	Correlation Coefficient	Significance
Age, years	- 0.05	0.77
BMI, Kg/m^2	- 0.16	0.29
Δ Renin, mU/l	- 0.18	0.24
Δ Aldosterone, pmol/l	-0.23	0.14
Δ VEGF-C, pg/ml	- 0.24	0.14

Correlations were analyzed using Spearman's correlation coefficient by rank. Δ represents change from placebo to slow sodium.

4.5.4 Skin capillaroscopy

3 non-Caucasian participants with dark skin were excluded from capillaroscopy analysis. Images for 20 participants were excluded as they were of inadequate quality and the software was unable to detect capillaries, as judged by both Dr Stephen Smith and myself. 5 participants were excluded as the SD for mean capillary density (MCD) exceeded 19/mm^2. The main baseline characteristics of the remaining 20 participants used for analysis are shown in Table 4.16. There were 12 men and baseline characteristics were comparable to the whole VARSITY study population. The main haemodynamic and biochemical responses to placebo vs. slow sodium for the 20 participants are shown in Table 4.17. Skin Na^+: K^+, night MAP and stroke volume were significantly higher post slow sodium compared to placebo, as seen in the main study population.

Table 4.16: Main baseline variables for the 20 participants used in capillaroscopy analysis.

Baseline variables	**(n=20)**
Age, years	31 ± 2
Ethnicity (Caucasian)	20/20
Sex (M/F)	12/8
BMI, kg ms^{-2}	23.2 (22.1 – 25.4)
Haemodynamic variables	
Supine SBP, mmHg	121 ± 2
Supine DBP, mmHg	70 ± 2
Supine MAP, mmHg	87 ± 2
24-hr MAP	95 ± 2
24-hr SBP	119 ± 2
24-hr DBP	75 ± 1
Biochemical variables	
Renin, mU/l	15.9 ± 2.0
Aldosterone, pmol/l	118 (84– 180)
24-hr Urine Na^+	113.0 ± 15.6

Normally distributed data presented as mean ± SEM. Non-normally distributed data are presented as median and IQR.

Table 4.17: Main haemodynamic and biochemical to placebo vs. slow sodium by sex for the 20 participants used in capillaroscopy analysis.

Variable	n=20		
	Placebo	Slow sodium	P-value
Haemodynamics			
Weight, kg	72.3 ± 2.7	73.5 ± 2.8	0.28
Clinic SBP, mmHg	115 ± 2	117 ± 2	0.29
Clinic DBP, mmHg	68 ± 2	68 ± 2	0.82
Supine MAP, mmHg	84 ± 2	84 ± 2	0.47
24-hr MAP, mmHg	96 ± 1	96 ± 1	0.18
Night MAP, mmHg	86 ± 2	89 ± 2	**0.03**
Stroke volume, ml	98.9 ± 5.1	109.5 ± 6.1	**0.02**
PVR, dynes s^{-1} cm^{-5}	1103 ± 62	1068 ± 79	0.52
Skin measurements			
Skin Na^+: K^+	2.76 ± 0.08	3.08 ± 0.14	**0.01**
Plasma measurements			
Renin, mU/l	20 (12 – 25)	7 (4 – 13)	**< 0.001**
Aldosterone, pmol/l	219 (82 – 361)	80 (69 – 88)	**< 0.001**
Urinary measurements			
Na^+, mmol/24hr	82.8 ± 11.8	226.0 ± 16.5	**< 0.001**

Normally distributed data presented as mean ± SEM. Non-normally distributed data are presented as median and IQR. Clinic BP refers to supine BP. Student's paired t-tests were applied to paired observations after placebo and slow sodium for normally distributed data and the Wilcoxon signed-rank test for non-normally distributed data.

Table 4.18 shows capillaroscopy data obtained at baseline (unoccluded) and after 2 min of venous occlusion at 60 mm Hg. Mean capillary density (MCD) at baseline was significantly lower after slow sodium (Figure 4.21).

Table 4.18: Changes in mean capillary density with salt intake in VARSITY methods.

Variable	n = 20 Placebo	Slow sodium	P-value
Mean Capillary density/mm^2			
Unoccluded	115.2 ± 4.3	106.4 ± 4.1	**0.01**
During venous occlusion	118.8 ± 4.8	121.5 ± 3.7	0.46
Absolute increase in capillary density/mm^2	3.6 ± 3.2	15.1 ± 3.1	**0.02**

Student's paired t-tests were applied to paired observations after placebo and slow sodium for normally distributed data and the Wilcoxon signed-rank test for non-normally distributed data.

Figure 4.21: Mean capillary density post placebo vs. slow sodium for the 20 participants.

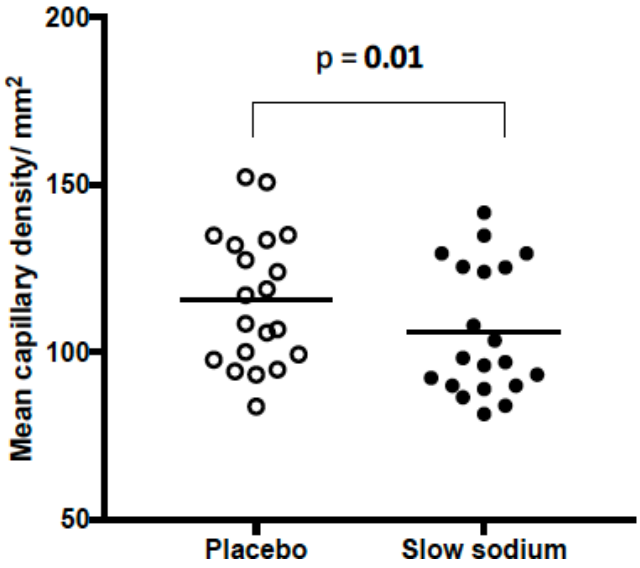

During venous occlusion, MCD increased post slow sodium but not post placebo (Figure 4.22). MCD post placebo and post slow sodium did not show any independent correlation with age, BMI or haemodynamic parameters (BP, stroke volume or PVR).

Figure 4.22: Effect of venous occlusion on mean capillary density post placebo (A) and post slow sodium (B) for the 20 participants used in capillaroscopy analysis.

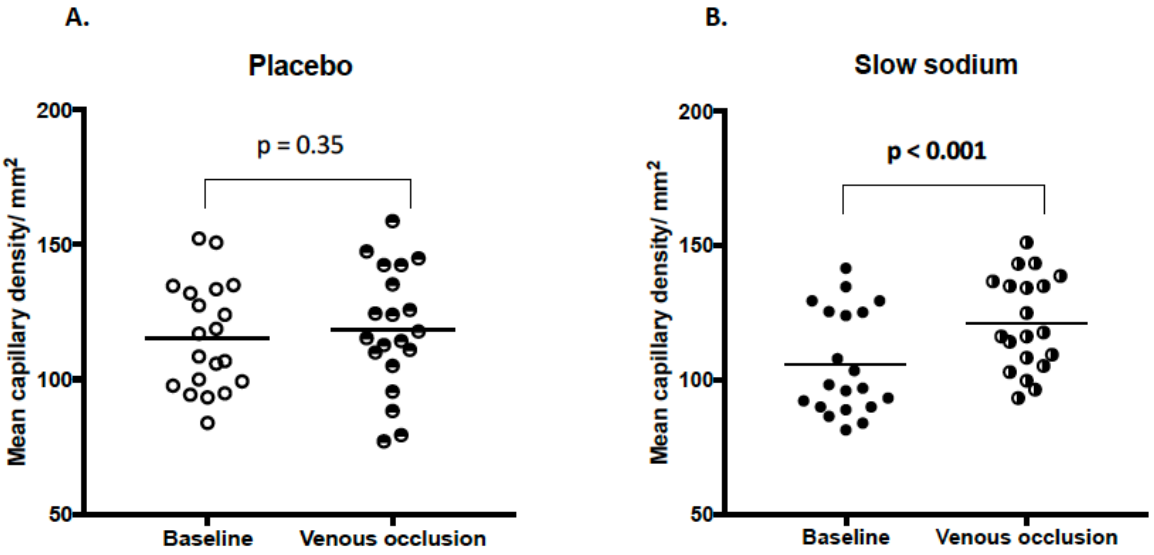

4.6 DISCUSSION

4.6.1 Main study

This study showed that skin sodium increases with dietary salt loading in healthy humans and this may occur in a sex-specific way. With dietary salt loading, men had a rise in skin Na^+:K^+ with no rise in BP, while women had a rise in ambulatory BP and no significant rise in skin Na^+:K^+. The dietary salt load used (200 mmol Na^+ for 7 days) is within the normal daily intakes of many individuals in urban societies, and thus would be clinically relevant. [36] The primary endpoint was significant, with skin Na^+:K^+ increasing between the placebo and slow sodium phases for the whole study population. This was mainly driven by men.

Skin measurements showed that women have lower skin K^+, as observed in the VARSITY methods pilot study (3.4.4) and consequently a higher Na^+:K^+ ratio (Table 4.7). The epidermis has previously found to have a significant K^+ content and this difference could be explained by the epidermis being thinner in women. [188,260] Therefore changes in Na^+:K^+ ratio with salt loading can be compared, but it is not possible to directly compare values for skin Na^+:K^+ between men and women.

Freeze-drying unfortunately could not remove moisture uniformly in small samples, particularly those below 10 mg (Figure 4.11), and it was not possible to use dry weight skin Na^+ and K^+ values as planned. The observed values for Na^+ and K^+ per unit wet weight fall within the range of previously published values [182,183,186]. To correct for sample hydration skin Na^+ was expressed as a ratio Na^+:K^+ because it was possible to measure K^+ reliably with ICPOES and evidence from animal work that skin K^+ remains stable with extremes of salt intake. [134,244,245] In our study skin K^+ did not change with salt loading. Furthermore, the Na^+ content of injected local anaesthetic did not appear to contaminate our skin samples (4.5.3.6).

Secondary analyses revealed that skin Na^+:K^+ had a significant interaction with sex and hence sex specific analyses were conducted. Unexpectedly the response to salt loading appeared to be different between men and women, with only men showing a significant increase in skin Na^+:K^+ . This difference was non-significant with formal ANOVA comparison,

and this was most probably due to small sample sizes. Women had a significant change in day and night ambulatory BP while men did not. This was associated with a significant gain in weight in women. This change in weight in women and lack thereof in men was in keeping with a greater sensitivity to dietary sodium in women. [118] Sex differences in baseline variables are in keeping with previous studies in healthy young adults. [258,269,289-291]. Augmentation index is higher in women and this is thought to be due to women having shorter stature and higher PVR, when corrected for body surface area. [269,292] Our study was not powered to show a difference in PVR, PWV. Or HRV.

There could be several explanations for the sex differences observed with salt loading. Sex differences in BP responses to dietary salt modulation (salt sensitivity), have previously been observed in large studies of healthy, young normotensive adults, as outlined in 1.5, with women showing a greater salt sensitivity. In this study the women had lower 24-hour UNaV post placebo than men (60.0 ± 6.8 vs. 86.3 ± 10.3 mmol; p=0.03) suggesting that they were more adherent to a low salt diet during placebo phase or ate less per se. This difference was statistically significant but modest. There are known limitations of using 24-hour UNaV to estimate Na^+ intake, with recent evidence showing ± 25 mmol deviations in urinary Na^+ from recorded Na^+ intake. [293] Nevertheless, differences in dietary salt restriction during the placebo phase is a possible reason why women had a greater salt sensitivity than men. An alternative explanation is that the men did not have BP changes with a short-term change in salt intake because they could buffer the additional dietary Na^+ with their skin via mechanisms described in animal studies, while in women this ability was attenuated.

In animals the skin buffers dietary salt, and a lower capacity to store Na^+ in the skin is associated with a greater BP rise during acute salt loading. [132] The sex differences could have been observed for 2 possible reasons. Firstly, men have a thicker skin at all ages and higher levels of dermal glycosaminoglycans. [261,262] This could imply that the skin is a more effective buffer for dietary Na^+ in men. In support of this, previous work in rats revealed that male rats had a higher capacity for osmotically inactive skin Na^+ storage compared to fertile female rats on a high salt intake. [132] Secondly, if we compare actual skin Na^+ measurements, which are not corrected for differences in sample hydration (table 4.7), there is a trend for

women to have a higher skin Na^+ post-placebo than men (2.15±0.05 vs 2.02±0.06 mg/g, p=0.08). This suggests that men had greater passage of Na^+ through the skin than women, as opposed to simply higher skin Na^+ storage, and the passage of Na^+ was protective in short-term salt loading. As shown in animal studies, the passage of skin Na^+ into the skin would have resulted in efflux of Na^+ via VEGF-C mediated lymphangiogenesis, which relates to NO production by VEGF-C. [133,134]. This is consistent with the known adaptation of salt-resistant subjects to a salt-load, which is vasodilation concomitant to the increase in cardiac output. [118,121,122]

There were significant correlations between skin Na^+:K^+ and various parameters in men, which were present regardless of salt intake. This suggests a physiological role for skin Na^+ or Na^+: K^+ ratio in regulating normal haemodynamics. Skin Na^+:K^+ was negatively correlated with stroke volume, which could be explained by higher Na^+:K^+ reflecting increased osmotically inactive Na^+ binding to glycosaminoglycans, allowing Na^+ without commensurate water accumulation, and therefore a less pronounced rise in circulatory volume. [64] Skin Na^+:K^+ was positively correlated with BP and PVR. The observations for BP and skin Na^+:K^+ support previous ^{23}Na MRI data, which showed skin Na^+ is positively associated with BP. [197] The mechanisms for these observations remain to be explained, but several possibilities exist. The skin is a rich source of nitric oxide, an important regulator of vascular tone. [211] Keratinocytes in the skin produce nitric oxide via nitric oxide synthase 2 (NOS-2) under the influence of hypoxia-inducible transcription factors, HIF-1a and HIF-2a, and these may be involved in modulation of dermal PVR. This is discussed further in 5.3. A further possible mechanism is dermal capillary rarefaction, which is discussed in 4.6.3. On univariate analysis, the only significant correlation for women was seen for skin or Na^+: K^+ and PVR post salt (r = 0.49, p=0.02). On multiple regression analysis, this correlation is not independent of age. In women contraceptive treatment did not seem to affect skin Na^+ or Na^+:K^+ response to salt loading, but skin K^+ was higher post salt ,and there was a trend for skin Na^+:K^+ to be lower in women on contraceptives (4.5.3.5). The reasons for this are unclear. Oestrogen administration increases epidermal thickness, which could partly explain this. [294] Therefore, the Na^+:K^+ ratio may have been less reliable for assessing correlations in women in our study.

No significant changes in plasma VEGF-C or sFLT4 were noted in either sex or the whole population between placebo and slow sodium phases. A previous study looking at plasma VEGF-C healthy adults noted no change on dietary salt loading. [159] This may be the first study looking at plasma sFLT4. Skin VEGF-C levels were not measured, which may not have been reflected by plasma levels, and therefore it may not be possible to make any conclusions on skin VEGF-C response. However, plasma VEGF-C in men correlated positively with skin Na^+:K^+ post slow sodium, which suggests increased in the salt-loaded state skin Na^+ induced VEGF-C production, as seen in animal studies. [133,134]

This study has several limitations. The study size was small, but we used a state-of-the art technique to measure skin Na^+, ICP-OES, which would have been more sensitive than ^{23}Na MRI. Our participants were non-resident and the control of Na^+ intake was challenging, especially in men. Dietary sodium intakes were not normalised for body weight. Participants also did not have their potassium and calorie intakes strictly controlled. Women were not salt loaded on the same day of the menstrual cycle. Our skin biopsies were small and taken from the lower back, and we had no means of ascertaining if they were representative of the whole skin or if skin Na^+ varies with region and time. Cl^-could not be measured with ICP-OES. The sex differences in BP and skin Na^+ are interesting but warrant further investigation and confirmation in larger studies. The use of ambulatory blood pressure monitoring made the detection of significant BP changes in women possible. Similar studies should also be conducted in older people, other ethnicities and hypertensives. In summary, it appears that the skin is a buffer for dietary salt, influencing the regulation of salt sensitivity, and this is affected by sex.

4.6.2 Salt taste sensitivity

This main finding of the salt taste sensitivity study was that salt detection threshold, or the lowest concentration at which participants could distinguish between ROS water and salt solution, increased with dietary salt loading. This implies that participants were less able to identify saltiness on a higher salt intake. No change in salt recognition threshold was noted. The observed salt recognition threshold range was similar to Choe et al[283]. Previous data in healthy humans have shown that detection thresholds decrease with dietary salt depletion and salt recognition threshold increased with dietary salt loading. [280,295] The methods and thresholds used in these studies varied, though they support the view that salt intake influences the appreciation of salt taste sensitivity. The mechanisms for this are uncertain. It is possible that the abundance of ENaC is altered by dietary salt loading, affecting the transduction of the taste of salt in the lingual epithelium. In this study and VEGF-C, renin and aldosterone levels did not clearly modulate this process, though lingual ENaC expression could have been reduced with decreased aldosterone levels post slow sodium in this study (Table 4.5). This would have implications for individuals moving to from rural societies to urbanised societies with higher salt intake, who may become less aware of the taste of salt, facilitating adaptation to a higher salt intake. There are several limitations for this study. The period of dietary salt modulation was short and dietary calorific and sugar intake was not controlled. The participants were presented salt solutions which may not have accurately simulated normal food substances.

4.6.3 Skin capillaroscopy

The main finding of the skin capillaroscopy study was that mean capillary density (MCD) at baseline was significantly lower after slow sodium, suggesting that capillary rarefaction had occurred with dietary salt loading (Figure 4.21).This observation is in keeping with data from He et al who showed that a significant increase in both basal and post venous occlusion MCD with dietary salt restriction in 169 subjects with untreated mild hypertension. [11] In this study venous congestion on significantly increased MCD post slow sodium, but not post placebo.

The mechanisms for capillary rarefaction are unclear, as outlined in 1.4, and is believed to represent a reduction in capillary blood flow and increase in PVR, raising BP. Greaney et al showed that high salt intake is associated with impaired dermal NO-mediated vasodilation in humans. [296] Helle et al showed that dermal pre-capillary skin vessels in rats on a high salt diet had increased vascular reactivity to noradrenaline. [297] These observations suggest that dietary salt affects vascular tone and could explain the positive correlation between skin Na^+ and BP as well as PVR the the VARSITY main study. The measured PVR in this group did not show significant change, with a trend for decrease in PVR (Table 4.17). The observation that capillary density increased with venous occlusion only post slow sodium suggests that blood flow in capillaries was attenuated with high salt intake. It is unknown if changes in PVR can occur in resistance vessels independent of systemic PVR.

A major limitation of this study was the significant number of images that were unsuitable for analysis, resulting in a small data set. Sub-group analyses were therefore not possible. Nevertheless, these findings highlight the possible role of dietary sodium in influencing dermal vascular tone.

4.6.4 Conclusions

In summary I conclude the following:

1. Skin Na^+ increases with dietary salt loading in humans.
2. The skin may buffer dietary Na^+, reducing the hemodynamic consequences of increased salt. This may be influenced by sex.
3. Skin Na^+ may influence blood pressure, stroke volume and PVR.
4. Increasing dietary salt may decrease salt taste sensitivity.

Chapter 5 CHANGES IN SKIN GENE EXPRESSION WITH DIETARY SALT MODULATION

5.1 INTRODUCTION

In Chapter 4 the change in skin Na^+ with dietary salt modulation and its relationship with hemodynamic variables were assessed. In this chapter, mechanisms explaining the link between skin Na^+ and systemic haemodynamics are explored.

Studies in rat models showed that dietary salt intake is directly linked to polymerization and sulphation of dermal glycosaminoglycans, providing an additional storage capacity for sodium. [130] GAG polymerisation was measured using messenger RNA (mRNA) levels of chondroitin synthase and xylose transferase, which are GAG polymerisation enzymes. [130] Evidence for this occurring in humans in lacking. Heer et al showed the mRNA expression for xeostosin-like glycosyltransferase 2 (EXTL2) (a heparan sulphate polymerisation enzyme) and hyaluronidase increased with dietary salt loading in 9 healthy men. The mean expression of mRNA for xylosyltransferase 1 (the rate-limiting key enzyme in the biosynthesis of the dermatan and heparan sulphate initiation linkage region) and chondroitin sulphate synthase 3 was not significantly increased during the high NaCl intake period. [298] Fischereder et al showed that skin GAGs content correlated with Na^+ concentration in renal transplant donors and recipients, suggesting that skin Na^+ storage is regulated by GAGs in humans. [143] The effect of dietary salt modulation on skin GAGs was not assessed.

Studies in rats also showed that macrophages exert a homeostatic function in the skin via TonEBP and VEGF-C, regulating clearance of osmotically inactive stored salt via lymphatic vessels. VEGF-C also induced expression of endothelial nitric oxide synthase (eNOS), causing vasodilation via nitric oxide (NO) production. [133,134] In these studies TonEBP and VEGF-C were quantified using western blotting and mRNA using real time polymerase chain reaction (rtPCR). eNOS was quantified using indirect immunofluorescence. [133,134] There is a paucity of evidence for the relationship between Ton-EBP, VEGF-C, BP and dietary salt in humans. Skin TonEBP and VEGF-C responses to dietary salt modulation in humans have not been

published.

The VARSITY study showed that skin sodium, expressed as skin Na^+:K^+, correlates with both MAP and peripheral vascular resistance in healthy humans (4.5.3.5). The mechanisms for this are unknown. The hypoxia inducible factor (HIF) transcription system plays a central role in a wide range of adaptive responses to changes in oxygenation. [216] As described in 1.4, the relative concentrations of HIF-1α and HIF-2α ratio in the skin affects MAP in humans, with a higher HIF-2α:HIF-1α ratio being associated with hypertension. [217] This occurs via differential effects on inducible nitric oxide synthase (iNOS) and regulation of nitric oxide (NO) equilibrium in the skin. [217] Furthermore, HIF-1α up-regulates VEGF A, which influences NO by upregulating eNOS via VEGFR2 receptors, influencing vascular tone. [219,220] HIF metabolism may also be related to dietary salt intake. In the rat kidney model, high salt intake has been shown to suppress prolyl hydroxylase domain 2 (PHD 2), which hydroxylates and degrades HIF-1α and HIF-2α. [299-301] The increase in HIF-1α alpha expression, resulting upregulation of heme oxygenase 1 (HO-1) 1 and cyclooxygenase 2 (COX-2), endothelin 1 and inducible nitric oxide synthase. This results in pressure natriuresis, counteracting the haemodynamic effects of dietary salt. [221,222] It would be plausible for a similar mechanism to exist in the skin whereby high salt intake alters levels of HIF isomers, potentially influencing PVR and BP (Figure 5.1).

Figure 5.1: A possible mechanism linking dietary salt intake, HIF isomers in the skin and BP. Keratinocytes in the skin produce nitric oxide via nitric oxide synthase 2 (NOS-2 or iNOS) under the influence of hypoxia-inducible transcription factors HIF-1α and HIF-2α, which act antagonistically. HIF-1α induces nitric oxide synthase 2 (NOS-2 or iNOS) which metabolises L-arginine , producing NO. HIF-2α induces arginase-1, which catalyses the hydrolysis of L-arginine to l-ornithine and urea, thus depleting L-arginine available for conversion to NO by iNOS [218,302,303] HIF-1α up-regulates VEGF A, which influences NO by upregulating eNOS via VEGFR2 receptors, influencing PV. The balance of dermal HIF-1α and HIF-2α influences BP by altering NO expression, which alters PVR. High salt intake suppresses PHD2, which degrades HIF-1a and HIF-2a, thus potentially influencing PVR.

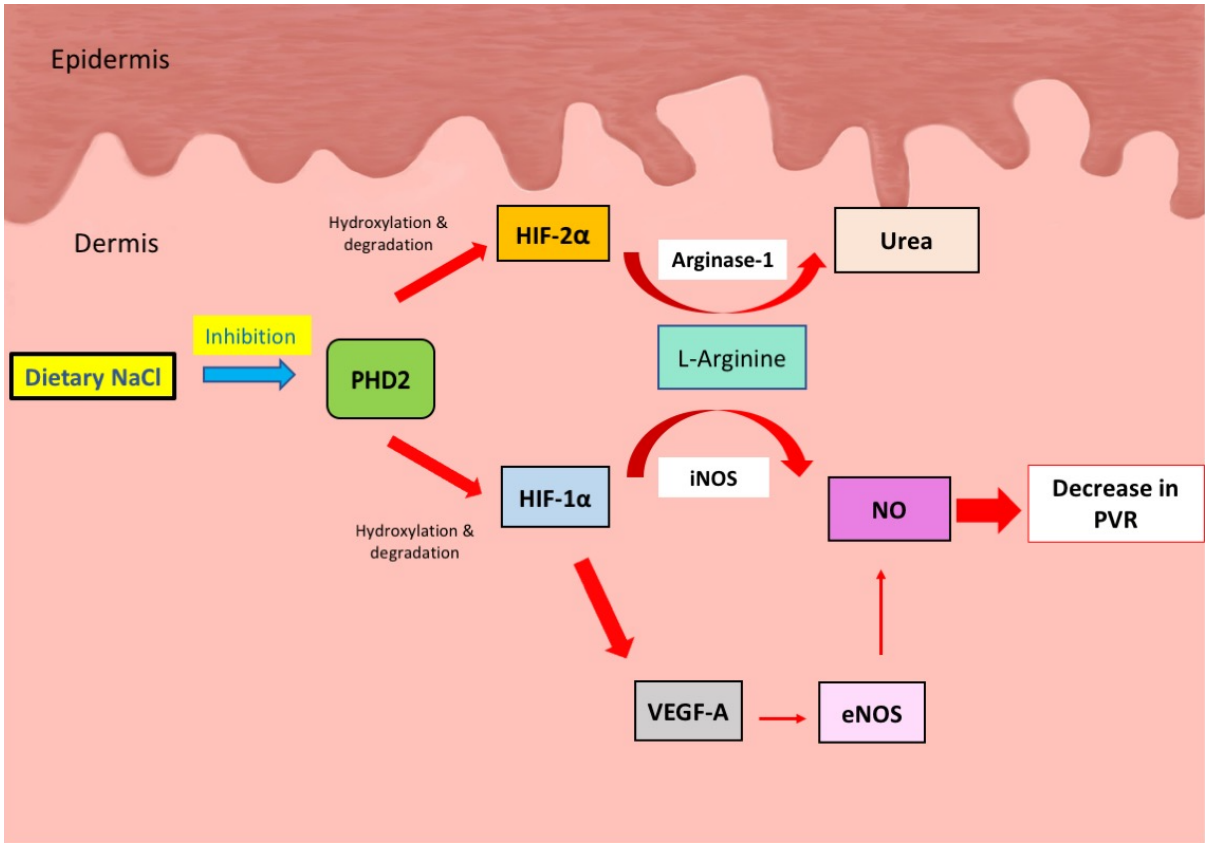

On this background changes in dermal gene expression of GAG-polymerisation enzymes, Ton-EBP, VEGF-C and HIF isomers with dietary salt modulation was conducted in a subset of VARSITY study participants. As a sex-specific difference in haemodynamic response to dietary salt was observed, a comparison was made between gene expression in men and women. All procedures involving the analysis of skin gene expression described in this chapter were carried out by QIAGEN in their service laboratory in Hilden, Germany.

5.2 HYPOTHESES

. Increased salt intake in humans leads to increased dermal gene expression of GAG-polymerisation enzymes, Ton-EBP and VEGF-C in humans.
. The dermal hypoxia inducible factor transcription system is altered by dietary salt loading and this relates to associated BP changes - an increase HIF-2α expression would raise BP while an increase HIF-1α would lower BP.
. Differences in gene expression in relation to salt intake may explain the sex-specific difference in BP response to dietary salt modulation observed in the VARSITY study.

5.3 AIMS

1. The primary aim of this study was to assess the difference in gene expression for GAG-polymerisation enzymes, Ton-EBP, VEGF-C and HIF isomers with different salt intakes.

2. The secondary aim was to assess sex-specific differences in gene expression.

5.4 METHODS

5.4.1 Subjects

20 participants for the VARSITY main study were selected if they had good dietary sodium compliance during placebo and slow sodium phases and sufficient skin tissue for analysis. These included 10 men and 10 women who were age matched.

5.4.2 Design and protocol

The VARSITY study design and protocol, as described in 4.4.1, was used for all 20 participants. Skin samples were obtained using methods described in 4.4.5 and 4.4.6 after placebo and slow sodium treatments. The remaining portion of each skin sample was stored at −80°C and transferred to the QIAGEN service laboratory in Hilden for PCR analysis using a custom quantitative PCR (qPCR) array. This was designed with genes of interest selected from QIAGEN's catalogue and conducted by QIAGEN using their own protocols, selected necessary housekeeper and internal control genes.

5.4.3 Custom quantitative PCR array

A brief overview of the custom quantitative PCR array carried out by QIAGEN is summarised below.

5.4.3.1 Genes of interest

The genes of interest included in the qPCR array are listed in table 5.1. These included genes for the following:

- Key GAG polymerisation enzymes such as chondroitin sulphate synthase (chondroitin sulphate elongation), dermatan sulphate epimerase (dermatan sulphate elongation),

xylosyl transferase 1 (dermatan or chondroitin sulphate initiation) and xylosyl transferase 2 (chondroitin or heparan sulphate elongation).

- The Ton-EBP - VEGF-C axis, including FLT-4, a tyrosine kinase receptor for vascular endothelial growth factor C.
- The HIF isomers and PHD2, which degrades HIF-1 α and HIF-2α.
- VEGF-A (a HIF-1 α target gene) and its tyrosine kinase receptor FLT-1.
- eNOS (NOS3) and iNOS(NOS2).
- 5 Housekeeping genes selected by QIAGEN

Table 5.1: The genes of interest included in the QIAGEN qPCR array.

Gene	Symbol
Vascular endothelial growth factor-A	VEGF-A
Vascular endothelial growth factor-C	VEGF-C
Fms-related tyrosine kinase 1	FLT-1 (VEGFR-1)
Fms-related tyrosine kinase 4	FLT-4 (VEGFR-3)
Ton-EBP (NFAT5)	Ton-EBP
Dermatan sulphate epimerase	DSE
Xylosyltransferase I	XYLT1
Xylosyltransferase II	XYLT2
Chondroitin sulphate synthase 1	CHSY1
Hypoxia inducible factor 1	HIF-1α
Endothelial PAS domain protein 1	HIF-2α
Egl nine homolog 1 (C. elegans)	PHD2
Inducible nitric oxide synthase 2	NOS2
Inducible nitric oxide synthase 3	NOS3
Housekeeping genes	
Hypoxanthine phosphoribosyl transferase 1	HPRT1
Ribosomal protein, large, P0	RPLP0
Actin, beta	ACTB
Glyceraldehyde-3-phosphate dehydrogenase	GAPDH
Beta-2-microglobulin	B2M

5.4.3.2 RNA Isolation and quality assessment

Skin tissue samples were first lysed in Buffer RLT and diluted before being treated with proteinase K. Debris were pelleted by centrifugation, and the supernatant is removed before being mixed with ethanol and then centrifuged through a RNeasy spin column. Traces of DNA copurified with the RNA were removed by DNase treatment on the silica membrane. DNase and any contaminants were washed away and RNA was eluted in RNase-free water. RNA quality and concentration are determined by using a Nanodrop spectrophotometer to measure the concentration and optical density (OD) 260/280 values of the samples.

5.4.3.3 cDNA Synthesis and Pre-amplification

The RT2 PreAMP complementary DNA (cDNA) Synthesis Kit (Cat. No. 330451) and RT2 PreAMP Pathway Primer Mixes (QIAGEN, Maryland, USA) were used to synthesis and pre-amplification of cDNA from total RNA samples, prior to gene expression analysis using a RT2 Profiler PCR array.

5.4.3.4 Real-time reverse transcription PCR

cDNA was mixed with a ready-to-use QIAGEN RT^2 SYBR® Green qPCR Master Mix. The mixture was added into a 96-well RT^2 mRNA PCR Array (SABiosciences) that contained primers for 84 tests and 5 housekeeping genes according to manufacturer's instruction. Thermal cycling was performed using ABI-7900 (Applied Biosystems, Foster, CA, USA).

5.4.3.5 Quality control methodologies

Quality control for qPCR was checked by assessing of PCR array reproducibility, reverse transcription efficiency and genomic DNA contamination. The Positive PCR Controls (PPC) were used to test the efficiency of the polymerase chain reaction using a pre-dispensed artificial DNA sequence and the primer set that detects it. Reverse transcription efficiency was assessed by testing the efficiency of the RT^2 First Strand Synthesis Kit (330401) reaction

with a primer set to detect template synthesized from the kit's built-in external RNA control. The DNA contamination control assay (GDC) was used to determine if genomic DNA was present in a skin sample at an amount that may affect PCR results. The GDC primers were used to specifically detect non-transcribed genomic DNA contamination, defined as Ct(GDC) < 30. In addition, control genes included in the array were used to assess the presence of impurities in RNA samples that affected the PCR amplification.

5.4.3.6 Data analysis and statistics

The QIAGEN PCR Array Data Analysis Web Portal (http://www.sabiosciences.com/pcrarraydataanalysis.php) automatically performed the above calculations and interpretation of the control wells upon including threshold cycle data from the real-time instrument (See Figure 5.2).

The threshold cycle (Ct) value is the cycle number at which the fluorescence generated within a reaction crosses the fluorescence threshold, which is a fluorescent signal significantly above the background fluorescence. At the threshold cycle, a detectable amount of amplicon product has been generated during the early exponential phase of the reaction. The threshold cycle is inversely proportional to the original relative expression level of the gene of interest. A Ct value equal to 35 was considered a negative call.

Figure 5.2: An example of how QIAGEN PCR Array Data Analysis Web Portal generates cycling curves and determines threshold cycle (Ct) value for each gene.

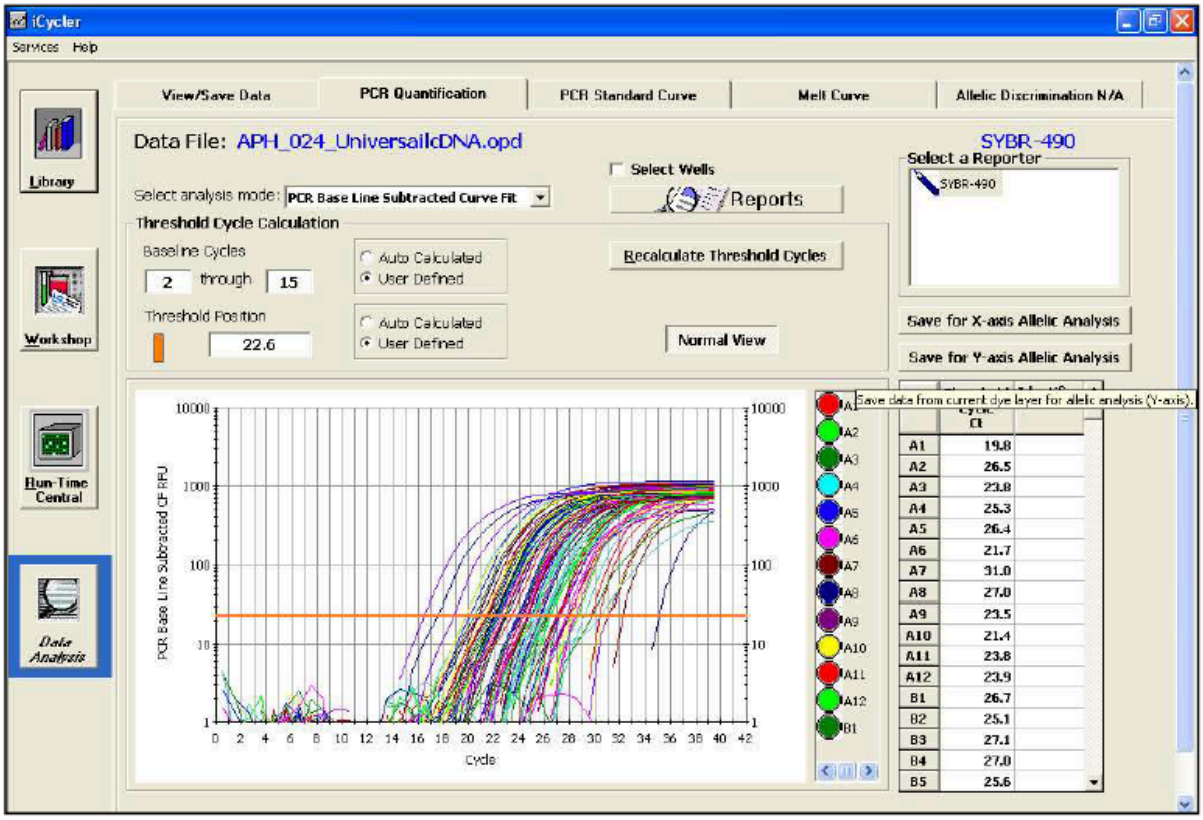

qPCR relative expression of genes of interest was determined with the double delta cycle threshold (ddCt or ΔΔCt) method as follows:

4. dCt = (Ct Gene of Interest) – (Ct Average of Housekeeping Genes)
5. ddCt = dCt (group 2) - dCt (group 1) where Group 1 refers to placebo and Group 2 refers to slow sodium

Differences in mRNA abundance and gene expression were expressed as fold changes (FC) and were calculated using 2^{-ddCt} method. A fold change > 1 represented an upregulation of a gene with slow sodium while a fold change of < 1 represented downregulation. Differences in gene expression for placebo vs. slow sodium treatments were analysed by Student's t-test. The p values were calculated based on a Student's t-test of the replicate 2^ (- Delta CT) values for each gene in the control group and treatment groups. A P value < 0.05 was considered to be statistically significant.

5.5 RESULTS

5.5.1 Analysis of whole study population

5.5.1.1 Baseline characteristics

The 20 participants (10 men, 10 women) had a mean age of 30 ± 2 years (range 18–49 years). Baseline characteristics are shown in Table 5.2. Our study sub-set had a low baseline sodium intake compared to the current average intake in England (approximately 130 mmol/day) and had similar baseline characteristics to the whole VARSITY study population. [256]

Table 5.2 : Baseline data for the 20 participants used in qPCR array.

Baseline variables	**(n=20)**
Age, years	31 ± 2
Ethnicity (Caucasian)	18/20
Sex (M/F)	10/10
BMI, kg ms^{-2}	24.1 ± 1
Haemodynamic variables	
Supine SBP, mmHg	119 ± 2
Supine DBP, mmHg	71 ± 2
Supine MAP, mmHg	87 ± 2
24-hr MAP	96 ± 2
24-hr SBP	120 ± 2
24-hr DBP	76 ± 2
Biochemical variables	
Renin, mU/l	14.1 ± 2.0
Aldosterone, pmol/l	110 (70 – 181)
24-hr Urine Na^+, mmol/24hr	80.0 ± 12.2

Normally distributed data presented as mean ± SEM. Non-normally distributed data are presented as median and IQR.

5.5.1.2 qPCR array quality assessment

All gene average threshold cycles were below the limit of 35. All samples passed PCR array reproducibility and reverse transcription efficiency tests using the QIAGEN PCR Array Data Analysis Web Portal. No significant genomic DNA contamination was detected.

5.5.1.3 Main haemodynamic and biochemical responses

The main haemodynamic and biochemical responses to placebo vs. slow sodium for the 20 participants are shown in Table 5.3. 24-hr MAP was significantly higher post slow sodium compared to placebo, as seen in the main study population.

Table 5.3: Main haemodynamic and biochemical responses to placebo vs. slow sodium for the 20 participants used in qPCR array.

Variable	n=20		
	Placebo	Slow sodium	P-value
Haemodynamics			
Weight, kg	67.9 ± 2.5	68.1 ± 2.4	0.50
Clinic SBP, mmHg	115 ± 2	117 ± 2	0.10
Clinic DBP, mmHg	70 ± 2	70 ± 2	0.66
Supine MAP, mmHg	85 ± 1	86 ± 2	0.27
24-hr MAP, mmHg	95 ± 1	98 ± 1	**0.04**
Day MAP, mmHg	99 ± 2	101 ± 1	0.10
Night MAP, mmHg	87 ± 2	90 ± 2	0.05
Stroke volume, ml	97.1 ± 4.7	103.7 ± 6.7	0.10
PVR, dynes s^{-1} cm^{-5}	1138 ± 67	1106 ± 82	0.36
Skin measurements			
Skin Na^+: K^+	2.91 ± 0.12	3.14 ± 0.16	0.10
Plasma measurements			
Renin, mU/l	219(10 – 27)	4(3 – 11)	**< 0.001**
Aldosterone, pmol/l	180 (92 – 407)	70 (65 – 80)	**< 0.001**
VEGF-C, pg/ml	632 ± 75	703 ± 90	0.52
sFlt-4, pg/ml	10.0 ± 1.2	10.4 ± 1.0	0.55
Urinary measurements			
Na^+, mmol/24hr	64.8 ± 7.0	261.0 ± 15.2	**< 0.001**

Normally distributed data presented as mean ± SEM. Non-normally distributed data are presented as median and IQR. Clinic BP refers to supine BP.

5.5.1.4 qPCR array results

Skin samples had a mean wet weight of 8.9 ± 0.7 mg. qPCR array results showing gene expression for slow sodium vs. placebo treatments are shown in Table 5.4. No significant changes were noted in gene expression for placebo compared to salt. There were trends for

increase in FLT-1 (VEGFR-1), HIF-2a, iNOS and eNOS with slow sodium treatment relative to placebo. VEGF-C showed a trend for decreased expression with slow sodium treatment relative to placebo (FC 0.59, p = 0.31). No change in gene expression for GAG polymerisation enzymes was seen with dietary salt loading.

Table 5.4: Changes in gene expression with placebo vs. slow sodium by sex for the 20 participants used in qPCR array.

Gene of interest	Symbol	Fold change	P-value
Vascular endothelial growth factor-A	VEGF-A	1.09	0.74
Vascular endothelial growth factor-C	VEGF-C	0.59	0.31
Fms-related tyrosine kinase 1	FLT-1 (VEGFR-1)	1.32	0.10
Fms-related tyrosine kinase 4	FLT-4 (VEGFR-3)	0.92	0.42
Ton-EBP (NFAT5)	Ton-EBP	1.06	0.50
Dermatan sulphate epimerase	DSE	0.96	0.68
Xylosyltransferase I	XYLT1	0.74	0.45
Xylosyltransferase II	XYLT2	1.09	0.53
Chondroitin sulphate synthase 1	CHSY1	1.11	0.30
Hypoxia inducible factor 1	HIF-1α	1.02	0.93
Endothelial PAS domain protein 1	HIF-2α	1.21	0.14
Egl nine homolog 1 (C. elegans)	PHD2	1.05	0.53
Inducible nitric oxide synthase 2	iNOS	1.48	0.11
Endothelial nitric oxide synthase 3	eNOS	1.30	0.09

Differences in mRNA abundance and gene expression were expressed as fold changes (slow sodium/ placebo) and were calculated using 2^{-ddCt} method. A fold change > 1 represented an upregulation of a gene with slow sodium compared to placebo while a fold change of < 1 represented downregulation. Fold-change values less than one indicate a negative or down-regulation. The p values are calculated based on a Student's t-test of the replicate 2^ (- Delta CT) values for each gene for placebo slow sodium treatments. P values less than 0.05 are considered significant.

5.5.2 Sex-specific analysis

5.5.2.1 Baseline characteristics

Sex-specific baseline characteristics are shown in Table 5.3. There were no significant differences in age or BMI between sexes. 4 women were on contraceptive treatment. Men had higher 24-hr SBP and renin, in keeping with the main VARSITY population.

Table 5.5: Sex-specific baseline characteristic for participants used in qPCR array.

Baseline variables	Males n = 10	Women n = 10	P value
Age, years	29 ± 3	33 ± 2	0.33
Ethnicity (Caucasian)	9/10	9/10	-
BMI, kg ms^{-2}	23.7 ± 1	24.6 ± 1	0.46
Haemodynamic variables			
Supine SBP, mmHg	122 ± 2	115 ± 3	0.13
Supine DBP, mmHg	70 ± 3	73 ± 2	0.42
Supine MAP, mmHg	87 ± 2	92 ± 2	0.21
24-hr MAP	100 ± 3	92 ± 2	0.06
24-hr SBP	126 ± 3	115 ± 2	**0.002**
24-hr DBP	78 ± 4	74 ± 1	0.38
Biochemical variables			
Renin, mU/l	20.0 ± 3.0	9.3 ± 2.0	**0.002**
Aldosterone, pmol/l	133.4 ± 16.3	134.5 ± 36.2	0.99
24-hr Urine Na^+, mmol/24hr	90.2 ± 20.9	66.2 ± 8.4	0.35

Normally distributed data presented as mean ± SEM. Non-normally distributed data are presented as median and IQR. The values for males and females was analyzed using the unpaired t test with normally distributed data and Man Whitney test for non-normal data. P value < 0.05 taken to be significant.

5.5.2.2 Main haemodynamic and biochemical responses

Sex-specific main haemodynamic and biochemical responses to placebo vs. slow sodium are shown in Table 5.6. Dietary salt compliance and difference in urinary sodium between placebo and slow sodium treatments was similar in men and women. In men there were no

differences in BP following salt loading, whilst women had higher 24-hour, day and night MAP. Only women had an increase in body weight post slow sodium (62.7 ± 1.4 vs. 63.5 ± 1.3 kg; p = 0.04). Men showed a rise in stroke volume and a trend for decrease in PVR with slow sodium, while in women this was not observed. Men had 9.3 % a rise skin Na^+:K^+ post slow sodium while in women this was 6.7 %, neither of which was statistically significant. In men there was a trend for higher plasma VEGF-C (840 ± 150 vs. 567 ± 77 pmol/l, p = 0.07) but in women this was not apparent (579 ± 96 vs 698 ± 131 pmol/l, p = 0.63). sFLT-4 did not change between treatments.

Table 5.6: Main haemodynamic and biochemical responses to placebo vs. slow sodium by sex for the 20 participants used in qPCR array.

Variable	Men (n=10)			Women (n=10)		
	Placebo	Slow sodium	P-value	Placebo	Slow sodium	P-value
Haemodynamics						
Weight, kg	73.1 ± 4.2	72.7 ± 4.3	0.32	62.7 ± 1.4	63.5 ± 1.3	**0.04**
Clinic SBP, mmHg	116 ± 2	119 ± 2	0.07	114 ± 3	116 ± 2	0.43
Clinic DBP, mmHg	68 ± 2	69 ± 2	0.64	71 ± 2	71 ± 2	0.87
Supine MAP, mmHg	84 ± 2	85 ± 2	0.26	85 ± 2	86 ± 2	0.59
24-hr MAP, mmHg	99 ± 2	100 ± 2	0.80	92 ± 1	96 ± 2	**0.003**
Day MAP, mmHg	101 ± 2	103 ± 2	0.91	97 ± 2	100 ± 2	**0.02**
Night MAP, mmHg	92 ± 2	93 ± 2	0.67	82 ± 1	87 ± 2	**0.006**
Stroke volume, ml	101.2 ± 7.1	116.4 ± 10.3	**0.01**	92.9 ± 6.1	91.0 ± 6.7	0.69
PVR, dynes s^{-1} cm^{-5}	1091 ± 88	1006 ± 114	0.08	1185 ± 103.6	1206 ± 115	0.68
Skin measurements						
Skin Na^+: K^+	2.67 ± 0.15	2.92 ± 0.19	0.16	3.15 ± 0.16	3.36 ± 0.24	0.37
Plasma measurements						
Renin, mU/l	23.6 ± 2.8	8.9 ± 1.6	**< 0.001**	15.2 ± 2.8	4.8 ± 1.2	**0.001**
Aldosterone, pmol/l	180 (93 – 268)	70 (68 – 118)	**0.01**	235 (69 – 455)	69 (65 – 74)	**0.02**
VEGF-C, pg/ml	567 ± 77	840 ± 150	0.07	698 ± 131	579 ± 96	0.38
sFlt-4, pg/ml	7.5 ± 1.8	7.9 ± 1.5	0.83	12.5 ± 1.2	13.0 ± 0.9	0.63
Urinary measurements						
Na^+, mmol/24hr	67.6 ± 10.7	260.1 ± 25.8	**< 0.001**	62.0 ± 9.6	261.9 ± 17.7	**< 0.001**

Normally distributed data presented as mean ± SEM. Non-normally distributed data are presented as median and IQR. Student's paired t-tests were applied to paired observations after placebo and slow sodium for normally distributed data and the Wilcoxon signed-rank test for non-normally distributed data. Clinic BP refers to supine BP.

5.5.2.3 qPCR array results

Sex specific qPCR array results showing gene expression for slow sodium vs. placebo treatments are shown below Table 5.7 and Figure 5.3. Women had a significant rise in HIF-2A gene expression with slow sodium compared to placebo (FC 1.43, p = 0.046) while in men this was attenuated (FC 1.17, p = 0.14). In men there was a trend for increase in iNOS and eNOS gene expression, in keeping with a trend for decrease in PVR with slow sodium compared to placebo. Both sexes showed a trend for decreased VEGF-C expression with slow sodium compared to placebo, though this was associated with wide 95% confidence intervals - (FC 0.67; CI 0.05, 1.29; p = 0.90) for men and (FC 0.54; CI 0.06, 1.02; p = 0.31) for women. In women there was a trend for increase in FLT-1 (FC 1.71, p = 0.11) with slow sodium treatment relative to placebo, while this was not seen in men (FC 1.07, p = 0.41). There was a trend for FLT4 expression to increase in men (FC 1.32, p = 0.26) and decrease in women (FC 0.64, p = 0.78). No change in gene expression for GAG polymerisation enzymes was seen with dietary salt loading in either sex.

Table 5.7: Sex-specific changes in gene expression with placebo vs. slow sodium by sex.

Gene of interest	Symbol	Men (n = 10)		Women (n = 10)	
		Fold change	P-value	Fold change	P-value
Vascular endothelial growth factor-A	VEGF-A	1.21	0.38	0.91	0.45
Vascular endothelial growth factor-C	VEGF-C	0.67	0.90	0.54	0.31
Fms-related tyrosine kinase 1	FLT-1 (VEGFR-1)	1.07	0.41	1.71	0.11
Fms-related tyrosine kinase 4	FLT-4 (VEGFR-3)	1.32	0.26	0.64	0.78
Ton-EBP (NFAT5)	Ton-EBP	1.07	0.35	1.00	0.97
Dermatan sulphate epimerase	DSE	0.91	0.54	0.97	0.92
Xylosyltransferase I	XYLT1	0.86	0.75	0.26	0.35
Xylosyltransferase II	XYLT2	0.97	0.79	1.26	0.48
Chondroitin sulphate synthase 1	CHSY1	1.03	0.77	1.17	0.31
Hypoxia inducible factor 1	HIF-1A	1.06	0.84	0.94	0.81
Endothelial PAS domain protein 1	HIF-2A	1.07	0.48	1.43	**0.046**
Egl nine homolog 1 (C. elegans)	PHD2	1.17	0.34	0.93	0.66
Inducible nitric oxide synthase 2	iNOS	1.43	0.24	1.24	0.53
Endothelial nitric oxide synthase 3	eNOS	1.45	0.16	1.13	0.38

Differences in mRNA abundance and gene expression were expressed as fold changes (slow sodium/ placebo) and were calculated using 2^{-ddCt} method. A fold change > 1 represented an upregulation of a gene with slow sodium compared to placebo while a fold change of < 1 represented downregulation. Fold-change values less than one indicate a negative or down-regulation. The p values are calculated based on a Student's t-test of the replicate 2^ (- Delta CT) values for each gene for placebo slow sodium treatments. P values less than 0.05 are considered significant.

Figure 5.3: Illustration of changes in gene expression for men and women for slow sodium vs. placebo. The diagrams show the mean fold changes and SEM.

A: HIF isomers and PHD-2.

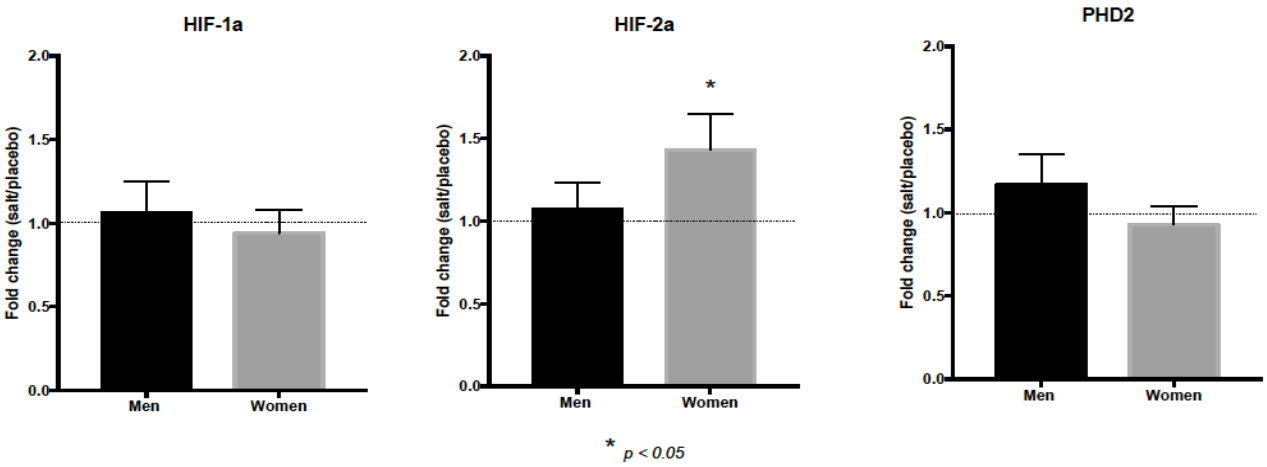

B. INOS and eNOS.

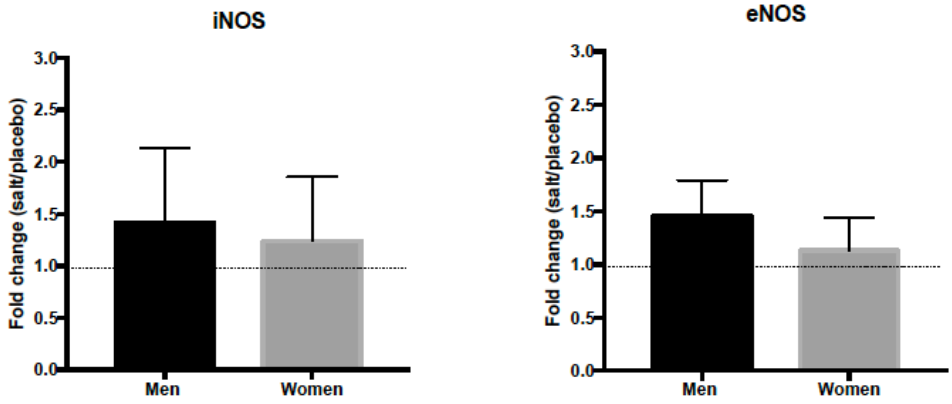

C. VEGF-A (a HIF-1α target gene) and its tyrosine kinase receptor FLT-1.

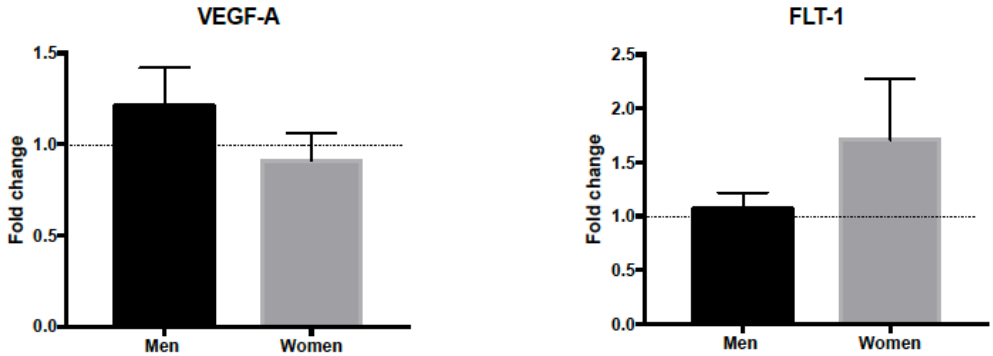

5.6 DISCUSSION

This analysis of specific dermal gene expression changes was carried out in a sub-set of 20 participants with characteristics and sex-specific differences similar to the main VARSITY study population. In analysis of all 20 participants an increase in 24-hr MAP was seen with salt loading and this was not associated with any clear change in GAG polymerisation, Ton-EBP, VEGF-C, VEGF-A or HIF isomers. In sex-specific analyses, women had a BP rise and increase in body weight with higher dietary salt while men did not, despite similar urinary sodium excretions in both groups. This sex-specific difference in haemodynamic response was associated with differences in dermal gene expression for HIF-2 and trends for differences in expression for eNOS, iNOS and FLT-1. There was no clear evidence that differences in the Ton-EBP-VEGF-C axis or polymerization and sulphation of dermal glycosaminoglycans explain the sex-specific difference in haemodynamic response.

Previous studies showing activation of the Ton-EBP-VEGF-C axis in rats used high salt intake of 4-8% NaCl over 4 weeks. [133,134] This represents an increase in salt intake of up to 15-fold compared to rats receiving a normal intake of 0.4% NaCl. [304] In the VARSITY study, 7 days of high salt intake (approximately 16 g of NaCl a day) were used, which is less than twice the average salt intake in current average intake in England (approximately 130 mmol/day). [256] This was a more relevant level of salt intake, but it may not have caused an adequate increase skin hypertonicity to induce Ton-EBP. In men there was a trend for increase in plasma VEGF-C and a trend in both sexes for a decrease in VEGF-C gene expression. Reasons for these observations are unclear and both plasma ELISA quantification and mRNA quantification showed significant variability, limiting the ability to observe trends. In rats both gene expression and protein quantification of Ton-EBP and VEGF-C was increased with higher salt intake. Skin tissue obtained in the VARSITY study were insufficient for protein analysis and therefore this could not be achieved.

In the only previous study of salt intake on GAG polymerisation enzymes, Heer et al showed the mRNA expression for xeostosin-like glycosyltransferase 2 (EXTL2) and hyaluronidase increased with dietary salt loading in 9 healthy men. These genes were not tested in this

qPCR array. In this study expression of xylosyltransferase 1 and chondroitin sulphate synthase 3 was not significantly increased, which concurs with the finding of this analysis. [298] GAG enzymes are a surrogate for GAG protein expression and may not reflect actual changes in GAG. The duration of salt loading in this study was shorter than previous work in rats (4 weeks) showing upregulation of GAG polymerisation enzymes. [130]

In this analysis, women had an increase in HIF-2α and an increase in ambulatory BP with increased salt intake while men showed no increased in either HIF-2α or BP. As described in 5.1, increased HIF-2α activity would induce arginase-1, which catalyses the hydrolysis of L-arginine to l-ornithine and urea, thus depleting L-arginine available for conversion to NO by iNOS [218,302,303] No difference in HIF-1α expression was seen, though it should be noted that HIF-1α mRNA has a relatively short half-life, while HIF-2a RNA has a remarkably longer half-life. [218] This could mean that changes in gene expression of HIF-1α could have been missed at 7 days. Both VEGF-A and its receptor FLT-1 (VEGF-1) are involved in regulating vasculogenesis and angiogenesis. [305] FLT-1 variants are increased in preeclamptic placentas compared with normotensive placentas. [306] In this analysis men had a modest trend for increase in VEGF-A (a target gene for HIF-1α) expression with salt loading (FC 1.21, p = 0.38). This could suggest increased HIF-1α expression or a reason for the trend for increase in eNOS expression. The basis and relevance for the trend for increase in in FLT-1 in women with slow sodium treatment relative to placebo is unclear and merits further study. In men a trend for decrease in PVR and increase in both eNOS and iNOS expression was seen. This could potentially explain why they did not have a rise in BP while women did. It is possible that differences in HIF-2A expression could partly account for this, but clearly further work would need to be done.

In summary, this qPCR analysis provides a unique insight into changes in gene expression with dietary salt loading. Results have to be interpreted with caution and are not conclusive as this is a small sample size and mRNA quantification in only a surrogate for protein expression.

Chapter 6 ELEMENTAL PROFILES AND THE EXISTENCE OF ENaC IN THE SKIN

6.1 INTRODUCTION

In Chapters 3 and 4 the functions of the skin as a repository for body sodium and a buffer for dietary sodium were explored using ICP-OES, which quantified skin sodium and potassium content. This technique could not be used to evaluate skin Cl^- concentrations or the distribution of elements in different layers or structures of the skin. In this chapter the development of techniques for analysing elemental distributions in the skin and the distribution of the epithelial sodium channel (ENaC) in keratinocytes are described. These would facilitate an understanding of mechanisms involved in sodium flux within the skin, a possible reason for the apparent sex-specific skin changes described in 4.5.2, potentially illuminating novel roles for skin Na^+.

The skin is a large, complex organ with a variety of structures and cells, including hairpin-like lymphatic and blood capillary structures (Figure 6.1). The distribution of sodium within these are largely unknown, as outlined in 1.3.4.

Figure 6.1: Structure of the skin and the different layers of the epidermis. The epidermis consists of continually keratinizing or cornifying, stratified non-vascularised epithelium terminating at mucocutaneous junctions such as the mouth. [178]. The stratum basale consists of keratinocytes, which are columnar epithelial cells on a basement membrane, undergoing cell division. The next layer, the stratum spinosum, consists of polyhedral cells connected by desmosomes, becoming progressively flatter upwards. Above this layer, the stratum granulosum, consists of flattened cells with numerous basophillic granules. Above this lies the stratum lucidum, consisting of packed squamous cells that lack organelles or nuclei. The outermost layer, the stratum corneum, is made of dead, anucleate cornified cells. [307]

:

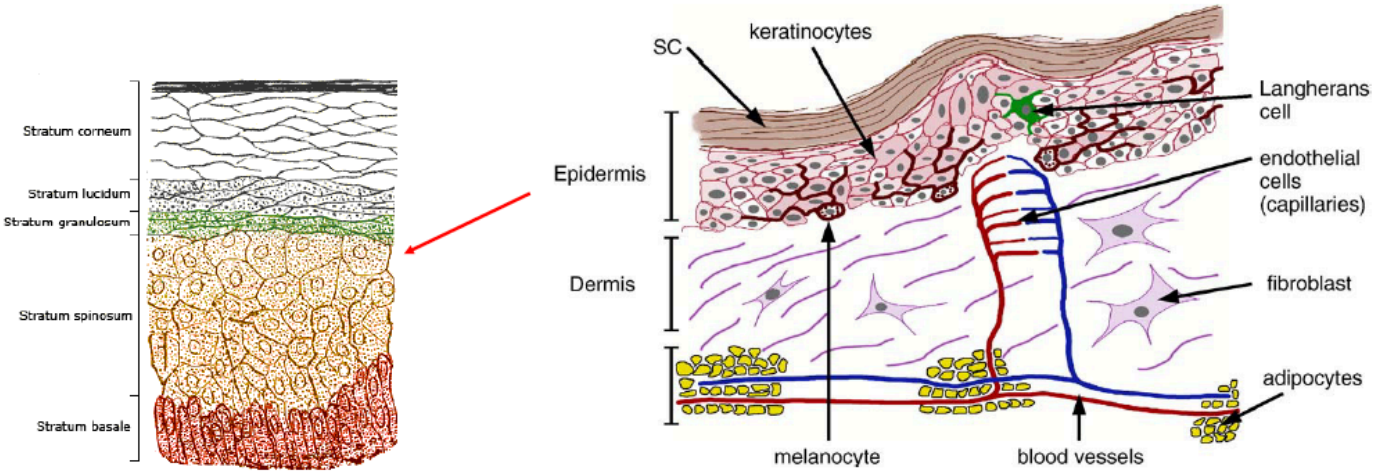

Few studies have analysed the distribution patterns of sodium and other elements in the skin. Over 30 years ago, electron probe analysis and X-ray microanalysis revealed sodium distribution patterns in the epidermis, with high levels in the keratinocytes of the lower epidermis. [308-310] The relevance of these patterns was unknown. Recently, ^{23}Na-MRI analysis of the skin at 7 tesla revealed an age-dependent increase in skin Na^+ content directly under the keratinocyte layer of the skin in humans. [199] This has given rise to notion that a kidney-like countercurrent system functions in the skin, whereby a Na^+ concentration gradient, believed to be generated by active transport in keratinocytes, forms an osmotic barrier. [208,209] It has been recently proposed that epithelial sodium channels (ENaC) are responsible for generating sodium gradients in keratinocytes. [135,311]

In the kidney, the amiloride-sensitive epithelial sodium channel (ENaC) plays a major role in the regulation of sodium transport in the collecting duct and is a well-known determinant of sodium homeostasis and BP. [312] The function of ENaC in human skin is unclear. Reptilian skin is known to be possess α , β and γ ENaC subunits in the apical membranes of keratinocytes within the stratum granulosum and the stratum spinosum, where they facilitate Na^+ transport and are believed to enable osmoregulation. [313,314] Mice having keratinocyte-

specific deletions of ENaC-α subunits have epidermal hyperplasia, suggesting a role for ENaC in in normal epidermal differentiation. [315,316] Studies assessing blood pressure and sodium homeostasis in these animals have not been published. Recently, ENaC-α subunits were localised in all epidermal layers in human skin except stratum corneum using confocal microscopy, as well as in the sebaceous glands, eccrine glands, arrector pili smooth muscle cells, and intra-dermal adipocytes. [317] It is unclear if sodium flux in the skin during periods of high salt intake is facilitated by ENaC. The distribution of chloride and potassium in the skin are poorly understood, with 1 previous study showing high potassium concentration in the epidermis as measured using flame photometry. [188]

In this chapter I will explore the feasibility of using SEM-EDX to show Na^+, K^+ and Cl^- patterns in the skin and how ENaC transporters are located relative to these patterns.

6.2 Hypotheses

On this background I propose the following hypotheses:

1. Skin sodium has distribution patterns in the epidermis and dermis, forming a barrier to water loss to the external environment.

2. ENaC facilitates the formation of this barrier and sodium flux between the epidermis and dermis.

6.3 Aims

The aims are to determine the following:

1. The feasibility of studying skin sodium distribution profiles using scanning electron microscopy with energy dispersive X-ray spectroscopy (SEM-EDX)

2. The feasibility of immunohistochemical localisation of ENaC in human skin.

6.4 Methods

6.4.1 Assessment of skin elemental distribution

6.4.1.1 SEM-EDX

Scanning electron microscopy with energy dispersive X-ray spectrometry (SEM–EDX) is a powerful tool for simultaneously examining the morphology and the elemental composition of solid structures, showing chemistry and morphology of particles as small as a few tenths of a micrometer. [318] It has been employed in the analysis of bullet wounds in forensic science and skin disease in dermatology. [319,320] The scanning electron microscope (SEM) is a type of electron microscope that creates images of the sample surface by scanning it with a high-energy electron beam, focussed on a field of interest. The electrons interact with the atoms that are in the sample to generate secondary electrons and backscattered electrons. Secondary electrons are emitted from the atoms occupying the top surface and produce a readily interpretable image of the surface which is three dimensional. Backscattered electrons show the distribution of different chemical phases in the sample and have less resolution. In the SEM EDX technique, the SEM image generated by secondary electrons is used to select the area of interest while an energy dispersive detector is used to measure the energies of emitted x-rays which are characteristic of the elements present. The energy of the primary electron beam is termed the accelerating voltage, which is adjustable to control image detail. The interaction between the primary electron beam and atoms in the sample causes inner electron shell transitions, which result in the emission of X-rays. A fraction of these X- rays are collected and analysed by means of an energy dispersive X-ray spectrometry. This detects and measures the characteristic X-ray energies, yielding an analysis of the elements present in the feature. Energy dispersive X-ray spectrometry can give a rapid, qualitative analysis, or, with adequate standards, quantitative analysis of elemental composition with a sampling depth of 1–2 µm. X-rays can be acquired in synchronization with the image-forming electron beam to form two-dimensional maps showing the distribution of elements in a sample surface. [318]

Thus, SEM-EDX can be used to derive elemental distribution patterns in solid structures,

including human tissue. The instruments and expertise for using this technique were available at the Cambridge Nanoscience Centre and Graphene Centre. For these reasons SEM-EDX was chosen for this thesis.

6.4.1.2 SEM-EDX instruments

The work in this thesis was developed initially at the Cambridge Nanoscience Centre and continued at the Cambridge Graphene Centre. Instruments were operated by Dr Yury Alaverdyan, Research Facilities Manager at Cambridge Graphene Centre, who developed the SEM-EDX techniques with me for this thesis. The first analysis was performed on the LEO GEMINI 1530VP FEG-SEM system at the Cambridge Nanoscience Centre (Figure 6.2). This consists of a scanning electron microscope coupled with an energy dispersive X-ray spectrometer (Inca Energy MX from Oxford Instruments Nanoanalysis). INCA software (version 4.02, Oxford Instruments) was used to process EDX outputs. The second analysis was performed at the Cambridge Graphene Centre on the on the FEI Magellan 400 XHR SEM coupled with a Bruker X-Flash EDX detector. OIM Analysis™ software (version 7, AMETEK) was used to process EDX outputs. (Figure 6.3)

Figure 6.2: The LEO GEMINI 1530VP FEG-SEM system at the Cambridge Nanoscience Centre.

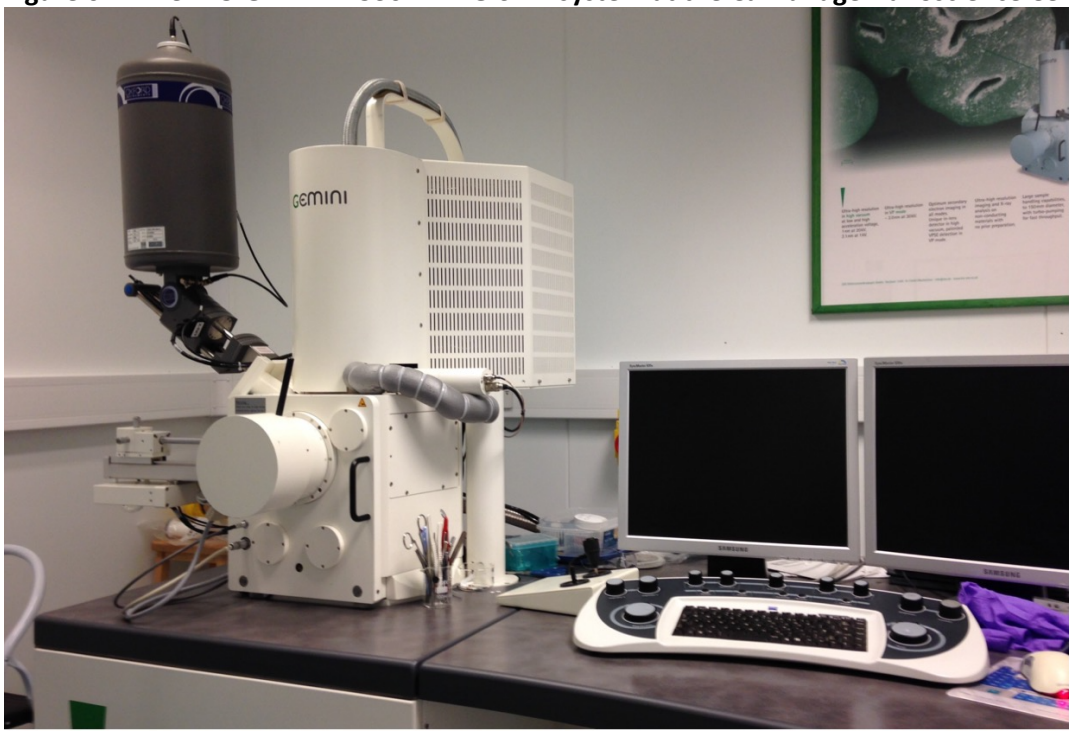

Figure 6.3: The FEI Magellan 400 XHR SEM coupled with a Bruker X-Flash EDX detector at the Cambridge Graphene Centre

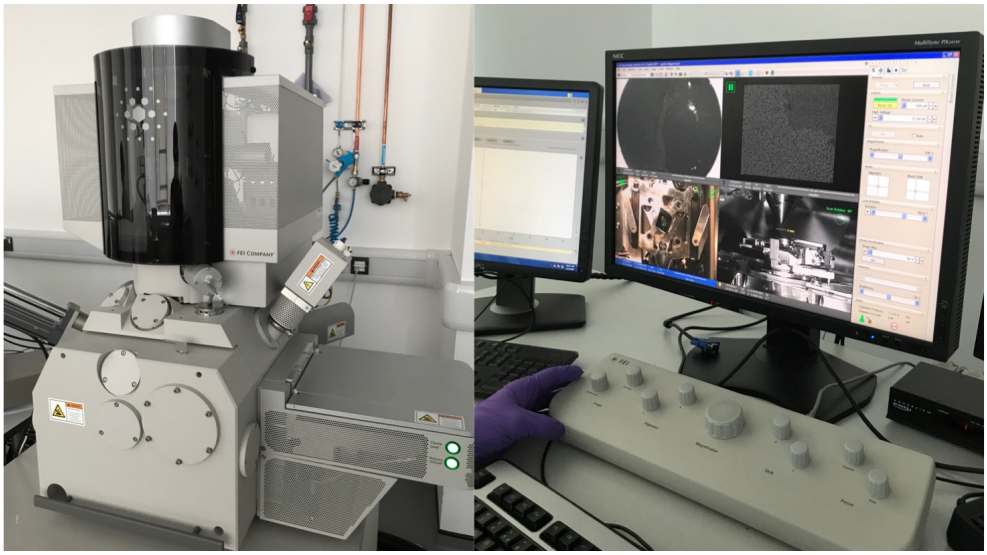

6.4.1.3 Samples

SEM-EDX analysis was performed on 2 remaining skin portions from the Tissue Bank samples, described in 2.5. These were healthy breast reduction surgical resections and were numbered sample 1 and 2. Skin Na^+ and K^+ had previously been determined by ICP-OES, as described in 2.5.3. The measures values for these elements using ICP-OES and the age of skin donors are shown in Table 6.1.

Table 6.1: Characteristics of Samples 1 and 2 used for SEM-EDX analysis.

Tissue Bank skin sample	Age	Skin Na^+_{Dry}, mg/g	Skin K^+_{Dry}, mg/g
1	47	5.57	0.76
2	45	4.06	1.66

6.4.1.4 Sample processing

Skin samples were stored at - 80 °C before undergoing cryosectioning in a Bright Clinicut cryostat in the EMIT unit. I cut Sample 1 at 30 micrometers (µm) at a chamber temperature of - 20 °C using O.C.T. Compound (Tissue-Tek, VWR) mounting medium. A frozen section of mounting medium was previously analysed using the LEO GEMINI 1530VP FEG-SEM system and found to have no sodium, potassium or chloride content. Samples were viewed with a light microscope (OLYMPUS 2467) under 20 x magnification to ensure intact epidermis and dermis portions were present. Sample 2 was sectioned at 35 µm at the Addenbrookes Hospital Tissue Bank using the same techniques. Frozen skin sections were mounted on 10 x 10 x 0.5 mm pre-cut undoped silicon slides obtained from the Cambridge Nanoscience Centre and stored at - 80 °C in the EMIT unit. Sample 1 was subsequently transferred to the Cambridge Nanoscience Centre and sample 2 to the Cambridge Graphene Centre on dry ice for SEM-EDX analysis. Sample thicknesses of 30-35 µm were chosen as it was felt this would include intact keratinocytes and samples were able to resist the damaging effects of freezing and thawing.

Figure 6.4: Skin sample preparation for SEM-EDX analysis. A: Sample 1 being cryosectioned in a Bright Clinicut cryostat. B: A frozen skin section on a silicon slide being prepared for SEM-EDX analysis.

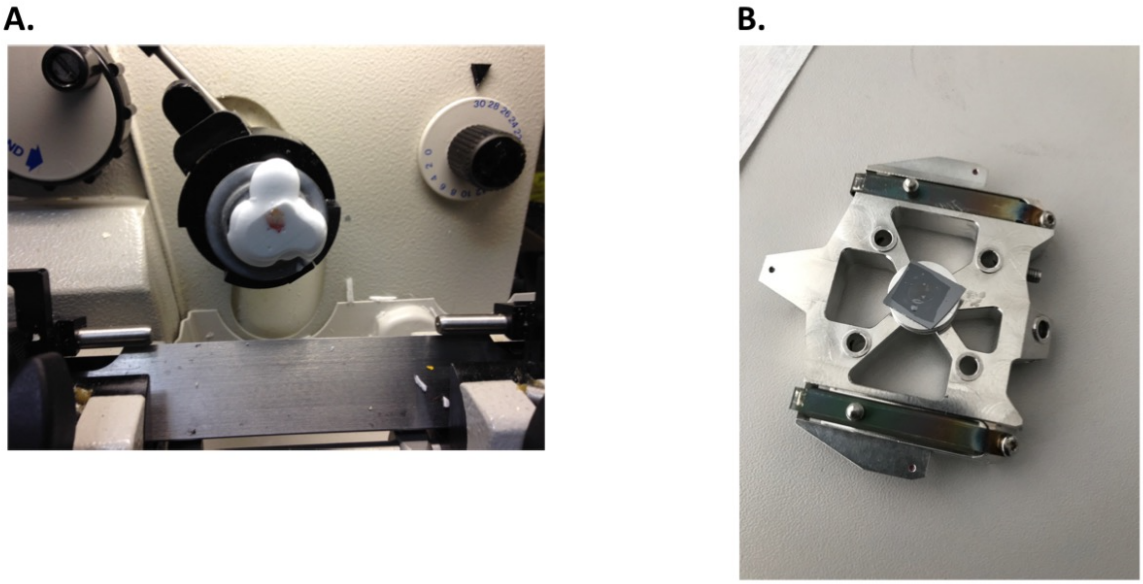

6.4.1.5 SEM-EDX procedure for skin analysis

Each skin section was placed in a drying cupboard at 60-70 °C for 1 hour to remove water content and prevent charging artefact (Figure6.4A). Sections were then viewed under a digital light microscope (OLYMPUS BX 51) at 20 x magnification to define an area of interest which included both the epidermis and dermis. An image of the area of interest was captured and used to guide the positioning of sections on sample holders and establishing starting fields X-ray microanalysis on the LEO GEMINI 1530VP FEG-SEM and FEI Magellan 400 XHR SEM (Figure 6.4B). Images were acquired over 1 hour. All analyses were run at an acceleration voltage of 15kV, a current of 100pA and an integration time of 100s. EDX spectra were used to ascertain elemental distributions for sodium, potassium or chloride in skin sections (Figure 6.5). For both samples, spectra were mapped to digital microscopic images of skin sections on silicon slides. For sample 2, in addition, a 4µm H&E section was cut at the Addenbrookes Hospital Tissue Bank and compared with elemental maps for sodium, potassium and chloride obtained from the FEI Magellan 400 XHR SEM.

Figure 6.4: Procedures prior to SEM-EDX. A: Skin sections on silicon slides were placed in a drying cupboard to remove moisture. B: Skin sections were then placed in the FEI Magellan 400 XHR SEM chamber for analysis with orientation guided by prior light microscopic assessment.

A.

B.

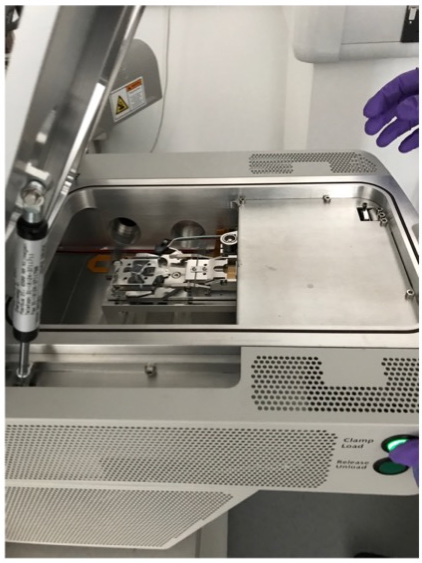

Figure 6.5: Examples of EDX spectra output. A: Output from the LEO GEMINI 1530VP FEG-SEM showing a SEM image of a sample and the area of interest in the yellow box and the elemental spectra detected within it. B: Output from the FEI Magellan 400 XHR SEM with SEM image of a sample and the area of interest in the green box and the elemental spectra detected within it, on the right.

A.

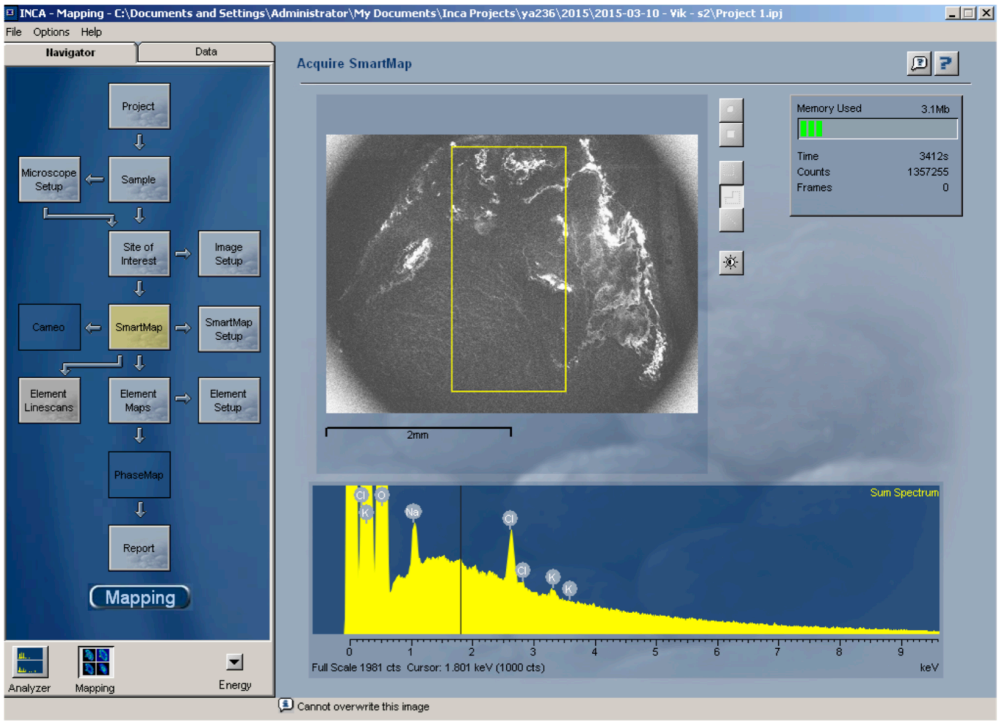

B.

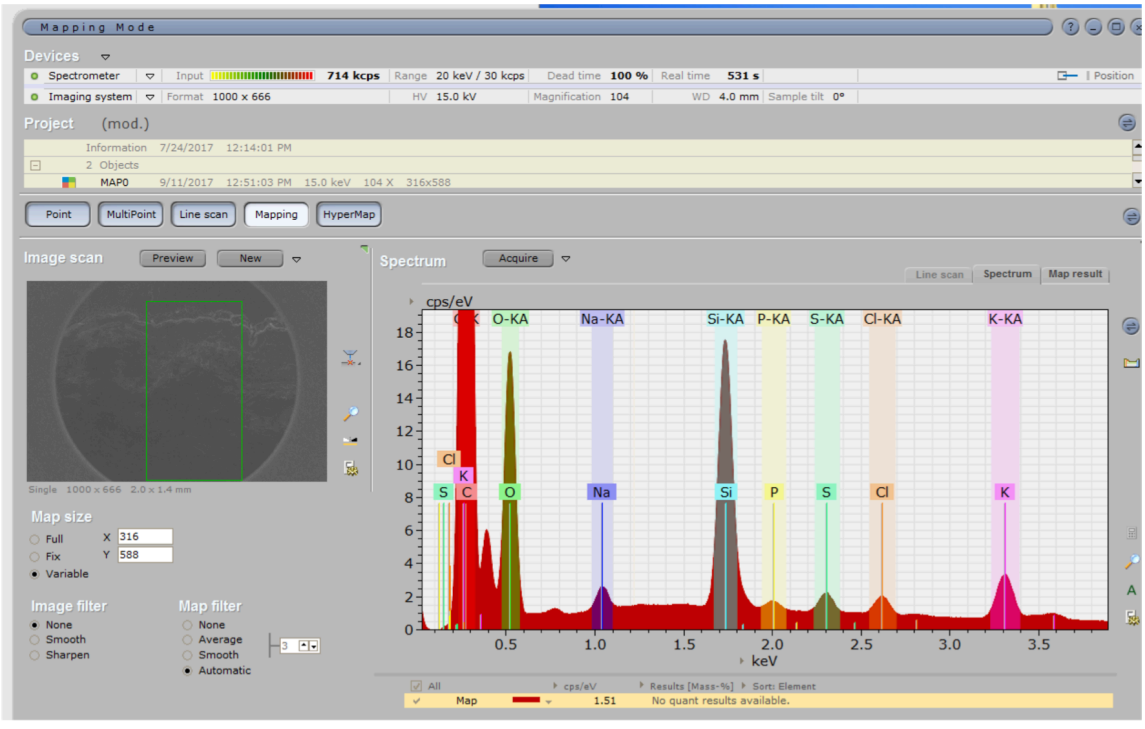

6.4.2 Skin immunohistochemical localisation of ENaC

6.4.2.1 Samples

Tissue bank skin sample from a 23-year-old woman and skin samples post-placebo and slow sodium for a 20-year-old male Caucasian VARSITY participant were used to assess the feasibility of immunohistochemical localisation of ENaC α subunits.

6.4.2.2 Paraffin embedding

4 µm sections were cut from 3 skin samples and embedded in paraffin by the Tissue Bank using their unit procedures.

6.4.2.3 Skin ENaC staining procedure

Staining procedure was carried out with DAKO Envision® Plus Kits (Denmark) by Miss Nichola Figg, Laboratory Manager at the EMIT unit using the following procedures.

Slides with skin sections from the Tissue Bank were deparaffinized through three changes of Histoclear, incubating slides for 10 min in each change. Slides were then rehydrated by dipping them decreasing strengths of ethanol followed by distilled water. Slides were placed in a microwave slide dish and covered with citrate buffer. Antigen retrieval was performed using the Prestige Medical 2100 Retriever and slides were allowed to cool for a minimum of 30 minutes before being rinsed in distilled water and placed in phosphate-buffered saline (PBS). Endogenous peroxidase activity was blocked using a pre-prepared solution from the DAKO kit and before rinsing in PBS. The primary antibody against ENaC α or negative control solution was then applied at a concentration of 1:10,000 and incubated for 2 hours at room temp. Rabbit anti-human epithelial sodium channel gamma antibody (ab3468, Abcam, UK) was used as the primary antibody against ENaC α. A rabbit IgG control antibody (DAKO, Denmark) was used for the negative control solution. Slides were then rinsed again with PBS. Counterstaining with haematoxylin (DAKO S3309) was carried out for 10 seconds. Slides were dipped five times in dilute ammonia water and then rinsed in tap water. Slides

were dehydrated in 95% ethanol followed by three changes of 100% ethanol. Slides were cleared in Histoclear and coverslips applied.

Skin sections were reviewed by myself under a digital light microscope (OLYMPUS BX51). Findings were confirmed with Dr George Meligonis, Consultant Pathologist at the Department of Pathology, Addenbrookes Hospital.

6.5 RESULTS

6.5.1 SEM-EDX

EDX spectra from the LEO GEMINI 1530VP FEG-SEM system for Sample 1 are shown below in Figure 6.5. Sample 1 was 3.72 mm long on its longitudinal axis. The intensities for sodium, potassium and chloride are given in keV and these show variations from epidermis to dermis layers. Sodium intensities were significant in the dermis and lower epidermis. Potassium intensities showed it was present in both layers. Chloride intensities were generally lower than sodium and potassium, and its distribution was mainly in the dermis.

Figure 6.6: EDX spectra for Sample 1 showing elemental intensity. The violet lines represent sodium, potassium and chloride elemental intensities along the epidermis and dermis, which are separated by the dotted green line. The 30 µm section used is shown on the right.

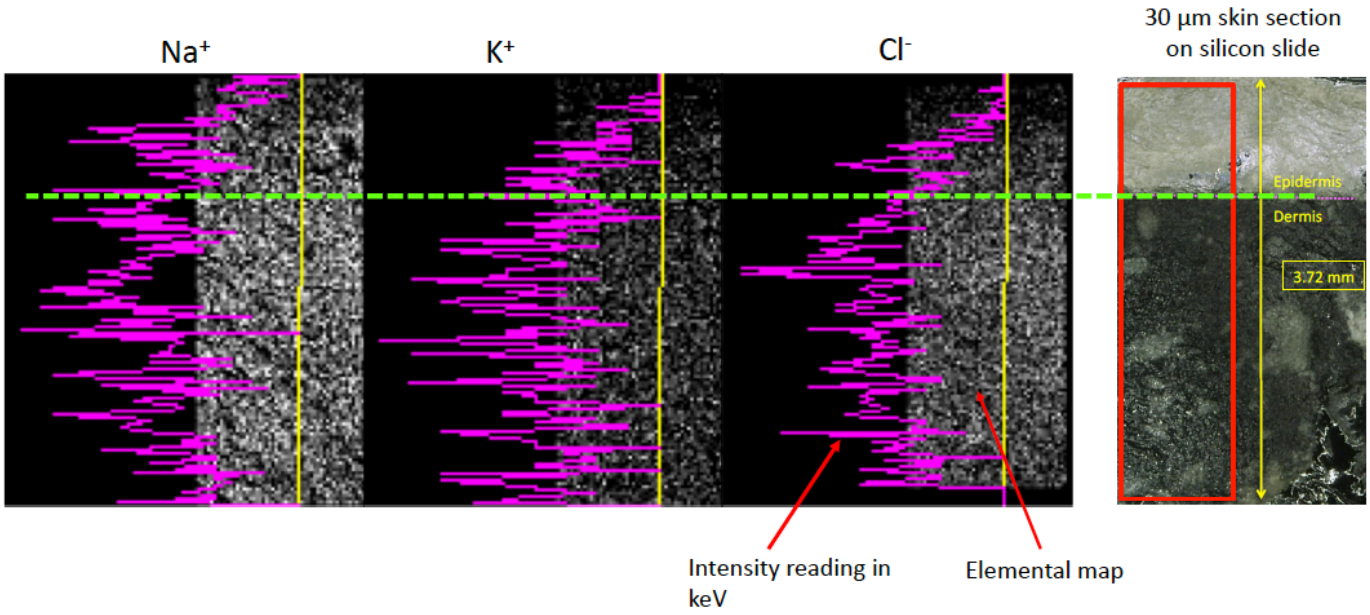

Elemental maps generated from the EDX spectra from the FEI Magellan 400 XHR SEM for sample 2 are shown below in Figure 6.7. Sample 2 was 1.5 mm long on its longitudinal axis. The colour intensities show elemental concentrations in the epidermal and dermal layers, separated by the dotted yellow lines. Sodium distribution was significant in the dermis and

lower epidermis. Distribution of potassium was decreased moving up the epidermis and generally lower than sodium in the dermis. Chloride did not show any clear variation in distribution in the epidermis or dermis.

Figure 6.7: EDX spectra for Sample 2 showing elemental maps sodium, potassium and chloride. Elemental intensities are denoted by intensity of colour. The epidermis and dermis are separated by the dotted yellow line. The 35 µm section used is showed second from the left, with skin layers identified and the defined area of interest shown in the red box. A corresponding H&E section for sample 2 is shown on the left.

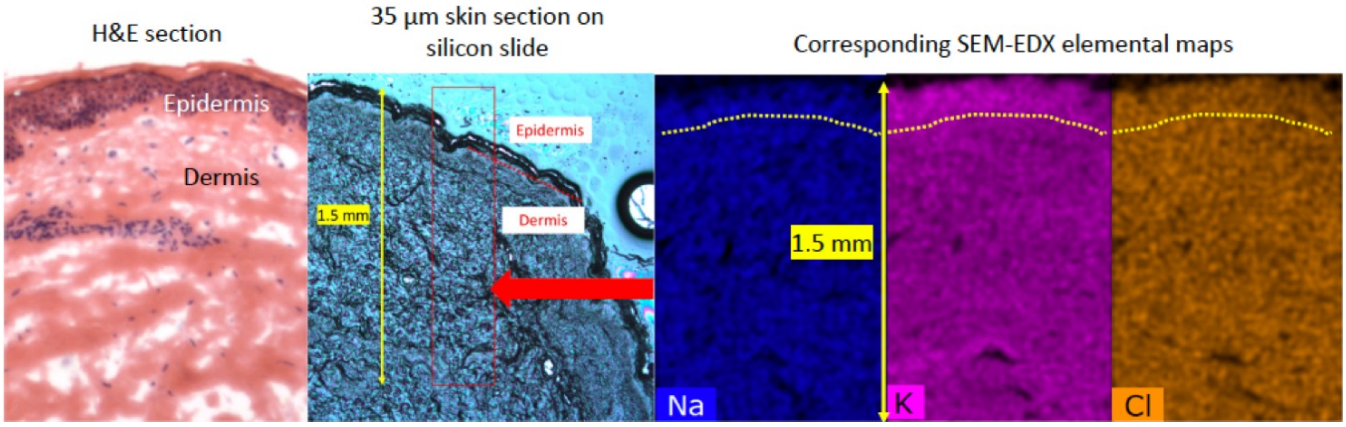

In both analyses, skin sections had to be replaced several times because of damage during the thawing procedure, resulting in skin tissue folding back off the silicon slide. This was detrimental for the structural integrity of the epidermis for analysis of elemental distributions.

6.5.2 Skin immunohistochemistry

Results for skin immunohistochemical localisation of ENaC-α are shown in Figures 6.8 - 6.10. In Figures 6.8 and 6.9, ENaC-α staining in breast skin appeared to be present mainly in the lower epidermis, corresponding with the stratum basale, stratum spinosum and granulosum in Figure 6.9. Under 20x magnification staining appeared to be nucleolar or cytoplasmic (Figure 6.9). A few regions of ENaC-α positivity are seen in the dermis, corresponding with

sebaceous glands.

Figure 6.8: ENaC-α staining in a 4 µm section of breast skin in a 23 year-old woman under 10x magnification. ENaC-α is distributed in the lower layers of epidermis. The corresponding negative control stain is shown on the left.

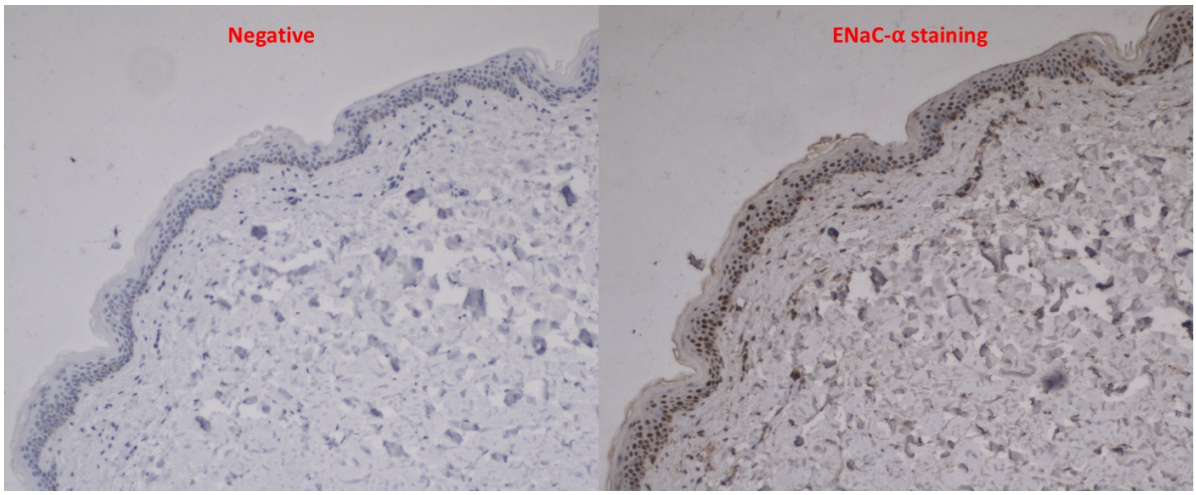

Figure 6.9: The same breast skin section under 20x magnification. ENaC-α staining (red arrow) appears to be in the nucleus or cytoplasm.

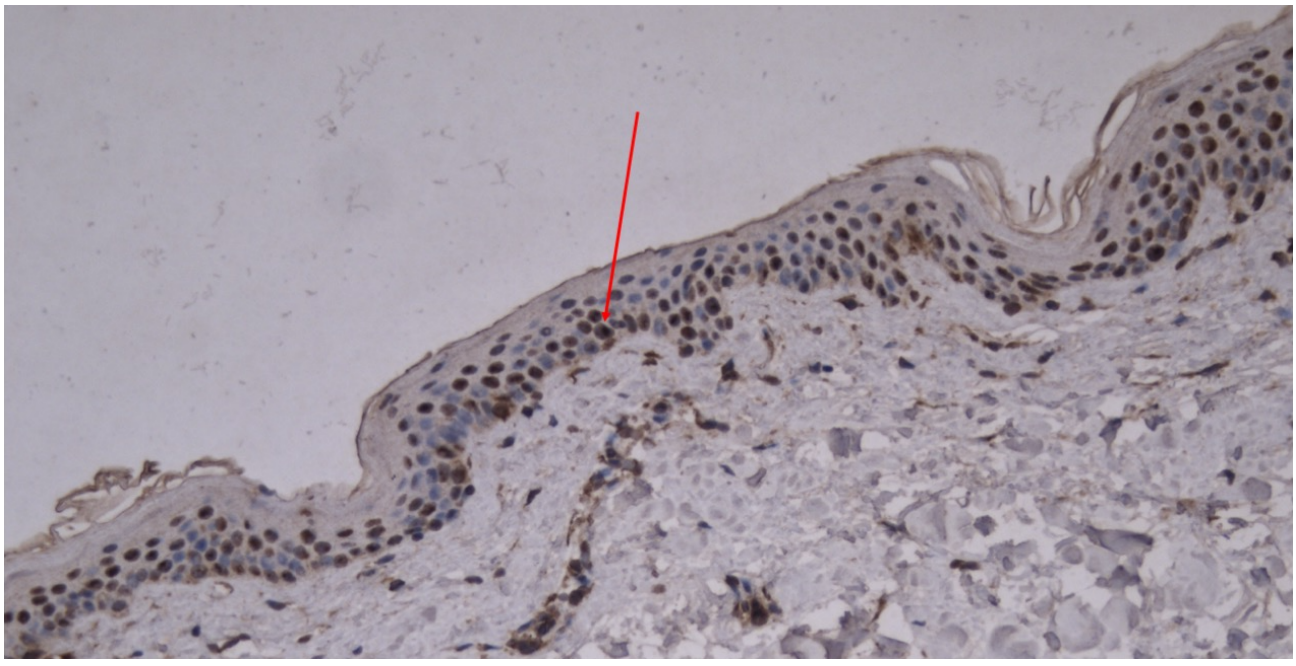

ENaC-α staining in the 20 year-old male Caucasian VARSITY participant is shown in Figure 6.10. Staining was evident in most of the epidermis and appeared to be more prominent on the low salt diet.

Figure 6.10: ENaC-α staining in a 4 µm section of lower back skin from a 20 year-old male Caucasian VARSITY participant under 20x magnification. ENaC-α distribution in the epidermis is shown during low and high salt intakes.

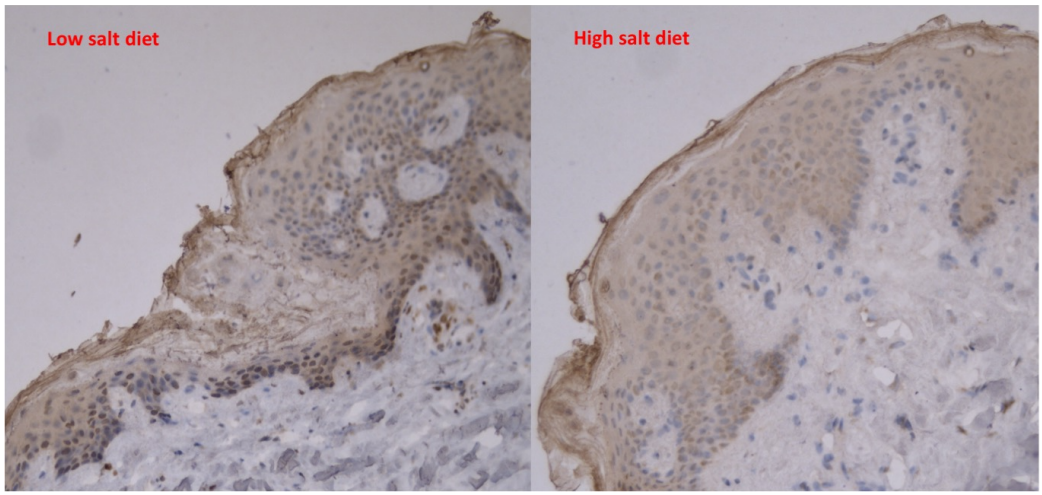

6.6 DISCUSSION

This study demonstrated that SEM-EDX can be used to study skin elemental patterns in human skin and that ENaC α immunohistochemical localisation is possible, showing significant ENaC presence in the epidermis.

In the SEM-EDX technique described, sodium, potassium and chloride distributions were seen in the epidermis and dermis. It was not possible to show the distribution of these elements in each layer of the epidermis as maintaining structural integrity of the epidermis was challenging and cryosections of less than 30μm repeatedly proved unsuccessful due to structural fragility during thawing. Sample 1 had a higher concentration of Na^+ as determined by ICP-OES, with evidence of a high 'band' of sodium in the epidermis which probably corresponded with the stratum basale, stratum spinosum and granulosum. This is in keeping with previous studies done with electron probe analysis and X-ray microanalysis in human skin. [308-310] In Sample 2 it was not possible to see a similar band using element intensity maps, which were less precise at showing the variation in element intensity. Samples 1 and 2 had a significant difference in skin K^+ as determined by ICP-OES (0.76 vs. 1.66 mg/g respectively). Sample 2 appeared to have a high potassium content in the epidermis as reflected in the element intensity map, while in Sample 1 potassium appeared to decrease moving up the layers of the epidermis, which could potentially occur with damage to the keratinocytes, releasing intracellular potassium during the skin sample preparation. Chloride levels appeared to be lower than sodium in both epidermis and dermis with no discernible pattern seen. The respective elemental intensity readings shown in Figure 6.6 correspond with animal data on skin Na^+, K^+ and Cl^- using atomic spectrometry. This showed that skin Cl^- was around 50-60% of skin Na^+ while skin K^+ was 60-70 % of skin Na^+. In Chapter 3, skin K^+ appeared to be lower in women than in men (Table 3.4) and lower in the Tissue Bank breast skin samples compared to VARSITY methods (Table 3.7). This could be explained by sex differences in epidermal thickness if there is a high concentration of K^+ in the epidermis, which is more cellular than the dermis. [188,260] This difference significantly affected the use of the Na^+:K^+ ratio in the VARSITY study.

The findings for immunohistochemical localisation of ENaC are preliminary and inconclusive but show that ENaC α has a significant presence in the epidermis. Several studies have assessed the presence of ENaC in human skin, yielding little insight into its function. [311,316,317,321,322] Recently Honukoglu et al mapped the sites of localization of ENaC α in the human skin by confocal microscopy using polyclonal antibodies generated against human ENaC α. They showed that ENaC α exists in all epidermal layers except stratum corneum, and also in the sebaceous glands, eccrine glands, arrector pili smooth muscle cells, and intra-dermal adipocytes. In the comparison of skin ENaC α staining during different salt intakes, there was an impression that ENaC expression was lower with high salt intake. This would concur with the decrease in aldosterone levels during high salt seen in the VARSITY study. The relevance of this to sodium homeostasis and BP is unclear. Hanukoglu et al observed that ENaC α had a cytoplasmic distribution, as seen in this analysis, the nature of which is not understood. [317] It would also be relevant to study the effects of increased ENaC activity in in humans with Liddle's syndrome to see the effects on skin sodium distribution.

In conclusion, this work shows that skin elemental distributions can be mapped out using SEM-EDX and immunohistochemical localisation of ENaC is feasible. Further development of these techniques to show better definition of epidermis elemental distribution patterns through better tissue preservation techniques and the possible use of confocal microscopy to ascertain the location of ENaC in the skin should be attempted. There were no conclusive findings regarding any possible underlying countercurrent system functioning in the skin, though was is a suggestion of high sodium distribution in the lower epidermis coinciding with the presence of ENaC α. Further work would be needed to confirm if ENaC is relevant to sodium in the epidermis and whether this influences sodium flux or storage in the skin.

Chapter 7 Conclusions and Future Directions

7.1 SUMMARY AND CONCLUSIONS

Excessive dietary sodium, principally as the chloride salt, has long been considered a pivotal factor in development of hypertension, an important modifiable risk factor for cardiovascular disease. [1,3,4,28] However, the haemodynamic response to salt intake is variable, with only some individuals showing salt sensitivity of blood pressure. [43,44] Current knowledge of the relationship between dietary sodium and BP fails to explain this heterogeneity in human response to sodium intake. We are now witnessing a paradigm shift away from the traditional nephrocentric view that pressure natriuresis exclusively determines salt sensitivity. The skin is now emerging as a potentially important site of extra-renal sodium homeostasis and BP regulation. Studies in rodent models have highlighted the relevance of interstitial electrolytes and the roles played by GAGs, the lymphatics and cells of the mononuclear phagocytotic system in buffering the haemodynamic effects of dietary salt. [133,134,152] It has been proposed that sodium in the skin may have certain distribution patterns that facilitate water conservation. [208] On this background, the principle hypothesis of this thesis is that the skin functions as a buffer for dietary sodium and modulates its haemodynamic effects.

In Chapters 2 and 3 the feasibility of measuring skin $Na^+$and K^+ concentrations using ICP-OES was shown using skin samples obtained from the Tissue Bank and skin biopsies in healthy volunteers. The values obtained for skin $Na^+$and K^+ were similar to previous studies of direct chemical measurements in full thickness human skin. The observed skin Na^+: water ratios support the existence of non-osmotic sodium storage in the skin, as seen in previous studies in rodents. [132,133,244,245] In Chapter 3 the observed average skin Na^+ concentration value of 2.15 mg/g of wet weight approximates to 10 - 14 % of total body sodium, suggesting that the skin is a reservoir for sodium in humans. [263] The water content in skin was found to be 62%. Thus, in a 70 kg human with 4.2 kg of skin, this would approximate to 2.6 litres of water. Skin Na^+ was not seen to increase with age, as shown in previous ^{23}Na-MRI studies, and this could have been due to the study size and narrow age rage in the study. [197,204] The

observed skin Na^+ values in mmol/l were lower than seen with ^{23}Na MRI. [195,197-204] It is possible that Na^+ bound to GAGs and ionised Na^+, as well as intracellular and extracellular sodium are detected differently by ^{23}Na MRI. This could lead to a discordance between direct chemical measurements and ^{23}Na MRI measurements or observed correlations. There was a trend for lower skin Na^+ in women in VARSITY methods, in keeping with the findings in ^{23}Na MRI data. This could be because men have a thicker epidermis and dermis at all ages and may have higher levels of dermal glycosaminoglycans, leading to sex-specific difference in skin Na^+ storage [261,262] Skin K^+ was lower in women and this be due to the epidermis being thinner in women. [188,260]

In Chapter 4 skin Na^+ and K^+ was measured in 48 healthy volunteers in the VARSITY study, using the techniques developed in Chapters 2 and 3, to observe the effects of varying salt intake on skin electrolytes alongside haemodynamic and biochemical measurements. In addition, the effects of varying salt intake on plasma VEGF-C, salt taste sensitivity and skin capillary density were examined. Skin sodium was expressed as the Na^+:K^+ ratio due to non-uniform water removal from samples. Skin Na^+:K^+ increased with dietary salt loading and showed a significant interaction with sex because women had lower skin K^+ and higher Na^+:K^+ ratios. Post-hoc sex-specific analyses showed that with dietary salt loading, men had a rise in skin Na^+:K^+ with no rise in BP, while women had a rise in ambulatory BP and no significant rise in skin Na^+:K^+. This supports the hypothesis that the skin buffers increase in body sodium and the degree of change in skin sodium with dietary salt loading relates to the BP change. In this study this occurred in a sex-specific manner. Possible explanations include sex-specific skin structural differences, as described above, and greater sodium flux in men, enabling skin in men to function as a more effective buffer in men. Plasma VEGF-C did not show change with dietary salt modulation and the relevance to skin VEGF-C are unclear. Correlations were seen between skin Na^+:K^+ and MAP, stroke volume and PVR during high and low salt intakes. Skin Na^+:K^+ correlated positively with plasma VEGF-C during high salt intake. These correlations were only observed in men, possibly because of the effects of contraceptive use on skin K^+ in women. A distinction should be made between the role of skin Na^+ in influencing BP in short term and long-term high-salt intake. In short-term salt loading, as in the case of the VARSITY study, dermal Na^+ storage may have buffered the BP response to salt. Long-term (months), the ability to maintain normal BP in the face of high

salt intake is dependent on the ability to decrease PVR. [323] The positive correlation seen between skin Na^+:K^+ and PVR suggests that skin Na^+ accumulation may, in the long-term, lead to higher BP by increasing PVR. This is supported by cross-sectional ^{23}Na MRI data showing that skin Na^+ storage higher in hypertensives and positively correlates with BP. [197,204] VARSITY was a short-term study and a salt loading over a longer period may not have been ethical. Chronic skin electrolyte changes in response to changes in salt intake may be different.

In the analysis of salt taste sensitivity, salt detection threshold, or the lowest concentration at which participants could distinguish between ROS water and salt solution, increased with dietary salt loading. Thus, participants were less able to identify saltiness on a higher salt intake. No change in salt recognition threshold was noted. This would suggest that individuals became less aware of the taste of salt with greater salt intake or adapted to a higher salt intake, supporting the role of habituation in determining salt intake, as previously described. [324]

In Chapter 4, skin capillary density was assessed in a group of 20 participants and appeared to decrease with dietary salt loading. This would imply that high salt intake decreases capillary blood flow in the skin. The observation that capillary density increased with venous occlusion only post slow sodium further supports the theory that blood flow in capillaries was attenuated with high salt intake. This could be explained by an increase in PVR in the skin due to increased arteriolar tone in the dermis. The measured PVR in this group did not show significant change, with a trend for decrease in PVR (Table 4.17). It is unknown if skin PVR changes can occur independent of PVR elsewhere in the body. The observation that blood flow in the skin is highly dynamic in mediating thermoregulation, ranging from as low as 1% rising to as high as 60-70%, may support this. [211,212]The finding that salt intake is linked to dermal vasculature is interesting and possible mechanisms would need to be explored in more detail in further studies.

In Chapter 5 specific skin gene expression changes were assessed in a sub-set of 20 participants with characteristics and sex-specific differences similar to the main VARSITY study population. This study found that women showed an increase in HIF-2α and an

increase in ambulatory BP with increased salt intake, while men showed no increase in either HIF-2α or BP. This would concur with studies in rodents, showing opposing effects of HIF-1α and HIF-2α on NO availability, with greater HIF-2α expression causing higher BP. [217] Changes in gene expression of HIF-1α and PHD2 could have been missed at 7 days. It is unknown if changes in skin Na^+, skin hypertonicity or systemic factors altered by dietary salt intake could have influenced PHD2 activity and consequently increased HIF-2α gene expression. It is also unclear if the difference in HIF-2 gene expression with salt loading represent sex differences or differences in salt sensitivity. Previous work on skin HIF isomers in rodents involved male animals and sex differences were not assessed. Very recent work in mice and humans in the MARS 500 study have shown that increased salt intake increases urea genesis by the liver and this accumulates in the renal medulla, acting as a driving force to facilitate renal water reabsorption. [325,326] This novel mechanism has been proposed as a means to limit water loss through natriuresis during dietary salt loading. Increased dermal HIF-2α expression with high salt intake would induce arginase-1, which catalyses the hydrolysis of L-arginine to l-ornithine and urea, increasing urea levels in the skin. [218,302,303] In support of this, recent work in rodents has shown that the urea gradient from the epidermis to dermis increased with salt loading, suggesting that high salt intake increases ureagenesis in keratinocytes. [327] This would reduce water loss in the skin and limit hypertonicity in the skin during periods of high salt intake. Thus, dermal HIF-2α could potentially complement the TonEBP - VEGF-C axis in addition to the haemodynamic response to salt loading. (Figure 7.1) No changes were observed in gene expression for GAG polymerisation, Ton-EBP or VEGF-C, which were shown in studies in rodents. [133,134,152] Possible explanations would include discordance between gene expression and protein expression for these factors in humans and the significantly greater duration and extent of salt loading in rodents compared to humans in the VARSITY study, implying that similar degrees of skin hypertonicity may not have been achieved.

Figure 7.1: The Ton EBP-VEGF-C axis and HIF-isomers in the skin responding to high salt intake. VEGF-C secretion expands dermal lymphatics, allowing movement of water and electrolytes from the skin to the systemic circulation. PHD2 inhibition by high salt intake results in increased expression of HIF-1α and HIF-2α. HIF-1α increases NO expression via action on iNOS while HIF-2α increases urea genesis. Urea causes an osmolyte gradient that could potentially limit water loss from the skin.

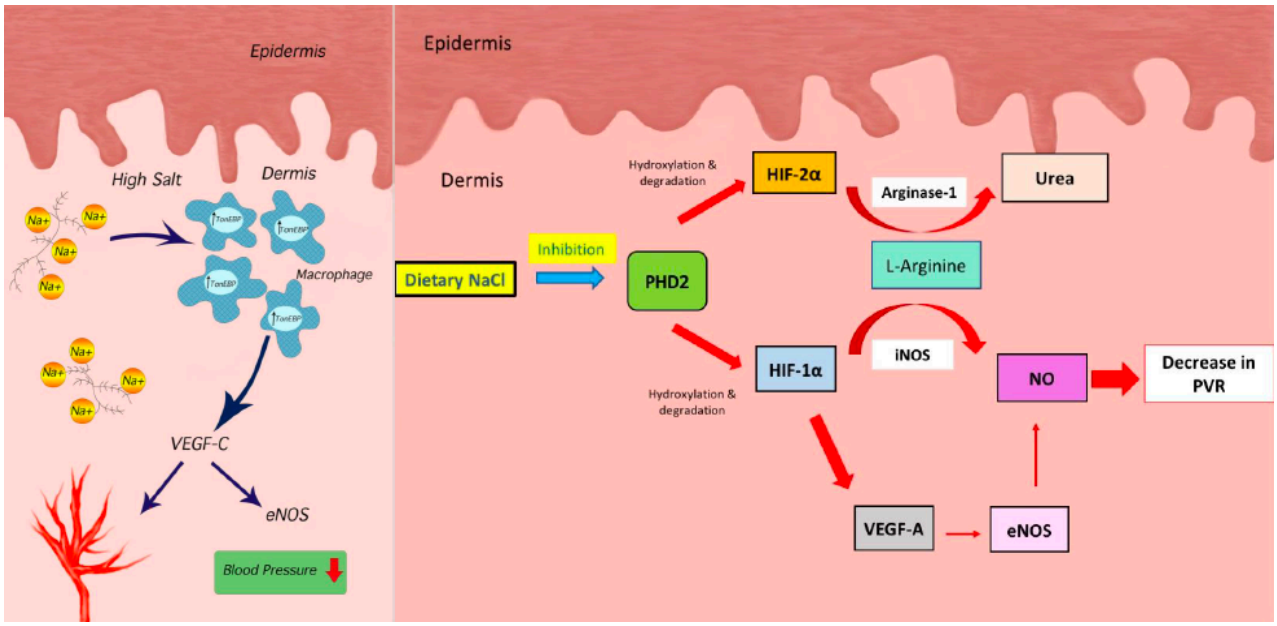

Chapter 6 addressed the feasibility of using SEM-EDX to study how sodium, potassium or chloride are distributed in the skin. The feasibility of immunohistochemical localisation of ENaC sodium transporter in the skin was also analysed with a view to assessing whether this is involved in skin sodium distribution. Using the LEO GEMINI 1530VP FEG-SEM and FEI Magellan 400 XHR SEM systems, skin distributions for sodium, potassium or chloride in skin sections were evaluated. Sodium appears to be present in the lower epidermis, where immunohistochemical localisation of ENaC was found. Adequate structural detail of sodium distribution in the epidermal layers was not possible and further work developing methods for skin section structural preservation during freezing and drying is required. It is possible that ENaC facilitates sodium flux between the epidermis and dermis. Sex steroids have recently been found to influence ENaC expression in animal models in various tissues and could potentially explain sex differences in sodium flux within the skin. [328-330] Chloride appears to exist within the dermis while potassium may be concentrated in the epidermis,

potentially explaining observed sex differences in skin potassium.

7.2 FUTURE WORK

There are several further studies that should be done to confirm and build on the findings of this thesis.

A study of dietary salt loading, similar to the VARSITY study, should be done with greater numbers to enable sex comparisons and comparisons between women on and without contraceptive treatment. Similar studies should also be conducted in older people, other ethnicities and hypertensives.

Currently, there is an ongoing study at the EMIT unit looking at the effects of sodium depletion with thiazide use on skin sodium. This study plans to validate a new ^{23}Na MRI technique in Cambridge by comparing sodium measurements obtained by direct chemical measurements (ICP-OES) and ^{23}Na MRI. Upon validation, this ^{23}Na MRI technique can eventually be used in larger cohorts such as the AIM-HY study, a multi-centre study running at the EMIT unit with the aim of identifying differential responses to antihypertensive drugs by ethnicity. This would show the effects of antihypertensives, diuretics in particular, on skin sodium and the relevance to BP response to treatment. This would potentially also show the effects of race on skin Na^+ responses.

Chloride could not be measured with ICP-OES, and techniques to evaluate skin chloride changes and how they relate to BP changes and other haemodynamic measurements are required.

The relevance of HIF isomers in modulating the effects of salt intake on systemic BP should be evaluated by salt loading keratinocyte-specific mutant mice with HIF-1α and HIF-2α deletions respectively, to see if the latter show greater salt sensitivity. Previous work by Cowburn et al could be repeated to include mice of both sexes, to see if HIF-1α or HIF-2α responses differ by sex.

Skin electrolytes, BP and response to dietary salt loading should be examined in the skin of mice in which the keratinocyte epithelial sodium channel alpha subunit had been deleted, to ascertain the influence of epidermal ENaC on these parameters. [315,316] SEM-EDX analysis of skin sodium distributions should be done in patients with Liddle's syndrome and compared to healthy volunteers, to observe the effects of increased ENaC activity on skin Na^+ quantity and distribution. This could reveal whether humans with this sodium channelopathy have extra-renal mechanisms for hypertension.

In summary, it appears that the skin is a buffer for dietary salt, influencing the regulation of salt sensitivity, and this is affected by sex. The skin has yet undefined pathways and mechanisms for sodium homeostasis and regulation of the vasculature that merit investigation. Some of these may explain sex differences in the haemodynamic response to salt intake.

References

1 Kearney PM, Whelton M, Reynolds K, Muntner P, Whelton PK, He J. Global burden of hypertension: analysis of worldwide data. *Lancet* 2005; **365**: 217–23.

2 Mills KT, Bundy JD, Kelly TN, *et al.* Global Disparities of Hypertension Prevalence and Control. *Circulation* 2016; **134**: 441–50.

3 Lawes CM, Hoorn SV, Rodgers A. Global burden of blood-pressure-related disease, 2001. *The Lancet* 2008; **371**: 1513–8.

4 Forouzanfar MH, Alexander L, Anderson HR, *et al.* Global, regional, and national comparative risk assessment of 79 behavioural, environmental and occupational, and metabolic risks or clusters of risks in 188 countries, 1990-2013: a systematic analysis for the Global Burden of Disease Study 2013. *Lancet* 2015; **386**: 2287–323.

5 Chobanian AV. Shattuck Lecture. The hypertension paradox--more uncontrolled disease despite improved therapy. *N Engl J Med* 2009; **361**: 878–87.

6 Lewington S, Clarke R, Qizilbash N, Peto R, Collins R, Prospective Studies Collaboration. Age-specific relevance of usual blood pressure to vascular mortality: a meta-analysis of individual data for one million adults in 61 prospective studies. *Lancet* 2002; **360**: 1903–13.

7 Beevers G, Lip GY, O'Brien E. ABC of hypertension: The pathophysiology of hypertension. *Br Med J* 2001; **322**: 912–6.

8 Lund-Johansen P. Hemodynamic trends in untreated essential hypertension. Preliminary report on a 10 year follow-up study. *Acta Med Scand Suppl* 1976; **602**: 68–76.

9 Conway J. Hemodynamic aspects of essential hypertension in humans. *Physiol Rev* 1984; **64**: 617–60.

10 Hughes AD, Martinez-Perez E, Jabbar A-S, *et al.* Quantification of topological changes in retinal vascular architecture in essential and malignant hypertension. *Journal of Hypertension* 2006; **24**: 889–94.

11 He FJ, Marciniak M, Markandu ND, Antonios TF, MacGregor GA. Effect of Modest Salt Reduction on Skin Capillary Rarefaction in White, Black, and Asian Individuals with Mild Hypertension. 2010; **56**: 253–9.

12 Cheriyan J, McEniery C, Wilkinson IB. Hypertension. Oxford University Press, 2009.

13 Safar ME, Blacher J, Pannier B, *et al.* Central Pulse Pressure and Mortality in End-Stage Renal Disease. *Hypertension* 2002; **39**: 735–8.

14 Roman MJ, Devereux RB, Kizer JR, *et al.* Central Pressure More Strongly Relates to Vascular Disease and Outcome Than Does Brachial Pressure: The Strong Heart Study. *Hypertension* 2007; **50**: 197–203.

15 Pini R, Cavallini MC, Palmieri V, *et al.* Central But Not Brachial Blood Pressure Predicts Cardiovascular Events in an Unselected Geriatric Population. *Hypertension* 2008; **51**: 2432–9.

16 McEniery CM, Cockcroft JR, Roman MJ, Franklin SS, Wilkinson IB. Central blood pressure: current evidence and clinical importance. *Eur Heart J* 2014; **35**: 1719–25.

17 Laurent S, Cockcroft J, Van Bortel L, *et al.* Expert consensus document on arterial stiffness: methodological issues and clinical applications. *Eur Heart J* 2006; **27**: 2588–605.

18 Franklin SS, Gustin W, Wong ND, *et al.* Hemodynamic patterns of age-related changes in blood pressure. The Framingham Heart Study. *Circulation* 1997; **96**: 308–15.

19 Sutton-Tyrrell K, Najjar SS, Boudreau RM, *et al.* Elevated aortic pulse wave velocity, a marker of arterial stiffness, predicts cardiovascular events in well-functioning older adults. *Circulation* 2005; **111**: 3384–90.

20 Chae CU, Pfeffer MA, Glynn RJ, Mitchell GF, Taylor JO, Hennekens CH. Increased Pulse Pressure and Risk of Heart Failure in the Elderly. *JAMA* 1999; **281**: 634–43.

21 Mitchell GF, Vasan RS, Keyes MJ, *et al.* Pulse Pressure and Risk of New-Onset Atrial Fibrillation. *JAMA* 2007; **297**: 709–15.

22 Payne RA, Wilkinson IB, Webb DJ. Arterial stiffness and hypertension: emerging concepts. *Hypertension* 2010; **55**: 9–14.

23 Shirwany NA, Zou M-H. Arterial stiffness: a brief review. *Nature Publishing Group* 2010; **31**: 1267–76.

24 Mattace-Raso FUS, van der Cammen TJM, Hofman A, *et al.* Arterial stiffness and risk of coronary heart disease and stroke: the Rotterdam Study. *Circulation* 2006; **113**: 657–63.

25 Vlachopoulos C, Aznaouridis K, Stefanadis C. Prediction of cardiovascular events and all-cause mortality with arterial stiffness: a systematic review and meta-analysis. *Hypertension* 2010; **55**: 1318–27.

26 Michell AR. The Clinical Biology of Sodium. Elsevier, 1995.

27 Sigel A, Sigel H, Sigel RKO. The Alkali Metal Ions: their Role for Life. Preface to Volume 16. *Met Ions Life Sci* 2016; **16**: vii–xi.

28 He FJ, MacGregor GA. A comprehensive review on salt and health and current experience of worldwide salt reduction programmes. *Journal of Human Hypertension* 2009; **23**: 363–84.

29 He FJ, MacGregor GA. Reducing Population Salt Intake Worldwide: From Evidence to Implementation. *Progress in Cardiovascular Diseases* 2010; **52**: 363–82.

30 Mozaffarian D, Fahimi S, Singh GM, *et al.* Global Sodium Consumption and Death from Cardiovascular Causes. *N Engl J Med* 2014; **371**: 624–34.

31 Adrogué HJ, Madias NE. Sodium and potassium in the pathogenesis of hypertension. *N Engl J Med* 2007; **356**: 1966–78.

32 Dahl LK, Love RA. Evidence for relationship between sodium (chloride) intake and human essential hypertension. *AMA Arch Intern Med* 1954; **94**: 525–31.

33 Joe B. Dr Lewis Kitchener Dahl, the Dahl rats, and the 'inconvenient truth' about the genetics of hypertension. *Hypertension* 2015; **65**: 963–9.

34 Intersalt Cooperative Research Group. Intersalt: an international study of electrolyte excretion and blood pressure. Results for 24 hour urinary sodium and potassium excretion. Intersalt Cooperative Research Group. *Br Med J* 1988; **297**: 319–28.

35 Sacks FM, Svetkey LP, Vollmer WM. Effects on Blood Pressure of Reduced Dietary Sodium and the Dietary Approaches to Stop Hypertension (DASH) Diet NEJM 2001;2001:3-10

36 Mente A, O'Donnell MJ, Rangarajan S, *et al.* Association of Urinary Sodium and Potassium Excretion with Blood Pressure. *N Engl J Med* 2014; **371**: 601–11.

37 Whelton PK, Appel LJ, Sacco RL, *et al.* Sodium, blood pressure, and cardiovascular disease: further evidence supporting the American Heart Association sodium reduction recommendations. *Circulation* 2012: 2880–9.

38 Cook NR, Appel LJ, Whelton PK. Lower levels of sodium intake and reduced cardiovascular risk. *Circulation* 2014; **129**: 981–9.

39 Cook NR, Appel LJ, Whelton PK. Sodium Intake and All-Cause Mortality Over 20 Years in the Trials of Hypertension Prevention. *Hypertension* 2016; **68**: 1609–17.

40 Beaglehole R, Bonita R, Horton R, *et al.* Measuring progress on NCDs: one goal and five targets. *Lancet* 2012; **380**: 1283–5.

41 Marrero NM, He FJ, Whincup P, MacGregor GA. Salt Intake of Children and Adolescents in South London: Consumption Levels and Dietary Sources. *Hypertension* 2014; **63**: 1026–32.

42 Elijovich F, Weinberger MH, Anderson CAM, *et al.* Salt Sensitivity of Blood Pressure: A Scientific Statement From the American Heart Association. *Hypertension* 2016; **68**: e7–e46.

43 Weinberger MH, Miller JZ, Luft FC, Grim CE, Fineberg NS. Definitions and characteristics of sodium sensitivity and blood pressure resistance. 1986; **8**: II127–34.

44 Overlack A, Ruppert M, Kolloch R, Gobel B, Kraft K. Divergent hemodynamic and hormonal responses to varying salt intake in normotensive subjects. *Journal of the American Heart Association* 1993; **22**: 331–8.

45 Oh YS, Appel LJ, Galis ZS, *et al.* National Heart, Lung, and Blood Institute Working Group Report on Salt in Human Health and Sickness: Building on the Current Scientific Evidence. *Hypertension* 2016; **68**: 281–8.

46 Weinberger MH, Fineberg NS. Sodium and Volume Sensitivity of Blood-Pressure - Age and Pressure Change Over Time. *Hypertension* 1991; **18**: 67–71.

47 Campese VM, Parise M, Karubian F, Bigazzi R. Abnormal renal hemodynamics in black salt-sensitive patients with hypertension. *Hypertension* 1991; **18**: 805–12.

48 Morimoto A, Uzu T, Fujii T, *et al.* Sodium sensitivity and cardiovascular events in patients with essential hypertension. *The Lancet* 1997; **350**: 1734–7.

49 Bragulat E, la Sierra de A, Antonio MT, COCA A. Endothelial dysfunction in salt-sensitive essential hypertension. *Hypertension* 2001; **37**: 444–8.

50 Weinberger MH, Fineberg NS, Fineberg SE, Weinberger M. Salt sensitivity, pulse pressure, and death in normal and hypertensive humans. *Hypertension* 2001; **37**: 429–32.

51 Martillotti G, Ditisheim A, Burnier M, Wagner G. Increased salt sensitivity of ambulatory blood pressure in women with a history of severe preeclampsia. *Hypertension* 2013;**62**: 802-8

52 Sullivan JM. Salt sensitivity. Definition, conception, methodology, and long-term issues. *Hypertension* 1991; **17**: I61–1.

53 Kawasaki T, Delea CS, Bartter FC, Smith H. The effect of high-sodium and low-sodium intakes on blood pressure and other related variables in human subjects with idiopathic hypertension. *The American Journal of Medicine* 1978; **64**: 193–8.

54 Weinberger MH. Salt sensitivity of blood pressure in humans. *Hypertension* 1996; **27**: 481–90.

55 la Sierra de A, Giner V, Bragulat E. Lack of correlation between two methods for the assessment of salt sensitivity in essential hypertension. *Journal of human hypertension.*2002;**16**:255-60

56 Felder RA, White MJ, Williams SM, Jose PA. Diagnostic tools for hypertension and salt sensitivity testing. *Current Opinion in Nephrology and Hypertension* 2013; **22**: 65–76.

57 Gu D, Zhao Q, Chen J, *et al.* Reproducibility of Blood Pressure Responses to Dietary Sodium and Potassium Interventions: The GenSalt Study. *Hypertension* 2013; **62**: 499–505.

58 He J, Gu D, Chen J, *et al.* Gender difference in blood pressure responses to dietary sodium intervention in the GenSalt study. *Journal of Hypertension* 2009; **27**: 48–54.

59 Aukland K, Reed RK. Interstitial-lymphatic mechanisms in the control of extracellular fluid volume. *Physiol Rev* 1993; **73**: 1–78.

60 Bhave G, Neilson EG. Body Fluid Dynamics: Back to the Future. *Journal of the American Society of Nephrology* 2011; **22**: 2166–81.

61 Cannon W. Organization for physiological homeostasis. *Am Physiological Soc* 1929; **9**: 399–431.

62 Davies KJA. Adaptive homeostasis. *Molecular Aspects of Medicine* 2016; **49**: 1–7.

63 Strauss MB, Lamdin E, Smith WP, Bleifer DJ. Surfeit and Deficit of Sodium : A Kinetic Concept of Sodium Excretion. *AMA archives of Arch Intern Med* 1958; **102**: 527–36.

64 Titze J. Water-Free Sodium Accumulation. *Seminars in Dialysis* 2009; **22**: 253–5.

65 Adrogué HJ, Madias NE. Sodium surfeit and potassium deficit: keys to the pathogenesis of hypertension. *J Am Soc Hypertens* 2014; **8**: 203–13.

66 Hall JE. Guyton and Hall Textbook of Medical Physiology, 12 edn. Elsevier Health Sciences, 2010.

67 Crowley SD, Gurley SB, Oliverio MI, *et al.* Distinct roles for the kidney and systemic tissues in blood pressure regulation by the renin-angiotensin system. *Journal of Clinical Investigation* 2005; **115**: 1092–9.

68 Lifton RP, Gharavi AG, Geller DS. Molecular mechanisms of human hypertension. *Cell* 2001; **104**: 545–56.

69 Ivy JR, Bailey MA. Pressure natriuresis and the renal control of arterial blood pressure. *The Journal of Physiology* 2014; **592**: 3955–67.

70 Meneton P, Jeunemaitre X, de Wardener HE, Macgregor GA. Links between dietary salt intake, renal salt handling, blood pressure, and cardiovascular diseases. *Physiol Rev* 2005; **85**: 679–715.

71 Visser FW, Krikken JA, Muntinga JHJ, Dierckx RA, Navis GJ. Rise in Extracellular Fluid Volume During High sodium Depends on BMI in Healthy Men. *Obesity* 2009; **17**: 1684–8.

72 Jung J, Basile DP, Pratt JH. Sodium Reabsorption in the Thick Ascending Limb in Relation to Blood Pressure: A Clinical Perspective. *Hypertension* 2011; **57**: 873–9.

73 Rettig R, Bandelow N, Patschan O, Kuttler B, Frey B, Uber A. The importance of the kidney in primary hypertension: insights from cross-transplantation. *Journal of Human Hypertension* 1996; **10**: 641–4.

74 Brands MW. Chronic blood pressure control. *Compr Physiol* 2012; **2**: 2481–94.

75 Kurtz TW, DiCarlo SE, Pravenec M, Schmidlin O, Tanaka M, Morris RC. An alternative hypothesis to the widely held view that renal excretion of sodium accounts for resistance to salt-induced hypertension. *Kidney International* 2016; **90**: 965–73.

76 Fournier D, Luft FC, Bader M, Ganten D, Andrade-Navarro MA. Emergence and evolution of the renin–angiotensin–aldosterone system. *J Mol Med* 2012; **90**: 495–508.

77 Rasmussen AS, Simonsen JA, Sandgaard N, Hoilund-Carlsen PF, Bie P. Mechanisms of acute natriuresis in normal humans on low sodium diet. *The Journal of Physiology* 2003; **546**: 591–603.

78 Cappuccio FP, Markandu ND, Sagnella GA, Macgregor GA. Sodium Restriction Lowers High Blood Pressure Through a Decreased Response of the Renin System: Direct Evidence Using Saralasin. *Journal of Hypertension* 1985; **3**: 243–7.

79 Weinberger MH, Stegner JE, Fineberg NS. A comparison of two tests for the assessment of blood pressure responses to sodium. *American Journal of Hypertension* 1993; **6**: 179–84.

80 Singer DR, Markandu ND, Morton JJ, Miller MA, Sagnella GA, MacGregor GA. Angiotensin II suppression is a major factor permitting excretion of an acute sodium load in humans. *Am J Physiol* 1994; **266**: F89–93.

81 Winternitz SR, Oparil S. Sodium-Neural Interactions in the Development of Spontaneous Hypertension. *Clinical & Experimental Hypertension* 1982; **4**: 751–60.

82 Luft FC, Rankin LI, Henry DP, Bloch R, 1979. Plasma and urinary norepinephrine values at extremes of sodium intake in normal man. *Hypertension* 1979; **1**: 261–6.

83 Campese VM, Romoff MS, Levitan D, Saglikes Y, Friedler RM, Massry SG. Abnormal relationship between sodium intake and sympathetic nervous system activity in salt-sensitive patients with essential hypertension. *Kidney International* 1982; **21**: 371–8.

84 Skrabal F, Herholz H, Neumayr M, *et al.* Salt sensitivity in humans is linked to enhanced sympathetic responsiveness and to enhanced proximal tubular reabsorption. *Hypertension* 1984; **6**: 152–8.

85 Sharma AM, Schattenfroh S, Thiede HM, Oelkers W, Distler A. Effects of sodium salts on pressor reactivity in salt-sensitive men. *Hypertension* 1992; **19**: 541–8.

86 Jin H, Chen YF, Yang RH, Oparil S. Atrial natriuretic factor in NaCl-sensitive and NaCl-resistant spontaneously hypertensive rats. *Hypertension* 1989; **14**: 404–12.

87 Lieb W, Pencina MJ, Jacques PF, *et al.* Higher aldosterone and lower N-terminal proatrial natriuretic peptide as biomarkers of salt sensitivity in the community. *Eur J Cardiovasc Prev Rehabil* 2011; **18**: 664–73.

88 Ferri C, Bellini C, Carlomagno A, Perrone A, Santucci A. Urinary kallikrein and salt sensitivity in essential hypertensive males. *Kidney International* 1994; **46**: 780–8.

89 Davenport AP, Hyndman KA, Dhaun N, *et al.* Endothelin. *Pharmacological Reviews* 2016; **68**: 357–418.

90 Hoffman A, Grossman E, Goldstein DS, Gill JR, Keiser HR. Urinary excretion rate of endothelin-1 in patients with essential hypertension and salt sensitivity. *Kidney International* 1994; **45**: 556–60.

91 Imanishi M, Okada N, Konishi Y, *et al.* Angiotensin II receptor blockade reduces salt sensitivity of blood pressure through restoration of renal nitric oxide synthesis in patients with diabetic nephropathy. *J Renin Angiotensin Aldosterone Syst* 2013; **14**: 67–73.

92 Miller JZ, Weinberger MH, Christian JC, Daugherty SA. Familial resemblance in the blood pressure response to sodium restriction. *Am J Epidemiol* 1987; **126**: 822–30.

93 Gu D, Rice T, Wang S, *et al.* Heritability of Blood Pressure Responses to Dietary Sodium and Potassium Intake in a Chinese Population. *Hypertension* 2007; **50**: 116–22.

94 Campese VM. Why is salt-sensitive hypertension so common in blacks? *Nephrol Dial Transplant* 1997; **12**: 399–403.

95 Doaei S, Gholamalizadeh M. The association of genetic variations with sensitivity of blood pressure to dietary salt: A narrative literature review. *ARYA Atheroscler* 2014; **10**: 169–74.

96 Luft FC. Molecular genetics of salt-sensitivity and hypertension. 2001: 500–4.

97 Sanada H, Jones JE, Jose PA. Genetics of Salt-Sensitive Hypertension. *Curr Hypertens Rep* 2010; **13**: 55–66.

98 Wain LV, Verwoert GC, O'Reilly PF, *et al.* Genome-wide association study identifies six new loci influencing pulse pressure and mean arterial pressure. *Nat Genet* 2011; **43**: 1005–11.

99 Boegehold MA, Kotchen TA. Importance of dietary chloride for salt sensitivity of blood pressure. *Hypertension* 1991; **17**: I158–8.

100 Luft FC, Zemel MB, Sowers JA, Fineberg NS, Weinberger MH. Sodium bicarbonate and sodium chloride: effects on blood pressure and electrolyte homeostasis in normal and hypertensive man. *Journal of Hypertension* 1990; **8**: 663–70.

101 Kurtz TW, Al-Bander HA, Morris RC. 'Salt-sensitive' essential hypertension in men. Is the sodium ion alone important? *N Engl J Med* 1987; **317**: 1043–8.

102 Hiraoka M, Kawano S, Hirano Y, Furukawa T. Role of cardiac chloride currents in changes in action potential characteristics and arrhythmias. *Cardiovasc Res* 1998; **40**: 23–33.

103 Yang H, Huang L-Y, Zeng D-Y, *et al.* Decrease of intracellular chloride concentration promotes endothelial cell inflammation by activating nuclear factor-κB pathway. *Hypertension* 2012; **60**: 1287–93.

104 Morris RC, Sebastian A, Forman A, Tanaka M, Schmidlin O. Normotensive salt sensitivity: effects of race and dietary potassium. 1999; **33**: 18–23.

105 Hedayati SS, Minhajuddin AT, Ijaz A, *et al.* Association of Urinary Sodium/Potassium Ratio with Blood Pressure: Sex and Racial Differences. *Clinical Journal of the American Society of Nephrology* 2012; **7**: 315–22.

106 Yang Q, Liu T, Kuklina EV, *et al.* Sodium and potassium intake and mortality among US adults: prospective data from the Third National Health and Nutrition Examination Survey. *Arch Intern Med* 2011; **171**: 1183–91.

107 Guyton AC. Long-term arterial pressure control: an analysis from animal experiments and computer and graphic models. *Am J Physiol* 1990; **259**: R865–77.

108 Ishii M, Atarashi K, Ikeda T, *et al.* Role of the aldosterone system in the salt-sensitivity of patients with benign essential hypertension. *Jpn Heart J* 1983; **24**: 79–90.

109 Wedler B, Brier ME, Wiersbitzky M, *et al.* Sodium kinetics in salt-sensitive and salt-resistant normotensive and hypertensive subjects. *Journal of Hypertension* 1992; **10**: 663–9.

110 Schmidlin O, Forman Anthony Sebastian A, Morris RC. What Initiates the Pressor Effect of Salt in Salt-Sensitive Humans? Observations in Normotensive Blacks. *Hypertension* 2007; **49**: 1032–9.

111 Schmidlin O, Forman A, Leone A, Sebastian A, Morris RC. Salt Sensitivity in Blacks: Evidence That the Initial Pressor Effect of NaCl Involves Inhibition of Vasodilatation by Asymmetrical Dimethylarginine. *Hypertension* 2011; **58**: 380–5.

112 Roman RJ, Osborn JL. Renal function and sodium balance in conscious Dahl S and R rats. *Am J Physiol* 1987; **252**: R833–41.

113 Nakamura K, Cowley AW. Sequential changes of cerebrospinal fluid sodium during the development of hypertension in Dahl rats. *Hypertension* 1989; **13**: 243–9.

114 Hu L, R D Manning J. Role of nitric oxide in regulation of long-term pressure-natriuresis relationship in Dahl rats. *Am J Physiol Heart Circ Physiol* 1995; **268**: H2375–83.

115 Kanagy NL, Fink GD. Losartan prevents salt-induced hypertension in reduced renal mass rats. *J Pharmacol Exp Ther* 1993; **265**: 1131–6.

116 Titze J, Krause H, Hecht H, *et al.* Reduced osmotically inactive Na storage capacity and hypertension in the Dahl model. *Am J Physiol Renal Physiol* 2002; **283**: F134–41.

117 Heer M, Baisch F, Kropp J, Gerzer R, Drummer C. High dietary sodium chloride consumption may not induce body fluid retention in humans. *Am J Physiol Renal Physiol* 2000; **278**: F585–95.

118 Laffer CL, Scott RC, Titze JM, Luft FC, Elijovich F. Hemodynamics and Salt-and-Water Balance Link Sodium Storage and Vascular Dysfunction in Salt-Sensitive Subjects. *Hypertension* 2016; **68**: 195–203.

119 Greene AS, Yu ZY, Roman RJ, A W Cowley J. Role of blood volume expansion in Dahl rat model of hypertension. *Am J Physiol Heart Circ Physiol* 1990; **258**: H508–14.

120 West SG, Light KC, Hinderliter AL, Stanwyck CL, Bragdon EE, Brownley KA. Potassium supplementation induces beneficial cardiovascular changes during rest and stress in salt sensitive individuals. *Health Psychol* 1999; **18**: 229–40.

121 Sullivan JM, Prewitt RL, Ratts TE, Josephs JA, Connor MJ. Hemodynamic characteristics of sodium-sensitive human subjects. *Hypertension* 1987; **9**: 398–406.

122 Schmidlin O, Forman A, Sebastian A, Morris RC. Sodium-selective salt sensitivity: its occurrence in blacks. 2007; **50**: 1085–92.

123 Palacios C, Wigertz K, Martin BR, *et al.* Sodium Retention in Black and White Female Adolescents in Response to Salt Intake. *The Journal of Clinical Endocrinology & Metabolism* 2009; **89**: 1858–63.

124 Titze J, Maillet A, Lang R, *et al.* Long-term sodium balance in humans in a terrestrial space station simulation study. *American Journal of Kidney Diseases* 2002; **40**: 508–16.

125 Rakova N, Jüttner K, Dahlmann A, *et al.* Long-Term Space Flight Simulation Reveals Infradian Rhythmicity in Human Na+ Balance. *Cell Metabolism* 2013; **17**: 125–31.

126 Lesperance LM, Gray ML, Burstein D. Determination of fixed charge density in cartilage using nuclear magnetic resonance. *Journal of Orthopaedic Research* 1992; **10**: 1–13.

127 Wheaton AJ, Borthakur A, Shapiro EM, *et al.* Proteoglycan Loss in Human Knee Cartilage: Quantitation with Sodium MR Imaging--Feasibility Study. *Radiology* 2004; **231**: 900–5.

128 Edelman IS, Leibman J. Anatomy of body water and electrolytes. *The American Journal of Medicine* 1959; **27**: 256–77.

129 Wahlgren V, Magnus R. Über die Bedeutung der Gewebe als Chlordepots. *Archiv f experiment Pathol u Pharmakol* 1909; **61**: 97–112.

130 Titze J, Shakibaei M, Schafflhuber M, *et al.* Glycosaminoglycan polymerization may enable osmotically inactive Na+ storage in the skin. *Am J Physiol Heart Circ Physiol* 2004; **287**: H203–8.

131 Ivanova LN, Archibasova VK, IS S. Sodium-depositing function of the skin in white rats. *Fiziol Zh SSSR Im I M Sechenova* 1978; **64**: 358–63.

132 Titze J, Lang R, Ilies C, *et al.* Osmotically inactive skin Na+ storage in rats. *Am J Physiol Renal Physiol* 2003; **285**: F1108–17.

133 Machnik A, Neuhofer W, Jantsch J, *et al.* Macrophages regulate salt-dependent volume and blood pressure by a vascular endothelial growth factor-C–dependent buffering mechanism. *Nature Medicine* 2009; **15**: 545–52.

134 Machnik A, Dahlmann A, Kopp C, *et al.* Mononuclear phagocyte system depletion blocks interstitial tonicity-responsive enhancer binding protein/vascular endothelial growth factor C expression and induces salt-sensitive hypertension in rats. *Hypertension* 2010; **55**: 755–61.

135 Wiig H, Luft FC, Titze JM. The interstitium conducts extrarenal storage of sodium and represents a third compartment essential for extracellular volume and blood pressure homeostasis. *Acta Physiol (Oxf)* 2018; **222**.

136 Comper WD, Laurent TC. Physiological function of connective tissue polysaccharides. *Physiol Rev* 1978; **58**: 255–315.

137 Schaefer L, Schaefer RM. Proteoglycans: from structural compounds to signaling molecules. *Cell Tissue Res* 2010; **339**: 237–46.

138 Lodish HF. Molecular Cell Biology. W.H. Freeman, 2012.

139 Chakrabarti B, Park JW, Stevens ES. Glycosaminoglycans: Structure and Interaction. *Critical Reviews in Biochemistry and Molecular Biology* 1980; **8**: 225–313.

140 Volpi N. Disaccharide analysis and molecular mass determination to microgram level of single sulfated glycosaminoglycan species in mixtures following agarose-gel electrophoresis. *Anal Biochem* 1999; **273**: 229–39.

141 Farber SJ. Mucopolysaccharides and Sodium Metabolism. 1960; **21**: 941–7.

142 Schafflhuber M, Volpi N, Dahlmann A, *et al.* Mobilization of osmotically inactive Na+ by growth and by dietary salt restriction in rats. *AJP: Renal Physiology* 2007; **292**: F1490–500.

143 Fischereder M, Michalke B, Schmöckel E, *et al.* Sodium storage in human tissues is mediated by glycosaminoglycan expression. *Am J Physiol Renal Physiol* 2017; **313**: F319–25.

144 Kirabo A. A new paradigm of sodium regulation in inflammation and hypertension. *AJP: Regulatory, Integrative and Comparative Physiology* 2017; **313**: R706–10.

145 Nijst P, Verbrugge FH, Grieten L, *et al.* The Pathophysiological Role of Interstitial Sodium in Heart Failure. *Hypertension* 2015; **65**: 378–88.

146 Harrison DG. Vascular inflammatory cells in hypertension. *Frontiers in Physiology* 2012; **3**: 1–8.

147 Wiktor-Jedrzejczak W, Gordon S. Cytokine regulation of the macrophage (M phi) system studied using the colony stimulating factor-1-deficient op/op mouse. *Physiol Rev* 1996; **76**: 927–47.

148 Wynn TA, Chawla A, Pollard JW. Macrophage biology in development, homeostasis and disease. *Nature* 2013; **496**: 445–55.

149 Mueller S, Quast T, Schroeder A, *et al.* Salt-Dependent Chemotaxis of Macrophages. *PLoS ONE* 2013; **8**. e73439

150 Zhang W-C, Zheng X-J, Du L-J, *et al.* High salt primes a specific activation state of macrophages, M(Na). *Cell Res* 2015; **25**: 893–910.

151 Berry MR, Mathews RJ, Ferdinand JR, *et al.* Renal Sodium Gradient Orchestrates a Dynamic Antibacterial Defense Zone. *Cell* 2017; **170**: 1–35.

152 Wiig H, Schröder A, Neuhofer W, *et al.* Immune cells control skin lymphatic electrolyte homeostasis and blood pressure. *Journal of Clinical Investigation* 2013; **123**: 2803–15.

153 Marvar PJ, Gordon FJ, Harrison DG. Blood pressure control: salt gets under your skin. *Nature Medicine* 2009; **15**: 487–8.

154 Ferrara N. Vascular endothelial growth factor: basic science and clinical progress. *Endocrine Reviews* 2004; **25**: 581–611.

155 Kruzliak P, Novak J, Novak M. Vascular Endothelial Growth Factor Inhibitor-Induced Hypertension: From Pathophysiology to Prevention and Treatment Based on Long-Acting Nitric Oxide Donors. *American Journal of Hypertension* 2013;**1**:3-13.

156 Lankhorst S, Saleh L, Danser AJ, van den Meiracker AH. Etiology of angiogenesis inhibition-related hypertension. *Current Opinion in Pharmacology* 2015; **21**: 7–13.

157 Hayman SR, Leung N, Grande JP, Garovic VD. VEGF Inhibition, Hypertension, and Renal Toxicity. *Curr Oncol Rep* 2012; **14**: 285–94.

158 Lankhorst S, Severs D, Markó L, *et al.* Salt Sensitivity of Angiogenesis Inhibition-Induced Blood Pressure Rise: Role of Interstitial Sodium Accumulation? *Hypertension* 2017; **69**: 919–26.

159 Slagman MCJ, Kwakernaak AJ, Yazdani S, *et al.* Vascular endothelial growth factor C levels are modulated by dietary salt intake in proteinuric chronic kidney disease patients and in healthy subjects. *Nephrology Dialysis Transplantation* 2012; **27**: 978–82.

160 Avolio AP, DENG FQ, LI WQ, *et al.* Effects of aging on arterial distensibility in populations with high and low prevalence of hypertension: comparison between urban and rural communities in China. 1985; **71**: 202–10.

161 Draaijer P, Kool MJ, Maessen JM, *et al.* Vascular distensibility and compliance in salt-sensitive and salt-resistant borderline hypertension. *Journal of Hypertension* 1993; **11**: 1199.

162 D'Elia L, Galletti F, La Fata E, Sabino P, Strazzullo P. Effect of dietary sodium restriction on arterial stiffness: systematic review and meta-analysis of the randomized controlled trials. *Journal of Hypertension* 2018; **36**: 734–43.

163 Dickinson KM, Keogh JB, Clifton PM. Effects of a low-salt diet on flow-mediated dilatation in humans. *Am J Clin Nutr* 2009; **89**: 485–90.

164 Todd AS, Macginley RJ, Schollum JBW, *et al.* Dietary sodium loading in normotensive healthy volunteers does not increase arterial vascular reactivity or blood pressure. *Nephrology* 2012; **17**: 249–56.

165 McMahon EJ, Bauer JD, Hawley CM, *et al.* A randomized trial of dietary sodium restriction in CKD. *Journal of the American Society of Nephrology* 2013; **24**: 2096–103.

166 Gijsbers L, Dower JI, Mensink M, Siebelink E, Bakker SJL, Geleijnse JM. Effects of sodium and potassium supplementation on blood pressure and arterial

stiffness: a fully controlled dietary intervention study. *Journal of Human Hypertension* 2015; : 1–7.

167 Jablonski KL, Fedorova OV, Racine ML, *et al.* Dietary sodium restriction and association with urinary marinobufagenin, blood pressure, and aortic stiffness. *Clinical Journal of the American Society of Nephrology* 2013; **8**: 1952–9.

168 He FJ, Marciniak M, Visagie E, *et al.* Effect of Modest Salt Reduction on Blood Pressure, Urinary Albumin, and Pulse Wave Velocity in White, Black, and Asian Mild Hypertensives. 2009; **54**: 482–8.

169 Pimenta E, Gaddam KK, Oparil S, *et al.* Effects of dietary sodium reduction on blood pressure in subjects with resistant hypertension: results from a randomized trial. 2009; **54**: 475–81.

170 Todd AS, Macginley RJ, Schollum JB, *et al.* Dietary salt loading impairs arterial vascular reactivity. *Am J Clin Nutr* 2010; **91**: 557–64.

171 Dickinson KM, Clifton PM, Keogh JB. A reduction of 3 g/day from a usual 9 g/day salt diet improves endothelial function and decreases endothelin-1 in a randomised cross_over study in normotensive overweight and obese subjects. *Atherosclerosis* 2014; **233**: 32–8.

172 Suckling RJ, He FJ, Markandu ND, Macgregor GA. Modest Salt Reduction Lowers Blood Pressure and Albumin Excretion in Impaired Glucose Tolerance and Type 2 Diabetes Mellitus: A Randomized Double-Blind Trial. *Hypertension* 2016; **67**: 1189–95.

173 van der Graaf AM, Paauw ND, Toering TJ, *et al.* Impaired sodium-dependent adaptation of arterial stiffness in formerly preeclamptic women: the RETAP-vascular study. *Am J Physiol Heart Circ Physiol* 2016; **310**: H1827–33.

174 Partovian C, Bénétos A, Pommiès JP, Mischler W, Safar ME. Effects of a chronic high-salt diet on large artery structure: role of endogenous bradykinin. *Am J Physiol* 1998; **274**: H1423–8.

175 Et-taouil K, Schiavi P, Levy BI, Plante GE. Sodium Intake, Large Artery Stiffness, and Proteoglycans in the Spontaneously Hypertensive Rat. *Hypertension* 2001; **38**: 1172–6.

176 Simon G, Abraham G, Altman S. Stimulation of vascular glycosaminoglycan synthesis by subpressor angiotensin II in rats. *Hypertension* 1994; **23**: I148–51.

177 Hollander W, Kramsch DM, Farmelant M, Madoff IM. Arterial wall metabolism in experimental hypertension of coarctation of the aorta of short duration. *Journal of Clinical Investigation* 1968; **47**: 1221–9.

178 Tobin DJ. Biochemistry of human skin—our brain on the outside. *Chem Soc Rev* 2006; **35**: 52.

179 Lambert PH, Laurent PE. Intradermal vaccine delivery: Will new delivery systems transform vaccine administration? *Vaccine* 2008; **26**: 3197–208.

180 Goldsmith LA. Physiology, biochemistry, and molecular biology of the skin. Oxford University Press, USA, 1991.

181 Brown H. The mineral content of human, dog, and rabbit skin. *Journal of Biological Chemistry* 1926; **68**: 729–36.

182 Brown H. The mineral content of human skin. *Journal of Biological Chemistry* 1927; **75**: 789–94.

183 Urbach E. Contributions to a physiological and pathological chemical of the skin II Note Water, common salt, residual nitrogen and fat content of the skin normally and under pathological relations. *Arch f Dermat* 1928; **156**: 73–101.

184 Cornbleet T, Ingraham RC, Schorr HC. Calcium potassium and sodium metabolism and the skin - The use of potassium chloride in certain allergic dermatoses. *Arch Derm Syphilol* 1942; **46**: 833–40.

185 Suntzeff V, Carruthers C. The Mineral Composition of Human Epidermis. *Journal of Biological Chemistry* 1945; **160**: 567–9.

186 Eisele CW, Eichelberger L. Water, Electrolyte and Nitrogen Content of Human Skin. *Proceedings of the Society for Experimental Biology and Medicine* 1945; **58**: 97–100.

187 Zheutlin H, Fox CL. Sodium and Potassium Content of Human Epidermis. *Arch Derm Syphilol* 1950; **61**: 397–400.

188 Hodgson C. The sodium and potassium content of the epidermis in eczema, psoriasis and lichen simplex. *British Journal of Dermatology* 1960; **72**: 409–15.

189 Padtberg JH. Über die Bedeutung der Haut als Chlordepot. *Archiv f experiment Pathol u Pharmakol* 1910; **63**: 60–79.

190 Urbach E, LeWinn EB. Skin Diseases, Nutrition and Metabolism. Grune & Stratton, 1946.

191 Carruthers C. Biochemistry of Skin in Health and Disease. 1962.

192 Shariatgorji M, Nilsson A, Bonta M, *et al.* Direct imaging of elemental distributions in tissue sections by laser ablation mass spectrometry. *Methods* 2016; **104**: 86–92.

193 Peitzman SJ. The flame photometer as engine of nephrology: a biography. *Am J Kidney Disease* 2010;**56**:379-86

194 Iyengar GV. Elemental Analysis of Biological Systems. CRC Press, 1989.

195 Kopp C, Linz P, Wachsmuth L, *et al.* 23Na Magnetic Resonance Imaging of Tissue Sodium. *Hypertension* 2011; **59**: 167–72.

196 Hilal SK, Maudsley AA, Ra JB, *et al.* In vivo NMR imaging of sodium-23 in the human head. *J Comput Assist Tomogr* 1985; **9**: 1–7.

197 Kopp C, Linz P, Dahlmann A, *et al.* 23Na magnetic resonance imaging-determined tissue sodium in healthy subjects and hypertensive patients. *Hypertension* 2013; **61**: 635–40.

198 Dahlmann A, Dörfelt K, Eicher F, *et al.* Magnetic resonance-determined sodium removal from tissue stores in hemodialysis patients. *Kidney International* 2015; **87**: 434–41.

199 Linz P, Santoro D, Renz W, *et al.* Skin sodium measured with 23Na MRI at 7.0 T. *NMR Biomed* 2014; **28**: 54–62.

200 Hammon M, Grossmann S, Linz P, *et al.* 23Na Magnetic Resonance Imaging of the Lower Leg of Acute Heart Failure Patients during Diuretic Treatment. *PLoS ONE* 2015; **10**: e0141336.

201 Dahlmann A, Kopp C, Linz P, *et al.* Quantitative assessment of muscle injury by (23)Na magnetic resonance imaging. *Springerplus* 2016; **5**: 661.

202 Kopp C, Beyer C, Linz P, *et al.* Na^+ deposition in the fibrotic skin of systemic sclerosis patients detected by ^{23}Na-magnetic resonance imaging. *Rheumatology (Oxford)* 2016; **56**: 371–560.

203 Wang P, Deger MS, Kang H, Ikizler TA, Titze J, Gore JC. Sex differences in sodium deposition in human muscle and skin. *Magnetic Resonance Imaging* 2017; **36**: 93–7.

204 Schneider MP, Raff U, Kopp C, *et al.* Skin Sodium Concentration Correlates with Left Ventricular Hypertrophy in CKD. *Journal of the American Society of Nephrology* 2017; **28**: 1867–76.

205 Madelin G, Regatte RR. Biomedical applications of sodium MRI in vivo. *J Magn Reson Imaging* 2013; **38**: 511–29.

206 Constantinides CD, Kraitchman DL, O'Brien KO, Boada FE, Gillen J, Bottomley PA. Noninvasive quantification of total sodium concentrations in acute reperfused myocardial infarction using 23Na MRI. *Magn Reson Med* 2001; **46**: 1144–51.

207 Madelin G, Babb J, Xia D, *et al.* Articular cartilage: evaluation with fluid-suppressed 7.0-T sodium MR imaging in subjects with and subjects without osteoarthritis. *Radiology* 2013; **268**: 481–91.

208 Hofmeister LH, Perisic S, Titze J. Tissue sodium storage: evidence for kidney-like extrarenal countercurrent systems? *Pflugers Arch - Eur J Physiol* 2015; **467**: 551–8.

209 Warner RR, Myers MC, Taylor DA. Electron probe analysis of human skin: determination of the water concentration profile. *Journal of Investigative …* 1988; **90**: 218–24.

210 Jantsch J, Schatz V, Friedrich D, *et al.* Cutaneous Na+ storage strengthens the antimicrobial barrier function of the skin and boosts macrophage-driven host defense. *Cell Metabolism* 2015; **21**: 493–501.

211 Johnson RS, Titze J, Weller R. Cutaneous control of blood pressure. *Current Opinion in Nephrology and Hypertension* 2016; **25**: 11–5.

212 Charkoudian N. Skin blood flow in adult human thermoregulation: how it works, when it does not, and why. *Mayo Clinic Proceedings* 2003; **78**: 603–12.

213 Mowbray M, McLintock S, Weerakoon R, *et al.* Enzyme-independent NO stores in human skin: quantification and influence of UV radiation. *Journal of Investigative Dermatology* 2009; **129**: 834–42.

214 Opländer C, Volkmar CM, Paunel-Görgülü A, *et al.* Whole Body UVA Irradiation Lowers Systemic Blood Pressure by Release of Nitric Oxide From Intracutaneous Photolabile Nitric Oxide Derivates. *Circulation Research* 2009; **105**: 1031–40.

215 Liu D, Fernandez BO, Hamilton A, *et al.* UVA irradiation of human skin vasodilates arterial vasculature and lowers blood pressure independently of nitric oxide synthase. *Journal of Investigative Dermatology* 2014; **134**: 1839–46.

216 Maxwell PH, Eckardt K-U. HIF prolyl hydroxylase inhibitors for the treatment of renal anaemia and beyond. *Nature Reviews Nephrology* 2016; **12**: 157–68.

217 Cowburn AS, Takeda N, Boutin AT, *et al.* HIF isoforms in the skin differentially regulate systemic arterial pressure. *Proc Natl Acad Sci USA* 2013; **110**: 17570–5.

218 Takeda N, O'Dea EL, Doedens A, *et al.* Differential activation and antagonistic function of HIF-alpha isoforms in macrophages are essential for NO homeostasis. *Genes & Development* 2010; **24**: 491–501.

219 Lin C, McGough R, Aswad B, Block JA, Terek R. Hypoxia induces HIF-1alpha and VEGF expression in chondrosarcoma cells and chondrocytes. *J Orthop Res* 2004; **22**: 1175–81.

220 Milkiewicz M, Hudlicka O, Brown MD, Silgram H. Nitric oxide, VEGF, and VEGFR-2: interactions in activity-induced angiogenesis in rat skeletal muscle. *Am J Physiol Heart Circ Physiol* 2005; **289**: H336–43.

221 Wang Z, Zhu Q, Xia M, Li PL, Hinton SJ, Li N. Hypoxia-Inducible Factor Prolyl-Hydroxylase 2 Senses High-Salt Intake to Increase Hypoxia Inducible Factor 1 Levels in the Renal Medulla. *Hypertension* 2010; **55**: 1129–36.

222 Zhu Q, Hu J, Han W-Q, *et al.* Silencing of HIF prolyl-hydroxylase 2 gene in the renal medulla attenuates salt-sensitive hypertension in Dahl S rats. *American Journal of Hypertension* 2014; **27**: 107–13.

223 Prasad A, Dunnill GS, Mortimer PS, MacGregor GA. Capillary rarefaction in the forearm skin in essential hypertension. *Journal of Hypertension* 1995; **13**: 265–8.

224 Antonios TFT, Singer DRJ, Markandu ND, Mortimer PS, MacGregor GA. Structural Skin Capillary Rarefaction in Essential Hypertension. 1999; **33**: 998–1001.

225 Debbabi H, Uzan L, Mourad J, Safar M, Levy B, Tibirica E. Increased Skin Capillary Density in Treated Essential Hypertensive Patients. *American Journal of Hypertension* 2006; **19**: 477–83.

226 Cheng C, Daskalakis C, Falkner B. Original Research: Capillary rarefaction in treated and untreated hypertensive subjects. *Therapeutic Advances in Cardiovascular Disease* 2008; **2**: 79–88.

227 Martens RJH, Henry RMA, Houben AJHM, *et al.* Capillary Rarefaction Associates with Albuminuria: The Maastricht Study. *J Am Soc Nephrol* 2016; : 1–10.

228 Serne EH, Gans ROB, Maaten ter JC, Tangelder GJ, Donker AJM, Stehouwer CDA. Impaired Skin Capillary Recruitment in Essential Hypertension Is Caused by Both Functional and Structural Capillary Rarefaction. 2001; **38**: 238–42.

229 Cutler JA, Sorlie PD, Wolz M, Thom T, Fields LE, Roccella EJ. Trends in hypertension prevalence, awareness, treatment, and control rates in United States adults between 1988-1994 and 1999-2004. *Hypertension* 2008; **52**: 818–27.

230 Sandberg KK, Ji HH. Sex differences in primary hypertension. *Biol Sex Differ* 2012; **3**: 7–7.

231 Maranon R, Reckelhoff JF. Sex and gender differences in control of blood pressure. *Clinical Science* 2013; **125**: 311–8.

232 Kojima S, Murakami K, Kimura G, *et al.* A Gender Difference in the Association Between Salt Sensitivity and Family History of Hypertension. *American Journal of Hypertension* 1992; **5**: 1–7.

233 Yanes LL, Sartori-Valinotti JC, Iliescu R, *et al.* Testosterone-dependent hypertension and upregulation of intrarenal angiotensinogen in Dahl salt-sensitive rats. *Am J Physiol Renal Physiol* 2009; **296**: F771–9.

234 Schulman IH, Aranda P, Raij L, Veronesi M, Aranda FJ, Martin R. Surgical Menopause Increases Salt Sensitivity of Blood Pressure. *Hypertension* 2006; **47**: 1168–74.

235 Pechere-Bertschi A, Maillard M, Stalder H, Brunner HR, Burnier M. Blood pressure and renal haemodynamic response to salt during the normal menstrual cycle. *Clin Sci* 2000; **98**: 697–702.

236 Pechère-Bertschi A, Maillard M, Stalder H, *et al.* Renal hemodynamic and tubular responses to salt in women using oral contraceptives. *Kidney International* 2003; **64**: 1374–80.

237 Smith RK. Laboratory Contamination. In: Interpretation of Inorganic Data. Genium Publishing Corporation, 2001.

238 Boss CB, Fredeen KJ. Concepts, instrumentation and techniques in inductively coupled plasma optical emission spectrometry. In: ICP-OES Instrumentation, 2nd edn. Perker Elmer, 1997.

239 Hou X, Jones BT. Inductively Coupled Plasma-Optical Emission Spectrometry. John Wiley & Sons Ltd, 2000: 9468–85.

240 Carpenter RC. The analysis of some evidential materials by inductively coupled plasma-optical emission spectrometry. *Forensic Sci Int* 1985; **27**: 157–63.

241 Jugdaohsingh R, Calomme MR, Robinson K, *et al.* Increased longitudinal growth in rats on a silicon-depleted diet. *Bone* 2008; **43**: 596–606.

242 Jugdaohsingh R, Anderson SHC, Lakasing L, Sripanyakorn S, Ratcliffe S, Powell JJ. Serum silicon concentrations in pregnant women and newborn babies. *BJN* 2013; **110**: 1–7.

243 Ghosh S, Prasanna VL, Sowjanya B. Inductively Coupled Plasma–Optical Emission Spectroscopy: A Review. *Asian J Pharm Ana* 2013; **3**.

244 Titze J, Bauer K, Schafflhuber M, *et al.* Internal sodium balance in DOCA-salt rats: a body composition study. *Am J Physiol Renal Physiol* 2005; **289**: F793–802.

245 Titze J, Luft FC, Bauer K, *et al.* Extrarenal Na+ balance, volume, and blood pressure homeostasis in intact and ovariectomized deoxycorticosterone-acetate salt rats. *Hypertension* 2006; **47**: 1101–7.

246 International Union of Pure and Applied Chemistry. Compendium of Chemical Terminology - Gold Book. 2014;892.

247 Ward AG, Courts A. The Science and Technology of Gelatin. Academic Press, 1977.

248 Smith CR. Osmosis and Swelling of Gelatine. *Journal of the American Chemical Society* 1921; **43**: 1350–66.

249 Scanlon JW. Electrolyte content of commercial gelatin products and sweetened liquid mixtures in treatment of diarrhea. *Clin Pediatr (Phila)* 1970; **9**: 508–9.

250 Loiselle RJ, Sawinski VJ, Goldberg AF. Local anesthetic solutions and associated response. *Anesth Prog* 1966; **13**: 95–6.

251 Brandis K. Alkalinisation of local anaesthetic solutions. *Issues* 2011; **34**: 173–5.

252 Liu S, Pollock JE, Mulroy MF, Allen HW, Neal JM, Carpenter RL. Comparison of 5% with Dextrose, 1.5% with Dextrose, and 1.5% Dextrose-Free Lidocaine Solutions for Spinal Anesthesia in Human Volunteers. *Anesthesia & Analgesia* 1995; **81**: 697.

253 Cepeda MS, Tzortzopoulou A, Thackrey M, Hudcova J, Arora Gandhi P, Schumann R. Adjusting the pH of lidocaine for reducing pain on injection. *Cochrane Database of Systematic Reviews* 2015; **22**: 216.

254 Bois Du D, Bois Du EF. A formula to estimate the approximate surface area if height and weight be known. 1916. 1989.

255 Levey AS, Bosch JP, Lewis JB, Greene T, Rogers N, Roth D. A More Accurate Method To Estimate Glomerular Filtration Rate from Serum Creatinine: A New Prediction Equation. *Ann Intern Med* 1999; **130**: 461–70.

256 Bates B, Cox L, Maplethorpe N, Mazumder A, Nicholson SEA. National diet and nutrition survey: assessment of dietary sodium in adults (aged 19 to 64 years) in England, 2014. Department of Health, 2016.

257 Shihab HM, Meoni LA, Chu AY, *et al.* Body mass index and risk of incident hypertension over the life course: the Johns Hopkins Precursors Study. *Circulation* 2012; **126**: 2983–9.

258 Berg UB. Differences in decline in GFR with age between males and females. Reference data on clearances of inulin and PAH in potential kidney donors. *Nephrol Dial Transplant* 2006; **21**: 2577–82.

259 Shapiro EM, Borthakur A, Dandora R, Kriss A, Leigh JS, Reddy R. Sodium visibility and quantitation in intact bovine articular cartilage using high field Na-23 MRI and MRS. *J Magn Reson* 2000; **142**: 24–31.

260 Sandby-Møller J, Poulsen T, Wulf HC. Epidermal thickness at different body sites: relationship to age, gender, pigmentation, blood content, skin type and smoking habits. *Acta dermato-venereologica* 2003; **83**: 410–3.

261 Giacomoni PU, Mammone T, Teri M. Gender-linked differences in human skin. *J Dermatol Sci* 2009; **55**: 144–9.

262 Oh J-H, Kim YK, Jung J-Y, Shin J-E, Chung JH. Changes in glycosaminoglycans and related proteoglycans in intrinsically aged human skin in vivo. *Experimental Dermatology* 2011; **20**: 455–6.

263 Ellis KJ, Vaswani A, Zanzi I, Cohn SH. Total body sodium and chlorine in normal adults. *Metab Clin Exp* 1976; **25**: 645–54.

264 Isezuo SA, Saidu Y, Anas S, Tambuwal BU, Bilbis LS. Salt taste perception and relationship with blood pressure in type 2 diabetics. *Journal of Human Hypertension* 2008; **22**: 432–4.

265 Málaga S, Díaz JJ, Arguelles J, Perillán C, Málaga I, Vijande M. Blood pressure relates to sodium taste sensitivity and discrimination in adolescents. *Pediatr Nephrol* 2003; **18**: 431–4.

266 Schiffman SS, Lockhead E, Maes FW. Amiloride reduces the taste intensity of Na+ and Li+ salts and sweeteners. *Proc Natl Acad Sci USA* 1983; **80**: 6136–40.

267 Heck GL, Mierson S, DeSimone JA. Salt taste transduction occurs through an amiloride-sensitive sodium transport pathway. *Science* 1984; **223**: 403–5.

268 Morris MJ, Na ES, Johnson AK. Salt craving: The psychobiology of pathogenic sodium intake. *Physiology & Behavior* 2008; **94**: 709–21.

269 McEniery CM, Yasmin, Hall IR, *et al.* Normal vascular aging: differential effects on wave reflection and aortic pulse wave velocity: the Anglo-Cardiff Collaborative Trial (ACCT). *Hypertension* 2005; **46**: 1753–60.

270 Clemensen P, Christensen P, Norsk P, Grønlund J. A modified photo- and magnetoacoustic multigas analyzer applied in gas exchange measurements. *J Appl Physiol* 1994; **76**: 2832–9.

271 Peyton PJ, Thompson B. Agreement of an Inert Gas Rebreathing Device with Thermodilution and the Direct Oxygen Fick Method in Measurement of Pulmonary Blood Flow. *J Clin Monit Comput* 2004; **18**: 373–8.

272 Peyton PJ, Bailey M, Thompson BR. Reproducibility of cardiac output measurement by the nitrous oxide rebreathing technique. *J Clin Monit Comput* 2009; **23**: 233–6.

273 Gabrielsen A, Videbaek R, Schou M, Damgaard M, Kastrup J, Norsk P. Non-invasive measurement of cardiac output in heart failure patients using a new foreign gas rebreathing technique. *Clin Sci* 2002; **102**: 247–52.

274 Agostoni P, Cattadori G, Apostolo A, *et al.* Noninvasive measurement of cardiac output during exercise by inert gas rebreathing technique: a new tool for heart failure evaluation. *Hypertension* 2005; **46**: 1779–81.

275 Mäki-Petäjä KM, Barrett SML, Evans SV, Cheriyan J, McEniery CM, Wilkinson IB. The Role of the Autonomic Nervous System in the Regulation of Aortic Stiffness. *Hypertension* 2016; **68**: 1290–7.

276 National Kidney Foundation. K/DOQI clinical practice guidelines for chronic kidney disease: evaluation, classification, and stratification. Am. J. Kidney Dis. 2002; **39**: S1–266.

277 Steinhäuslin F, Burnier M, Magnin JL, *et al.* Fractional excretion of trace lithium and uric acid in acute renal failure. *J Am Soc Nephrol* 1994; **4**: 1429–37.

278 Cornsweet TN. The Staircase-Method in Psychophysics. *The American Journal of Psychology* 1962; **75**: 485.

279 Giguère J-F, de Moura Piovesana P, Proulx-Belhumeur A, Doré M, de Lemos Sampaio K, Gallani M-C. Reliability of a Simple Method for Determining Salt Taste Detection and Recognition Thresholds. *Chemical Senses* 2016; **41**: 205–10.

280 Huggins RL, Di Nicolantonio R, Morgan TO. Preferred salt levels and salt taste acuity in human subjects after ingestion of untasted salt. *Appetite* 1992; **18**: 111–9.

281 DiNicolantonio R, Teow BH, Morgan TO. Sodium Sodium detection threshold and preference for sodium chloride in humans on high and low sodium diets. *Clinical and Experimental Pharmacology and Physiology* 1984; **11**: 335–8.

282 Rabin M, Poli de Figueiredo CE, Wagner MB, Antonello ICF. Salt taste sensitivity threshold and exercise-induced hypertension. *Appetite* 2009; **52**: 609–13.

283 Choe J-S, Kim E-K, Kim E-K. Comparison of salty taste acuity and salty taste preference with sodium intake and blood pressure based on zinc nutritional status in two rural populations in Korea. *Nutr Res Pract* 2012; **6**: 534.

284 Antonios TF, Rattray FE, Singer DR, Markandu ND, Mortimer PS, MacGregor GA. Maximization of skin capillaries during intravital video-microscopy in essential

hypertension: comparison between venous congestion, reactive hyperaemia and core heat load tests. *Clin Sci* 1999; **97**: 523–8.

285 Fredly S, Fugelseth D, Wester T, Häggblad E, Kvernebo K. Skin microcirculation in healthy term newborn infants--assessment of morphology, perfusion and oxygenation. *Clin Hemorheol Microcirc* 2015; **59**: 309–22.

286 Hills M, Armitage P. The two-period cross-over clinical trial. *Br J Clin Pharmacol* 1979; **8**: 7–20.

287 Wiggins WS, Manry CH, Lyons RH, Pitts RF, Barrett M, Dumas B. The Effect of Salt Loading and Salt Depletion on Renal Function and Electrolyte Excretion in Man. *Circulation* 1951; **3**: 275–81.

288 Roos JC, Koomans HA, Mees EJD, Delawi IM. Renal sodium handling in normal humans subjected to low, normal, and extremely high sodium supplies. *Am J Physiol Renal Physiol* 1985; **249**: F941–7.

289 Ogawa T, Spina RJ, Martin WH, *et al.* Effects of aging, sex, and physical training on cardiovascular responses to exercise. *Circulation* 1992; **86**: 494–503.

290 Wiinberg N, Høegholm A, Christensen HR, *et al.* 24-h ambulatory blood pressure in 352 normal Danish subjects, related to age and gender. *American Journal of Hypertension* 1995; **8**: 978–86.

291 James GD, Sealey JE, Müller F, Alderman M, Madhavan S, Laragh JH. Renin relationship to sex, race and age in a normotensive population. *J Hypertens Suppl* 1986; **4**: S387–9.

292 Middlemiss JE, Miles KL, McDonnell BJ, *et al.* Mechanisms underlying elevated SBP differ with adiposity in young adults. *Journal of Hypertension* 2016; **34**: 290–7.

293 Lerchl K, Rakova N, Dahlmann A, *et al.* Agreement Between 24-Hour Salt Ingestion and Sodium Excretion in a Controlled Environment. *Hypertension* 2015; **66**: 850–7.

294 Stevenson S, Thornton J. Effect of estrogens on skin aging and the potential role of SERMs. *Clin Interv Aging* 2007; **2**: 283–97.

295 Beauchamp GK, Bertino M, Burke D, Engelman K. Experimental sodium depletion and salt taste in normal human volunteers. *The American journal Clin Nutr* 1990;**51**:881-9

296 Greaney JL, DuPont JJ, Lennon-Edwards SL, Sanders PW, Edwards DG, Farquhar WB. Dietary sodium loading impairs microvascular function independent of blood pressure in humans: role of oxidative stress. *The Journal of Physiology* 2012; **590**: 5519–28.

297 Helle F, Karlsen TV, Tenstad O, Titze J, Wiig H. High Salt Diet Increases Hormonal Sensitivity In Skin Pre-Capillary Resistance Vessels. *Acta Physiol* 2013; **207**: 577-81

298 Heer M, Frings-Meuthen P, Titze J, *et al.* Increasing sodium intake from a previous low or high intake affects water, electrolyte and acid–base balance differently. *BJN* 2009; **101**: 1286.

299 Masson N, Willam C, Maxwell PH, Pugh CW, Ratcliffe PJ. Independent function of two destruction domains in hypoxia-inducible factor-alpha chains activated by prolyl hydroxylation. *EMBO J* 2001; **20**: 5197–206.

300 Zhu Q, Wang Z, Xia M, Li P-L, Zhang F, Li N. Overexpression of HIF-1α transgene in the renal medulla attenuated salt sensitive hypertension in Dahl S rats. *Biochimica et Biophysica Acta (BBA) - Molecular Basis of Disease* 2012; **1822**: 936–41.

301 Penna Della SL, Cao G, Carranza A, *et al.* Renal Overexpression of Atrial Natriuretic Peptide and Hypoxia Inducible Factor-1 αas Adaptive Response to a High Salt Diet. *BioMed Research International* 2014; **2014**: 1–10.

302 Iyer R, Jenkinson CP, Vockley JG, Kern RM, Grody WW, Cederbaum S. The human arginases and arginase deficiency. *J Inherit Metab Dis* 1998; **21**: 86–100.

303 Jenkinson CP, Grody WW, Cederbaum SD. Comparative properties of arginases. *Comp Biochem Physiol B, Biochem Mol Biol* 1996; **114**: 107–32.

304 Luft FC. Rats, Salt, and History. *Cell Metabolism* 2012; **15**: 129–30.

305 Shibuya M. Vascular Endothelial Growth Factor (VEGF) and Its Receptor (VEGFR) Signaling in Angiogenesis: A Crucial Target for Anti- and Pro-Angiogenic Therapies. *Genes & Cancer* 2012; **2**: 1097–105.

306 Jebbink J, Keijser R, Veenboer G, van der Post J, Ris-Stalpers C, Afink G. Expression of placental FLT1 transcript variants relates to both gestational hypertensive disease and fetal growth. *Hypertension* 2011; **58**: 70–6.

307 Ovalle WK, Nahirney PC, Netter FH. Netter's Essential Histology, 2nd edn. Elsevier Health Sciences, 2013.

308 Wei X, Roomans GM, Forslind B. Elemental distribution in guinea-pig skin as revealed by X-ray microanalysis in the scanning transmission microscope. *J Invest Dermatol* 1982; **79**: 167–9.

309 Warner RR, Myers MC, Taylor DA. Electron probe analysis of human skin: element concentration profiles. *Journal of Investigative Dermatology* 1988; **90**: 78–85.

310 Zglinicki Von T, Lindberg M, Roomans GM, Forslind B. Water and ion distribution profiles in human skin. *Acta dermato-venereologica* 1993; **73**: 340.

311 Xu W, Hong SJ, Zeitchek M, *et al.* Hydration status regulates sodium flux and inflammatory pathways through epithelial sodium channel (ENaC) in the skin. *Journal of Investigative Dermatology* 2015; **135**: 796–806.

312 Hamm LL, Feng Z, Hering-Smith KS. Regulation of sodium transport by ENaC in the kidney. *Current Opinion in Nephrology and Hypertension* 2010; **19**: 98–105.

313 Ussing HH, Zerahn K. Active transport of sodium as the source of electric current in the short-circuited isolated frog skin. *Acta Physiol Scand* 1951; **23**: 110–27.

314 Kaneko Y, Fujimaki-Aoba K, Watanabe S-I, Hokari S, Takada M. Localization of ENaC subunit mRNAs in adult bullfrog skin. *Acta Histochem* 2012; **114**: 172–6.

315 Mauro T, Guitard M, Behne M, *et al.* The ENaC channel is required for normal epidermal differentiation. *J Invest Dermatol* 2002; **118**: 589–94.

316 Yang HY, Charles RP, Hummler E, Baines DL, Isseroff RR. The epithelial sodium channel mediates the directionality of galvanotaxis in human keratinocytes. *J Cell Sci* 2013; **126**: 1942–51.

317 Hanukoglu I, Boggula VR, Vaknine H, Sharma S, Kleyman T, Hanukoglu A. Expression of epithelial sodium channel (ENaC) and CFTR in the human epidermis and epidermal appendages. *Histochem Cell Biol* 2017; **38**: 484.

318 Willis RD, Blanchard FT, Connor TL. Guidelines for the application of SEM/EDX analytical techniques to particulate matter samples. Environmental Protection Agency, 2002.

319 Forslind B. Clinical applications of scanning electron microscopy and energy dispersive X-ray analysis in dermatology--an up-date. *Scanning Microsc* 1988; **2**: 959–76.

320 Zadora G, Brożek-Mucha Z. SEM–EDX—a useful tool for forensic examinations. *Materials Chemistry and Physics* 2003; **81**: 345–8.

321 Brouard M, Casado M, Djelidi S, Barrandon Y, Farman N. Epithelial sodium channel in human epidermal keratinocytes: expression of its subunits and relation to sodium transport and differentiation. *J Cell Sci* 1999; **112**: 3343–52.

322 Xu W, Hong SJ, Zhong A, *et al.* Sodium channel Nax is a regulator in epithelial sodium homeostasis. *Science Translational Medicine* 2015; **7**: 312ra177–7.

323 Sullivan JM, Ratts TE. Hemodynamic mechanisms of adaptation to chronic high sodium intake in normal humans. *Hypertension* 1983; **5**: 814–20.

324 Epstein LH, Temple JL, Roemmich JN, Bouton ME. Habituation as a determinant of human food intake. *Psychological Review* 2009; **116**: 384–407.

325 Kitada K, Daub S, Zhang Y, *et al.* High salt intake reprioritizes osmolyte and energy metabolism for body fluid conservation. *Journal of Clinical Investigation* 2017; **127**: 1944–59.

326 Rakova N, Kitada K, Lerchl K, *et al.* Increased salt consumption induces body water conservation and decreases fluid intake. *Journal of Clinical Investigation* 2017; **127**: 1932–43.

327 Nikpey E, Karlsen TV, Rakova N, Titze JM, Tenstad O, Wiig H. High-Salt Diet Causes Osmotic Gradients and Hyperosmolality in Skin Without Affecting Interstitial Fluid and Lymph. *Hypertension* 2017; **69**: 660-668

328 Kienitz T, Allolio B, Strasburger CJ, Quinkler M. Sex-specific regulation of ENaC and androgen receptor in female rat kidney. *Horm Metab Res* 2009; **41**: 356–62.

329 Yang GZ, Nie HG, Lu L, *et al.* Estrogen regulates the expression and activity of epithelial sodium channel in mouse osteoblasts. *Cell Mol Biol* 2011; **57 Suppl**: OL1480–6.

330 Haase M, Laube M, Thome UH. Sex-specific effects of sex steroids on alveolar epithelial Na +transport. *American Journal of Physiology-Lung Cellular and Molecular Physiology* 2017; **312**: L405–14

Appendix A

Contributions to this thesis

I would also like to acknowledge the contributions made by of the following people for the work described in this thesis:

- Dr Kaisa Mäki-Petäjä from the EMIT unit gave me guidance for the statistical methods used in this thesis.
- Skin and gelatine elemental analysis with ICPOES described in Chapter 2 and 3 were carried out by Miss Liliana Pedro and Dr Sylvaine Bruggraber at the Cambridge MRC Elsie Widdowson Lab.
- Skin elemental analysis with ICPOES described in Chapter 4 for the VARSITY study was carried out by me under the guidance of Miss Liliana Pedro and Dr Sylvaine Bruggraber at the Cambridge MRC Elsie Widdowson Lab.
- ELISA assays for VEGF-C and sFLT4 were operated by Mr Keith Burling and his team at the Addenbrookes Core Biochemical Assay Laboratory.
- The recruitment and assessment of the first 36 participants of the Varsity Methods study was carried out by Miss Anna Goodheart (medical student) and Mr Iqbal Mohammed (MPhil student), at the EMIT unit. Skin biopsies for the first 36 participants were carried out by Dr Maysoon Elkhawad under the guidance of Dr Paul Norris (Consultant Dermatologist), both of whom subsequently trained me to perform the procedure. I subsequently recruited, assessed and carried out skin biopsies for the remaining 12 participants in the study and collated the data for all 48 patients.
- Dr Stephen Smith wrote the computer program for capillary counting in Chapter 4.
- Dr Yury Alaverdyan, Research Facilities Manager at Cambridge Graphene Centre operated the LEO GEMINI 1530VP FEG-SEM at the Cambridge Nanoscience Centre and FEI Magellan 400 XHR SEM systems at the Cambridge Graphene Centre for me and supervised the interpretation of SEM EDX data for the work described in Chapter 6.
- Dr George Meligonis, Consultant Pathologist at Addenbrookes Hospital gave guidance for the interpretation of skin sections described in Chapter 6. Cambridge University Hospitals NHS Foundation Trust Human Research Tissue Bank carried

Publications and Presentations arising from this thesis

Publications

1. **Selvarajah V**, Maki-Petaja K, Pedro L, Bruggraber SFA, Goodhart AK, Brown MJ, McEniery CM, Wilkinson IB. A novel mechanism for buffering dietary salt in humans: effects of salt loading on skin sodium, VEGF-C and blood pressure. Hypertension 2017;70(5):930-937

Presentations (Oral)

1. **Novel mechanisms for salt sensitive hypertension in humans: Effects of salt loading on skin sodium, VEGF-C and blood pressure.** AHA Scientific Council on Hypertension Meeting, Orlando, 16th Sep 2016

2. **Novel mechanisms for salt sensitive hypertension in humans: Effects of salt loading on skin sodium, VEGF-C and blood pressure.** British Hypertension Society Meeting, Dublin, 20th Sep 2016 (Awarded Young Investigator's Award)

3. **Novel mechanisms for salt sensitive hypertension in humans: Effects of salt loading on skin sodium, VEGF-C and blood pressure.** AHA Scientific Council on Hypertension Meeting/American Society of Hypertension Meeting, San Francisco, 15th Sep 2017

Presentations (Poster)

1. Selvarajah V, Maki-Petaja K, Pedro L, Bruggraber SFA, McEniery CM, Wilkinson IB. Novel mechanisms for salt sensitive hypertension in humans: Effects of salt loading on skin sodium, VEGF-C and blood pressure. American Society of Nephrology Meeting, San Diego 5th Nov 2015